Engineered surfaces for binding carbamylated proteins

by Yuhao Ma

A thesis submitted in partial fulfillment of the requirements for the degree of

Doctor of Philosophy

Department of Biomedical Engineering
University of Alberta

Abstract

For patients with decreased kidney function, waste materials accumulate within the blood compartment. Although not all of these chemical species have been directly linked to a specific toxicity, they are generally referred to as uremic toxins. Of particular interest are protein bound uremic toxins for they are extremely difficult to remove using membrane technology. One type of protein bound uremic toxin involves protein carbamylation. Carbamylation of albumin (cHSA) has shown that both extent of carbamylation and concentration of carbamylated albumin are associated with significantly elevated risk of all-cause mortality. Currently there has been no effective method for specifically targeting and removing cHSA from the blood. We believe small peptides, stabilized through immobilization on surfaces, can be employed as high affinity, cheap ligands to target and remove cHSA from blood.

For the first phase we studied the effect of carbamylation on three proteins, cHSA, carbamylated fibrinogen (cFgn) and carbamylated α-lactalbumin (cLA), in terms of physiological aspects. While the molecular integrity and secondary structure were preserved after carbamylation, it was found carbamylation increases the surface charge negativity of protein and significantly altered its tertiary structure. For HSA and LA, carbamylation increased the accessibility of fluorescence quencher. For Fgn, carbamylation increased the fraction of accessible tryptophan. Also, all studied carbamylated proteins

were found to have reduced interaction with surrounding water. Protein adsorption studies revealed that carbamylated proteins generally had a lower amount of adsorption, and the type of substrates influenced the overall amount of adsorption.

After this study, phage display was performed against carbamylated HSA to determine the potential ligand for carbamylated protein. A total of seven candidate phage clones were identified from phage display. ELISA results showed that these phage clones had specificity towards cHSA compared to native HSA. Isothermal titration calorimetry was used to determine that the peptide GSAARTISPSLL (cH2-p1) had a dissociation constant (Kd) of 1.0×10^{-4} M when binding to cHSA, and was almost one magnitude lower than its Kd to native HSA. The binding affinity for cH2-p1 towards cHSA was found to be little influenced by the extent of carbamylation. Moreover, cH2-p1 was found to preferentially bind cFgn, with a similar Kd (8.4×10^{-5} M) as cHSA while there seems to be no interaction between cH2-p1 and native Fgn. All above results suggest that the candidate peptide cH2-p1 can specifically bind to carbamylated protein and recognize only homocitrulline residues as the main target.

The peptide, cH2p1, was immobilized so as to investigate the possibility of using this ligand for selective binding and removal of cHSA. A p(HEMA) coating was formed, and the peptide cH2p1 was tethered to the polymer film through either C terminal (NH-cH2p1) or N terminal (CO-cH2p1) binding. To investigate the surface binding carbamylated and

native HSA or carbamylated and native Fgn were labeled with radioactive ^{125}I. Both cH2-p1 functionalized surfaces show selective binding features towards cHSA and cFgn, compared to their native protein form, with NH-cH2p1 of superior selectivity than CO-cH2p1. Both surfaces also show a high carbamylated protein binding ability in diluted plasma, with an ultralow Fgn adsorption observed for NH-cH2p1.

The results of the study suggest that the candidate peptide cH2-p1 immobilized p(HEMA) surface had specific affinity to carbamylated cHSA. The potential of the proof-of-concept surface platform shown in this work makes it possible to build adsorbent materials based on surface immobilized peptide ligands for removing carbamylated proteins from CKD patients and benefit hemodialysis treatment.

Preface

This thesis is an original work by Yuhao Ma. Contents in Chapter 2 has been submitted to *Microporous and Mesoporous Materials* as a review paper for review; works in Chapter 3 has been submitted to *Colloids and Surfaces B: Biointerfaces* for review; works in Chapter 4 has been accepted by *ACS Omega*.

Acknowledgements

I would like to give my sincere thanks and respects to Dr. Larry Unsworth as my supervisor. I would thank him for choosing me to undertake this exciting research program, guiding me to explore in the world of biomaterials with his knowledge, experience and brilliance. I could not have these ideas of reasearch and achieved so much without his supervision. Also I should thank a lot to Dr. Doschak, for providing all the radiolabeling facilities and guiding me a lot in radiolabeling research. It would be much more difficult without all these help.

For my work, it would be impossible to finish my study without the assitance of the following technicians. I need to give thanks to Bradley Smith for providing me techniques in SI-ATRP, Rajesh Pillai in help gold sputtering, Khalid Azyat in teaching me organic synthesis, Zhimin Yan in training me to use NMR for T_2 relaxation. Also, I would thank Ravichandran Kollarigowda and Shuhui Li for their contribution in my paper writings.

I cannot go so far without the help from my group members. Here I shall thank Abdullah Alshememry and Markian Bahniuk in their help in SDS-PAGE, Mehdi Ghaffari Sharaf in phage display, Shuhui Li in ITC, Kosala Waduthanthri in lab organization and Shanna Banman in lab safety. Also, I want to thank NINT and Nanofab staff members for their kindly support.

Finally, I would like to give my deepest gratitude to my mom and dad for raising me and giving me so much. Also, for my wife who has spent all these time with me, I owe her a heartfelt gratitude.

Table of Contents

List of Tables

List of Figures

Chapter 1: Introduction

1.1 Protein bound uremic toxins

1.1.1 Health issues caused by protein bound uremic toxins

Uremic toxins are waste products formed during metabolism that are usually removed by healthy kidneys, but could become toxic upon accumulation in the blood due to kidney failure. As chronic kidney disease (CKD) develops, further complications may be induced by these retained toxins, including cardiovascular diseases, bone weakening, anemia, nervous system damage, decreased immune response, pericarditis and pregnancy complications. They could be any biologically active compounds including urea, amino acids derivates, salts and impaired biomacromolecules. Around 150 solutes have been identified that accumulate within the blood compartment as kidney disease develops and are commonly referred to as uremic toxins [1]. These toxins have a diverse molecular weight range from 60 (i.e. urea) to 32,000 Da (i.e. IL-1) [1]. Toxin concentrations (C_U) may vary a lot, and be quite different than that found within the population of people with normal kidney function (C_N). Uremic toxins with the highest concentrations include urea, uric acid, creatine, creatinine, myoinositol, retinol-binding protein, Ig light chain [2]. Uremic toxins with the highest C_U/C_N ratio include Guanidinosuccinic acid, Methylguanidine, Indoxyl sulfate, Indole-3-acetic acid, Hippuric acid, 1-methylinosine and p-cresol. A majority of them have small molecular weight (MW < 500 Da), with the property of small size and hydrophilic, these toxins are easy to pass through dialysis membrane to be removed [1]. Middle-sized toxins have a MW > 500 Da and require large pore membranes (high flux dialysis) to achieve any clearance, but often result in only a limited removal rate. The remaining toxins have a high molecular weight range from 0.5

to 60 kDa and are featured by protein-bound toxins that are unable to be removed using only dialysis techniques because (i) they have a strong binding affinity to much larger sized protein and (ii) membranes cannot discriminate between native proteins and modified ones [3]. Uremic toxins can bind to proteins through covalent bonding, as in the case of carbamylated proteins that lysines were chemically modified by isocyanate [4]. Also, they can be trapped physically into protein molecules, like indoxyl sulfate that bound inside albumin through physical linking.

Recent work suggests that the presence of uremic toxins bound to proteins (i.e.. covalent or physical) may contribute to the uremic syndrome: high levels of albumin covalently altered through carbamylation are strongly and independently associated with cardiac damage, congestive heart failure, and sudden cardiac death [4]. Physically incorporated indoxyl sulfate with albumin in patients with renal dysfunction has been associated with renal scarring and chronic renal failure [5].

1.1.2 Limitation of current techniques to remove protein bound uremic toxins

Although being the most effective technique to sustain life for uremic patients, modern hemodialysis still has significant limitations. First, the average costs per patient is as high as $120,000 per year and could be significantly higher when complications occur. Second, it is associated with high rates of mortality. For instance, the average life expectancy of a person on hemodialysis is less than 3 years [6]. Hemodialysis treatment severely reduces patient quality of life. This situation has not been improved significantly for the last 30 years, yet hemodialysis technology has had very little improvements over this period. To overcome barriers that restrict improvement of hemodialysis, it is important to determine

the substances that accumulated due to kidney failure and identify their role in symptoms and complications caused by kidney failure. Being lack of knowledge of these substances on their molecular weight, structure, charge and extent of protein binding, advancement of strategy to remove them was greatly hampered.

Since hemodialysis works solely by controlling diffusion through pore size, it has only a limited clearance rate for middle molecules and even worse for protein bound uremic toxins. Therefore, membrane-based purification techniques are not able to differentiate between native and toxin bound proteins, that is, it is nearly impossible to remove selectively these modified proteins without removing normal proteins.

The two most studied protein bound toxin models for evaluating adsorbent are indoxyl sulfate (IS) and p-cresyl sulfate, and they have been shown to play a prominent role in the progression of CKD [5, 7, 8]. IS in the body is synthesized as the final metabolite of tryptophan [9]. As a uremic toxin, pathophysiologic effects of IS include an increase in renal oxidative stress (ROS), a release of endothelial microparticles into endothelium system, and an increase of the fibrosis and angiotensinogen expression in the kidney. p-cresyl sulfate is the main conjugate form (>95%) of p-cresol circulating *in vivo* [10, 11]. p-cresol is metabolized through conjugation, mainly sulphation and glucuronidation [12, 13]. Studies have identified the contribution of p-cresyl sulfate to CKD related insulin resistance [14] and p-cresyl sulfate also causes renal tubular cell damage by inducing oxidative stress [15]. For both IS and p-cresyl sulfate, albumin was found to be the main binding protein and the clearance of IS and p-cresyl sulfate through hemodialysis is limited. For instance, up to 90 % of IS in the blood compartment can bind reversibly to albumin with a dissociation constant of 13.2 μM [16-18]. This binding by albumin renders the majority of indoxyl sulfate effectively inaccessible to be removed by traditional

hemodialysis. Even unbound indoxyl sulfate within the blood is hard to remove from the blood compartment using either conventional or high flux dialysis techniques [19, 20], [21]. The ineffective removal of middle and protein bound toxins by hemodialysis motivates studies of other blood clearance techniques, and adsorbent based removal might be the one with the greatest potential.

1.2 Risks of carbamylated proteins

1.2.1 Chemistry of carbamylation

Carbamylation (a.k.a carbamoylation) is the reaction of primary amines or sulfhydryl groups with isocyanate to form carbamyl (carbamoyl) group (R-C=O-NH_2) (Figure 1-1). As a post-translational modification, protein carbamylation irreversibly occurs as a result of *in vivo* urea degradation [22]. The chemistry for carbamylation has been discussed in the literature as early as the 1960s [23-25]. Isocyanic acid is a natural decomposition product of urea that is in equilibrium with urea [26]. Increased urea concentration leads to increased isocyanic acid concentration, which further increases their propensity to react with N-terminal or ε-amino groups in proteins. Generally, terminal amino groups react faster than ε-amino groups due to a lower pKa, and the reaction can be accelerated in acidic pH. For carbamylation of α-crystallins, it was determined that lysines at different locations have different rate constant of carbamylation [27]. Similarly, carbamylation of HSA was found not equal for all lysines, whereby two specific lysines had a higher extent of carbamylation than others through both *in vitro* and *in vivo* carbamylation [28]. It has been suggested that the carbamylation reactivity of ε-amino group was determined by both the solvent accessibility and pK_a value upon protonation [27]. Besides the susceptibility of NH_2 in lysine or guanidine, other protein groups such as reduced thiols are also targets for carbamylation [29].

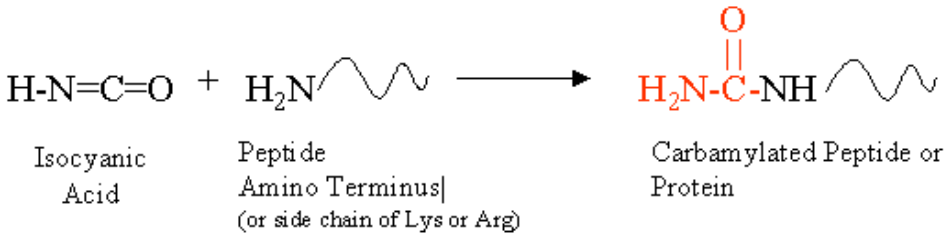

Figure 1-1 Protein carbamylation reaction, as illustrated using the terminal amine group.

1.2.2 Effects of carbamylation on proteins

In general, it has been established that carbamylation largely consumes positively charged primary amines of lysine and forms carbamyl groups to give uncharged homocitrulline [30]. For example, isoelectric focusing (IEF) of αA-crystallin exhibited a gradual shift toward a lower pH as a function of the average number of carbamylated lysines (1.2~2.7 per molecule) [23]. That said, however, this may have great implications on protein function. Slightly carbamylated collagen shows distinct changes in the packing distance of the collagen fibers and changes in the environment surrounding the lysine side chains; although the triple helix conformation was conserved and no denaturation of the secondary structure was observed. Further experiments suggest that carbamylated type I collagen was not able to polymerize into normal fibrils [31]. When incubated with potassium cyanate, bovine serum albumin (BSA) exhibited a slight increase in Stoke's radius from 3.51 to 3.96 nm [32]. Additionally, the carbamylation of crystallin resulted in exposed thiol groups that become oxidized or more reactive with other thiol groups, rendering it an aggregation center for cataract progression [33]. It has been suggested carbamylated albumin may cause enhanced tubular cell damage and promote peritubular fibrosis [34]. Also for rheumatoid arthritis (RA) patients, carbamylation had an adverse impact by triggering autoimmune

response [35].

However, the implications of carbamylation and human health outcomes are just now being explored. Briefly, this modification may cause structural changes and loss of functions for affected proteins. Carbamylation of proteins has been linked to an increasing number of diseases, including cataract formation, enhanced extracellular degradation, reduced enzymatic activity, rheumatoid arthritis, athlerosclerosis, and some misfolded protein diseases [36]. In particular, attention on carbamylation of albumin has shown that both extent of carbamylation and concentration of carbamylated albumin are associated with significantly elevated risk of all-cause mortality and has been proposed as a potential biomarker of cardiovascular disease (CVD) risk [37].

1.3 Antibody mimic peptide by phage display for selective protein binding

1.3.1 Principle of phage display and M13 phage library

Bacteriophages (a.k.a. phage) are bacterial viruses used extensively for biopanning studies to identify small peptide fragments that can bind many types of surfaces or molecules with antibody-like affinities, as summarized elsewhere [38-40]. Phage display has advantages in its simplicity of use, high target yield, large and diverse initial library, and low cost and has been applied for determining targets specific to peptide, proteins, and antibodies [41, 42]. During a typical phage display process, the first step is to prepare the library containing a large number of phage clones with unique peptide or proteins displayed on its surface. Then the library is introduced to targets immobilized on certain substrate (plate, beads) and

incubated to allow for phage-target specific interactions. Phage bound to the targets of choice are captured, amplified (i.e. grown up) with bacteria, and DNA sequenced to confirm retained consensus sequences that are enriched upon further rounds of biopanning. Candidate phages are characterized using enzyme-linked immunosorbent assay (ELISA) to verify binding affinities, there DNA sequenced to identify the surface-displayed peptide motif.

Numerous types of phages have been used for phage display, such as filamentous M13, T7, bacteriophage lambda (λ phage), and T4 phage. M13 (Figure 1-2) are the focus of the work presented herein and has one circular ssDNA of 6407 nucleotides encapsulated within five types of coat proteins (PVIII, PIX, PVII,PVI, PIII). The ssDNA encodes ~ 2700-3000 copies of the coat protein PVIII, five copies of the other four types of proteins located at the terminal. Although the M13 is not lytic to its host, a decreased growth has been noted for its infected hosts. Based on the fusion position, a peptide library can be inserted into two coat proteins (PIII and PVIII). In PVIII library thousands of copies can be displayed on the side wall. In PIII library, only five copies of peptides are displayed at the tip of phage. The limitation of PVIII library lies in that large fusion proteins would influence its host infection capability due to increased steric hinderance, the PIII library allows for large protein fusion without getting its infection ability affected. Still there are problems to display cytoplasmic proteins on M13 phages, and only peptides or proteins with the cell membrane penetration ability can be displayed with corrected conformations [43].

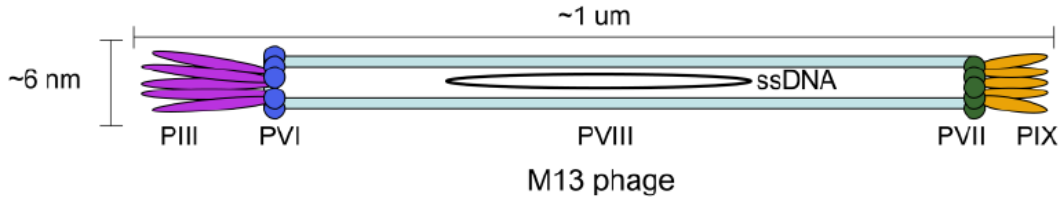

M13 phage

Figure 1-2 The structure of M13 phage

1.3.2 Application of filamentous phage display in identifying highly specific binding peptide

M13 phage display has been based on the construction of a variety of library types, including an antibody library [44], peptide library [41], and even protein library with segments of interests as variants [45]. The peptide library has been used to search for ligands to receptors with significant medical roles like erythropoietin [46]. Peptide library was also used for targeting tumor-associated vasculature [47]. Antibody phage library has been used for identifying therapeutic antibody against certain antigens [48].

For specific protein binding, phage displayed has been used as a tool to search for peptide targeting various proteins. Albumin binding peptides with the core sequence DICLPRWGCLW has been identified from phage display serum albumin against multiple species [49], and the cross-binding of peptide to albumin from different species has been observed. No cross-binding was observed for ovalbumin. Streptavidin has been widely used for bind biotinylated targets, and the streptavidin binding peptides have been selected using phage display with the biotin mimic motif, HPQ, at different locations within the peptide sequence [50]. Besides that, other plasma proteins such as IgG [51], fibrinogen [52] and fibrin [53] have been used as targets in phage display to determine its high affinitive binding peptide.

1.3.3 Polyclonal antibody against carbamylated albumin: comparison to phage display derived peptides

Antibodies have been widely prepared through hybridoma techniques, which involves a costly and complicated preparation process that includes animal immunization and hybridoma cell culture, with only limited yield and poor repeatability [54]. In comparison, phage display techniques allow for antibody-like peptide generation with an easier procedure and a larger scale of production [39]. Besides costs of construction and determination, small peptides can be immobilized on surfaces with both a higher density as well as with a controlled orientation compared to antibodies. In addition, small peptides may have a higher stability within complex media (like blood), making them suitable for long term applications such as sensor surfaces or substrates for adsorption [43]. Antibodies against carbamylated protein have been identified [55] and the monoclonal antibody prepared by way of hybridoma [56, 57], proving that it is possible to target carbamylated proteins. Hitherto, no peptide has been identified for carbamylated protein, not even any sequence of antibody for homocitrulline containing protein has been reported to our best knowledge.

1.4 Peptide modified surface for binding target proteins

1.4.1 Protein non-specific adsorption on biomaterial surface

Proteins play the most important role in operation of living organisms. To do so, most proteins fold to a globular shape, in order to realize their biological functions. The folded conformations were generally 5 to 10 kcal/mol more stable than unfolded, biologically

inactive conformations under physiological conditions [58]. Several forces are known involved in maintaining the folded structure including Electrostatic forces, Van der Waals forces, hydrogen bonding, and hydrophobic effect. The entropy driven hydrophobic effect was considered to be the dominant force in maintaining the fold structure, as it minimized the energetically unfavorable interaction between non-polar moieties of protein and water molecules while keeping the nonpolar interactions within its structure. Even though, the thermodynamically unfavorable interaction between non-polar part and water still exist, known as clathrate hydrate, or clathrate cage. Once a protein reaches a surface capable of forming non-polar interactions. The hydrophobic effect will force the protein to refold and attach its non-polar part to adsorb to surface in order to gain entropy and further avoid the formation of clathrate structure [59]. Therefore, in many cases protein adsorption is energetically more favorable than self-folding.

Prevention of protein adsorption, or biofouling, has remained great challenges in many fields of applications. Marine biofouling is a worldwide problem. The marine organism adhesion on ship hull greatly increases its surface roughness and creates more drags while ship body moves through water to waste a lot of fuel consumptions [60]. For biosensors sensitive to changes on surface, nonspecific protein adsorption may degrades its performance or even disables its function. For biomaterials used *in vivo*, protein adsorption and biofouling are not favored in many cases. Biomaterials prepared in non-sterile environment is susceptible to bacteria adhesion, which may induce problem such as chronic inflammation, tissue, necrosis, or even septicemia [61]. For degradable materials for drug release, protein adsorption may cause inconsistent release profile [62]. For blood contacting biomaterials, even a small amount of protein adsorption could be damaging. It was found that only 5 ng/cm^2 of fibrinogen is sufficient to enable platelet adhesion and subsequent coagulation events [63], and this would set a very high standards on maximum

protein adsorption for hemocompatible materials.

1.4.2 Non-fouling polymer brushes to minimize protein non-specific adsorption

Current studies have shown that for both polyhydrophilic and polyzwitterionic brushes, the nonfouling properties against protein adsorption is due to formation of a hydration layer on the surface. It was thought that a tightly bound water layer surrounding the polymer brushes serve as an energetic barrier to prevent protein adsorption on the underlying surface [64].

Poly(ethylene glycol) (PEG) has been widely used as nonfouling polymers [65]. Despite its good nonfouling performance, question arises when it's exposed to environment with oxygen and transition-metal, as presence in many solutions used biomedically. PEG may undergo oxidation to break its chain and get the brush structure damaged in these cases [65-67]. Other hydrophilic materials such as tetraglyme [68], dextran[69], mannitol [67] and glycerol dendron [70] and poly(hydroxy-functional methacrylates) (pHEMA) [71] can be surface hydrated through hydrogen bonding. In comparison, zwitterionic polymers such as 2-methacryloyloxyethyl phosphorylcholine, poly(sulfobetaine methacrylate) [72, 73] and poly(carboxybetaine methacrylate) [74] were hydrated through ionic interactions with water molecules.

1.4.3 Surface modification for immobilization of bioactive molecules on non-fouling polymer film

With the ability to prevent non-specific protein adsorption, nonfouling surface has the potential to be bioactive by immobilization of bioactive molecules. This is usually done through covalent binding through functional groups with bioactive molecules. The functional group could be -NH_2, -COOH, -NHS, -OH, which allows for easy conjugation with bioactive molecules through different chemistry. To achieve an effective hydration layer for nonfouling, a high grafting density of polymer brushes is usually required. Compared to "graft-to" method by which polymer chains were anchored to the surface directly, "graft-from" method immobilize the initiator molecules firstly on surface and then enable the polymerization based on surface. A high packing density of brush is usually achieved through "graft-from" method, since the steric hinderance in "graft-to" method often limit the immobilization of polymers in close distance. Also "graft-from" method allow for better control of the brush thickness and structure [75]. Several controlled surface-initiated polymerization techniques have been developed for the preparation of surface brushes, including atom-transfer radical polymerization (ATRP) [76, 77], reversible addition–fragmentation chain-transfer (RAFT) polymerization [78], and nitroxide-mediated polymerization (NMP) [79]. Also this technique has been developed for immobilization of initiators on various substrate, including silicon [80, 81], gold [82, 83], silica [84-87], mica [88, 89], graphene [90, 91], cellulose [92], nanofibers [93], and polymers [94-96].

One important feature of polymer brush is the grafting density, or number of chains per area. If grafted with high density, the polymer chains tend to extend more and form "brush"

regime. On contrary if grafted with low density, the polymer chains tend to form coils and isolated from each other, as in the form of “mushroom” regime. The boundary between “mushroom” and “brush” regime depends on the structure of monomers, solvent, and underlying substrate [97, 98]. Another feature characterizing polymer brush is the thickness. The thickness of polymer brush layer can vary in a large range as the parameters for polymerization changes. Controlled surface-initiated polymerization allows for precise control of thickness within nanometers. Studies have been performed on the nonfouling performance of polymer brush layer with varied thickness [71].

The application of nonfouling, bioactive surfaces has included, but is not limited to, areas like biosensors [99], affinity chromatography [100], protein purification, anticoagulation [101], cell proliferation and differentiation [102, 103], gene and drug delivery [104-106], antibiofouling [107]. Our particular interest is the selective protein binding by bioactive molecules located on a nonfouling surface. Due to the extremely high association constant, streptavidin/biotin binding has been extensively used for functionalization of nonfouling polymer brushes [108-110]. Streptavidin has been covalently immobilized through various coupling agents such as succinic anhydride, pentafluoropyridine, 3-chloropropionaldehyde diethylacetal, nitrophenyl chloroformate, tresyl chloride and disuccinimidyl carbonate (DSC), with DSC found to be the most efficient one for capturing streptavidin [108]. Likewise, biotin was immobilized onto pOEGMA film through click chemistry, and its specific recognition of streptavidin was demonstrated [110]. Another type of bioactive molecules immobilized for protein binding is antibodies. Various polymer brushes have been functionalized with antibodies for protein sensing [111, 112].

Immobilization of bioactive molecules have also been found to influence the nonfouling properties of polymer brush. Among three typical nonfouling platform, poly(2-

hydroxyethyl methacrylate) (pHEMA), carboxy-functional poly(carboxybetaine acrylamide) (pCBAA), and a standard OEG-based carboxy-functional alkanethiolate self-assembled monolayer (AT-SAM), it was found only pCBAA maintained the overall fouling resistance after anti-E.coli and anti-Salm immobilization through EDC/NHS chemistry [113], and it was suggested the increased fouling was possibly due to film property change. To improve the loading capacity of the polymer brushes, one strategy is to introduce a secondary layer of polymer brush grown by partial deactivation of terminal bromine group of the first layer, and it was shown an increased amount of immobilized antibody was achieved, and an improved antigen detecting sensitivity was resulted [114].

1.5 Research objective

With the purpose of selective removal of carbamylated protein, the key part of the project is to identify carbamylation specific peptide, with specificity to carbamylated HSA. Phage display library is to be used to search for carbamylated protein binding peptides. Before phage display work, a comprehensive study of effect of carbamylation on protein structure and properties is to be performed, in order for a better understanding of the carbamylation process and verify feasibility of the subsequent work. After the carbamylation specific peptide been identified, immobilization of the candidate peptides on surface will be studied on nonfouling polymer film. Once peptide been successfully immobilized and the nonfouling performance been verified, the surface will be put into test for adsorption of carbamylated protein, with the native uncarbamylated protein as a comparison, to study the effectiveness of resulting adsorbent surface.

Phage-derived peptides will have similar affinities as antibodies, should be relatively cheap to express. It is hypothesized that cost effective interfaces that specifically bind these

carbamylated protein can be formed through the combination of non-fouling polymers and peptide identified using phage display techniques. It is thought that through surface engineering of a film using peptides, these specific proteins can be selectively bound and removed from the blood during dialysis.

1.6 Scope of the Thesis

The thesis includes six chapters. The scope for each chapter is listed below:

Chapter 1 is the introduction of thesis, including backgrounds on protein bound uremic toxins, phage displayed peptides, and nonfouling bioactive surface. The research objective and significance of thesis are also given in this chapter.

Chapter 2 introduces the current adsorbent materials that have been used for removal of uremic toxins, including activated carbon, zeolite, mesoporous silica and polymers, etc. Clinical applications of several adsorbents for CKD treatment are introduced. For this chapter my group member Shuhui Li made some contributions in reference data search and writings.

Chapter 3 focuses on the characterization of carbamylated proteins. Changes in charge, tertiary structure and water bound states have been identified for carbamylated proteins. Adsorption of carabamylated proteins is studied on several model SAM surfaces. For this chapter my group member Dr. Abdullah Alshememry made some contributions in SDS-PAGE, and Dr. Ravichandran Kollarigowda made some contributions in writings.

Chapter 4 works on searching for carbamylation specific peptide through phage display. Candidate peptides are identified from biopanning against cHSA, and their binding affinity towards carbamylated proteins are tested. For the peptide (cH2-p1) showing preferrable binding towards carbamylated HSA and carbamylated Fgn over their native forms, the binding mechanism is studied through molecular docking of homocitrulline residues with

the cH2-p1. For this chapter my group member Shuhui Li made some contributions in collecting ITC data, and my group member Dr. Mehdi Ghaffari Sharaf made some contributions in phage display work.

Chapter 5 works on preparation of p(HEMA) brushes bound with candidate peptide, cH2-p1. In addition to characterization of polymer film, the nonfouling performance is also tested. Immobilization of cH2-p1 is done through both C-terminal and N-terminal coupling. Adsorption of carbamylated HSA and carbamylated Fgn is done on p(HEMA) surface bound with candidate peptide through radiolabeling. Competitive adsorption between carbamylated and native protein in PBS and diluted plasma is done to explore the potential of the model surface to capture carbamylated proteins. For this chapter Dr. Khalid Azyat made some contributions in synthesis of initiator for SI-ATRP.

Chapter 6 presents the conclusion of thesis, with the limitation and implication discussed. Future works and perspectives of the research are also suggested.

1.7 References

[1] R. Vanholder, R. De Smet, G. Glorieux, A. Argiles, U. Baurmeister, P. Brunet, W. Clark, G. Cohen, P.P. De Deyn, R. Deppisch, B. Descamps-Latscha, T. Henle, A. Jorres, H.D. Lemke, Z.A. Massy, J. Passlick-Deetjen, M. Rodriguez, B. Stegmayr, P. Stenvinkel, C. Tetta, C. Wanner, W. Zidek, E. Grp, Review on uremic toxins: Classification, concentration, and interindividual variability, Kidney international 63(5) (2003) 1934-1943.

[2] R. Vanholder, R. De Smet, G. Glorieux, A. Argiles, U. Baurmeister, P. Brunet, W. Clark, G. Cohen, P.P. De Deyn, R. Deppisch, B. Descamps-Latscha, T. Henle, A. Jorres, H.D. Lemke, Z.A. Massy, J. Passlick-Deetjen, M. Rodriguez, B. Stegmayr, P. Stenvinkel, C. Tetta, C. Wanner, W. Zidek, G. European Uremic Toxin Work, Review on uremic toxins: classification, concentration, and interindividual variability, Kidney Int 63(5) (2003) 1934-43.

[3] H.A. Mutsaers, E.G. Stribos, G. Glorieux, R. Vanholder, P. Olinga, Chronic kidney disease and fibrosis: the role of uremic retention solutes, Frontiers in medicine 2 (2015) 60.

[4] C. Drechsler, S. Kalim, J.B. Wenger, P. Suntharalingam, T. Hod, R.I. Thadhani, S.A. Karumanchi, C. Wanner, A.H. Berg, Protein carbamylation is associated with heart failure and mortality in diabetic patients with end-stage renal disease, Kidney international 87(6) (2015) 1201-1208.

[5] R. Vanholder, E. Schepers, A. Pletinck, E.V. Nagler, G. Glorieux, The Uremic Toxicity of Indoxyl Sulfate and p-Cresyl Sulfate: A Systematic Review, Journal of the American Society of Nephrology 25(9) (2014) 1897-1907.

[6] J.B. Stokes, Consequences of frequent hemodialysis: comparison to conventional hemodialysis and transplantation, Trans Am Clin Climatol Assoc 122 (2011) 124-36.

[7] S. Liabeuf, T.B. Drueke, Z.A. Massy, Protein-Bound Uremic Toxins: New Insight from Clinical Studies, Toxins 3(7) (2011) 911-919.

[8] L. Dou, E. Bertrand, C. Cerini, V. Faure, J. Sampol, R. Vanholder, Y. Berland, P. Brunet, The uremic solutes p-cresol and indoxyl sulfate inhibit endothelial proliferation and wound repair, Kidney international 65(2) (2004) 442-451.

[9] S.C. Leong, T.L. Sirich, Indoxyl sulfate—review of toxicity and therapeutic strategies, Toxins 8(12) (2016) 358.

[10] A.W. Martinez, N.S. Recht, T.H. Hostetter, T.W. Meyer, Removal of p-cresol sulfate by hemodialysis, Journal of the American Society of Nephrology 16(11) (2005) 3430-3436.

[11] H. de Loor, B. Bammens, P. Evenepoel, V. De Preter, K. Verbeke, Gas chromatographic-mass spectrometric analysis for measurement of p-cresol and its conjugated metabolites in uremic and normal serum, Clinical chemistry 51(8) (2005) 1535-1538.

[12] T. Niwa, K. Maeda, T. Ohki, A. Saito, K. Kobayashi, A gas chromatographic-mass spectrometric analysis for phenols in uremic serum, Clinica chimica acta; international journal of clinical chemistry 110(1) (1981) 51-57.

[13] N. Ogata, N. Matsushima, T. Shibata, Pharmacokinetics of wood creosote: glucuronic acid and sulfate

conjugation of phenolic compounds, Pharmacology 51(3) (1995) 195-204.
[14] L. Koppe, N.J. Pillon, R.E. Vella, M.L. Croze, C.C. Pelletier, S. Chambert, Z. Massy, G. Glorieux, R. Vanholder, Y. Dugenet, H.A. Soula, D. Fouque, C.O. Soulage, p-Cresyl Sulfate Promotes Insulin Resistance Associated with CKD, Journal of the American Society of Nephrology 24(1) (2013) 88-99.
[15] H. Watanabe, Y. Miyamoto, D. Honda, H. Tanaka, Q. Wu, M. Endo, T. Noguchi, D. Kadowaki, Y. Ishima, S. Kotani, M. Nakajima, K. Kataoka, S. Kim-Mitsuyama, M. Tanaka, M. Fukagawa, M. Otagiri, T. Maruyama, p-Cresyl sulfate causes renal tubular cell damage by inducing oxidative stress by activation of NADPH oxidase, Kidney international 83(4) (2013) 582-592.
[16] T. Niwa, Uremic Toxicity of Indoxyl Sulfate, Nagoya journal of medical science 72(1-2) (2010) 1-11.
[17] L. Viaene, P. Annaert, H. de Loor, R. Poesen, P. Evenepoel, B. Meijers, Albumin is the main plasma binding protein for indoxyl sulfate and p-cresyl sulfate, Biopharmaceutics & drug disposition 34(3) (2013) 165-75.
[18] E. Devine, D.H. Krieter, M. Ruth, J. Jankovski, H.D. Lemke, Binding Affinity and Capacity for the Uremic Toxin Indoxyl Sulfate, Toxins 6(2) (2014) 416-429.
[19] A. Dhondt, R. Vanholder, W. Van Biesen, N. Lameire, The removal of uremic toxins, Kidney international 58 (2000) S47-S59.
[20] A. Enomoto, M. Takeda, A. Tojo, T. Sekine, S.H. Cha, S. Khamdang, F. Takayama, I. Aoyama, S. Nakamura, H. Endou, T. Niwa, Role of organic anion transporters in the tubular transport of indoxyl sulfate and the induction of its nephrotoxicity, Journal of the American Society of Nephrology 13(7) (2002).
[21] T. Niwa, Removal of Protein-Bound Uraemic Toxins by Haemodialysis, Blood purification 35 (2013) 20-25.
[22] C.M. Balion, T.F. Draisey, R.J. Thibert, Carbamylated hemoglobin and carbamylated plasma protein in hemodialyzed patients, Kidney international 53(2) (1998) 488-495.
[23] W. Qin, J.B. Smith, D.L. Smith, Rates of Carbamylation of Specific Lysyl Residues in Bovine Alpha-Crystallins, Journal of Biological Chemistry 267(36) (1992) 26128-26133.
[24] S.S. Sun, J.Y. Zhou, W.M. Yang, H. Zhang, Inhibition of protein carbamylation in urea solution using ammonium-containing buffers, Analytical biochemistry 446 (2014) 76-81.
[25] P.M. Angel, R. Orlando, Quantitative carbamylation as a stable isotopic labeling method for comparative proteomics, Rapid Commun Mass Sp 21(10) (2007) 1623-1634.
[26] J.J.T. Gerding, A. Koppers, P. Hagel, H. Bloemendal, Cyanate Formation in Solutions of Urea .I. Effect of Urea on Eye Lens Protein Alpha-Crystallin, Biochimica et biophysica acta 243(3) (1971) 374-+.
[27] W. Qin, J.B. Smith, D.L. Smith, Rates of carbamylation of specific lysyl residues in bovine alpha-crystallins, The Journal of biological chemistry 267(36) (1992) 26128-33.
[28] A.H. Berg, C. Drechsler, J. Wenger, R. Buccafusca, T. Hod, S. Kalim, W. Ramma, S.M. Parikh, H. Steen, D.J. Friedman, J. Danziger, C. Wanner, R. Thadhani, S.A. Karumanchi, Carbamylation of Serum Albumin as a Risk Factor for Mortality in Patients with Kidney Failure, Science translational medicine 5(175) (2013).
[29] G.R. Stark, [53] Modification of proteins with cyanate, Methods in enzymology 25 (1972) 579-84.
[30] L. Gorissea, C. Pietrement, V. Vuiblet, C.E.H. Schmelzer, M. Kohler, L. Duca, L. Debelle, P. Fornes,

S. Jaisson, P. Gillery, Protein carbamylation is a hallmark of aging, Proceedings of the National Academy of Sciences of the United States of America 113(5) (2016) 1191-1196.
[31] S. Jaisson, S. Lorimier, S. Ricard-Blum, G.D. Sockalingum, C. Delevallee-Forte, G. Kegelaer, M. Manfait, R. Garnotel, P. Gillery, Impact of carbamylation on type I collagen conformational structure and its ability to activate human polymorphonuclear neutrophils, Chem Biol 13(2) (2006) 149-159.
[32] K.M. Fazili, M.M. Mir, M.A. Qasim, Changes in Protein Stability Upon Chemical Modification of Lysine Residues of Bovine Serum-Albumin by Different Reagents, Biochem Mol Biol Int 31(5) (1993) 807-816.
[33] H.T. Beswick, J.J. Harding, High-Molecular-Weight Crystallin Aggregate Formation Resulting from Nonenzymatic Carbamylation of Lens Crystallins - Relevance to Cataract Formation, Experimental eye research 45(4) (1987) 569-578.
[34] M.-L.P. Gross, G. Piecha, A. Bierhaus, W. Hanke, T. Henle, P. Schirmacher, E. Ritz, Glycated and carbamylated albumin is more" nephrotoxic" than unmodified albumin in the amphibian kidney, American Journal of Physiology-Heart and Circulatory Physiology (2011).
[35] J. Shi, P.A. van Veelen, M. Mahler, G.M.C. Janssen, J.W. Drijfhout, T.W.J. Huizinga, R.E.M. Toes, L.A. Trouw, Carbamylation and antibodies against carbamylated proteins in autoimmunity and other pathologies, Autoimmunity reviews 13(3) (2014) 225-230.
[36] F.H. Verbrugge, W.H.W. Tang, S.L. Hazen, Protein carbamylation and cardiovascular disease, Kidney international 88(3) (2015) 474-478.
[37] B.G. Stegmayr, New insight in impaired binding capacity for albumin in uraemic patients, Acta Physiol 215(1) (2015) 5-8.
[38] B.P. Gray, K.C. Brown, Combinatorial Peptide Libraries: Mining for Cell-Binding Peptides, Chemical reviews 114(2) (2014) 1020-1081.
[39] J. Pande, M.M. Szewczyk, A.K. Grover, Phage display: Concept, innovations, applications and future, Biotechnol Adv 28(6) (2010) 849-858.
[40] G.P. Smith, V.A. Petrenko, Phage display, Chemical reviews 97(2) (1997) 391-410.
[41] J.K. Scott, G.P. Smith, Searching for Peptide Ligands with an Epitope Library, Science 249(4967) (1990) 386-390.
[42] J. Mccafferty, A.D. Griffiths, G. Winter, D.J. Chiswell, Phage Antibodies - Filamentous Phage Displaying Antibody Variable Domains, Nature 348(6301) (1990) 552-554.
[43] Y.Y. Tan, T. Tian, W.L. Liu, Z. Zhu, C.Y.J. Yang, Advance in phage display technology for bioanalysis, Biotechnology journal 11(6) (2016) 732-745.
[44] C.F. Barbas, A.S. Kang, R.A. Lerner, S.J. Benkovic, Assembly of Combinatorial Antibody Libraries on Phage Surfaces - the Gene-Iii Site, Proceedings of the National Academy of Sciences of the United States of America 88(18) (1991) 7978-7982.
[45] H.B. Lowman, S.H. Bass, N. Simpson, J.A. Wells, Selecting High-Affinity Binding-Proteins by Monovalent Phage Display, Biochemistry 30(45) (1991) 10832-10838.
[46] N.C. Wrighton, F.X. Farrell, R. Chang, A.K. Kashyap, F.P. Barbone, L.S. Mulcahy, D.L. Johnson, R.W. Barrett, L.K. Jolliffe, W.J. Dower, Small peptides as potent mimetics of the protein hormone erythropoietin,

Science 273(5274) (1996) 458-463.
[47] W. Arap, R. Pasqualini, E. Ruoslahti, Cancer treatment by targeted drug delivery to tumor vasculature in a mouse model, Science 279(5349) (1998) 377-380.
[48] J. Andris-Widhopf, P. Steinberger, C.F. Barbas Iii, Bacteriophage Display of Combinatorial Antibody Libraries, eLS (2001).
[49] M.S. Dennis, M. Zhang, Y.G. Meng, M. Kadkhodayan, D. Kirchhofer, D. Combs, L.A. Damico, Albumin binding as a general strategy for improving the pharmacokinetics of proteins, Journal of Biological Chemistry 277(38) (2002) 35035-35043.
[50] L.B. Giebel, R. Cass, D.L. Milligan, D. Young, R. Arze, C.J.B. Johnson, Screening of cyclic peptide phage libraries identifies ligands that bind streptavidin with high affinities, 34(47) (1995) 15430-15435.
[51] M. Krook, K. Mosbach, O.J.J.o.i.m. Ramström, Novel peptides binding to the Fc-portion of immunoglobulins obtained from a combinatorial phage display peptide library, 221(1-2) (1998) 151-157.
[52] C. Heilmann, M. Herrmann, B.E. Kehrel, G.J.T.J.o.i.d. Peters, Platelet-binding domains in 2 fibrinogen-binding proteins of Staphylococcus aureus identified by phage display, 186(1) (2002) 32-39.
[53] A.F. Kolodziej, S.A. Nair, P. Graham, T.J. McMurry, R.C. Ladner, C. Wescott, D.J. Sexton, P.J.B.c. Caravan, Fibrin specific peptides derived by phage display: characterization of peptides and conjugates for imaging, 23(3) (2012) 548-556.
[54] F.W. Falkenberg, Monoclonal antibody production: problems and solutions, Res Immunol 149(6) (1998) 542-547.
[55] J. Shi, R. Knevel, P. Suwannalai, M.P. van der Linden, G.M.C. Janssen, P.A. van Veelen, N.E.W. Levarht, A.H.M. van der Helm-van Mil, A. Cerami, T.W.J. Huizinga, R.E.M. Toes, L.A. Trouw, Autoantibodies recognizing carbamylated proteins are present in sera of patients with rheumatoid arthritis and predict joint damage, Proceedings of the National Academy of Sciences of the United States of America 108(42) (2011) 17372-17377.
[56] J.S. Dekkers, M.K. Verheul, J.N. Stoop, B.S. Liu, A. Ioan-Facsinay, P.A. van Veelen, A.H. de Ru, G.M.C. Janssen, M. Hegen, S. Rapecki, T.W.J. Huizinga, L.A. Trouw, R.E.M. Toes, Breach of autoreactive B cell tolerance by post-translationally modified proteins, Annals of the rheumatic diseases 76(8) (2017) 1449-1457.
[57] S. Turunen, M.K. Koivula, L. Risteli, J. Risteli, Anticitrulline Antibodies Can Be Caused by Homocitrulline-Containing Proteins in Rabbits, Arthritis Rheum 62(11) (2010) 3345-3352.
[58] C.N. Pace, Conformational stability of globular proteins, Trends in biochemical sciences 15(1) (1990) 14-7.
[59] V. Hlady, J. Buijs, Protein adsorption on solid surfaces, Curr Opin Biotech 7(1) (1996) 72-77.
[60] M.E. Callow, J.A. Callow, Marine biofouling: a sticky problem, Biologist 49(1) (2002) 1-5.
[61] R.J.C. McLean, M. Whiteley, D.J. Stickler, W.C. Fuqua, Evidence of autoinducer activity in naturally occurring biofilms, FEMS microbiology letters 154(2) (1997) 259-263.
[62] G. Crotts, T.G. Park, Protein delivery from poly(lactic-co-glycolic acid) biodegradable microspheres: release kinetics and stability issues, Journal of microencapsulation 15(6) (1998) 699-713.
[63] W.B. Tsai, J.M. Grunkemeier, T.A. Horbett, Human plasma fibrinogen adsorption and platelet

adhesion to polystyrene, J Biomed Mater Res 44(2) (1999) 130-139.
[64] S. Herrwerth, W. Eck, S. Reinhardt, M. Grunze, Factors that determine the protein resistance of oligoether self-assembled monolayers - Internal hydrophilicity, terminal hydrophilicity, and lateral packing density, Journal of the American Chemical Society 125(31) (2003) 9359-9366.
[65] J.M. Harris, Introduction to biomedical and biotechnical applications of polyethylene glycol., Abstr Pap Am Chem S 213 (1997) 21-Poly.
[66] M.C. Shen, L. Martinson, M.S. Wagner, D.G. Castner, B.D. Ratner, T.A. Horbett, PEO-like plasma polymerized tetraglyme surface interactions with leukocytes and proteins: in vitro and in vivo studies, Journal of Biomaterials Science-Polymer Edition 13(4) (2002) 367-390.
[67] Y.Y. Luk, M. Kato, M. Mrksich, Self-assembled monolayers of alkanethiolates presenting mannitol groups are inert to protein adsorption and cell attachment, Langmuir 16(24) (2000) 9604-9608.
[68] M.C. Shen, M.S. Wagner, D.G. Castner, B.D. Ratner, T.A. Horbett, Multivariate surface analysis of plasma-deposited tetraglyme for reduction of protein adsorption and monocyte adhesion, Langmuir 19(5) (2003) 1692-1699.
[69] S. Martwiset, A.E. Koh, W. Chen, Nonfouling characteristics of dextran-containing surfaces, Langmuir 22(19) (2006) 8192-8196.
[70] M. Wyszogrodzka, R. Haag, Synthesis and Characterization of Glycerol Dendrons, Self-Assembled Monolayers on Gold: A Detailed Study of Their Protein Resistance, Biomacromolecules 10(5) (2009) 1043-1054.
[71] C. Zhao, L.Y. Li, Q.M. Wang, Q.M. Yu, J. Zheng, Effect of Film Thickness on the Antifouling Performance of Poly(hydroxy-functional methacrylates) Grafted Surfaces, Langmuir 27(8) (2011) 4906-4913.
[72] Z. Zhang, S.F. Chen, Y. Chang, S.Y. Jiang, Surface grafted sulfobetaine polymers via atom transfer radical polymerization as superlow fouling coatings, Journal of Physical Chemistry B 110(22) (2006) 10799-10804.
[73] G. Cheng, Z. Zhang, S.F. Chen, J.D. Bryers, S.Y. Jiang, Inhibition of bacterial adhesion and biofilm formation on zwitterionic surfaces, Biomaterials 28(29) (2007) 4192-4199.
[74] W. Yang, H. Xue, W. Li, J.L. Zhang, S.Y. Jiang, Pursuing "Zero" Protein Adsorption of Poly(carboxybetaine) from Undiluted Blood Serum and Plasma, Langmuir 25(19) (2009) 11911-11916.
[75] R. Barbey, L. Lavanant, D. Paripovic, N. Schuwer, C. Sugnaux, S. Tugulu, H.A. Klok, Polymer Brushes via Surface-Initiated Controlled Radical Polymerization: Synthesis, Characterization, Properties, and Applications, Chemical reviews 109(11) (2009) 5437-5527.
[76] K. Matyjaszewski, Atom Transfer Radical Polymerization (ATRP): Current Status and Future Perspectives, Macromolecules 45(10) (2012) 4015-4039.
[77] D.J. Siegwart, J.K. Oh, K. Matyjaszewski, ATRP in the design of functional materials for biomedical applications, Progress in Polymer Science 37(1) (2012) 18-37.
[78] G. Moad, E. Rizzardo, S.H. Thang, Radical addition-fragmentation chemistry in polymer synthesis, Polymer 49(5) (2008) 1079-1131.
[79] R.B. Grubbs, Nitroxide-Mediated Radical Polymerization: Limitations and Versatility, Polym Rev

51(2) (2011) 104-137.
[80] W. Feng, R.X. Chen, J.L. Brash, S.P. Zhu, Surface-initiated atom transfer radical polymerization of oligo(ethylene glycol) methacrylate: Effect of solvent on graft density, Macromolecular rapid communications 26(17) (2005) 1383-1388.
[81] A.A. Brown, N.S. Khan, L. Steinbock, W.T.S. Huck, Synthesis of oligo(ethylene glycol) methacrylate polymer brushes, Eur Polym J 41(8) (2005) 1757-1765.
[82] D.M. Jones, A.A. Brown, W.T.S. Huck, Surface-initiated polymerizations in aqueous media: Effect of initiator density, Langmuir 18(4) (2002) 1265-1269.
[83] C.D. Bain, E.B. Troughton, Y.T. Tao, J. Evall, G.M. Whitesides, R.G. Nuzzo, Formation of Monolayer Films by the Spontaneous Assembly of Organic Thiols from Solution onto Gold, Journal of the American Chemical Society 111(1) (1989) 321-335.
[84] C. Perruchot, M.A. Khan, A. Kamitsi, S.P. Armes, T. von Werne, T.E. Patten, Synthesis of well-defined, polymer-grafted silica particles by aqueous ATRP, Langmuir 17(15) (2001) 4479-4481.
[85] K. Ohno, T. Morinaga, K. Koh, Y. Tsujii, T. Fukuda, Synthesis of monodisperse silica particles coated with well-defined, high-density polymer brushes by surface-initiated atom transfer radical polymerization, Macromolecules 38(6) (2005) 2137-2142.
[86] C.L. Huang, T. Tassone, K. Woodberry, D. Sunday, D.L. Green, Impact of ATRP Initiator Spacer Length on Grafting Poly(methyl methacrylate) from Silica Nanoparticles, Langmuir 25(23) (2009) 13351-13360.
[87] H.W. Ma, D.J. Li, X. Sheng, B. Zhao, A. Chilkoti, Protein-resistant polymer coatings on silicon oxide by surface-initiated atom transfer radical polymerization, Langmuir 22(8) (2006) 3751-3756.
[88] B. Lego, M. Francois, W.G. Skene, S. Giasson, Polymer Brush Covalently Attached to OH-Functionalized Mica Surface via Surface-Initiated ATRP: Control of Grafting Density and Polymer Chain Length, Langmuir 25(9) (2009) 5313-5321.
[89] B. Lego, W.G. Skene, S. Giasson, Unprecedented covalently attached ATRP initiator onto OH-functionalized mica surfaces, Langmuir 24(2) (2008) 379-382.
[90] M. Steenackers, A.M. Gigler, N. Zhang, F. Deubel, M. Seifert, L.H. Hess, C.H.Y.X. Lim, K.P. Loh, J.A. Garrido, R. Jordan, M. Stutzmann, I.D. Sharp, Polymer Brushes on Graphene, Journal of the American Chemical Society 133(27) (2011) 10490-10498.
[91] A. Badri, M.R. Whittaker, P.B. Zetterlund, Modification of graphene/graphene oxide with polymer brushes using controlled/living radical polymerization, J Polym Sci Pol Chem 50(15) (2012) 2981-2992.
[92] J. Majoinen, A. Walther, J.R. McKee, E. Kontturi, V. Aseyev, J.M. Malho, J. Ruokolainen, O. Ikkala, Polyelectrolyte Brushes Grafted from Cellulose Nanocrystals Using Cu-Mediated Surface-Initiated Controlled Radical Polymerization, Biomacromolecules 12(8) (2011) 2997-3006.
[93] T. Ameringer, F. Ercole, K.M. Tsang, B.R. Coad, X.L. Hou, A. Rodda, D.R. Nisbet, H. Thissen, R.A. Evans, L. Meagher, J.S. Forsythe, Surface grafting of electrospun fibers using ATRP and RAFT for the control of biointerfacial interactions, Biointerphases 8 (2013).
[94] A.M. Telford, C. Neto, L. Meagher, Robust grafting of PEG-methacrylate brushes from polymeric coatings, Polymer 54(21) (2013) 5490-5498.

[95] A. Hucknall, A.J. Simnick, R.T. Hill, A. Chilkoti, A. Garcia, M.S. Johannes, R.L. Clark, S. Zauscher, B.D. Ratner, Versatile synthesis and micropatterning of nonfouling polymer brushes on the wafer scale, Biointerphases 4(2) (2009) Fa50-Fa57.
[96] F.J. Xu, Z.H. Wang, W.T. Yang, Surface functionalization of polycaprolactone films via surface-initiated atom transfer radical polymerization for covalently coupling cell-adhesive biomolecules, Biomaterials 31(12) (2010) 3139-3147.
[97] A.M. Jonas, Z.J. Hu, K. Glinel, W.T.S. Huck, Effect of Nanoconfinement on the Collapse Transition of Responsive Polymer Brushes, Nano Letters 8(11) (2008) 3819-3824.
[98] T. Wu, K. Efimenko, J. Genzer, Combinatorial study of the mushroom-to-brush crossover in surface anchored polyacrylamide, Journal of the American Chemical Society 124(32) (2002) 9394-9395.
[99] M. Furuya, M. Haramura, A. Tanaka, Reduction of nonspecific binding proteins to self-assembled monolayer on gold surface, Bioorganic & medicinal chemistry 14(2) (2006) 537-543.
[100] M. Furuya, Y. Tsushima, S. Tani, T. Kamimura, Development of affinity chromatography using a bioactive peptide as a ligand, Bioorganic & medicinal chemistry 14(15) (2006) 5093-5098.
[101] H. Chen, Y. Chen, H. Sheardown, M.A. Brook, Immobilization of heparin on a silicone surface through a heterobifunctional PEG spacer, Biomaterials 26(35) (2005) 7418-7424.
[102] H.W. Liu, C.H. Chen, C.L. Tsai, I.H. Lin, G.H. Hsiue, Heterobifunctional poly(ethylene glycol)-tethered bone morphogenetic protein-2-stimulated bone marrow mesenchymal stromal cell differentiation and osteogenesis, Tissue Eng 13(5) (2007) 1113-1124.
[103] J.E. Raynor, J.R. Capadona, D.M. Collard, T.A. Petrie, A.J. Garcia, Polymer brushes and self-assembled monolayers: Versatile platforms to control cell adhesion to biomaterials (Review), Biointerphases 4(2) (2009) Fa3-Fa16.
[104] M.A. Mintzer, E.E. Simanek, Nonviral Vectors for Gene Delivery, Chemical reviews 109(2) (2009) 259-302.
[105] D. Oupicky, Design and development strategies of polymer materials for drug and gene delivery applications, Adv Drug Deliver Rev 60(9) (2008) 957-957.
[106] D.W. Pack, A.S. Hoffman, S. Pun, P.S. Stayton, Design and development of polymers for gene delivery, Nat Rev Drug Discov 4(7) (2005) 581-593.
[107] W.J. Yang, K.G. Neoh, E.T. Kang, S.S.C. Lee, S.L.M. Teo, D. Rittschof, Functional polymer brushes via surface-initiated atom transfer radical graft polymerization for combating marine biofouling, Biofouling 28(9) (2012) 895-912.
[108] J. Trmcic-Cvitas, E. Hasan, M. Ramstedt, X. Li, M.A. Cooper, C. Abell, W.T.S. Huck, J.E. Gautrot, Biofunctionalized Protein Resistant Oligo(ethylene glycol)-Derived Polymer Brushes as Selective Immobilization and Sensing Platforms, Biomacromolecules 10(10) (2009) 2885-2894.
[109] J. Trmcic-Cvitas, E. Hasan, M. Ramstedt, X. Li, M.A. Cooper, C. Abell, W.T. Huck, J.E.J.B. Gautrot, Biofunctionalized protein resistant oligo (ethylene glycol)-derived polymer brushes as selective immobilization and sensing platforms, 10(10) (2009) 2885-2894.
[110] B.S. Lee, J.K. Lee, W.-J. Kim, Y.H. Jung, S.J. Sim, J. Lee, I.S.J.B. Choi, Surface-initiated, atom transfer radical polymerization of oligo (ethylene glycol) methyl ether methacrylate and subsequent click

chemistry for bioconjugation, 8(2) (2007) 744-749.
[111] N.D. Brault, A.D. White, A.D. Taylor, Q. Yu, S.J.A.c. Jiang, Directly functionalizable surface platform for protein arrays in undiluted human blood plasma, 85(3) (2013) 1447-1453.
[112] H. Vaisocherová, V. Ševců, P. Adam, B. Špačková, K. Hegnerová, A. de los Santos Pereira, C. Rodriguez-Emmenegger, T. Riedel, M. Houska, E.J.B. Brynda, Bioelectronics, Functionalized ultra-low fouling carboxy-and hydroxy-functional surface platforms: functionalization capacity, biorecognition capability and resistance to fouling from undiluted biological media, 51 (2014) 150-157.
[113] H. Vaisocherova, V. Sevcu, P. Adam, B. Spackova, K. Hegnerova, A.D. Pereira, C. Rodriguez-Emmenegger, T. Riedel, M. Houska, E. Brynda, J. Homola, Functionalized ultra-low fouling carboxy- and hydroxy-functional surface platforms: functionalization capacity, biorecognition capability and resistance to fouling from undiluted biological media, Biosensors & bioelectronics 51 (2014) 150-157.
[114] N.D. Brault, H.S. Sundaram, C.-J. Huang, Y. Li, Q. Yu, S.J.B. Jiang, Two-layer architecture using atom transfer radical polymerization for enhanced sensing and detection in complex media, 13(12) (2012) 4049-4056.

Chapter 2. Adsorbent based strategy for removal of uremic toxins

2.1 Porous or membrane based adsorbents for clearance of uremic toxins

Research involving adsorbents integrated with current hemodialysis systems can be described either as column-based or membrane-based (Figure 2-1). For column adsorbents, porous material beads (i.e. activated charcoal) or resin are loaded into a column that then can be used to remove toxins from media. Directing anticoagulated blood through a column is known as hemoperfusion [115]. In this process small molecules get trapped into pores of the adsorbent, but blood cells or large biomolecules can pass through the column and return to the body without loss of content. Hemoperfusion with some resin materials (polystyrene) are highly effective in removing lipid-soluble toxins. Charcoal-based hemoperfusion has been involved in the treatment of many conditions [116]. Charcoal may get coated with an antibody or antigen for treatment of autoimmune diseases such as systemic lupus erythematosus [117], rheumatoid arthritis [118, 119], and in the removal of pathogenic antibodies [120]. Middle molecular weight molecules that are not removed effectively by hemodialysis, β2-microglobulin for example, can be removed by hemoperfusion [121]. Although adsorbent beads are loaded into the column, adsorbent material may still make their way into blood through microparticle formation [122] or dissolvation [123] to cause other health issues.

Dialysate, instead of blood, can be passed through the column adsorbent so as to remove uremic toxins that have passed through the membrane from the blood [124]. This has been

done to enhance the concentration gradient, and thus molecular flux, across the membrane to enhance clearance of the toxin from the blood [125]. In effect, this doesn't necessarily have a large effect on clearance as much as it can allow for similar clearance using less dialysate. A highly porous adsorbent with a large capacity of toxin adsorption is favored for purpose of dialysate adsorption. Activated carbon and zeolite have been the most common adsorbents used, for they are both capable of adsorption of a variety of uremic toxins and can be prepared at a relatively low cost compared to other types of materials. Use of dialysate adsorbent satisfies the need to develop miniaturized or wearable dialyzer that can constantly remove dialysate toxins with an enclosed dialysate cycling system [126]. The toxin removal efficiency for adsorbent is highly addressed in order to scale down the existing wearable hemodialysis system [127-129].

Membrane-based adsorbents use the dialysis membrane, or its modified form, for toxin adsorption directly. Synthetic membranes currently used, like hydrophobic membranes composed of various polymers (PAN, PMMA, Polysulfone, polyamide), are shown to adsorb proteins or peptide nonspecifically. There are examples (adsorption of factor D, endotoxin, cytokine, and β_2m) that such adsorption properties are beneficial in lowing morbidity and mortality during hemodialysis. In the case of dialysis-related amyloid (DRA) contributed by β_2m, adsorption of β_2m to dialysis membranes appeared to be an important way for β_2m removal [130]. Despite that, nonspecific adsorption is not beneficial. One big issue is that adsorbed fibrinogen may promote platelet adhesion and trigger severe clotting of a dialysis membrane to render its utility failed [131]. In contradictory to the benefits brought by its adsorption properties, adsorption or deposition of any protein or peptide will gradually affect its permeation efficiency by irreversibly surface binding and plugging its semi-permeable pores [132]. Plus, the capacity of adsorption for the membrane is very limited compared to porous adsorbent particles. All these drawbacks indicate that the semi-permeable membrane cannot work by itself as a good adsorbent. Therefore the so-called

sorbent membrane [133-136] or mixed matrix membrane (MMM) [137] were developed to strengthens the role of adsorbent, and will be reviewed more detailed later.

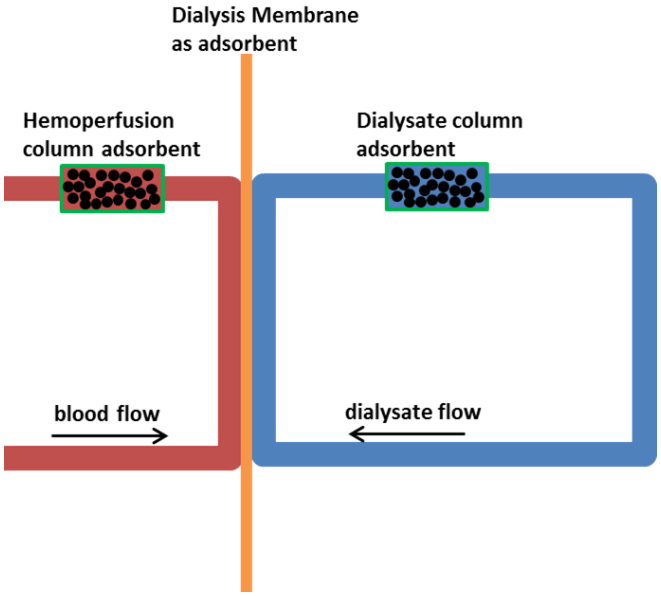

Figure 2-1 Illustration of column and membrane adsorbents used in hemodialysis systems.

For both column and membrane adsorbent, the basic principles determining their ability are the porous structure and surface chemistry. For certain type of adsorbent, there are various studies performed to investigate their potential, by some modifications either to enhance their adsorption capacity or to address issues that limit their further advancement, and these will be reviewed in detail. In addition, we reviewed some *in vivo* studies involving the use of adsorbents for treatment of uremic models, with comparison to routine hemodialysis.

2.2 Adsorbents based on different materials

Porous adsorbents are defined by having a pore structure. The dimension of pores ranges from micrometers to the order of magnitude of molecular dimensions. A large internal surface area can provide high adsorption properties for various substances such as solutes,

gas vapors and aerosols. For this ability porous adsorbents were used extensively in the application of uremic solutes adsorption. Table 2-1 compares the advantages and disadvantages of several adsorbent materials that have been used for removal of uremic toxins.

Table 2-1 Summary of advantages and disadvantages of several adsorbent materials used for removal of uremic toxins.

Adsorbent type	Advantages	Disadvantages
Activated carbon	-High adsorption capacity -Immunizing inert -Low cost	-Property not tunable -Poor hemocompatibility -Lack of selective adsorption
Zeolite	-Uniform pore size -Allow sieving small toxin molecules -Tunable physical properties by various frameworks	-Partial dissolvation in dialysate -Adsorption of cations from blood/dialysate
Mesoporous silica	-Uniform pore size -Pore size highly variable for different sizes of toxin molecules -Easy surface functionalization	-Limited industrial yield -Limited structure stability -Mechanisms not well understood
Polymer	-Different adsorbent forms (membrane, gel, resin) available -Highly flexible ways of modification (surface chemistry, copolymerization, blending)	-Poor hemocompatibility -Uneven pore size/shape -May trigger immunogenic response

The earliest and most studied porous adsorbent is activated carbon, also called activated charcoal. Activated carbon is produced from carbonaceous sources like wood, coal, and nutshell. Activation of these source materials, either through physical or chemical activation, is required to carbonization and generate a highly porous structure. In physical activation, carbonization is done by pyrolyzing the precursor at a temperature between 600 and 800^{o}C, under inert gas atmospheres like argon or nitrogen. Activation or oxidation is then performed by exposing carbonized material to oxidizing atmospheres, such as carbon

dioxide or oxygen, at a temperature above 250°C. In chemical activation, the precursor is impregnated with chemicals such as phosphoric acid or strong bases or salts like zinc chloride and is then treated at temperatures ranging from 450 to 900°C for carbonization. For one gram of activated carbon, a surface area of in excess of 3,000 m^2 can be achieved [138]. As early as 1969, Chang had attempted using activated charcoal to lower the level of a uremic marker, creatinine [139]. Activated carbon is still considered the most common adsorbent, which is due to its high adsorption potential, has rapid adsorption dynamics, and is chemically inert, and stable within complex physiological conditions [140]. Although activated carbon is involved in almost every artificial kidney device, carbon actually does not show the highest affinity toward any individual uremic toxin. An evident example is in adsorption of urea, the major uremic toxin component, where activated carbon has the lowest urea adsorption as compared to various uremic toxin adsorbents [124, 141]. Activated carbon is also found to have inadequate removal of middle molecular weight substances [142]. Another issue using activated carbon is that it adsorbs both uremic toxins and other organic molecules, like nutrients [143, 144].

As an alternative material, zeolite is being researched as another porous uremic toxin adsorbent. Zeolite is an aluminum silicate which can be both occurred in nature and produced synthetically. It is composed of SiO_4 and AlO_4 tetrahedra joined together, with the stoichiometric unit cell formula [145]:

$$M_{x/m}\,[(AlO_2)_x\,(SiO_2)_y]\,z\,H_2O$$

Where M is the cation type with the valence value m, and z represents the number of water molecules in each unit cell. To balance the negative charge due to the substitution of Si^{4+} by Al^{3+}, a cation is needed. Zeolite can afford many cations such as K^+, Na^+, Mg^{2+}, Ca^{2+} and so on, which are exchangeable under salt solution. The ionic nature makes most zeolite generally more hydrophilic than activated carbon [146]. Besides variations in the cationic

composition, it is also possible to modify the Si/Al ratio, in this way zeolites can be generated with different natures like framework structure and hydrophobicity and tailored properties for specific adsorption can be possible. Till now there are over 200 unique zeolite frameworks been synthesized. With a crystal structure, zeolite also features itself by a uniform distribution of pore sizes, for which reason they are capable of separating molecules based on size differences and are known as molecular sieves. Zeolite has superior adsorption towards *p*-cresol [123, 147]. However, one big concern of zeolite as an adsorbent used under liquid is that they may get dissolved into the media [148]. The desolvation of zeolite would allow aluminum or silicon to enter the blood, directly or indirectly from the dialysate. Unlike activated carbon with a wide range of pore dimensions, zeolites may get the pore size tuned to fit that of uremic toxins to exclude some organic molecules [147]. Nevertheless, zeolite may still adsorb sodium, calcium and potassium ions from blood or dialysate, thereby these ions has to be re-added in extra to compensate their loss [148].

Besides zeolite, another possible alternative porous adsorbent is mesoporous silica. Hexagonal pores arranged MCM-41 and SBA-15 are two most common types of mesoporous silica-based materials. Mesoporous silica can be prepared by reacting tetraethyl orthosilicate with the presence of a template material made of micellar rods. After self-organization and condensation of tetraethyl orthosilicate around a micellar template, the arranged tunnels are formed inside silica. Finally, surfactant can be removed by washing with a solvent adjusted to the proper pH [149]. The whole preparation process is illustrated in Figure 2-2. Like zeolite, an uniform pore distribution is also featured by mesoporous silica, but with a much larger scale of size variation (2 to 200 nm), making it more modifiable in its properties [150]. Besides, mesoporous silica can be modified with different chemicals to introduce functionality. It was found amino- and carboxylic-containing molecules can be grafted onto silica surface through chemisorption [151-154],

another advantage which zeolite does not possess.

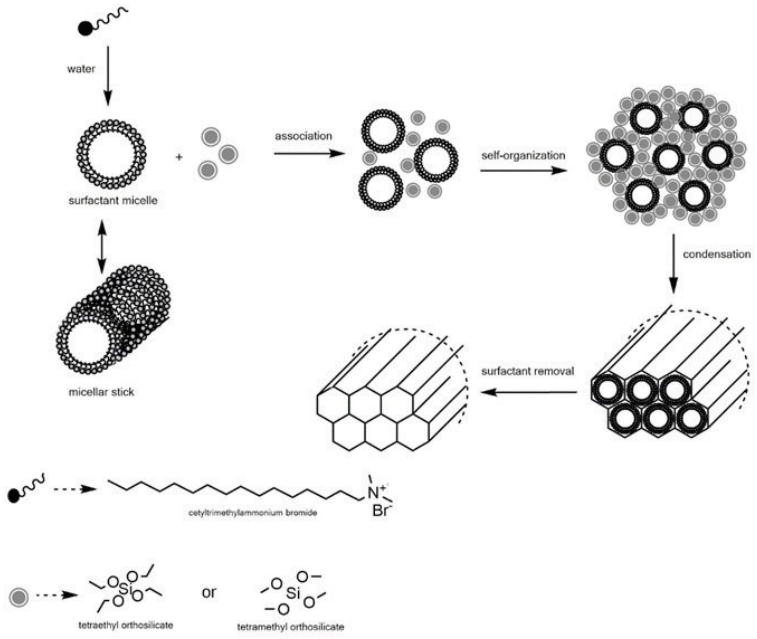

Figure 2-2 Process of silica-based mesoporous materials synthesis. Reproduced with permission from [155]. Copyright CEON/CEES 2001-2018.

In recent years, a rising number of studies have utilized polymer materials to discover novel adsorbents. Superior properties that make polymer a suitable adsorbent include various processing methods that allow for different final forms such as membrane, fiber or resin beads, modifiable mechanical and chemical properties, as well as numerous environmental (pH, temperature, irradiation) responsive properties. Monomer properties could also improve adsorption or make adsorption selective, these features allow polymer adsorbents preferable and versatile qualities compared with activated carbon, zeolite and silica. Dialysis membranes based on synthetic polymers (for example PMMA) show good solute permeability and a higher degree of biocompatibility than natural polymers (for example cellulose-based) [130, 156]. It was found that during dialysis, replacing PMMA membrane

in each dialysis session resulted in the reduction of a large-sized uremic toxin, free immunoglobulin light chains (sFLC), which suggests PMMA may serve as sFLC adsorbent. [157]. Polysulfone and polyamide were found with a high adsorption capacity for *p*-cresol. In study of adsorbent for middle-sized uremic toxins, such as β_2-microglobulin (β2M) and α-1-microglobulin(α-1-m), commercially available columns based on cellulose [158-161], polystyrene [162-164], and styrene-divinylbenzene copolymers [165] have been used to achieve the highest removal performance ever reported at 99% decrease in β2M; far exceeding that for high-flux dialysis membranes that only reduced the plasma β2M levels by 23~37% [166].

One common problem for these porous adsorbents used *in vivo* is the indiscriminate adsorption between toxins and non-toxins, which may reduce some essential nutrient levels during circulation and it would be necessary to supplement these nutrients after adsorption. For application in hemoperfusion, the performance of porous adsorbents has been significantly weakened by their poor hemocompatibility. Take activated carbon for example, non-specific blood protein adsorption cannot be avoided once activated carbon is exposed to blood, and this can cause big clinic problems, including particulate microemboli formation, hemolysis, and coagulation [167-169]. To overcome these limitations, further surface functionalization or surface modification are then required.

One main concern for using activated carbon in hemoperfusion is on its poor hemocompatibility, this may result in either reduced adsorption ability or blood coagulation [170]. In general, changing a hydrophobic surface into a hydrophilic surface will improve its hemocompatibility [171]. To this end, several attempts to generate a more hydrophilic surface of activated carbons have been made. Chang et al. first prepared heparin-complexed and albumin coated collodion microencapsulated activated carbon. Both modified activated carbons were found to maintain the arterial platelet level and not release

embolizing particles. Both modified activated carbons performed nearly as efficient as normally activated carbon in lowering blood creatinine, with albumin coated activated carbon more efficient than the heparin-complexed form.

Hydrogels are the cross-linked form of polymers that can maintain high amounts of water, and can provide some level of biocompatibility. Hydrogels have been used as a coating to enhance hemocompatibility of activated carbon. Zhang developed a zwitterionic poly-carboxybetaine (PCB) hydrogel coated on powdered activated carbon (PAC). The activated carbon particles were embedded into hydrogels by *in situ* crosslinking. The PCB-PAC complex showed negligible hemolysis and low levels of nonspecific protein adsorption, without sacrificing its adsorption performance [172]. Lee et al. attempted improving the blood hemocompatibility of spherical activated carbon (SAC) by coating with poly(hydroxyethyl methacrylate) (p(HEMA)). The reduction of platelet adsorption for SAC-p(HEMA) was as good as commercial hemoperfusion particles (Kuraray's DHP). It also confirmed that p(HEMA) coatings have a slight effect on the adsorption capacity of creatinine on SAC particles [173]. Another study chose dextran as a coating for activated carbo. The dextran-coated AC withstood several ISO recommended tests including inflammatory response, fibrinogen adsorption and complement generation to be proved hemocompatible. However, the coating still adversely affects the adsorption by decreasing the pore size and adsorption capacity of activated carbon.

Activated carbon can be modified or activated in ways that suit certain adsorption scenarios. For removal of uric acid, Liang et al. modified spherical activated carbon (PSAC) by chemical vapor deposition of NH_3 (NH_3-CVD). It was found NH_3-CVD significantly changed the surface properties, such as increased surface basicity and pH_{PZC} (point of zero charge), and these changes promoted adsorption of uric acid [174]. Nishiyama et al. activated mesoporous carbon with KOH for indole adsorption. The KOH activated

mesoporous carbon was found to have a higher porosity. The KOH-AC exhibits rapid indole adsorption [175]. Chang et al. prepared microencapsulated activated carbon by coating of poly(vinylidene fluoride) and of poly(vinylidene chloride/vinyl chloride) and used it as adsorbent for large lipophilic molecules (e.g. vitamin B_{12}) and small hydrophilic molecules (e.g. creatinine). Removal of large lipophilic molecules was rapid and complete for polymer-coated activated carbon, similar to that for uncoated activated carbon, and was little influenced by coating concentration of polymers. However, removal of small hydrophilic molecules was severely affected by coating concentration of polymers. Even with the lowest coating concentration test, the excluding efficiency was 80~85 % and was not as good as uncoated activated carbon with ~100% clearance [176]. As mentioned earlier in this review, certain polymeric adsorbents were found suitable to remove middle molecules, and this is because of the presence of a large amount of the so-called mesopores of 2-30 nm [177]. By taking advantage of such mesoporous structure, Malik et al. prepared spherical carbons with two different sulphonated styrene divinylbenzene copolymers, and was further activated using carbon dioxide [177]. It was found that activation would lead to loss of some mechanical strength. For adsorption of an inflammatory cytokine (IL-1β), a "trade-off" between adsorption capability and mechanical strength was determined, which means in order to achieve higher IL-1β uptake, some of the mechanical strength has to be sacrificed.

The use of activated carbon has been made into a composite with other materials for better adsorption performance. Zhao et al. prepared Poly(ether sulfone)/activated carbon (PES–AC) hybrid beads [178]. In this case, adsorption of creatinine was primarily determined by the AC content, where PES works as a substrate to incorporate and fix AC. By adding propylene glycol (PG), which is to promote penetration, into preparation solution, creatinine adsorption rate was also found increased. In another study, alginate and activated carbon were co-deposited onto steel wire mesh to create a novel sorbent material, by way

of electrophoretic deposition [179]. This sorbent uses alginate as a gel matrix forming agent to enhance the activated carbon loading. Such sorbent material absorbed creatinine, ammonia and uric acid in significant quantities, but still not on par with current materials.

There are also studies using particular precursors to prepare higher efficient or more cost-effective activated carbon. Jia et al. prepared activated carbon powders based on Polyaniline-poly(styrene sulfonate) (PAn-PSS) hydrogels [180]. The prepared particles were found with mesopores with pore ratio of 54 % and average pore diameter of 2.87 nm. This adsorbent featured itself by a high amine content, which may help intensify interaction with certain adsorbates by the formation of hydrogen bond. Compared to coconut shell activated carbon, PAn-PSS hydrogel activated carbon exhibited higher adsorption capacity of creatinine. Surendra et al. prepared activated carbon from parthenium weed, an inexpensive and easily available carbonaceous source materials [181]. Compared to commercial grade activated carbon, parthenium based activated carbon was found to remove *p*-cresol with close but still lower equilibrium amount, up to an equilibrium adsorbent concentration of 500 mg/L. Another study done by Bakas et al. compared *p*-cresol adsorption between granular activated alumina and granular activated charcoal [182]. They found that granular activated alumina and granular activated charcoal have very similar maximum monolayer adsorption capacity of 55.80 mg/g and 56.61 mg/g for *p*-cresol adsorption, therefore activated alumina might be considered as another low-cost option with similar adsorption capacity as activated charcoal.

Table 2-2 Summary of work done by researchers using adsorbent for removal of uremic toxins

Adsorbent type	Uremic toxins	Removal rate/ Saturated adsorption amount	Reference
Activated Carbon (AC)			
heparin-complex	creatinine	16%	[139]
albumin coating	creatinine	37%	[139]
zwitterionic poly-carboxybetaine (PCB) hydrogel coating	bilirubin	95%	[172]
poly(hydroxyethyl methacrylate) coating	creatinine	71.4%	[173]
dextran coating	bilirubin	< 8.7 mg/g	[169]
NH_3 deposition	uric acid	333.1 mg/g	[174]
KOH activation	indole	79%	[183]
poly(vinylidene fluoride) + PEG coating	Urea, creatinine	60% 24%	[184]
4% poly(vinylidene chloride/vinyl chloride) coating	creatinine	92%	[185]
CO_2 activation	Interleukin 1β	CT275-C1-A1 140ng/g MN500HSC1-A6 60ng/g	[186]
Poly(ether sulfone)/activated carbon (PES–AC) hybrid beads	creatinine	80%	[187]

codeposition with alginate	Uric acid, creatinine, ammonia, urea	99.0 ± 1.1%, 38.3 ± 1.1%, 13.7 ± 2.2%, 3.7 ± 1.0%.	[179]
zeolite			
Ca^{2+} and K^{+} exchanged framework	Urease	80IU/ml	[188]
Mordenite	Creatinine Indoxyl sulfate	37500 ug/g 3700 ug/g	[189]
poly(ethylene-co-vinyl alcohol) (EVOH)-zeolite–polymer composite nanofibers	Creatinine	220umol/g	[190]
polyacrylonitrile (PAN)-zeolite composite nanofiber	Creatinine	52%	[191]
zeolites and polyethersulfone-zeolite composite membranes	Indoxyl sulfate	1300ug/g	[192]
polymer			
cellulose membrane	creatinine/urea	70%/76%	[193]
polyamide membrane	*p*-cresol	21 mg/g	[194]
poly(acrylonitrile) membrane	*p*-cresol	0.3 mg/g	[123]
polysulfone membrane	*p*-cresol	37.3 mg/g	[123]
cellulose column	β_2-microglobulin (β2M)	16.5 %	[159]
polystyrene column	β_2-microglobulin (β2M)	96%	[195]
styrene divinylbenzene copolymer column	β_2-microglobulin	99%	[196]

poly(cyclodextrins)	(β2M)	80%	[197]
Seed-Conjugated Polymer Beads	indoxyl sulfate	40%	[198]
carbonylated hypercrosslinked chloromethylated poly(styrene-co-divinylbenzene)	β_2-microglobulin (β2M) p-cresol	1.3 mmol/g	[198]
Molecularly Imprinted Polymer (MIP)			
creatinine-imprinted poly(β-cyclodextrin)	creatinine	6mg/g	[199]
creatinine-imprinted	creatinine	0.86mg/g	[200]
mixed matrix membrane (MMM)	creatinine		
cellulose acetate matrix	creatinine	25mg/g	[201]
poly(ethersulfone)/poly(vinylpyrrolidone) polymer blend matrix	creatinine	48mg/g	[202]
Poly heparin-mimicking polymers	creatinine	1400ug/g	[203]

As been introduced earlier, several non-AC materials are available as uremic toxin adsorbents. This includes zeolite with different framework types, mesoporous silica with surface modified, and different polymers. Being another uremic toxin adsorbent, zeolite has been studied systematically in terms of the physical and chemical properties (pore size, hydrophobicity, grain size, charge compensating cations etc.) in order to properly tune its adsorption performance. In this work, zeolites with different framework types were prepared, and both free water-soluble toxins (urea etc.) and protein-bound uremic toxins (*p*-Cresol etc.) were used in adsorption test. Specific adsorption towards uremic toxins was proposed for zeolite, due to the findings that zeolite pores and uremic toxins are similar in size, which enables entrapments of uremic toxins. With a higher Si/Al ratio, the zeolite

channel becomes more hydrophobic and favors adsorption of *p*-cresol much more than that with equal or similar amount of Si and Al. However, for adsorption of indoxyl sulfate, no such advantage was observed for high Si/Al ratio samples. Al-Si frameworks are negatively charged and therefore need to be compensated by cations. The adsorption of uric acid on Ca^{2+} and K^{+} exchanged framework are comparatively higher than on Na^{+} exchanged framework. The adsorption of indoxyl sulfate on K^{+} exchanged framework is comparatively higher than on the other cation exchanged framework and is as high as that on hydrophobic uncharged framework. Other factors like grain size and hydrothermal treatment were also found to influence the adsorption properties. Interestingly, the adsorption result for creatinine shows that Z9, a framework type called MOR (Mordenite) with a high Si/Al ratio and low Na^{+} content, has a specific high affinity towards creatinine than any other framework. Further mechanism study revealed that by adsorption onto Mordenite, creatinine was protonated [204]. When adsorption was performed on partially exchanged forms of mordenite, it is possible that a cationic exchange between the protonated creatinine and other cations occurred. Anyway, specific removal of creatinine might be a property for mordenite that can work with hemodialysis to eliminate this single toxin molecule, and further *in vivo* test is still required to prove this specificity in a more complex blood environment.

For successful integration of zeolite into a practical blood purification system, zeolite has been integrated with multiple types of substrate, such as nanofiber matrix and membranes. Such composite structure would ensure immobilization of zeolite particles, while also aims to minimize the adverse effect on solution exposure and adsorption capability of zeolite. Mitsuhiro et al. developed a zeolite-polymer composite nanofiber mesh incorporated into a portable blood purification system [205]. The nanofiber is made from poly(ethylene-co-vinyl alcohol) (EVOH) by electrospinning of its solution with zeolite particles dispersion. Zeolite was found incorporated into nanofibers as a bead-like structure p(EVOH).

Adsorption of creatinine with several commercial zeolite species was measured. Although the zeolite type, 940-HOA, was identified with optimal adsorption capacity, the p(EVOH) matrix do have some adverse barrier effect on adsorption, and the adsorption efficiency decreased when more zeolite was incorporated into the nanofiber matrix. Another interesting finding by this work is that under continuous flow condition, creatinine adsorption was found to be much lower than that without flow. Therefore, flow rate and area are important factors to be considered for the design of the setup to maximize the adsorption capacity. To overcome the barrier effect of nanofiber matrix, the same group continued their work by varying the composition of ethylene in EVOH, thus resulted in a less crystallized structure and a higher creatinine adsorption [206]. The composite fibers also showed much less cytotoxicity than free zeolite particles which kills more than 95% of cells. Similarly, John et al. prepared polyacrylonitrile (PAN)-zeolite nanofiber membranes through electrospinning, with zeolite incorporated by dispersion in PAN solution [207]. Also, 940-HOA was identified with the zeolite type with the highest adsorption capacity. When compared with free zeolite powders, both 840 and 940 zeolites incorporated in membranes exhibited even higher adsorption capacity, which seems to be contradictory to the barrier effect put by the nanofibers. For such a surprising result, the experiment itself might be arguable because different testing protocols were used for free powders and nanofiber composite, thus may put control powder samples less exposed to creatinine solutions. Another work done by John et al. is the preparation of PES-zeolite composite membrane for indoxyl sulfate removal [208]. The composite membrane was fabricated by a spin-coating method followed by liquid-liquid phase separation in water. Among 10 types of zeolite with 5 different frameworks, only P87 and P371 have adsorption of indoxyl sulfate. P87 incorporated into PES membrane showed a similar removal rate of inodxyl sulfate compared to P87 powder. Further experiments suggested that electrostatic attraction is the main force responsible for indoxyl sulfate adsorption.

Silica features itself for easy surface functionality, which may allow for various surface chemistry to be conducted to introduce wanted functional moiety. For example, amine-functionalized mesoporous silica has been synthesized and characterized by Fei-Yee et al [150]. In this study, 3-aminopropyl was chemically introduced onto the mesoporous silica surface, and this brought about a slight decrease in pore diameter. Through urea adsorption study, both the amine modified mesoporous silica and unmodified mesoporous silica exhibited much higher adsorption capacity than commercially used activated carbon, despite the fact that activated carbon owns much lower pore diameter and higher BET surface area. What the author addressed more attention is that not only the amine modified mesoporous silica gave the highest adsorption capacity, but also showed much higher nominal rate constant than any other tested subject, and the author further suggested that such an advantage would allow for increased dialysate flow to achieve a higher uremic toxin clearance efficiency.

With a large variety of species and compositions, polymer adsorbent can be made with different adsorption properties based on their structural diversity and high potential for functionalization. Poly-β-cyclodextran has been used for removal of indoxyl sulfate. Jia et al. prepared cross-linked poly-β-cyclodextrins (PCDs) as a water-soluble adsorbent for IS [209]. PCDs has an inner hydrophobic cavity and an external hydrophilic shell, therefore the cavity is able to accommodate diverse hydrophobic molecules and IS adsorption was proved to be the hydrophobic interactions between indole ring and cavity of β-CD, plus hydrogen bonding. Binding capability of 45 mg/g was achieved by PCD. In addition, PCDs demonstrated improved removal rate of IS when introduced into dialysis systems. As is known, dialysis-related amyloidosis (DRA) is caused by the accumulation of β2M which then turns to amyloid fibrils. Seung et al. found one peptide segment (Lys - Asp - Trp - Ser - Phe - Tyr - Leu - Leu - Tyr - Tyr) derived from β2M are capable of forming amyloid fibrils. After immobilization of this peptide on polymer beads of HiCore resin, the

peptide is able to accrete β2M in the form of fibrils on the bead surface [210]. It is suggested that these seed-immobilized beads work as a highly specific β2M removal system. For removal of phenolic compounds like *p*-cresol, commercially available Amberlite XAD-4 resin has been recognized as the best synthetic polymer adsorbent. However, its capability of adsorption is compromised by its hydrophobic surface when removing toxins from aqueous solution. To this end, Huang prepared a hypercrosslinked polymeric adsorbent HJ-1 from chloromethylated poly(styrene-co-divinylbenzene) (PS) [211]. The modified resin (HJ-1) exhibited higher polarity compared to chloromethylated poly(styrene-co-divinylbenzene) and was even more polar than non-polar XAD-4. Adsorption test under aqueous solution revealed that HJ-1 has a higher adsorption capacity of phenol and *p*-cresol compared to commercial XAD-4 resin. Polymeric microspheres are also used as an adsorbent for uremic toxins. Zhang et al. prepared copolymer p(HEMA-co-NVP) microspheres, which was cross-linked with N,N'-methylene bisacrylamide (MBA) [212]. The microspheres were chemically modified with 3,5-dinitrobenzoyl chloride (DNBC), to obtain 3,5-dinitrobenzoate group (DNBZ) bound surface. The DNBZ bound p(HEMA-co-NVP) microspheres have a fairly high adsorption capacity for creatinine with the saturated adsorption amount of 25 mg/g, 20 times as compared to unmodified p(HEMA-co-NVP) microspheres.

2.3 Molecularly imprinted polymer (MIP) and Mixed matrix membrane (MMM) for removal of uremic toxins

Molecularly imprinted polymer (MIP) system has been recognized recently as a promising tool in applications like sensors [213] and adsorbent [214]. MIP is a polymer substrate which can bind with high specificity towards target molecules (Figure 2-3). In brief, monomers are polymerized and cross-linked around a template molecule. While MIP is formed either non-covalent or reversible covalent interaction may occur between MIP and

template. Upon template removal, a binding pocket specific for this template molecule is then left [215].

Figure 2-3 Basics of molecularly imprinted polymer (MIP). (1) The template molecule (T) forms complex with functional monomers (M); (2) Copolymerization occurs with both M and cross-linker (CL) to form polymeric network around the template; (3) Removal of template to create complementary binding cavities that can bind template molecules with high specificity. Reproduced with permission from [216]. Copyright 2003 American Chemical Society.

MIP has been utilized for specific binding of uremic toxins, with creatinine being the most used molecules for imprinting. Syu et al. prepared creatinine imprinted MIP, using β-Cyclodextrin as the monomer and epichlorohydrin as the crosslinking agent. The molar ratio between monomer to template and monomer to the cross-linking agent were optimized for maximum adsorption of creatinine. Creatinine, N-hydroxysuccinimide, and 2-pyrrolidinone were chosen for comparison of their adsorption. The results of adsorption on binary and ternary mixture solution suggest that the creatinine imprinted poly(β-CD) has recognition ability towards creatinine. The specific binding effect of MIP to creatinine was further confirmed by capping hydroxyl groups of the imprinted poly(β-CD) with chlorotrimethylsilane (CTMS). Another work by the same group was done on the preparation of creatinine imprinted sol-gel [217], an inorganic polymer matrix that has ever been used as a matrix for molecularly imprinting. The study suggested that solvent played an important role in specific binding, that the imprinting factor, measured by comparing adsorbed creatinine amount in imprinted sol-gel to non-imprinted sol-gel, in water was much higher than that in methanol. It was found solvent also affect the competitive

adsorption. Under methanol solution, adsorption by the imprinted sol-gel on mixture solution of N-hydroxysuccinimide/2-pyrrolidinone/creatinine failed to show any selectivity towards creatinine. While in water the imprinted sol-gel did have the highest bound amount of creatinine than other compounds, so did it in binary mixture solutions comprised of creatinine and other compounds.

Since the use of adsorbent with the aim to strengthen dialysis technology, the so-called sorbent membranes had been developed in the late 1970s by Enka [218-222]. However, it turned out to be a failed commercializing practice, due to problems in fabrication, adsorbent purification and other issues cannot be solved properly [133, 134]. One advancement appeared recently is a new type of diffusion and adsorption combined membrane, the so-called mixed matrix membrane (MMM) [137, 223, 224]. In MMM, the adsorptive particles are embedded in a membrane serves as a macroporous matrix, and another particle-free membrane layer is introduced with direct blood contact, in order to minimize hemocompatibility issue (Figure 2-4). Compared to column adsorbent, MMM embeds AC particles more firmly to prevent release, while the membrane still maintains high diffusion transparency. Cellulose acetate and polyethersulfone (PES)/polyvinylpyrrolidone (PVP) polymer blend (PES as a membrane-forming polymer blended with PVP to improve hydrophilicity) [137, 224, 225] have been used for macroporous matrix, and activated carbon was used in both cases as the adsorptive particle. With heparin-mimicking polymers grafted carbon nanotubes (f-CNT), Zhao et al. prepared a hemocompatibility enhanced MMM [226]. Blending of f-CNT into PES membrane remarkably improved both hemocompatibility and removal efficiency of uremic toxin. Although the advancement in MMM has proved a more promising way of clearing uremic toxins, it should be noted that this technique, in essence, is still membrane based that rely on diffusion of uremic toxin. Large biomolecules bound with uremic toxins with high affinity are unable to diffuse into MMM and would remain in circulation that would possess

risks of their associated CKD complications.

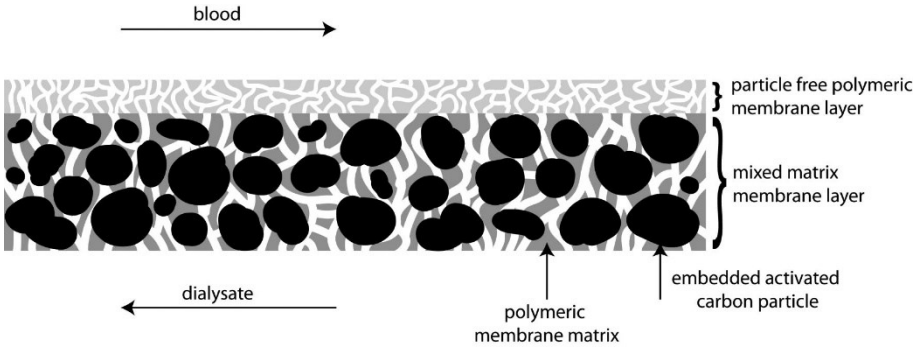

Figure 2-4 Schematic illustration of mixed matrix membrane (MMM) for blood purification. Reproduced with permission from. Copyright 2012 ELSEVIER.

2.4 *In vivo* test performances of several adsorbent systems

Although hemodialysis is considered as the necessary treatment for CKD patients, protein-bound uremic toxins are actually poorly removed by current dialysis. Hemodialysis alone does not help too much in reducing indoxyl sulfate and *p*-cresyl sulfate levels which are associated with cardiovascular disease (CVD) such as atherosclerosis [193, 227, 228]. Contemporary adsorbent technique was found to be a more efficient therapy in this issue. Most of the *in vivo* test or treatments were conducted in either of two forms: oral adsorption or extracorporeal adsorption.

The oral AC based adsorbent AST-120 (Kremezin®), as a pre-dialysis serving agent, has been used in renal failure patients to adsorb uremic toxins contained in the gastrointestinal tract (GI) in order to prolong the progression of CKD [229, 230]. AST-120 is composed of spherical particles (~ 0.2–0.4 mm) which are mainly carbon [231]. Administration of AST-120 in nephrectomy animal models resulted in a decreased level of serum creatinine and urinary protein [229]. More specific studies revealed that by decreasing IS levels in *vivo*,

AST-120 significantly reduced the ratio of oxidized albumin, and therefore the role of AST-120 in inhibiting oxidative stress in CKD was determined [232]. In addition, AST-120 has been reported to improve low bone turnover that results from uremia, another IS associated disease [233]. Over decades, clinic data has supported the efficacy of AST-120 in delaying the initiation time of hemodialysis treatment and slowing decrease of glomerular filtration rate [234, 235].

For better removal of protein-bound toxins, one technique called fractionated plasma separation and adsorption (FPSA) was created. In FPSA system, the albumin fraction is first separated by filtration through an albumin permeable membrane, and is then purified by perfusion over a neutral resin adsorbent and an anion exchanger and then flow back to the plasma [236, 237]. The whole blood is then dialyzed through the high-flux dialyzer (Figure1-7). The system has been commercialized with the brand name Prometheus®. For liver or kidney failure issue, FPSA was specifically designed to remove albumin-bound toxins, as albumin was considered to be the main binding protein for hydrophobic solutes [17]. *In vivo* study in CKD patients showed that the reduction rate of *p*-cresyl sulfate by FPSA exceeded the reduction rate given by high-flux hemodialysis [238]. In a similar study, the removal rate on FPSA treated patients for several protein-bound uremic toxins including phenylacetic acid, indoxyl sulfate and *p*-cresol were increased by 130%, 187% and 127% in comparison to conversional high-flux hemodialysis [239]. The present studies have proved that FPSA is more capable of removing albumin bound toxins in CKD patients than high-flux hemodialysis. Nevertheless, it should be noted that FPSA compromised a lot at *in vivo* removal rate compared to that at *in vitro*. By filtration in order to separate albumin, a sieving effect has been observed that a large portion of albumin failed to cross Albuflow® for secondary circuit. For this reason, it makes sense that some of the toxins that bound to albumin can be retained back to circulation as well. To achieve optimal albumin separation, more precisely determined membrane cut-off sizes is to be expected.

In early FPSA system, fibrinogen was only little involved in the secondary circuit, but there were studies blame coagulation abnormality for CKD patients to toxin binding of fibrinogen [240], and therefore fibrinogen or even other minor proteins may have to be involved for clearance. Although the adsorbents used exhibit high capacity of toxin binding and high ability of lowering the concentration, non-specific adsorption is still unavoidable. Adsorption of both pro- and anticoagulant factors onto the anion exchange resin has been reported leading to severe thrombosis issues. Other safety parameters such as cortisol, triiodothyronine, or total plasma protein seems did not change a lot to be concerned, investigation addressing these issues is still lacking. It is known that toxin binding impairs protein function by influencing the complex-forming properties. Albumin from chronic hemodialysis patients underwent significant conformational changes and got a decreased capacity of binding pharmaceuticals [241]. Nikolaev proved carbonic hemosorbents (HSGD®) coated with albumin as a promising method to deligand these protein-bound toxins such as bilirubin [242], fatty and bile acids, phenols, CMPF, hippuric acid and IS [243] from albumin. Molecular level restoration of human serum albumin in terms of conformation and ligand-binding activity was confirmed by this method. After extracorporeal treatment by deliganding adsorbent, restoration of conformation and complex-forming capacity occurred for uremic albumin [244].

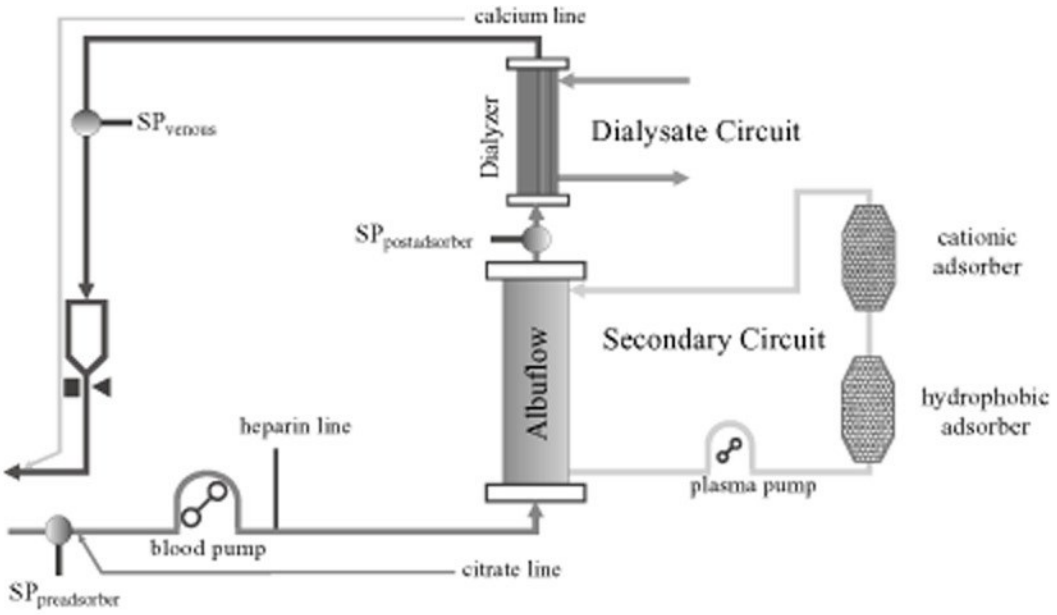

Figure 2-5 Schematic illustration of fractionated plasma separation and adsorption (FPSA) system. Reproduced with permission from [239]. Copyright 2013 John Wiley & Sons

2.5 Challenges for removal of protein bound uremic toxins

Unlike small free water-soluble uremic toxins, protein-bound and middle uremic toxins cannot be removed well enough by conventional hemodialysis and were found associated with CKD or CVD related diseases. In this area, better solutions may be proposed with the use of adsorbent materials. Although each type of porous material discussed in this review own their unique property and may exhibit suitability under certain scenarios, AC based adsorbent is by far the most studied material and to our knowledge included in most commercialized adsorbent systems. Despite the fact that the superior removal rate has been achieved by these adsorbents over hemodialysis, there are still some challenges to be addressed in future studies, like being more hemocompatible without sacrificing the adsorption capacity, or being specific toxin binders without affecting normal healthy biomolecules.

2.6 References

[17] L. Viaene, P. Annaert, H. de Loor, R. Poesen, P. Evenepoel, B. Meijers, Albumin is the main plasma binding protein for indoxyl sulfate and p-cresyl sulfate, Biopharmaceutics & drug disposition 34(3) (2013) 165-75.
[115] M.H. Rahman, S.S. Haqqie, M.D. McGoldrick, Acute hemolysis with acute renal failure in a patient with valproic acid poisoning treated with charcoal hemoperfusion, Hemodialysis international. International Symposium on Home Hemodialysis 10(3) (2006) 256-9.
[116] J. Winchester, A. Boldur, C. Oleru, C. Kitiyakara, Use of dialysis and hemoperfusion in treatment of poisoning, Handbook of dialysis. Boston: Boston Little Brown (1994).
[117] D.S. Terman, G. Buffaloe, G. Cook, M. Sullivan, C. Mattioli, R. Tillquist, J.C. Ayus, Extracorporeal Immunoadsorption - Initial Experience in Human Systemic Lupus-Erythematosus, Lancet 2(8147) (1979) 824-826.
[118] A. Ault, New direction for treatment of rheumatoid arthritis offered in USA, Lancet 353(9158) (1999) 1071-1071.
[119] J. Caldwell, R.M. Gendreau, D. Furst, A pilot study using a staph protein A column (Prosorba (R)) to treat refractory rheumatoid arthritis, Journal of Rheumatology 26(8) (1999) 1657-1662.
[120] R.M. Hakim, E. Milford, J. Himmelfarb, R. Wingard, J.M. Lazarus, R.M. Watt, Extracorporeal Removal of Anti-Hla Antibodies in Transplant Candidates, American Journal of Kidney Diseases 16(5) (1990) 423-431.
[121] S. Yamamoto, J.J. Kazama, T. Wakamatsu, Y. Takahashi, Y. Kaneko, S. Goto, I. Narita, Removal of uremic toxins by renal replacement therapies: a review of current progress and future perspectives, Renal Replacement Therapy 2(1) (2016) 43.
[122] R.A. Van Wagenen, M. Steggall, D.J. Lentz, J.D. Andrade, Activated carbons for medical applications. In vitro microparticle characterization and solute adsorption, Biomaterials, medical devices, and artificial organs 3(3) (1975) 319-64.
[123] V. Wernert, O. Schaf, V. Faure, P. Brunet, L. Dou, Y. Berland, P. Boulet, B. Kuchta, R. Denoyel, Adsorption of the uremic toxin p-cresol onto hemodialysis membranes and microporous adsorbent zeolite silicalite, Journal of biotechnology 123(2) (2006) 164-173.
[124] G. Dunea, Replacement of Renal-Function by Dialysis - a Textbook of Dialysis, 2nd Edition - Drukker,W, Parsons,Fm, Maher,Jf, Jama-J Am Med Assoc 252(13) (1984) 1768-1768.
[125] J. Mulder, Basic principles of membrane technology, Springer Science & Business Media2012.
[126] V. Gura, C. Ronco, A. Davenport, The Wearable Artificial Kidney, Why and How: From Holy Grail to Reality, Seminars in dialysis 22(1) (2009) 13-17.
[127] C. Ronco, A. Davenport, V. Gura, Toward the wearable artificial kidney, Hemodialysis International 12 (2008) S40-S47.
[128] C. Ronco, A. Davenport, V. Gura, A wearable artificial kidney: dream or reality?, Nat Clin Pract

Nephr 4(11) (2008) 604-605.
[129] H.D. Polaschegg, Wearable Dialysis: What is Missing?, Hemodialysis: New Methods and Future Technology 171 (2011) 226-230.
[130] M. Pascual, N. TolkoffRubin, J.A. Schifferli, Is adsorption an important characteristic of dialysis membranes?, Kidney international 49(2) (1996) 309-313.
[131] A.K. Cheung, Biocompatibility of Hemodialysis Membranes, Journal of the American Society of Nephrology 1(2) (1990) 150-161.
[132] H. Vonbaeyer, F. Kochinke, R. Schwerdtfeger, Cascade Plasmapheresis with Online Membrane Regeneration - Laboratory and Clinical-Studies, J Membrane Sci 22(2-3) (1985) 297-315.
[133] G.V. Chapman, P.W.E. Hone, W. Bolton, A. Blogg, C. Stokoe, T. Cahill, J.F. Mahony, P.C. Farrell, Evaluation of Hemodiafiltration and Sorbent Membrane Dialysis .1. Invivo and Invitro Dialyzer Performance, Dialysis Transplant 11(9) (1982) 758-&.
[134] G.V. Chapman, P.W.E. Hone, M.J. Shirlow, W. Bolton, A. Blogg, C. Stokoe, T. Cahill, J.F. Mahony, P.C. Farrell, Evaluation of Hemodiafiltration and Sorbent Membrane Dialysis .2. Clinical, Nutritional, and Middle Molecule Assessment, Dialysis Transplant 11(10) (1982) 871-&.
[135] K. Maeda, A. Saito, S. Kawaguchi, R. Sezaki, T. Niwa, M. Naotsuka, K. Kobayashi, H. Asada, Y. Yamamoto, K. Ohta, Problems with Activated-Charcoal and Alumina as Sorbents for Medical Use, Artificial organs 3(4) (1979) 336-340.
[136] D.H. Randerson, H.J. Gurland, B. Schmidt, P.C. Farrell, P.W.E. Hone, C. Stokoe, A. Zuber, A. Blogg, A. Fatehmoghadam, I. Marschner, W. Kopcke, Sorbent Membrane Dialysis in Uremia, Contributions to nephrology 29 (1982) 53-64.
[137] M.S.L. Tijink, M. Wester, J.F. Sun, A. Saris, L.A.M. Bolhuis-Versteeg, S. Saiful, J.A. Joles, Z. Borneman, M. Wessling, D.F. Stamatialis, A novel approach for blood purification: Mixed-matrix membranes combining diffusion and adsorption in one step, Acta Biomaterialia 8(6) (2012) 2279-2287.
[138] E.C. Dillon, J.H. Wilton, J.C. Barlow, W.A. Watson, Large Surface-Area Activated-Charcoal and the Inhibition of Aspirin Absorption, Ann Emerg Med 18(5) (1989) 547-552.
[139] T.M.S. Chang, Removal of Endogenous and Exogenous Toxins by a Microencapsulated Absorbent, Can J Physiol Pharm 47(12) (1969) 1043-&.
[140] H. Marsh, F. Rodríguez-Reinoso, CHAPTER 1 - Introduction to the Scope of the Text, in: H. Marsh, F. Rodríguez-Reinoso (Eds.), Activated Carbon, Elsevier Science Ltd, Oxford, 2006, pp. 1-12.
[141] S. Stefoni, L. Coli, G. Feliciangeli, L. Baldrati, V. Bonomini, Regular Hemoperfusion in Regular Dialysis Treatment - a Long-Term Study, International Journal of Artificial Organs 3(6) (1980) 348-353.
[142] J. Chen, W. Han, J. Chen, W. Zong, W. Wang, Y. Wang, G. Cheng, C. Li, L. Ou, Y. Yu, High performance of a unique mesoporous polystyrene-based adsorbent for blood purification, Regenerative biomaterials 4(1) (2016) 31-37.
[143] R.C. Bansal, J.-B. Donnet, F. Stoeckli, Active carbon, Marcel Dekker1988.
[144] M.C. Annesini, V. Piemonte, L. Turchetti, Removal of albumin-bound toxins from albumin-containing solutions: Tryptophan fixed-bed adsorption on activated carbon, Chem Eng Res Des 88(8A) (2010) 1018-1023.
[145] Crystallization, Air–Water Operations, Drying, Adsorption, Membrane Separations, and Other Mass Transfer Processes, Fluid Mechanics, Heat Transfer, and Mass Transfer.

[146] J. Pires, M.L. Pinto, A. Carvalho, M.B. de Carvalho, Assessment of hydrophobic-hydrophilic properties of microporous materials from water adsorption isotherms, Adsorption 9(4) (2003) 303-309.
[147] V. Wernert, O. Schaf, H. Ghobarkar, R. Denoyel, Adsorption properties of zeolites for artificial kidney applications, Micropor Mesopor Mat 83(1-3) (2005) 101-113.
[148] R.R. Willis, D.S. Bem, D.L. Ellig, Process and composition for removing toxins from bodily fluids, Google Patents, 2003.
[149] B.G. Trewyn, J.A. Nieweg, Y. Zhao, V.S.Y. Lin, Biocompatible mesoporous silica nanoparticles with different morphologies for animal cell membrane, penetration, Chem Eng J 137(1) (2008) 23-29.
[150] W.K. Cheah, Y.L. Sim, F.Y. Yeoh, Amine-functionalized mesoporous silica for urea adsorption, Mater Chem Phys 175 (2016) 151-157.
[151] D. Fine, A. Grattoni, R. Goodall, S.S. Bansal, C. Chiappini, S. Hosali, A.L. van de Ven, S. Srinivasan, X.W. Liu, B. Godin, L. Brousseau, I.K. Yazdi, J. Fernandez-Moure, E. Tasciotti, H.J. Wu, Y. Hu, S. Klemm, M. Ferrari, Silicon Micro- and Nanofabrication for Medicine, Adv Healthc Mater 2(5) (2013) 632-666.
[152] Q. Wei, H.Q. Chen, Z.R. Nie, Y.L. Hao, Y.L. Wang, Q.Y. Li, J.X. Zou, Preparation and characterization of vinyl-functionalized mesoporous SBA-15 silica by a direct synthesis method, Mater Lett 61(7) (2007) 1469-1473.
[153] G.S. Wu, P.H. Li, H.Q. Feng, X.M. Zhang, P.K. Chu, Engineering and functionalization of biomaterials via surface modification, Journal of Materials Chemistry B 3(10) (2015) 2024-2042.
[154] K.Y. Ho, G. McKay, K.L. Yeung, Selective adsorbents from ordered mesoporous silica, Langmuir 19(7) (2003) 3019-3024.
[155] M.D. Branković, A.R. Zarubica, T.D. Anđelković, D.H. Anđelković, Mesoporous silica (MCM-41): Synthesis/modification, characterization and removal of selected organic micro-pollutants from water, Advanced Technologies 6(1) (2017) 50-57.
[156] H. Sugaya, Y. Sakai, Polymethylmethacrylate: from polymer to dialyzer, Polymethylmethacrylate, Karger Publishers1999, pp. 1-8.
[157] P. Fabbrini, S. Sirtori, E. Casiraghi, F. Pieruzzi, S. Genovesi, D. Corti, R. Brivio, G. Gregorini, G. Como, M.L. Carati, M.R. Vigano, A. Stella, Polymethylmethacrylate Membrane and Serum Free Light Chain Removal: Enhancing Adsorption Properties, Blood purification 35 (2013) 52-58.
[158] S. Furuyoshi, M. Nakatani, J. Taman, H. Kutsuki, S. Takata, N. Tani, New Adsorption Column (Lixelle) to Eliminate (β2-Microglobulin for Direct Hemoperfusion, Therapeutic Apheresis 2(1) (1998) 13-17.
[159] T. Abe, K. Uchita, H. Orita, M. Kamimura, M. Oda, H. Hasegawa, H. Kobata, M. Fukunishi, M. Shimazaki, T. Abe, T. Akizawa, S. Ahmad, Effect of beta(2)-microglobulin adsorption column on dialysis-related amyloidosis, Kidney international 64(4) (2003) 1522-1528.
[160] N. Homma, F. Gejyo, S. Hasegawa, T. Teramura, I. Ei, H. Maruyama, M. Arakawa, Effects of a new adsorbent column for removing beta-2-microglobulin from circulating blood of dialysis patients, Dialysis-Related Amyloidosis 112 (1995) 164-171.
[161] F. Gejyo, T. Teramura, I. Ei, M. Arakawa, R. Nakazawa, N. Azuma, M. Suzuki, S. Furuyoshi, T. Nankou, S. Takata, A. Yasuda, Long-term clinical evaluation of an adsorbent column (BM-O1) of direct hemoperfusion type for beta(2)-microglobulin on the treatment of dialysis-related amyloidosis, Artificial organs 19(12) (1995) 1222-1226.

[162] V. Davankov, L. Pavlova, M. Tsyurupa, J. Brady, M. Balsamo, E. Yousha, Polymeric adsorbent for removing toxic proteins from blood of patients with kidney failure, Journal of Chromatography B 739(1) (2000) 73-80.
[163] E. Menegatti, C. Ronco, J.F. Winchester, A. Dragonetti, D. Di Simone, A. Davit, G. Mengozzi, G. Marietti, G. Loduca, M. Mansouri, G.P. Sancipriano, L.M. Sena, D. Roccatello, Absence of NF-kappa B activation by a new polystyrene-type adsorbent designed for hemoperfusion, Blood purification 23(1) (2005) 91-98.
[164] M. Santin, M.A. Wassall, G. Peluso, S.P. Denyer, Adsorption of alpha-1-microglobulin from biological fluids onto polymer surfaces, Biomaterials 18(11) (1997) 823-827.
[165] M.D. Morena, D.Q. Guo, V.S. Balakrishnan, J.A. Brady, J.F. Winchester, B.L. Jaber, Effect of a novel adsorbent on cytokine responsiveness to uremic plasma, Kidney international 63(3) (2003) 1150-1154.
[166] R.A. Odell, P. Slowiaczek, J.E. Moran, K. Schindhelm, Beta2-Microglobulin Kinetics in End-Stage Renal-Failure, Kidney international 39(5) (1991) 909-919.
[167] K.E. Hagstam, L.E. Larsson, H. Thysell, Experimental Studies on Charcoal Haemoperfusion in Phenobarbital Intoxication and Uraemia Including Histopathologic Findings, Acta Med Scand 180(5) (1966) 593-+.
[168] M. Ghannoum, J. Bouchard, T.D. Nolin, G. Ouellet, D.M. Roberts, Hemoperfusion for the Treatment of Poisoning: Technology, Determinants of Poison Clearance, and Application in Clinical Practice, Seminars in dialysis 27(4) (2014) 350-361.
[169] C.A. Howell, S.R. Sandeman, Y. Zheng, S.V. Mikhalovsky, V.G. Nikolaev, L.A. Sakhno, E.A. Snezhkova, New dextran coated activated carbons for medical use, Carbon 97 (2016) 134-146.
[170] N.N. Cai, Q.S. Li, J.M. Zhang, T. Xu, W.Q. Zhao, J. Yang, L. Zhang, Antifouling zwitterionic hydrogel coating improves hemocompatibility of activated carbon hemoadsorbent, Journal of colloid and interface science 503 (2017) 168-177.
[171] J.D. Andrade, K. Kunitomo, Vanwagen.R, B. Kastigir, D. Gough, W.J. Kolff, Coated Adsorbents for Direct Blood Perfusion - Hema/Activated Carbon, T Am Soc Art Int Org 17(Apr) (1971) 222-&.
[172] N. Cai, Q. Li, J. Zhang, T. Xu, W. Zhao, J. Yang, L. Zhang, Antifouling zwitterionic hydrogel coating improves hemocompatibility of activated carbon hemoadsorbent, Journal of colloid and interface science 503 (2017) 168-177.
[173] C.J. Lee, S.T. Hsu, Preparation of Spherical Encapsulation of Activated Carbons and Their Adsorption Capacity of Typical Uremic Toxins, J Biomed Mater Res 24(2) (1990) 243-258.
[174] C.J. Liu, X.Y. Liang, X.J. Liu, Q. Wang, L. Zhan, R. Zhang, W.M. Qiao, L.C. Ling, Surface modification of pitch-based spherical activated carbon by CVD of NH(3) to improve its adsorption to uric acid, Applied Surface Science 254(21) (2008) 6701-6705.
[175] T. Mitome, Y. Uchida, Y. Egashira, K. Hayashi, A. Nishiura, N. Nishiyama, Adsorption of indole on KOH-activated mesoporous carbon, Colloid Surf. A-Physicochem. Eng. Asp. 424 (2013) 89-95.
[176] R. Sipehia, R.A.B. Bannard, T.M.S. Chang, Poly(Vinylidene Fluoride)-Coated or Poly(Vinylidene Chloride Vinyl Chloride)-Coated Activated-Charcoal for the Adsorption of Large Lipophilic Molecules with Exclusion of Small Hydrophilic Molecules, J Membrane Sci 47(3) (1989) 293-299.
[177] D.J. Malik, G.L. Warwick, M. Venturi, M. Streat, K. Hellgardt, N. Hoenich, J.A. Dale, Preparation of novel mesoporous carbons for the adsorption of an inflammatory cytokine (IL-1 beta), Biomaterials 25(15)

(2004) 2933-2940.
[178] X.P. Deng, T. Wang, F. Zhao, L.J. Li, C.S. Zhao, Poly(ether sulfone)/activated carbon hybrid beads for creatinine adsorption, J Appl Polym Sci 103(2) (2007) 1085-1092.
[179] C. Jackson, Design and In-vitro Characterisation of Novel Sorbent Device for Extracorporeal Blood Filtration and Other Applications, McGill University, 2012.
[180] Y.J. Jia, X.Y. Li, J.C. Jiang, K. Sun, Adsorption of creatinine on polyaniline-poly(styrene sulfonate) hydrogels based activated carbon particles, Iran Polym J 24(9) (2015) 775-781.
[181] R.K. Singh, S. Kumar, S. Kumar, A. Kumar, Development of parthenium based activated carbon and its utilization for adsorptive removal of p-cresol from aqueous solution, J Hazard Mater 155(3) (2008) 523-535.
[182] I. Bakas, K. Elatmani, S. Qourzal, N. Barka, A. Assabbane, I. Aît-Ichou, A comparative adsorption for the removal of p-cresol from aqueous solution onto granular activated charcoal and granular activated alumina, J. Mater. Environ. Sci 5(3) (2014) 675-682.
[183] V.K. Upadhyayula, S. Deng, M.C. Mitchell, G.B. Smith, Application of carbon nanotube technology for removal of contaminants in drinking water: a review, Science of the total environment 408(1) (2009) 1-13.
[184] K.H. Chan, E.T. Wong, M.I. Khan, A. Idris, N.M. Yusof, Fabrication of polyvinylidene difluoride nano-hybrid dialysis membranes using functionalized multiwall carbon nanotube for polyethylene glycol (hydrophilic additive) retention, Journal of Industrial and Engineering Chemistry 20(5) (2014) 3744-3753.
[185] R. Sipehia, R. Bannard, T. Chang, Poly (vinylidene fluoride)-or poly (vinylidene chloride/vinyl chloride)-coated activated charcoal for the adsorption of large lipophilic molecules with exclusion of small hydrophilic molecules, Journal of membrane science 47(3) (1989) 293-299.
[186] D. Malik, G. Warwick, M. Venturi, M. Streat, K. Hellgardt, N. Hoenich, J. Dale, Preparation of novel mesoporous carbons for the adsorption of an inflammatory cytokine (IL-1β), Biomaterials 25(15) (2004) 2933-2940.
[187] X. Deng, T. Wang, F. Zhao, L. Li, C. Zhao, Poly (ether sulfone)/activated carbon hybrid beads for creatinine adsorption, Journal of applied polymer science 103(2) (2007) 1085-1092.
[188] S.R. Ash, Dialysis material and method for removing uremic substances, Google Patents, 1986.
[189] V. Wernert, O. Schäf, H. Ghobarkar, R. Denoyel, Adsorption properties of zeolites for artificial kidney applications, Microporous and Mesoporous Materials 83(1-3) (2005) 101-113.
[190] K. Namekawa, M.T. Schreiber, T. Aoyagi, M. Ebara, Fabrication of zeolite–polymer composite nanofibers for removal of uremic toxins from kidney failure patients, Biomaterials Science 2(5) (2014) 674-679.
[191] L. Lu, C. Samarasekera, J.T. Yeow, Creatinine adsorption capacity of electrospun polyacrylonitrile (PAN)-zeolite nanofiber membranes for potential artificial kidney applications, Journal of Applied Polymer Science 132(34) (2015).
[192] L. Lu, J.T. Yeow, An adsorption study of indoxyl sulfate by zeolites and polyethersulfone–zeolite composite membranes, Materials & Design 120 (2017) 328-335.
[193] G. Lesaffer, R. De Smet, N. Lameire, A. Dhondt, P. Duym, R. Vanholder, Intradialytic removal of protein-bound uraemic toxins: role of solute characteristics and of dialyser membrane, Nephrol Dial Transpl 15(1) (2000) 50-57.

[194] V. Wernert, O. Schäf, V. Faure, P. Brunet, L. Dou, Y. Berland, P. Boulet, B. Kuchta, R. Denoyel, Adsorption of the uremic toxin p-cresol onto hemodialysis membranes and microporous adsorbent zeolite silicalite, Journal of biotechnology 123(2) (2006) 164-173.
[195] V. Davankov, L. Pavlova, M. Tsyurupa, J. Brady, M. Balsamo, E. Yousha, Polymeric adsorbent for removing toxic proteins from blood of patients with kidney failure, Journal of Chromatography B: Biomedical Sciences and Applications 739(1) (2000) 73-80.
[196] M.D. Morena, D. Guo, V.S. Balakrishnan, J.A. Brady, J.F. Winchester, B.L. Jaber, Effect of a novel adsorbent on cytokine responsiveness to uremic plasma, Kidney international 63(3) (2003) 1150-1154.
[197] J. Li, L. Han, S. Liu, S. He, Y. Cao, J. Xie, L. Jia, Removal of indoxyl sulfate by water-soluble poly-cyclodextrins in dialysis, Colloids and Surfaces B: Biointerfaces 164 (2018) 406-413.
[198] S. Kang, J.E. Yang, J. Kim, M. Ahn, H.J. Koo, M. Kim, Y.S. Lee, S.R. Paik, Removal of intact β2-microglobulin at neutral ph by using seed-conjugated polymer beads prepared with β2-microglobulin-derived peptide (58–67), Biotechnology progress 27(2) (2011) 521-529.
[199] H.-A. Tsai, M.-J. Syu, Synthesis of creatinine-imprinted poly (β-cyclodextrin) for the specific binding of creatinine, Biomaterials 26(15) (2005) 2759-2766.
[200] H.-A. Tsai, M.-J. Syu, Preparation of imprinted poly (tetraethoxysilanol) sol–gel for the specific uptake of creatinine, Chemical engineering journal 168(3) (2011) 1369-1376.
[201] M. Tijink, J. Kooman, M. Wester, J. Sun, S. Saiful, J. Joles, Z. Borneman, M. Wessling, D. Stamatialis, Mixed matrix membranes: a new asset for blood purification therapies, Blood purification 37(1) (2014) 1-3.
[202] M.S. Tijink, M. Wester, G. Glorieux, K.G. Gerritsen, J. Sun, P.C. Swart, Z. Borneman, M. Wessling, R. Vanholder, J.A. Joles, Mixed matrix hollow fiber membranes for removal of protein-bound toxins from human plasma, Biomaterials 34(32) (2013) 7819-7828.
[203] C. Nie, L. Ma, Y. Xia, C. He, J. Deng, L. Wang, C. Cheng, S. Sun, C. Zhao, Novel heparin-mimicking polymer brush grafted carbon nanotube/PES composite membranes for safe and efficient blood purification, Journal of Membrane Science 475 (2015) 455-468.
[204] D. Berge-Lefranc, H. Pizzala, R. Denoyel, V. Hornebecq, J.L. Berge-Lefranc, R. Guieu, P. Brunet, H. Ghobarkar, O. Schaf, Mechanism of creatinine adsorption from physiological solutions onto mordenite, Micropor Mesopor Mat 119(1-3) (2009) 186-192.
[205] K. Namekawa, M.T. Schreiber, T. Aoyagi, M. Ebara, Fabrication of zeolite-polymer composite nanofibers for removal of uremic toxins from kidney failure patients, Biomater Sci-Uk 2(5) (2014) 674-679.
[206] R. Takai, R. Kurimoto, Y. Nakagawa, Y. Kotsuchibashi, K. Namekawa, M. Ebara, Towards a Rational Design of Zeolite-Polymer Composite Nanofibers for Efficient Adsorption of Creatinine, J Nanomater (2016).
[207] L.M. Lu, C. Samarasekera, J.T.W. Yeow, Creatinine adsorption capacity of electrospun polyacrylonitrile (PAN)-zeolite nanofiber membranes for potential artificial kidney applications, J Appl Polym Sci 132(34) (2015).
[208] L.M. Lu, J.T.W. Yeow, An adsorption study of indoxyl sulfate by zeolites and polyethersulfone-zeolite composite membranes, Mater Design 120 (2017) 328-335.
[209] J.Y. Li, L.L. Han, S.X. Liu, S. He, Y.M. Cao, J. Xie, L.Y. Jia, Removal of indoxyl sulfate by water-

soluble poly-cyclodextrins in dialysis, Colloid Surf. B-Biointerfaces 164 (2018) 406-413.
[210] S. Kang, J.E. Yang, J. Kim, M. Ahn, H.J. Koo, M. Kim, Y.S. Lee, S.R. Paik, Removal of Intact beta 2-Microglobulin at Neutral pH by Using Seed-Conjugated Polymer Beads Prepared with beta 2-Microglobulin-Derived Peptide (58-67), Biotechnol Progr 27(2) (2011) 521-529.
[211] J.H. Huang, Treatment of phenol and p-cresol in aqueous solution by adsorption using a carbonylated hypercrosslinked polymeric adsorbent, J Hazard Mater 168(2-3) (2009) 1028-1034.
[212] B.J. Gao, Y. Yang, J. Wang, Y. Zhang, Preparation and adsorption characteristic of polymeric microsphere with strong adsorbability for creatinine, J Biochem Mol Toxic 22(3) (2008) 166-174.
[213] G. Selvolini, G. Marrazza, MIP-based sensors: Promising new tools for cancer biomarker determination, Sensors 17(4) (2017) 718.
[214] H.A. Tsai, M.J. Syu, Synthesis of creatinine-imprinted poly(beta-cyclodextrin) for the specific binding of creatinine, Biomaterials 26(15) (2005) 2759-2766.
[215] C. Baggiani, L. Anfossi, C. Giovannoli, Molecular imprinted polymers as synthetic receptors for the analysis of myco-and phyco-toxins, Analyst 133(6) (2008) 719-730.
[216] K. Haupt, Peer Reviewed: Molecularly Imprinted Polymers: The Next Generation, Analytical chemistry 75(17) (2003) 376 A-383 A.
[217] H.A. Tsai, M.J. Syu, Preparation of imprinted poly(tetraethoxysilanol) sol-gel for the specific uptake of creatinine, Chem Eng J 168(3) (2011) 1369-1376.
[218] P.S. Malchesky, W. Varnes, W. Piatkiewicz, Y. Nose, Membranes Containing Sorbents for Blood Detoxification, T Am Soc Art Int Org 23 (1977) 659-666.
[219] E. Denti, J.M. Walker, D. Brancaccio, V. Tessore, Evaluation of Novel Sorbent Systems for Joint Hemodialysis and Hemoperfusion, Med Instrum 11(4) (1977) 212-216.
[220] P.S. Malchesky, W. Piatkiewicz, W.G. Varnes, L. Ondercin, Y. Nose, Sorbent Membranes - Device Designs, Evaluations and Potential Applications, Artificial organs 2(4) (1978) 367-371.
[221] E. Klein, F.F. Holland, K. Eberle, F.C. Morton, I. Cabasso, Sorbent-Filled Hollow Fibers for Hemopurification, T Am Soc Art Int Org 24 (1978) 127-130.
[222] H.J. Gurland, L.A. Castro, W. Samtleben, J.C. Fernandez, Combination of Hemodialysis and Hemoperfusion in a Single Unit for Treatment of Uremia, Clinical nephrology 11(3) (1979) 167-172.
[223] S. Saiful, Mixed matrix membrane adsorbers for protein and blood purification, (2007).
[224] M.S.L. Tijink, M. Wester, G. Glorieux, K.G.F. Gerritsen, J.F. Sun, P.C. Swart, Z. Borneman, M. Wessling, R. Vanholder, J.A. Joles, D. Stamatialis, Mixed matrix hollow fiber membranes for removal of protein-bound toxins from human plasma, Biomaterials 34(32) (2013) 7819-7828.
[225] D. Pavlenko, E. van Geffen, M.J. van Steenbergen, G. Glorieux, R. Vanholder, K.G.F. Gerritsen, D. Stamatialis, New low-flux mixed matrix membranes that offer superior removal of protein-bound toxins from human plasma, Scientific reports 6 (2016).
[226] C.X. Nie, L. Ma, Y. Xia, C. He, J. Deng, L.R. Wang, C. Cheng, S.D. Sun, C.S. Zhao, Novel heparin-mimicking polymer brush grafted carbon nanotube/PES composite membranes for safe and efficient blood purification, J Membrane Sci 475 (2015) 455-468.
[227] S. Ito, M. Yoshida, Protein-Bound Uremic Toxins: New Culprits of Cardiovascular Events in Chronic Kidney Disease Patients, Toxins 6(2) (2014) 665-678.
[228] D.H. Krieter, A. Hackl, A. Rodriguez, L. Chenine, H.L. Moragues, H.D. Lemke, C. Wanner, B.

Canaud, Protein-bound uraemic toxin removal in haemodialysis and post-dilution haemodiafiltration, Nephrol Dial Transpl 25(1) (2010) 212-218.
[229] Y. Yoshida, T. Sakai, M. Ise, Effects of Oral Adsorbent in the Rat Model of Chronic-Renal-Failure, Nephron 62(3) (1992) 305-314.
[230] P. Owada, M. Nakao, J. Koike, K. Ujiie, K. Tomita, T. Shiigai, Effects of oral adsorbent AST-120 on the progression of chronic renal failure: A randomized controlled study, Kidney international (1997) S188-S190.
[231] T. Miyazaki, I. Aoyama, M. Ise, H. Seo, T. Niwa, An oral sorbent reduces overload of indoxyl sulphate and gene expression of TGF-beta 1 in uraemic rat kidneys, Nephrol Dial Transpl 15(11) (2000) 1773-1781.
[232] K. Shimoishi, M. Anraku, K. Kitamura, Y. Tasaki, K. Taguchi, M. Hashimoto, E. Fukunaga, T. Maruyama, M. Otagiri, An oral adsorbent, AST-120 protects against the progression of oxidative stress by reducing the accumulation of indoxyl sulfate in the systemic circulation in renal failure, Pharmaceut Res 24(7) (2007) 1283-1289.
[233] Y. Iwasaki, H. Yamato, T. Nii-Kono, A. Fujieda, M. Uchida, A. Hosokawa, M. Motojima, M. Fukagawa, Administration of oral charcoal adsorbent (AST-120) suppresses low-turnover bone progression in uraemic rats, Nephrol Dial Transpl 21(10) (2006) 2768-2774.
[234] M. Asai, S. Kumakura, M. Kikuchi, Review of the efficacy of AST-120 (KREMEZIN((R))) on renal function in chronic kidney disease patients, Renal failure 41(1) (2019) 47-56.
[235] G. Schulman, R. Vanholder, T. Niwa, AST-120 for the management of progression of chronic kidney disease, International journal of nephrology and renovascular disease 7 (2014) 49-56.
[236] D. Falkenhagen, W. Strobl, G. Vogt, A. Schrefl, I. Linsberger, F.J. Gerner, M. Schoenhofen, Fractionated plasma separation and adsorption system: A novel system for blood purification to remove albumin bound substances, Artificial organs 23(1) (1999) 81-86.
[237] W. Laleman, A. Wilmer, P. Evenepoel, C. Verslype, J. Fevery, F. Nevens, Review article: non-biological liver support in liver failure, Aliment Pharm Therap 23(3) (2006) 351-363.
[238] B.K. Meijers, V. Weber, B. Bammens, W. Dehaen, K. Verbeke, D. Falkenhagen, P. Evenepoel, Removal of the uremic retention solute p-Cresol using fractionated plasma separation and adsorption, Artificial organs 32(3) (2008) 214-219.
[239] F. Brettschneider, M. Tolle, M. von der Giet, J. Passlick-Deetjen, S. Steppan, M. Peter, V. Jankowski, A. Krause, S. Kuhne, W. Zidek, J. Jankowski, Removal of protein-bound, hydrophobic uremic toxins by a combined fractionated plasma separation and adsorption technique, Artificial organs 37(4) (2013) 409-16.
[240] V. Binder, B. Bergum, S. Jaisson, P. Gillery, C. Scavenius, E. Spriet, A.K. Nyhaug, H.M. Roberts, I.L.C. Chapple, A. Hellvard, N. Delaleu, P. Mydel, Impact of fibrinogen carbamylation on fibrin clot formation and stability, Thromb Haemostasis 117(5) (2017) 899-910.
[241] V.V. Sarnatskaya, A.I. Ivanov, V.G. Nikolaev, E. Rotellar, K. von Appen, M. Haspar, V.N. Maslenny, H. Klinkmann, Structure and binding properties of serum albumin in uremic patients at different periods of hemodialysis, Artificial organs 22(2) (1998) 107-115.
[242] V.V. Sarnatskaya, W.E. Lindup, P. Walther, V.N. Maslenny, L.A. Yushko, A.S. Sidorenko, A.V. Nikolaev, V.G. Nikolaev, Albumin, bilirubin, and activated carbon: New edges of an old triangle, Artificial Cells Blood Substitutes and Immobilization Biotechnology 30(2) (2002) 113-126.

[243] V.G. Nikolaev, V.V. Sarnatskaya, A.N. Sidorenko, K.I. Bardakhivskaya, E.A. Snezhkova, L.A. Yushko, V.N. Maslenny, L.A. Sakhno, S.V. Mikhalovsky, O.P. Kozynchenko, A.V. Nikolaev, Deliganding Carbonic Adsorbents for Simultaneous Removal of Protein-Bound Toxins, Bacterial Toxins and Inflammatory Cytokines, Nato Sci Peace Sec A (2011) 289-+.
[244] V.V. Sarnatskaya, L.A. Yushko, L.A. Sakhno, V.G. Nikolaev, A.V. Nikolaev, D.V. Grinenko, S.V. Mikhalovsky, New approaches to the removal of protein-bound toxins from blood plasma of uremic patients, Artif Cell Blood Sub 35(3) (2007) 287-308.

Chapter 3: Carbamylation of several plasma proteins

3.1 Introduction

It has been suggested carbamylated albumin may cause enhanced tubular cell damage and promote peritubular fibrosis [34]. The finding implies that removal of C-Alb would lead to better clinical outcomes. A better understanding of the structural and functional changes that carbamylation produces in blood proteins would be a first step toward this goal. Besides human serum albumin (HSA), we considered two other proteins found in human blood. Fibrinogen (Fgn) is the third most abundant protein in plasma whose major role is to form insoluble fibrin clots during coagulation [245]. Coagulation abnormalities that cannot be managed with hemodialysis frequently appear in patients with end-stage renal disease [246]. Despite that some important mechanisms for abnormalities in stages of platelet adhesion, secretion and aggregation have been discovered, the involvement of carbamylation in the aberrant fibrin clot formation was identified [240]. α-lactalbumin (LA) is a 14 kDa milk transport protein for items like essential amino acids and calcium, but can also function as a bactericidal agent [247] and in this study serves as a small molecule probe for the surface to understand size effects on the adsorption process. Together, the three selected proteins (HSA, Fgn, LA) represent a range of molecular sizes from small (~10 kDa) to large (~340 kDa).

All three proteins are slightly negatively charged at neutral pH, with their isoelectric point, size, and shape listed in Table 3-1. Unlike the globular HSA and α-lactalbumin, fibrinogen has an elongated shape with the dimension of 9 × 47.5 × 6 nm [248]. To determine the structural and property changes that carbamylation produces in these three proteins, we evaluated secondary and tertiary structure as well as zeta-potential. We measured NMR

transverse relaxation (T_2) to study the interaction between water and the carbamylated proteins.

Table 3-1 Molecular weight (Mw), isoelectric point, and Stokes radius for Albumin, Fibrinogen and α-lactalbumin

Protein	Mw (kDa)	Isoelectric Point		Stokes radius[a] (nm)	
Serum Albumin	66.5	5.0	[249]	3.5	[250]
Fibrinogen	340	5.5	[251]	10.7	[250]
α-lactalbumin	14.2	4.2	[252]	1.9	[253]

[a] Stokes radius in references was calculated by means of the Stokes-Einstein equation: $a=kT/6\pi\eta D$

Self-assembled monolayers (SAM) are a common platform for studying protein adsorption [254-258], where a well ordered layer of alkanethiols chemisorb to the Au interface. SAMs allow a great variety of functional terminal groups and were chosen here as a gold-standard, well-characterized surface to study adsorption properties of these altered proteins. Generally, a more hydrophobic surface can be formed using $–CH_3$ as the terminal chemistry rather than –OH, and has generally been shown to have a greater affinity toward plasma proteins like HSA or Fgn [255, 256].

In this work, $–CH_3$ and –OH SAMs on gold surfaces were formed according to well-established protocols and employed to evaluate the adsorption of carbamylated proteins. Our aim here is to analyze how protein modification *via* carbamylation directly affects protein-surface interactions, with the intention to correlate the results to the structural changes that occur upon carbamylation.

3.2 Experiments

3.2.1 Materials

Albumin from human serum (HSA, lyophilized, fatty acid free), fibrinogen from bovine plasma (Fgn, ≥75% clottable) and α-lactalbumin from human milk (LA) were purchased from Sigma-Aldrich (Canada). Sodium cyanate, 2-aminobenzoic acid (ABA), trichloroacetic acid (TCA), sodium tetraborate (ST), 2,4,6-trinitrobenzenesulfonic acid (TNBS), acrylamide, 1-Dodecanethiol (DT) and 1-Mercapto-1-undecanol (MUOH) were also provided by Sigma-Aldrich (Canada). All dilutions and buffers were prepared with syringe filtered (0.22 μm) milli-Q deionized water. Silicon wafers (single side polished) were purchased from University Wafer Co., and were sputtered with an adhesion layer of Ti/W (10% Ti, 90% W, 20 nm) followed by a 20 nm Au layer before use.

3.2.2 *In vitro* carbamylation of albumin, fibrinogen and α-lactalbumin

In vitro Carbamylation was carried out by incubating protein sample (6.25 mg/ml) under 0.1 M phosphate buffer (PB, pH 7.4) with 96 mM sodium cyanate at room temperature. After certain period, unbound cyanate was removed by ultrafiltration with PB for several cycles. ABA assay, as reported elsewhere [107, 259], was used to prove absence of residual cyanate. In brief, 0.5 ml of solution that may contain residual cyanate was added into a solution of 6 N HCl with 2-aminobenzoic acid for 1 min in boiling water bath and then cooled to room temperature, and the absorbance at 310 nm was recorded for quantification of residual cyanate. Solution protein concentration was determined using UV-Vis and

diluted to desired concentrations. The residual cyanate concentration and removal rate measured by ABA assay after each ultrafiltration was provided in Table 3-2. Determination of the degree of carbamylation was accomplished using the TNBS assay [260]. In brief, 25 μl of 0.03 M TNBS solution was added into 1 ml of sample solution. After agitation and standing for 30 min at room temperature, absorbance at 420 nm was recorded for quantification.

Table 3-2 Residual cyanate concentration and removal rate after each spin of ultrafiltration

Spin No.	Cyanate Concentration After Spin	Cyanate Removal Percent
1	32.5 mg/ml	95%
2	1.625 mg/ml	99.75%
3	0.08125 mg/ml	99.99%
4	0.0039 mg/ml	100%

3.2.3 Characterization of carbamylated proteins

3.2.3.1 Secondary structure characterization

Circular dichroism (CD) was conducted using a Jasco J-810 Spectropolarimeter. Protein solution was diluted to 0.1 mg/ml with PB (pH 7.4, 0.1 M) and was then loaded on a 0.5 mm pathlength cell for spectra collecting. All spectra (190~260 nm) are averages of 5 measurements obtained at the scanning speed of 100 nm/min under room temperature. Background spectrum of 0.1 M PB was collected and subtracted from sample spectra [261]. CDNN software was used to deconvolute the spectra into each secondary structure component.

3.2.3.2 Zeta-potential characterization

Zeta-potential was measured using Malvern Nano-ZS DLS. Protein solution was concentrated to 8 mg/ml with 1 mM PB (pH 7.4) and all measurements were taken under 25 ^{o}C.

3.2.3.3 Tertiary structure characterization

Tertiary structure analysis was conducted using a PTI fluorescence spectrophotometer, with excitation wavelength fixed at 295 nm and emission wavelength ranged from 300~450 nm. The wavelength at which the peak intensity appeared in the emission scan was used as single emission wavelength for the quenching tests, where the emission intensity was collected repeatedly for 10 seconds to get the average intensity [262].

3.2.3.4 Characterization of protein hydration state through transverse relaxation measurements (T_2)

Protein solution was solvent exchanged by phosphate buffer (0.1 M, pH 7.4, deuterium oxide (D_2O)) through ultrafiltration and was then concentrated to required concentration. NMR relaxation test was performed on a 600 MHz SB Varian VNMRS NMR Spectrometer. T_2 measurement was carried out using a Carr–Purcell–Meiboom–Gill (CPMG) sequence [263]. The 90~180^{o} pulse spacing was 962.7 μs. Data points were obtained over 10 acquisitions (τ values array from 0.025 to 12.83 s) under 22 ^{o}C with a recycle delay of 10 s to avoid saturation [264]. The data points were then fitted using processing modules of VnmrJ 4.2 software to obtain T_2 values. T-test was done for slopes to be compared by doing univariate analysis of variance for linear model.

3.2.4 Protein adsorption on self-assembly monolayer (SAM) surface

3.2.4.1 Preparation of self-assembly monolayer (SAM) on gold

After deposition of gold, all wafers were then sliced into 10 mm x 10 mm pieces and cleaned using fresh hot piranha solution and rinsed with deionized water and 2-propanol and dried with nitrogen flow. For SAM preparation, 1 mM of DT or MUOH solution in ethanol was prepared and degassed by nitrogen bubbling for 30 mins, which was then transferred into jars containing gold wafer under nitrogen atmosphere and was kept overnight at room temperature. Unattached thiols were removed *via* repeated ultrasonication in ethyl acetate and then ethanol and the wafers were then dried through nitrogen stream. SAM modified wafers were sealed under nitrogen atmosphere before use. X-ray photoelectron spectroscopy (Kratos AXIS 165) and contact angle measurement were used to characterize the SAM with oligomer chain ended with $-CH_3$ (Au-CH_3) and –OH (Au-OH) separately. The thickness of the formed SAM layer was measured using ellipsometry and was fitted by Cauchy model (An=1.30, Bn=0.01, Cn=0.001, n=1.33 at 632.8 nm [265]). The optical constant (k_s, n_s) and gold layer thickness was obtained for bare gold sputtered wafers prior to SAM formation and was used in fitting of substrate model.

3.2.4.2 Protein adsorption study

Protein samples were diluted to 1 mg/ml by 0.1 M PB (pH 7.4) for adsorption test. Au or SAM modified Au surfaces were incubated with 200 μL of this solution under room temperature and were sealed for 30 min to prevent evaporation. Each wafer was then rinsed with Milli-Q water, dried under nitrogen flow and further dried under vacuum overnight.

Ellipsometry (M-2000V J.A. Woollam Ellipsometer) was used to quantify the amount of adsorbed protein. The optical constant (k_s, n_s) and thickness of the pre-existing surface (Au or Au-SAM) was obtained prior to protein adsorption and used in fitting of substrate model. Scanning wavelength was ranged from 300~1000 nm and three incidental angles (65^o, 70^o, 75^o) were applied. For ellipsometry measurement, the thickness of protein adhesion layer was fitted through Cauchy models (An=1.45, Bn=0.01, Cn=0.001) [266].

3.3 Result

3.3.1 Determination of degree of carbamylation

The degree of carbamylation was determined using an improved TNBS assay. Standard curve was plotted using virgin protein solutions of different concentrations and was shown in Figure 3-1. Calibration curves for all three proteins have high linearity (R^2>0.99). At least four different carbamylation periods were applied to each protein. The results in Figure 3-2a show that HSA has a higher carbamylation rate than other two proteins, with carbamylated lysine at 33% after the initial 5 hours, more than 20% higher than Fgn and LA ($p<0.01$). Fgn and LA have very similar carbamylation curves.

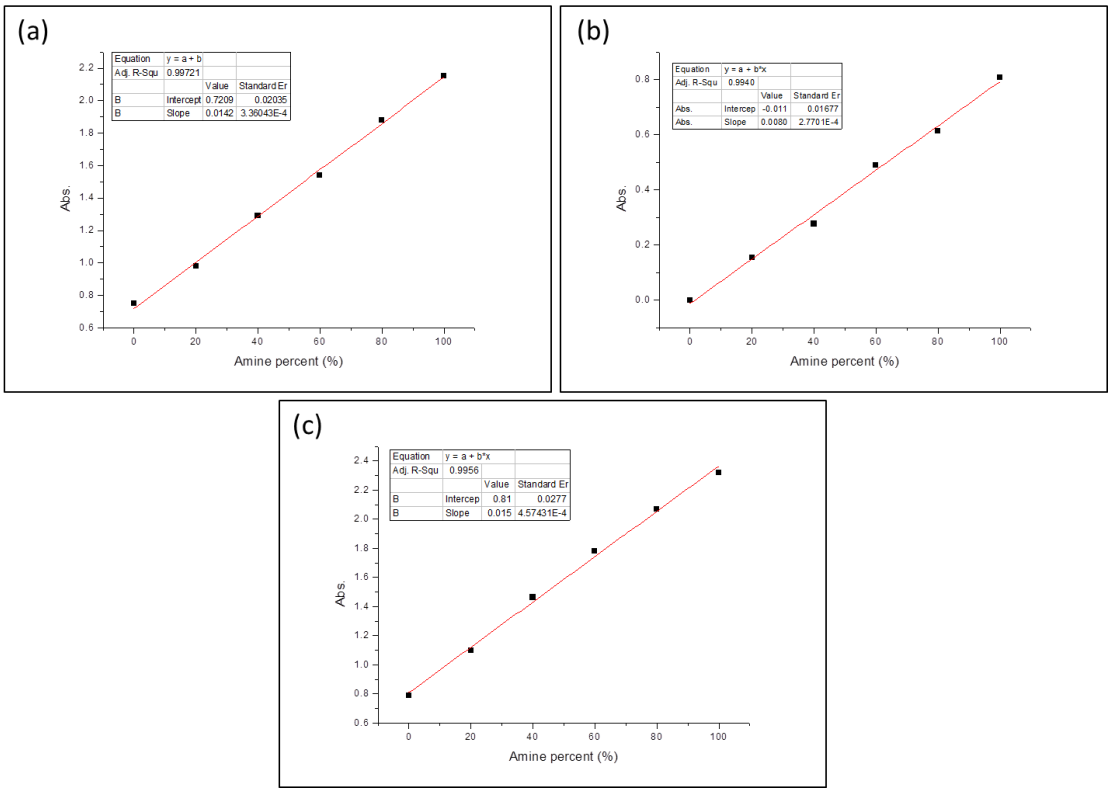

Figure 3-1 Standard curve of virgin (a) HSA, (b) Fgn (c) LA for amine conversion calibration through TNBS assay. Amine percent represents the relative concentration to virgin samples (2.5 mg/ml, 0.1 M PB at pH 7.4 and 25 oC.).

As expected, it was observed that increasing the degree of carbamylation reduces the number of positive charges found on proteins (Figure 3-2b). Both HSA and Fgn are slightly negatively charged proteins and LA has the lowest isoelectric point among the three proteins and exhibits the lowest zeta-potential. Interestingly, carbamylation of lysozyme, which is a positively charged protein, resulted in immediate and irreversible turbidity; causing us to remove this protein from further study. In addition to above findings, we also noticed a shift of isoelectric point (pI) caused by carbamylation. For HSA as an example, pI determined through zeta-potential was 4.85 for normal HSA and 4.17 for C-HSA-2d.

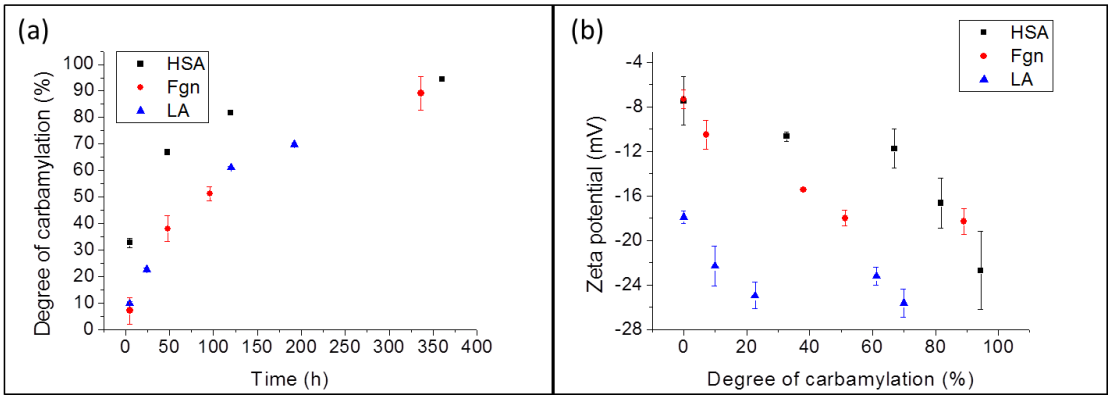

Figure 3-2 (a) Degree of carbamylation of HSA, Fgn and LA as a function of reaction time as determined using a TNBS assay. Data represent mean ±1 SD, n=3. (b) Zeta-potential of HSA, Fgn and LA as a function of degree of carbamylation with concentration of 8 mg/ml in 1 mM PB at pH 7.4 and 25 oC. Data represent mean ±1 SD, n=3.

3.3.2 Secondary and tertiary structure analysis

Circular dichroism (CD) spectra were collected to determine the effect of carbamylation on protein secondary structure (Figure 3-3a-c). Carbamylation yielded no extra peaks in the CD spectra of all three proteins, nor was there a significant change in the intensity of observed peaks relative to the control. From deconvolution of these curves (CDNN) no significant changes in terms of each structural component was observed.

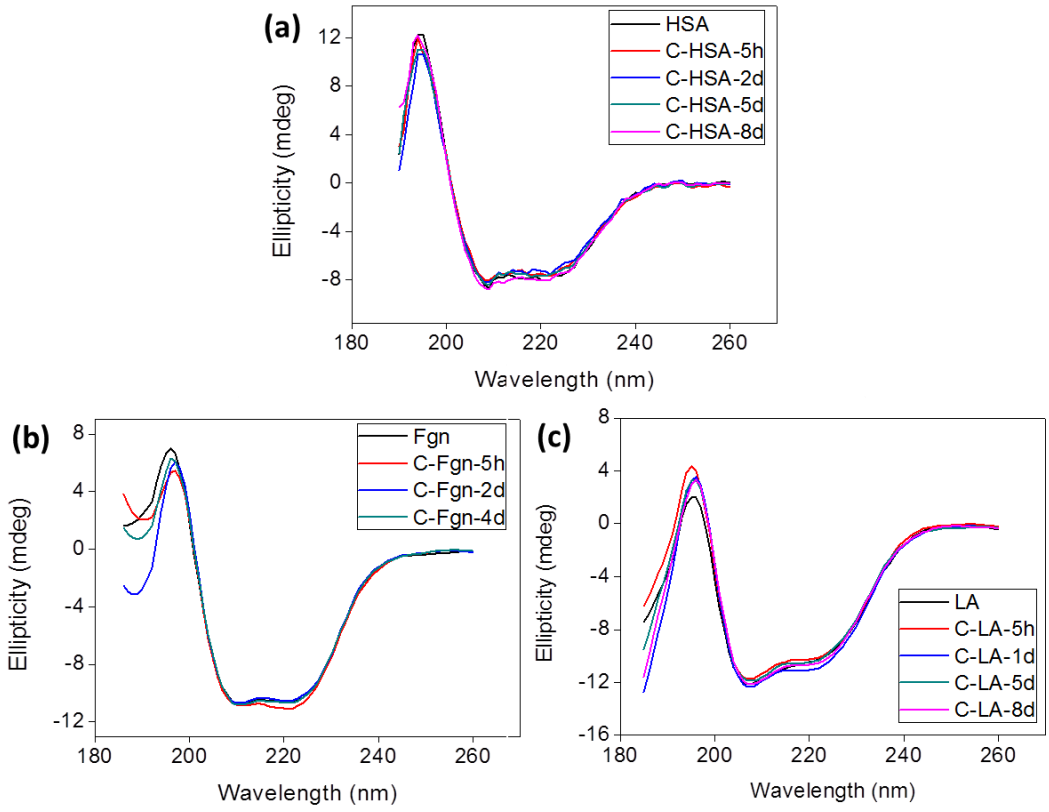

Figure 3-3 Circular dichroism spectra of native and carbamylated (a) HSA, (b) Fgn and (c) LA of different carbamylation period of 0.1 mg/ml in 0.1 M PB at pH 7.4 and room temperature. Data represent the average of n = 5 measurements.

To gain insight on how carbamylation affects tertiary protein structure, fluorescence spectroscopy was used to monitor any changes in the accessibility of tryptophans to acrylamide quenchers. Emission peaks obtained from these proteins using an excitation wavelength of 295 nm, are summarized in Table 3-3. For these data a blue shift in emission indicates that tryptophan residues reside within a less polar environment, and a red shift indicates the opposite. For HSA, the emission spectra was relatively broad with a similar ~333.5 nm peak for carbamylated samples. For Fgn and LA, a slight 1~1.5 nm blue shift of the emission peak was observed upon carbamylation. The plots of

fluorescence intensity as a function of acrylamide concentration were analyzed using the Stern−Volmer model. These data indirectly suggest that possible tertiary structure changes occur due to differences in ability of the acrylamide to access the tryptophans. Obtained spectra were corrected for dilution effects as well as acrylamide absorbance using a molar extinction coefficient at 295 nm of 0.23 and the following equation:

$$I_{corr} = I_{measured} \times 10^{0.23[acrylamide]/2}$$

For a protein with both accessible and inaccessible fluorophores, Stern−Volmer fits relationship can be expressed as:

$$\frac{I_0}{I_0 - I} = \frac{1}{f_a} + \frac{1}{f_a K_{sv}[Q]}$$

where I_0 is the unquenched intensity, I is the intensity with quenching, f_a is the fraction of quenched fluorophore, K_{sv} is the Stern-Volmer constant (M^{-1}), and [Q] is the concentration of quencher in [M]. For HSA, Fgn and LA, pristine and other two carbamylated samples were tested for quenching studies. The linearity of Stern-Volmer plots shown in Figure 3-4 a-c demonstrates the accessibility of both buried and exposed tryptophan to quencher [267]. T-test was done for slopes to be compared by doing univariate analysis of variance for linear model.

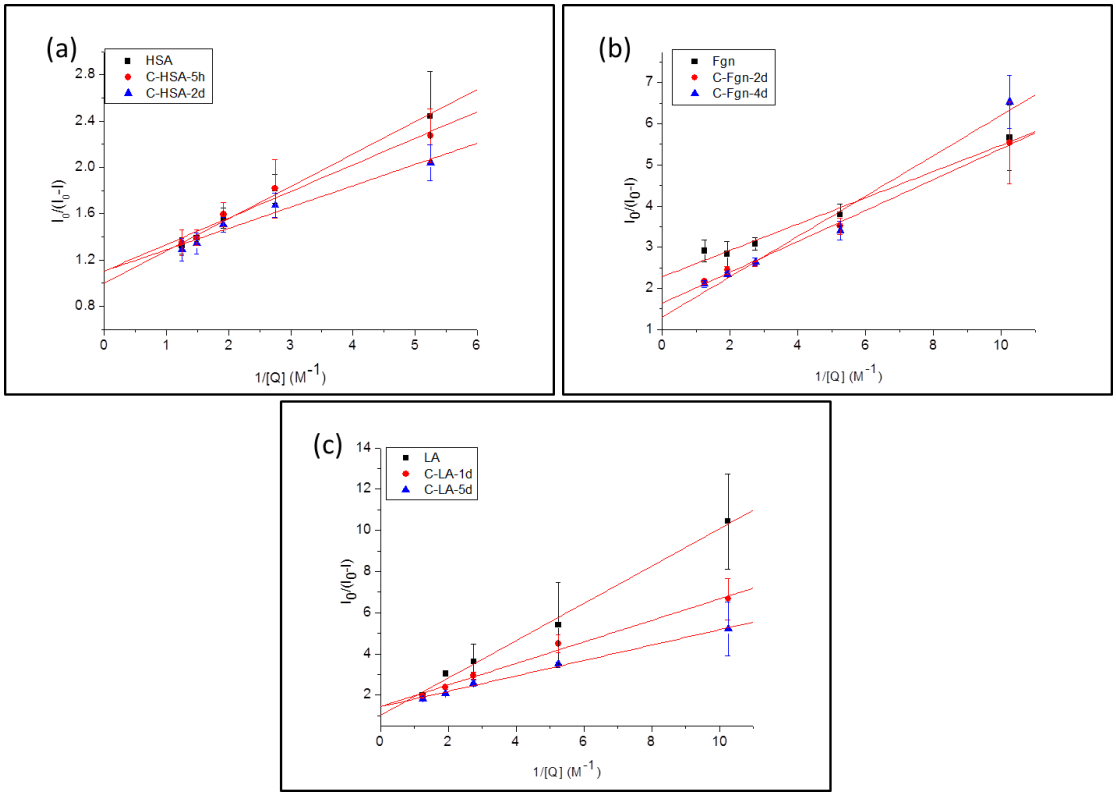

Figure 3-4 Modified Stern–Volmer plots of carbamylated (a) HSA, (b) Fgn and (c) LA. Intensity readings were corrected for acrylamide absorbance at 295 nm and dilution of the sample. Data represent mean ±1 SD, n=3. Linear fitting was achieved by weighted least-square method.

Table 3-3 Degree of carbamylation for each sample tested, wavelength with maximum fluorescence intensity (λmax) and Stern–Volmer Constants (Ksv) and Fraction of Accessible Tryptophan (fa) derived from the Linear Modified Stern–Volmer Fits

Sample	degree of carbamylation	λmax (nm)	f_a	K_{sv}
HSA	0	333.5	0.92	3.63
C-HSA-5h	32.7	333.5	0.82	5.14
C-HSA-2d	67.0	333.5	0.83	6.40
Fgn	0	338	0.44	7.16
C-Fgn-2d	38.0	336.5	0.61	4.38
C-Fgn-4d	51.4	336.5	0.77	2.66
LA	0	334	0.99	1.11
C-LA-1d	22.7	333	0.70	2.75
C-LA-5d	69.9	332.5	0.70	3.82

3.3.3 NMR water proton transverse relaxation time

NMR was used to study the water state in the solution of the tested proteins. NMR water proton transverse relaxation time is known to be sensitive to the protein solute [268]. The addition of the protein increases the NMR relaxation rate (T_2^{-1}) for water protons and a linear relationship can be established between T_2^{-1} and protein concentration, but it has to be below certain concentrations where the cooperative effect of adjacent protein molecules does not occur [269]. As shown in Figure 3-5b, d for HSA and LA with or without carbamylation, the expected linear relationship between relaxation rate and concentration

was established. For all three proteins, we observed that carbamylated proteins give lower slope values ($p<0.01$ for HSA and Fgn, $p<0.1$ for LA). For HSA samples the slope decreases from 0.88 to 0.32 s^{-1} wt.%$^{-1}$ for uncarbamylated and C-HSA-8d systems, respectively (Figure 3-5a, b). For LA samples the slope decreases from 0.91 to 0.38 s^{-1} wt.%$^{-1}$ for uncarbamylated and C-LA-5d systems, respectively (Figure 3-5c, d). For Fgn samples the slope decreases from 0.61 s^{-1} wt.%$^{-1}$ for uncarbamylated Fgn to -0.05 (approximately 0) s^{-1} wt.%$^{-1}$ for C-Fgn-4d (Figure 3-5e, f).

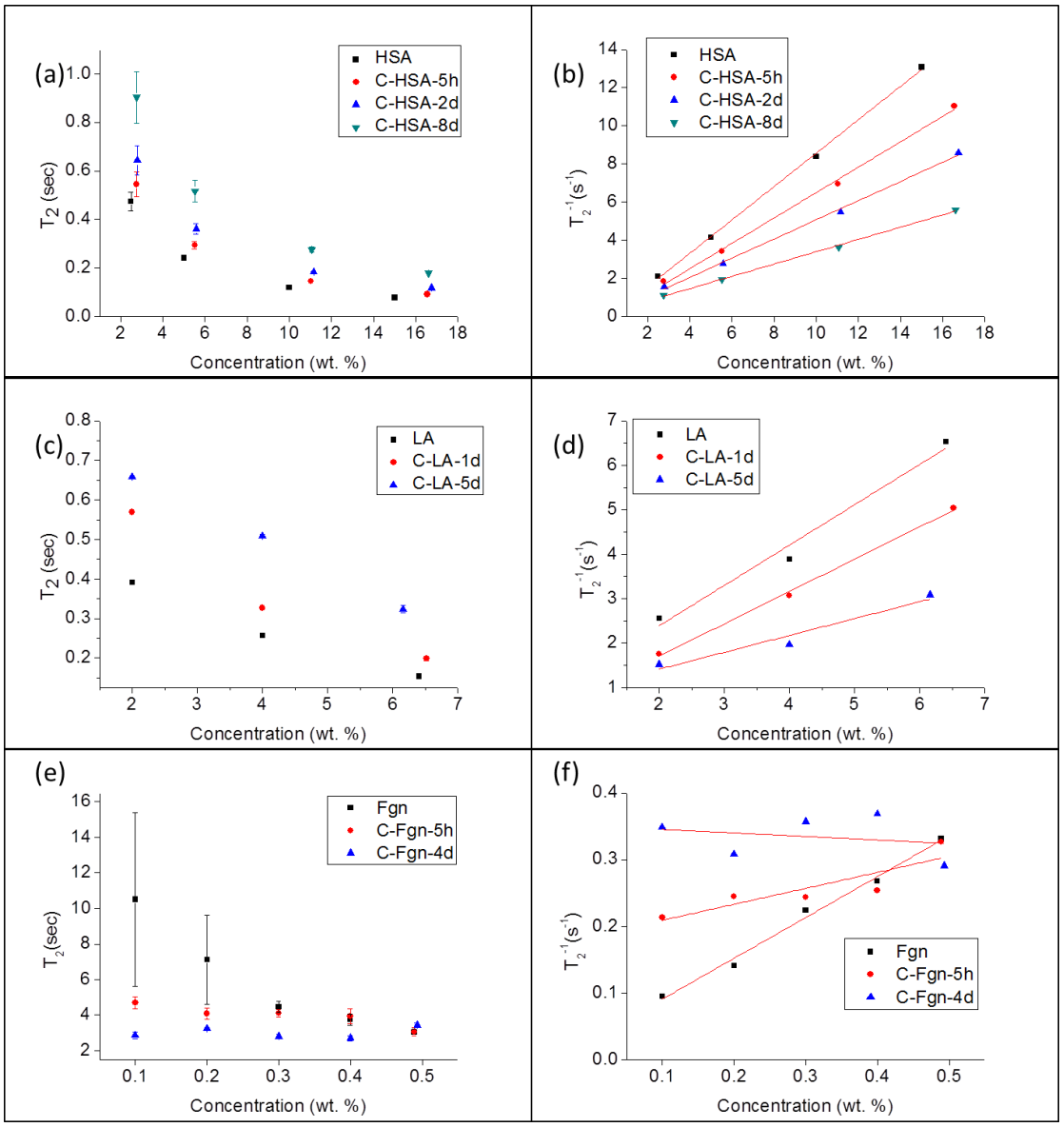

Figure 3-5 NMR spin-spin relaxation time (T2) of (a) normal and carbamylated HSA with different concentrations; (c) normal and carbamylated LA with different concentrations; (e) normal and carbamylated Fgn with different concentrations. Linear fitted NMR spin-spin relaxation rate (T2-1) of (b) normal and carbamylated HSA with different concentrations; (d) normal and carbamylated LA with different concentrations; (f) normal and carbamylated Fgn with different concentrations. Samples were dissolved in 0.1 M PB (pH=7.4, in D2O) and NMR tests were measured at 22 ^{o}C. T2 data represent mean ±1 SD, n=3.

3.3.4 Protein adsorption on Au and Au-SAM surface

SAMs were formed on Au coated surfaces using two alkyl thiols. Formed films were characterized using X-ray photoelectron spectroscopy (XPS). From the survey scan (Figure 3-6), only peaks corresponding to Au, C, O, and S were detected, with no additional peaks observed. Hi-Resolution XPS scans were obtained for Au 4f, C 1s, O 1s and S 2p peaks (Figure 3-7, 3-8). The chemical composition of three elements (C, O and S) was calculated by taking into account the relative sensitivity of their signal in XPSCasa. The results, together with the expected theoretical values, are summarized in Table 3-4. The S 2p content for both SAMs are lower than theoretical value, presented by a higher C/S ratio. The Au-OH surface seems to present a lower sulfur atomic percentage than Au-CH_3 surface. Compared to bare Au, both SAMs present a higher C/O ratio. SAM thickness (Table 3-4) was measured using ellipsometry, where DT and MUOH films were found to be 1.04 and 1.01 nm thick when dried, respectively. Contact angle measurement (Table 3-4) show that Au-CH_3 surface has higher sessile and dynamic contact angles than Au-OH or Au controls, whereas Au-OH has a slightly lower contact angle than unmodified Au.

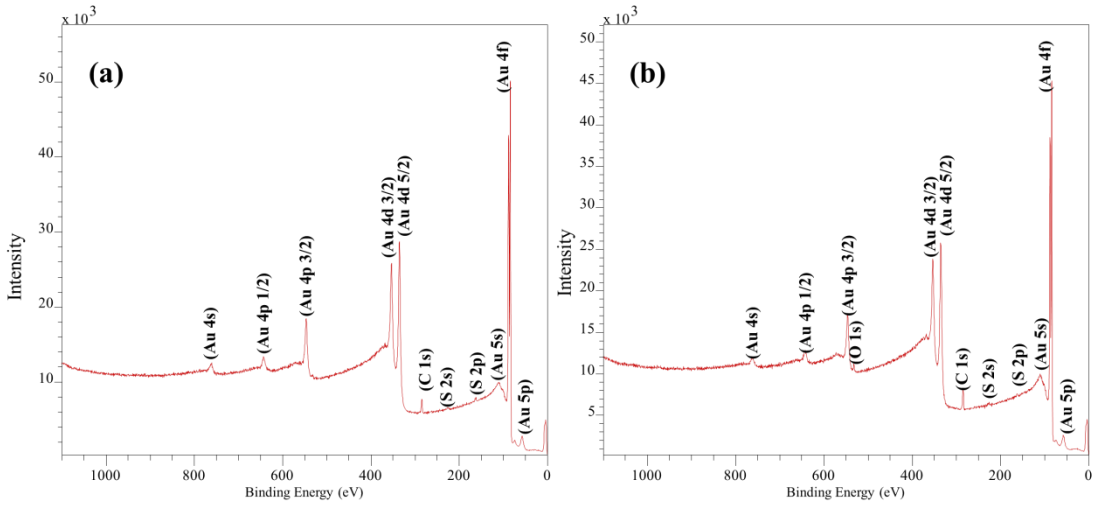

Figure 3-6 XPS survey scan for (a) Au-CH3 and (b) Au-OH

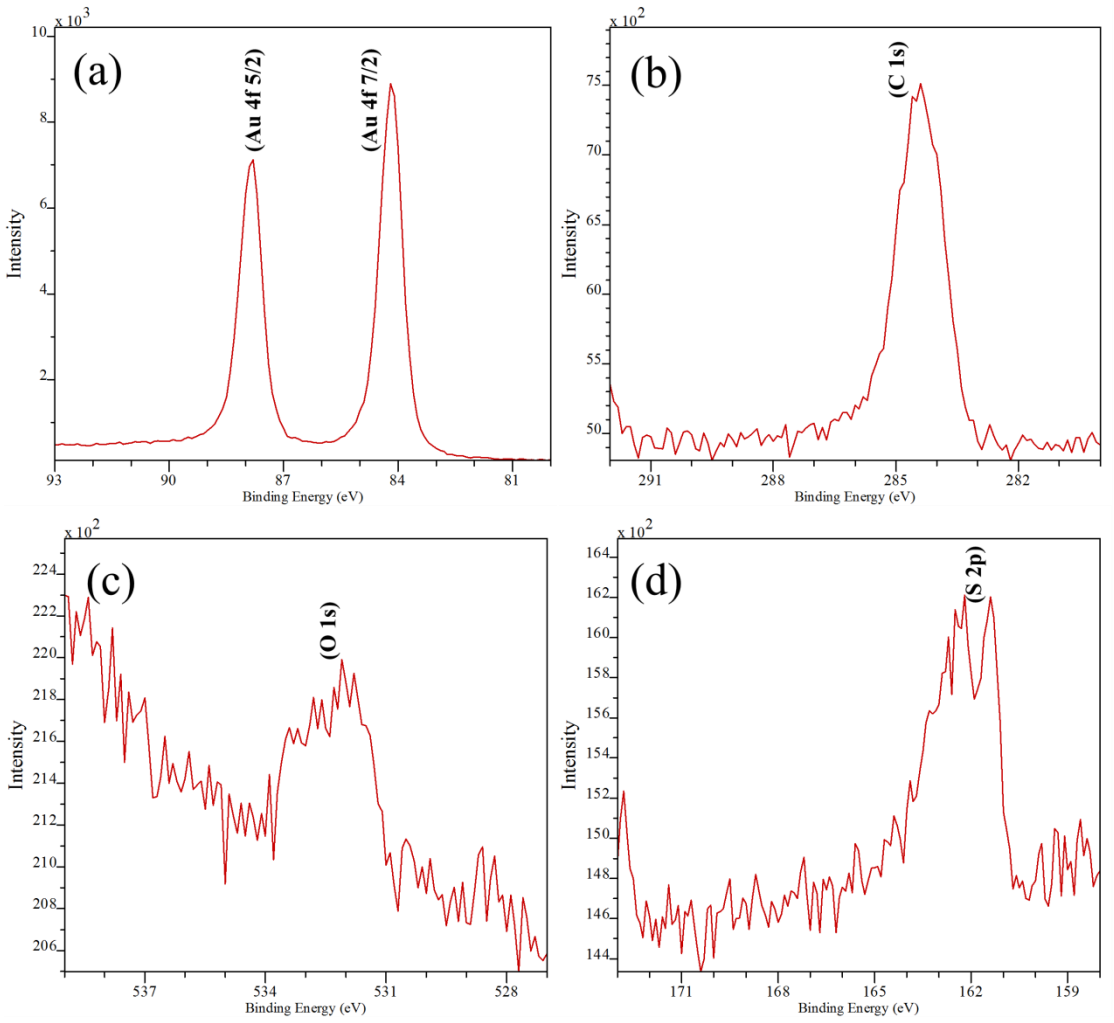

Figure 3-7 XPS high resolution scan of (a) Au 4f, (b) C 1s, (c) O 1s and (d)S 2p for Au-CH3

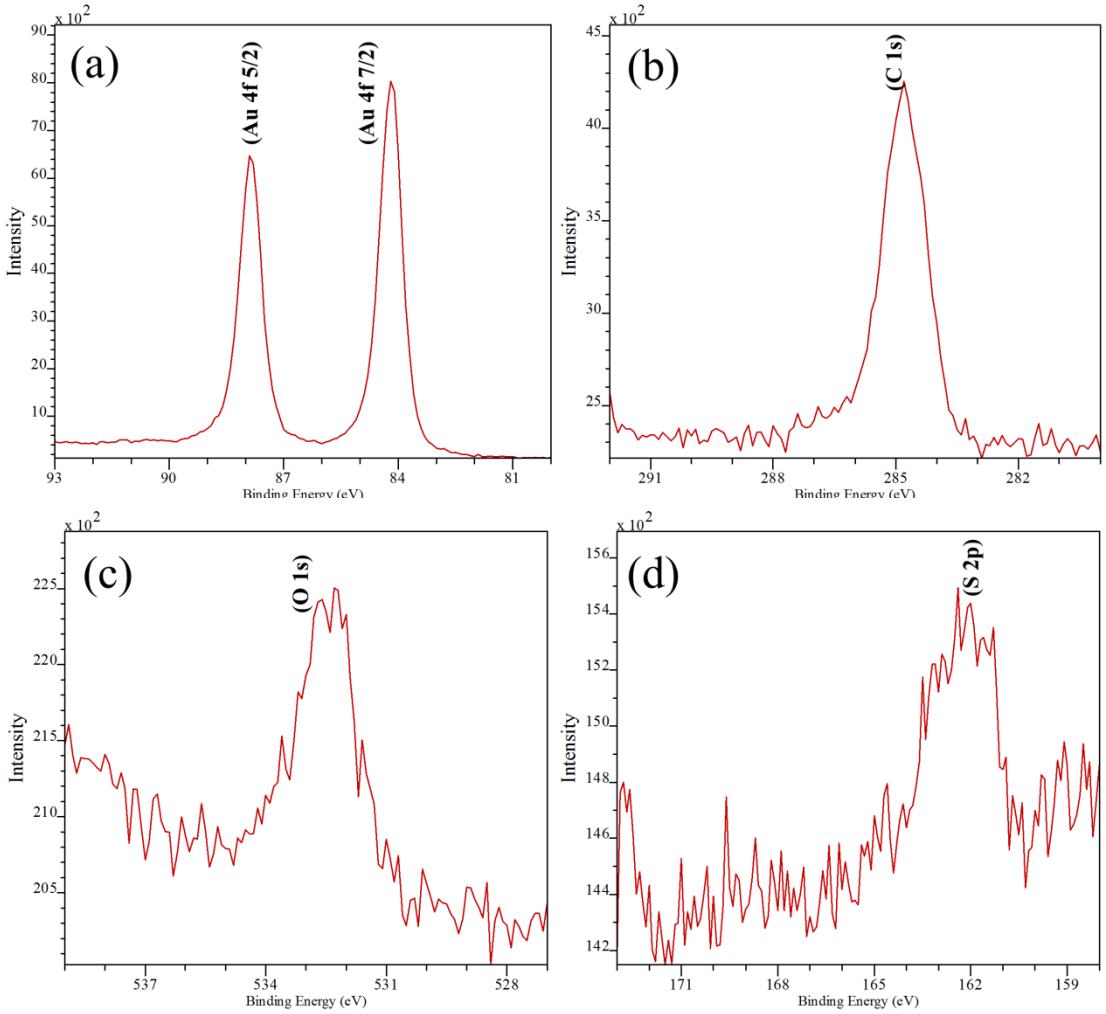

Figure 3-8 XPS high resolution scan of (a) Au 4f, (b) C 1s, (c) O 1s and (d)S 2p for Au-OH

Table 3-4 XPS elemental composition, thickness, and water contact angle of DT/MUOH SAM on Au. XPS test was performed with a take-off angle of 90°, and thickness and contact angle data represent average of n=3 measurements.

Sample	Elemental composition (%)			C/O	C/S	Thickness (nm)	Contact angle (°)			
	C 1s	O 1s	S 2p				Sessile	Advancing	Receding	hysteresis
Au-CH_3 (theoretical)	91.7	0	8.3	N/A	11.0	N/A	N/A	N/A	N/A	N/A
Au-OH (theoretical)	84.6	7.7	7.7	11.0	11.0	N/A	N/A	N/A	N/A	N/A
Au	79.6	20.4	0	3.9	N/A	N/A	74.9±4.6	84.4±2.0	36.5±1.4	47.9
Au-CH_3	84.1	10.7	5.2	7.9	16.0	1.04±0.11	103.5±1.2	104.6±2.0	66.0±0.8	38.6
Au-OH	82.1	14.9	3.0	5.5	27.6	1.01±0.14	56.1±3.0	82.4±4.6	30.8±1.5	51.6

With a similar degree of carbamylation (slightly higher than 50%), the adsorption result of C-HSA-2d, C-Fgn-4d, and C-LA-5d on bare Au surface suggested a significant decrease in C-Fgn-4d adsorption relative to virgin Fgn, but neither HSA nor LA exhibited significant differences upon carbamylation, shown in (Figure 3-9).

Adsorption onto the SAM modified surfaces (Figure 3-9) showed that on average more proteins adsorbed to Au-CH_3 than Au-OH, especially for Fgn and C-Fgn-4d. For -CH_3 terminated SAMs the carbamylated samples have generally lower layer thicknesses than those without carbamylation. A similar trend was observed for adsorption to the -OH

terminated SAMs, where carbamylated samples have a reduced thickness on average. The contrast in thickness between the carbamylated and non-carbamylated sample was more significant in Fgn or LA than in HSA.

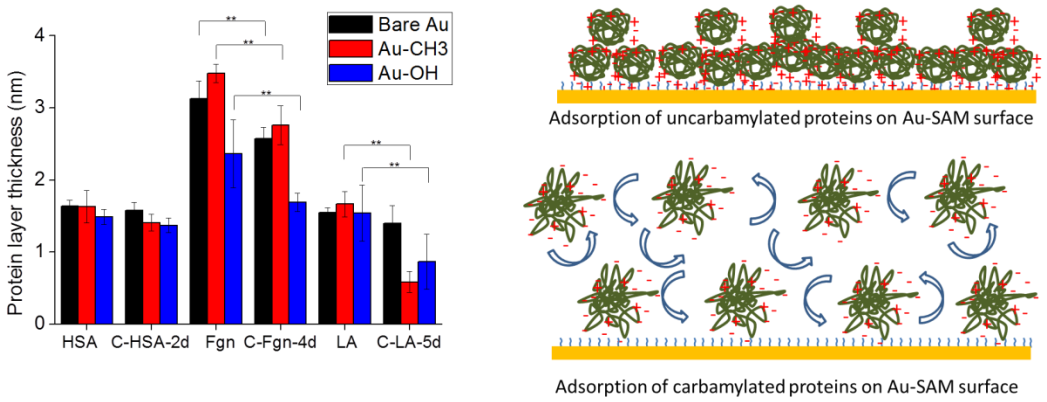

Figure 3-9 Left: Dry thickness of adsorbed protein on bare Au and SAM-modified Au measured using ellipsometry. Data represent mean ±1 SD, n=3; *, p < 0.1 (one way ANOVA); **, p<0.05 (one way ANOVA)). Right: Graphic illustration of adsorption difference between uncarbamylated and carbamylated protein.

For a protein monolayer on a surface, the following equation can be used to estimate the protein density [270-272]:

$$\Gamma = \delta(\frac{M}{A_r})(\frac{n^2-1}{n^2+2})$$

where Γ is the protein surface density (ng/cm^2), δ (nm) is the ellipsometry-measured protein layer thickness, M the molecular weight (g mol^{-1}), and Ar is the molar refractivity (cm^3 mol^{-1}). For simplicity, the ratio for protein samples measured is M/Ar = 4.12 g cm^{-3} [273], n is refractive index for the adsorbed 'dry' protein layer (approx. as 1.53). For estimation of theoretical monolayer density, the projection area for both HSA and LA were calculated based on a globular structure, and projected area for Fgn was calculated based on a rod

model with a side-on orientation.

3.4 Discussion

3.4.1 Characterization of degree of carbamylation

Protein carbamylation was quantified through the change in free amines as a function of incubation time using a TNBS assay (Figure 3-2). As a negative control, virgin proteins were incubated in a cyanate free PB buffer to determine if the time of incubation affected the stability and structure of protein. It was observed that there was very little change in both structure and charge caused only by sample aging. In our study sodium dodecyl sulfate polyacrylamide gel electrophoresis (SDS-PAGE) was also used to assess the decomposition of proteins before and after carbamylation (Figure 3-10). The results show that all three proteins retain integrity of their components after the longest solution incubation times used for carbamylation. For HSA samples (MW 66.5 kDa) additional bands appeared at 150~200 kDa, which are commonly associated with impurities (less than 4% by agarose gel) found in commercial albumin [274]. Upon carbamylation these SDS-PAGE bands were similar to the virgin samples. These results suggest no decomposition or aggregation occurred throughout our study. However, it is still noteworthy that long solution incubation times are not appropriate for Fgn, as it will gradually aggregate and become unstable in solution at room temperature [275]. For this reason, we incubated the Fgn samples for no more than 4 days. Results of degree of carbamylation shown in (Figure 3-2a) suggests that under the same period of incubation with isocyanate, HSA has a higher extent of carbamylated lysines. A total number of available lysines for carbamylation for HSA, Fgn and LA is found to be 59, 208 and 11, respectively. Our results suggest that HSA is more susceptible to carbamylation than the other two proteins. Clinical studies have reported that the average percentage of carbamylated lysines for HSA at a single position

in the protein (lys549) for uremic patients is 0.9%, or twice that of non-uremic patients [28]. However, this may not represent the actual carbamylation extent as it may reflect a large fraction of HSA that is uncarbamylated for uremic patients, while also not characterizing any other carbamylation throughout the protein. By adding sodium cyanate dropwise into a well stirred protein solution, all proteins are supposed to be equally carbamylated, and throughout the molecule. We also observed that for all three types of protein, surface charges became more negative with increased degree of carbamylation (Figure 3-2b), which is consistent with the assumption that carbamylation would reduce the number of positive charges of proteins.

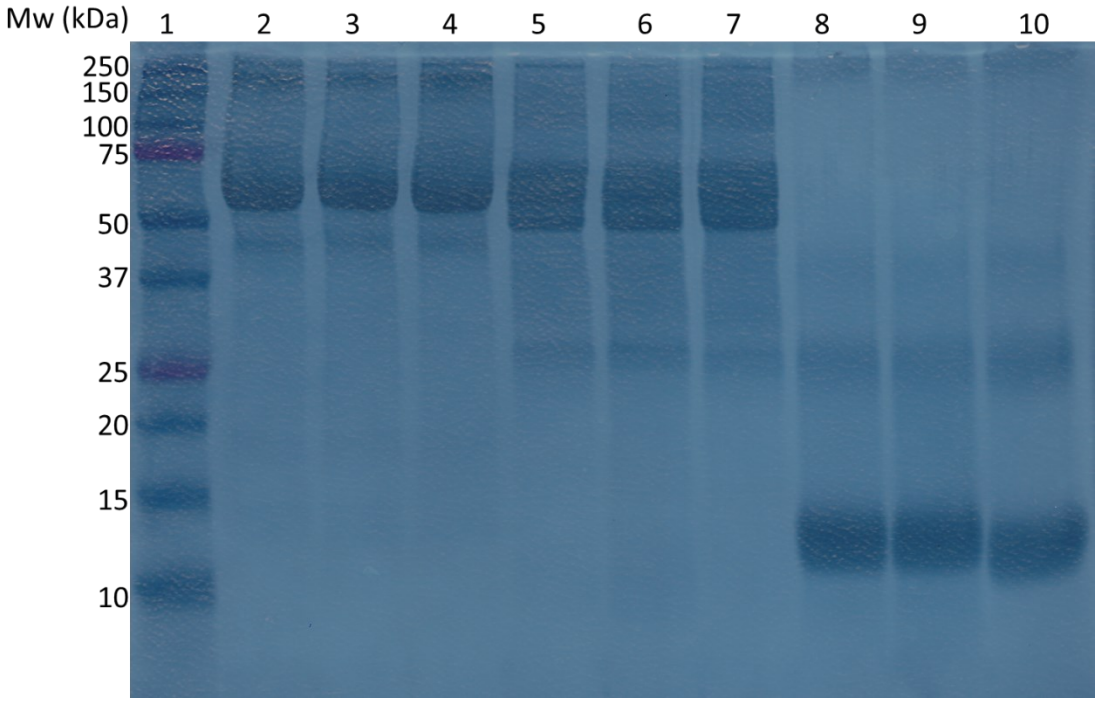

Figure 3-10 SDS-PAGE of 1. molecular weight ladder; 2~4. Fresh HSA, HSA after incubation for 8 days in PB (pH 7.4, 0.1 M) at room temperature, C-HSA-8d; 5~7. Fresh Fgn, Fgn after incubation for 4 days in PB (pH 7.4, 0.1 M) at room temperature, C-Fgn-4d; 8~10. Fresh LA, LA after incubation for 8 days in PB (pH 7.4, 0.1 M) at room temperature, C-LA-8d

3.4.2 Carbamylation affects tertiary structure more than secondary

Protein secondary structure studies did not show any peak shifts or any trend in peak intensity as a function of the extent of carbamylation. Overall CD spectra for these proteins did not change greatly upon carbamylation, nor were the relative composition of the secondary structures greatly affected. Although lysine has a low propensity to be found in alpha helices and lysine carbamylation might weaken this propensity, the helical content is the en masse average and is not significantly altered upon carbamylation.

In fluorescence spectra, we observed a very slight blue shift in λ_{max} after carbamylation, which may reflect the expected reduction in polar environment around the tryptophans upon carbamylation. The linearity of the data (Figure 3-4) is interpreted to mean that no unfolding or other significant conformation change occured during acrylamide titration. For native HSA an f_a of 92% shows that almost all tryptophans are able to be quenched. Carbamylation of HSA showed a reduction in f_a to ~0.83 after both 5 h to 2 days of reaction ($p<0.01$), indicating that there is a stable number of unquenched tryptophans for HSA. We may imagine that some carbamylated lysines would lose charge, becoming less polar and then entropically driven toward a more hydrophobic domain; as it has been recognized that more than 95 % of charged groups are exposed with high solvent-accessibility [276], it is possible that losing charges and carbamylation could decrease the acrylamide accessibility to the tryptophans around them. A more significant change was observed for the K_{sv} value for HSA, which was 3.63 for native protein and then 5.14 and 6.40 for 5 h and 2 day reacted protein. A K_{sv} increase indicates an increased quenching efficiency, thus, the tryptophans that are being quenched are done so with a higher

efficiency. This might be expected as the tryptophans that are no longer being quenched (~9%) may represent a subpopulation with low quenching efficiency and, when inaccessible, causes an increase in K_{sv}. The slight blue shift upon carbamylation may support this proposed mechanism. However, it is possible that since carbamylation reduces the positive charges and, hence, the protein becomes more negatively charged, enhanced repulsion between negatively charged residues might cause neighboring tryptophan to become more exposed to solvent [277]. The overall effect is enhanced quenching efficiency. Stronger repulsion forces should render the global structure more expanded, and this has been evidenced by increased Stoke's radius of BSA after carbamylation [32]. Either way, these data suggest a tertiary rearrangement has occurred for HSA upon carbamylation.

Native Fgn has a very low amount of accessible tryptophans, with only 43.8% of tryptophans able to be quenched by acrylamide. This low accessibility could be due to the large molecular weight and subchain entanglement of Fgn, which contains more inaccessible tryptophan than that of HSA. The carbamylated sample substantially increases the accessible fraction, to around 76.6% of accessible tryptophan for 51.35% carbamylated Fgn ($p<0.05$). Similar to HSA, Fgn was slightly negatively charged at pH 7.4. Carbamylation disrupts the balance of this charge to make it more negative, and this may disentangle subchains from each other or separate aggregated Fgn molecules, to get tryptophan more exposed to the solvent. However this makes the overall quenching efficiency drop from 7.16 to 2.66, which may be because the accessible tryptophan arising from inaccessible ones are not completely free from structural restrictions. For LA, a very significant decrease of accessible tryptophan was shown for the carbamylated sample, from 0.99 to 0.70 ($p<0.01$). There are some similarities between LA and HSA, both have their f_a decreased and K_{sv} increased after carbamylation. The observation of such change could be due to similar reasons.

3.4.3 Characterization of hydration state of carbamylated protein

With decreased charged groups, which mainly reside at the surface region of a protein, there may be less water molecules around the outer layer and this could cause carbamylated proteins to behave with more hydrophobic features. ^{1}H-NMR relaxation time informs water proton states. The linear relationship between relaxation rate and concentration has been described for protein solution by a well-established model, which takes three different protons into consideration: free water protons, hydration water protons and water protons in exchange with exchangeable protein protons, with free water protons as a slow relaxation component and the other two protons as a rapid relaxation component [278]. In this three-site exchange model the increase in observed relaxation rate is actually due to the contribution of both hydration water protons and exchangeable protons. Furthermore, each of the three proteins after carbamylation has a lower slope. In the three-site exchange model the slope is represented by $n(R_{2b}-R_{2a})$, where n is the hydration number, and R_{2b} and R_{2a} is the spin-spin relaxation rate of hydration water and bulk water, respectively. The lower slope is commonly attributed to either a lower fraction of hydrated water or decreased relaxation rate for hydration water protons [278]. The distribution coefficient, LogD, is the ratio of a compound (in both ionized and un-ionized form) in each of two different phases (usually water and octanol) and can be used to compare the lipophilicity of different compounds [279]. It is known that carbamylation of lysine leads to the formation of homocitrulline residues. LogD for lysine and homocitrulline at pH 7.4 was predicted by ACD/LogP DB Suite Version 9.0 (Advanced Chemistry Development, Inc. (ACD Labs)) to be -4.73 and -3.58, respectively. The high negative LogD value means both amino acids can be well hydrated in aqueous solution, and lysine with a more negative LogD should have a higher tendency to form hydrogen bond over hydrophobic interactions than

homocitrulline, and this supports the findings of weakened hydration observed in ^{1}H-NMR T_2 relaxation time for carbamylated proteins.

3.4.4 Characterization of SAMs and protein adsorption on SAMs

The adsorption of both native and carbamylated protein to bare Au surfaces and surfaces modified with $–CH_3$ and –OH terminated SAMs were conducted [255]. XPS results (Table 3-4) show a low S 2p content for both SAMs, which is commonly observed and likely a result of the signal being suppressed by the presence of the SAM monolayer [280]. The presence of C or O signal on bare Au surface is due to the so-called adventitious carbon (AdC) that appears as a contaminant when sputtered surface is exposed to air before testing [281]. The increased C/O ratio for Au-CH_3 and Au-OH indicates the presence of DT or MUOH and was similar to previously reported results for SAM modified Au surfaces [83, 255]. Ellipsometry returned thicknesses of $–CH_3$ and –OH SAMs were measured to be 1.04 ± 0.11 and 1.01 ± 0.14 nm, also similar to previously reported 11-carbon alkyl chain SAMs [265, 282]. The surface hydrophobicity change was characterized through water contact angle (Table 3-4) and an increased sessile contact angle for Au-CH_3 indicates the surface is more hydrophobic than Au, while a decreased sessile contact angle for Au-OH indicates the surface is more hydrophilic. A relatively high bare Au contact angle is commonly observed and attributed to carbonaceous contamination.

Protein adsorption experiments were done using a 30 min incubation time, and it was shown by many studies that 30 mins is enough to reach saturated protein adsorption on a SAM surface [255, 283, 284]. Adsorption of carbamylated HSA does not exhibit any significant difference compared to native HSA, nor did their adsorption differ on different types of surface. Both C-Fgn-4d and C-LA-5d have a lower adsorbed protein layer thickness, compared to native samples on any tested surface.

The layer densities for adsorbed proteins and expected amounts for a monolayer are detailed in Table 3-5. Adsorbed amounts of native HSA and C-HSA-2d are lower than the expected monolayer density of 261 ng/cm^2. This monolayer density is calculated from a rigid model of HSA molecules that does not undergo any conformational change upon adsorption. Previous reports indicate adsorbed amount of HSA can be lower than the expected monolayer coverage, due to adsorption-induced conformational and multilayer adsorption may be impeded by electrostatic repulsion [285],[286]. The surface property, either -CH_3 terminated or -OH terminated SAM, has almost no influence on adsorption density of HSA and C-HSA-2d. For LA, the experimental value measured was close to the monolayer value, while a lower than monolayer density value was observed for C-LA-5d on Au-CH_3 and Au-OH. Conformational change was found to occur for LA upon adsorption [287]. Unlike HSA with an almost complete unfolding upon adsorption [288], adsorption of LA results in a intermediate partially folded conformations, or the so called molten globule state [287]. The molten globule state was considered a compact conformation and may have a similar surface coverage to a native folded conformation, so it is possible the experimentally obtained LA density would resemble the density estimated for the monolayer. The decreased C-LA-5d adsorption on Au-CH_3 and Au-OH may suggest a larger extent of unfolding when carbamylated LA interacts with the SAM. For Fgn and C-Fgn-4d, the experimental values are intermediate between estimated side-on and end-on monolayer model. Rearrangement from side-on to end-on orientation has been observed for Fgn adsorption on -CH_3 and -OH terminated surface [288]. Upon carbamylation the charge profile of the protein becomes increasingly negative as the extent of carbamylation increases (Figure 3-2b), where zeta-potential differences ($\Delta\zeta$) with their native forms are -4.3 mV for HSA, -10.7 mV for Fgn, and -7.8 mV for LA. It should be noted that HSA with the lowest $\Delta\zeta$ shows the most insignificant adsorption difference between carbamylated and native form among all three proteins. It may be that the first adsorbed proteins are

affecting subsequent adsorption, where the lowest change in zeta-potential for HSA leads to less protein-protein interaction between vicinal proteins and yields similar adsorbed amounts compared to the native HSA. Whereas significant changes in zeta-potential may lead to more electrostatic repulsion between vicinal proteins and reduced amounts adsorbed. Therefore, we may speculate that a higher $\Delta\zeta$ may increase the protein repellence and lead to a less adsorbed amount (schematic illustration of Figure 3.9). However, it should be noted that electrostatic repulsion is only one of many factors involved in the complicated adsorption process with protein rearrangement and should not be seen as the only determining factor.

We have determined in NMR T_2 test that carbamylated proteins are less hydrated than native ones. Although the slope of linear regression representing the hydration state for all three proteins were shifted by -0.38 s^{-1} $wt.\%^{-1}$, -0.56 s^{-1} $wt.\%^{-1}$ and -0.66 s^{-1} $wt.\%^{-1}$ by C-HSA-2d, C-LA-5d and C-Fgn-4d, the weakened hydration did not result in increased adsorption density for all three carbamylated proteins, on any tested surface. One big difference between the charge and hydration is that charges presents only on protein surface, while hydration water is throughout the molecule. Therefore, the charge interaction should be more important when proteins interact with each other upon adsorption. In addition to this, it should be noted that carbamylated lysine (homocitrulline) is still a residue that can be hydrated and therefore the propensity for interaction of hydrophobic domains with the surface may not be significantly altered upon carbamylation. Thus, the on average reduced adsorption of HSA and significant ($p<0.05$) decrease for Fgn and LA adsorption to SAM surfaces may be influenced by the increased ratio of negative charges.

Table 3-5 Summary of dried protein adhesion layer thickness and estimated surface density. Each data point represents the average of n=3 measurements.

	Substrate	Average Thickness (nm)	Experimental density (ng/cm^2)	Theoretical Monolayer density (ng/cm^2)
HSA	Au	1.64±0.08	208±11	261
C-HSA-2d	Au	1.58±0.11	201±14	261
Fgn	Au	3.13±0.25	398±32	180-952
C-Fgn-4d	Au	2.58±0.16	328±20	180-952
LA	Au	1.55±0.07	197±9	189
C-LA-5d	Au	1.40±0.24	178±31	189
HSA	$Au-CH_3$	1.63±0.23	207±29	261
C-HSA-2d	$Au-CH_3$	1.41±0.11	179±15	261
Fgn	$Au-CH_3$	3.48±0.13	442±16	180-952
C-Fgn-4d	$Au-CH_3$	2.76±0.27	351±34	180-952
LA	$Au-CH_3$	1.67±0.18	212±22	189
C-LA-5d	$Au-CH_3$	0.58±0.14	74±18	189
HSA	Au-OH	1.49±0.11	189±13	261
C-HSA-2d	Au-OH	1.37±0.10	174±13	261
Fgn	Au-OH	2.37±0.47	301±60	180-952
C-Fgn-4d	Au-OH	1.69±0.13	215±17	180-952
LA	Au-OH	1.54±0.39	196±50	189
C-LA-5d	Au-OH	0.86±0.38	109±48	189

3.5 Conclusion

Protein carbamylation was studied in terms of its effects on protein property and adsorption behavior. It was found that carbamylation irreversible altered the protein charge and tertiary structure of albumin, fibrinogen and -lactalbumin. In addition, carbamylation also affected the water binding states of proteins, by weakening the protein's hydration. Adsorption studies revealed that carbamylated Fgn and LA were adsorbed at a lower amount to SAM surfaces than their native forms.

3.6 Reference

[28] A.H. Berg, C. Drechsler, J. Wenger, R. Buccafusca, T. Hod, S. Kalim, W. Ramma, S.M. Parikh, H. Steen, D.J. Friedman, J. Danziger, C. Wanner, R. Thadhani, S.A. Karumanchi, Carbamylation of Serum Albumin as a Risk Factor for Mortality in Patients with Kidney Failure, Science translational medicine 5(175) (2013).

[32] K.M. Fazili, M.M. Mir, M.A. Qasim, Changes in Protein Stability Upon Chemical Modification of Lysine Residues of Bovine Serum-Albumin by Different Reagents, Biochem Mol Biol Int 31(5) (1993) 807-816.

[34] M.-L.P. Gross, G. Piecha, A. Bierhaus, W. Hanke, T. Henle, P. Schirmacher, E. Ritz, Glycated and carbamylated albumin is more" nephrotoxic" than unmodified albumin in the amphibian kidney, American Journal of Physiology-Heart and Circulatory Physiology (2011).

[83] C.D. Bain, E.B. Troughton, Y.T. Tao, J. Evall, G.M. Whitesides, R.G. Nuzzo, Formation of Monolayer Films by the Spontaneous Assembly of Organic Thiols from Solution onto Gold, Journal of the American Chemical Society 111(1) (1989) 321-335.

[107] W.J. Yang, K.G. Neoh, E.T. Kang, S.S.C. Lee, S.L.M. Teo, D. Rittschof, Functional polymer brushes via surface-initiated atom transfer radical graft polymerization for combating marine biofouling, Biofouling 28(9) (2012) 895-912.

[240] V. Binder, B. Bergum, S. Jaisson, P. Gillery, C. Scavenius, E. Spriet, A.K. Nyhaug, H.M. Roberts, I.L.C. Chapple, A. Hellvard, N. Delaleu, P. Mydel, Impact of fibrinogen carbamylation on fibrin clot formation and stability, Thromb Haemostasis 117(5) (2017) 899-910.

[245] M.W. Mosesson, Fibrinogen and fibrin structure and functions, Journal of Thrombosis and Haemostasis 3(8) (2005) 1894-1904.

[246] D. Brian, P. Chowdary, Coagulation in Kidney Disease, in: M. Harber (Ed.), Practical Nephrology, Springer London, London, 2014, pp. 603-612.

[247] E.A. Permyakov, L.J. Berliner, alpha-Lactalbumin: structure and function, FEBS letters 473(3) (2000) 269-274.

[248] S.Y. Jung, S.M. Lim, F. Albertorio, G. Kim, M.C. Gurau, R.D. Yang, M.A. Holden, P.S. Cremer, The Vroman effect: A molecular level description of fibrinogen displacement, Journal of the American Chemical Society 125(42) (2003) 12782-12786.

[249] T. Peters, Serum-Albumin, Adv.Protein Chem. 37 (1985) 161-245.

[250] L.M. Siegel, K.J. Monty, Determination of Molecular Weights and Frictional Ratios of Proteins in Impure Systems by Use of Gel Filtration and Density Gradient Centrifugation . Application to Crude Preparations of Sulfite and Hydroxylamine Reductases, Biochimica et biophysica acta 112(2) (1966) 346-&.

[251] H.O. Ho, C.C. Hsiao, T.D. Sokoloski, C.Y. Chen, M.T. Sheu, Fibrin-Based Drug-Delivery Systems .3. The Evaluation of the Release of Macromolecules from Microbeads, Journal of Controlled Release 34(1) (1995) 65-70.

[252] C. Bramaud, P. Aimar, G. Daufin, Whey protein fractionation: Isoelectric precipitation of alpha-lactalbumin under gentle heat treatment, Biotechnology and bioengineering 56(4) (1997) 391-397.

[253] K. Gast, D. Zirwer, M. Muller-Frohne, G. Damaschun, Trifluoroethanol-induced conformational transitions of proteins: Insights gained from the differences between alpha-lactalbumin and ribonuclease A, Protein Science 8(3) (1999) 625-634.
[254] K.L. Prime, G.M. Whitesides, Adsorption of Proteins onto Surfaces Containing End-Attached Oligo(Ethylene Oxide) - a Model System Using Self-Assembled Monolayers, Journal of the American Chemical Society 115(23) (1993) 10714-10721.
[255] M.C.L. Martins, B.D. Ratner, M.A. Barbosa, Protein adsorption on mixtures of hydroxyl- and methylterminated alkanethiols self-assembled monolavers, Journal of Biomedical Materials Research Part A 67A(1) (2003) 158-171.
[256] S.N. Rodrigues, I.C. Goncalves, M.C.L. Martins, M.A. Barbosa, B.D. Ratner, Fibrinogen adsorption, platelet adhesion and activation on mixed hydroxyl-/methyl-terminated self-assembled monolayers, Biomaterials 27(31) (2006) 5357-5367.
[257] V.A. Tegoulia, S.L. Cooper, Leukocyte adhesion on model surfaces under flow: Effects of surface chemistry, protein adsorption, and shear rate, J Biomed Mater Res 50(3) (2000) 291-301.
[258] J.C. Lin, W.H. Chuang, Synthesis, surface characterization, and platelet reactivity evaluation for the self-assembled monolayer of alkanethiol with sulfonic acid functionality, J Biomed Mater Res 51(3) (2000) 413-423.
[259] M. Guilloton, F. Karst, A Spectrophotometric Determination of Cyanate Using Reaction with 2-Aminobenzoic Acid, Analytical biochemistry 149(2) (1985) 291-295.
[260] S.L. Snyder, P.Z. Sobocinski, An improved 2, 4, 6-trinitrobenzenesulfonic acid method for the determination of amines, Analytical biochemistry 64(1) (1975) 284-288.
[261] M. Binazadeh, H. Zeng, L.D. Unsworth, Effect of peptide secondary structure on adsorption and adsorbed film properties on end-grafted polyethylene oxide layers, Acta Biomaterialia 10(1) (2014) 56-66.
[262] S. Abraham, A. So, L.D. Unsworth, Poly(carboxybetaine methacrylamide)-Modified Nanoparticles: A Model System for Studying the Effect of Chain Chemistry on Film Properties, Adsorbed Protein Conformation, and Clot Formation Kinetics, Biomacromolecules 12(10) (2011) 3567-3580.
[263] S. Meiboom, D. Gill, Modified Spin-Echo Method for Measuring Nuclear Relaxation Times, Rev Sci Instrum 29(8) (1958) 688-691.
[264] B.P. Hills, S.F. Takacs, P.S. Belton, The Effects of Proteins on the Proton Nmr Transverse Relaxation-Times of Water .1. Native Bovine Serum-Albumin, Mol Phys 67(4) (1989) 903-918.
[265] T.T. Ehler, N. Malmberg, L.J. Noe, Characterization of self-assembled alkanethiol monolayers on silver and gold using surface plasmon spectroscopy, The Journal of Physical Chemistry B 101(8) (1997) 1268-1272.
[266] M.C. Sun, J. Deng, Z.C. Tang, J.D. Wu, D. Li, H. Chen, C.Y. Gao, A correlation study of protein adsorption and cell behaviors on substrates with different densities of PEG chains, Colloid Surf. B-Biointerfaces 122 (2014) 134-142.
[267] L.C. Kurz, D. LaZard, C. Frieden, Protein structural changes accompanying formation of enzymic transition states: tryptophan environment in ground-state and transition-state analog complexes of adenosine deaminase, Biochemistry 24(6) (1985) 1342-1346.
[268] J. Oakes, Protein hydration. Nuclear magnetic resonance relaxation studies of the state of water in native bovine serum albumin solutions, Journal of the Chemical Society, Faraday Transactions 1: Physical

Chemistry in Condensed Phases 72 (1976) 216-227.
[269] J. Clifford, J. Oakes, G. Tiddy, Nuclear magnetic resonance studies of water in disperse systems, Special Discussions of the Faraday Society 1 (1970) 175-186.
[270] P.A. Cuypers, J.W. Corsel, M.P. Janssen, J.M.M. Kop, W.T. Hermens, H.C. Hemker, The Adsorption of Prothrombin to Phosphatidylserine Multilayers Quantitated by Ellipsometry, Journal of Biological Chemistry 258(4) (1983) 2426-2431.
[271] S.J. McClellan, E.I. Franses, Adsorption of bovine serum albumin at solid/aqueous interfaces, Colloid Surf. A-Physicochem. Eng. Asp. 260(1-3) (2005) 265-275.
[272] M. Dargahi, S. Omanovic, A comparative PM-IRRAS and ellipsometry study of the adsorptive behaviour of bovine serum albumin on a gold surface, Colloid Surf. B-Biointerfaces 116 (2014) 383-388.
[273] P.A. Cuypers, J.W. Corsel, M.P. Janssen, J. Kop, W.T. Hermens, H.C. Hemker, The adsorption of prothrombin to phosphatidylserine multilayers quantitated by ellipsometry, Journal of Biological Chemistry 258(4) (1983) 2426-2431.
[274] J.-F. Hsieh, S.-T. Chen, Comparative studies on the analysis of glycoproteins and lipopolysaccharides by the gel-based microchip and SDS-PAGE, Biomicrofluidics 1(1) (2007) 014102.
[275] P. Weathersby, T. Horbett, A. Hoffman, Solution stability of bovine fibrinogen, Thromb Res 10(2) (1977) 245-252.
[276] A.A. Rashin, B. Honig, On the environment of ionizable groups in globular proteins, Journal of molecular biology 173(4) (1984) 515-521.
[277] C. Koro, A. Hellvard, N. Delaleu, V. Binder, C. Scavenius, B. Bergum, I. Główczyk, H.M. Roberts, I.L. Chapple, M.M. Grant, Carbamylated LL-37 as a modulator of the immune response, Innate immunity 22(3) (2016) 218-229.
[278] A. Le Dean, F. Mariette, M. Marin, (1)H nuclear magnetic resonance relaxometry study of water state in milk protein mixtures, Journal of agricultural and food chemistry 52(17) (2004) 5449-5455.
[279] G.H. Goetz, M. Shalaeva, Leveraging chromatography based physicochemical properties for efficient drug design, Admet Dmpk 6(2) (2018) 85-104.
[280] I. Zaccari, B.G. Catchpole, S.X. Laurenson, A.G. Davies, C. Walti, Improving the Dielectric Properties of Ethylene-Glycol Alkanethiol Self-Assembled Monolayers, Langmuir 30(5) (2014) 1321-1326.
[281] G. Greczynski, L.J.P.i.M.S. Hultman, X-ray photoelectron spectroscopy: Towards reliable binding energy referencing, 107 (2020) 100591.
[282] Y. Kamon, Y. Kitayama, A.N. Itakura, K. Fukazawa, K. Ishihara, T. Takeuchi, Synthesis of grafted phosphorylcholine polymer layers as specific recognition ligands for C-reactive protein focused on grafting density and thickness to achieve highly sensitive detection, Physical Chemistry Chemical Physics 17(15) (2015) 9951-9958.
[283] Y. Arima, H. Iwata, Effects of surface functional groups on protein adsorption and subsequent cell adhesion using self-assembled monolayers, Journal of Materials Chemistry 17(38) (2007) 4079-4087.
[284] L.Y. Li, S.F. Chen, S.Y. Jiang, Protein adsorption on alkanethiolate self-assembled monolayers: Nanoscale surface structural and chemical effects, Langmuir 19(7) (2003) 2974-2982.
[285] D.K. Goyal, A. Subramanian, In-situ protein adsorption study on biofunctionalized surfaces using spectroscopic ellipsometry, Thin Solid Films 518(8) (2010) 2186-2193.
[286] J. Benesch, A. Askendal, P. Tengvall, Quantification of adsorbed human serum albumin at solid

interfaces: a comparison between radioimmunoassay (RIA) and simple null ellipsometry, Colloid Surf. B-Biointerfaces 18(2) (2000) 71-81.
[287] M.F.M. Engel, C.P.M. van Mierlo, A.J.W.G. Visser, Kinetic and structural characterization of adsorption-induced unfolding of bovine alpha-lactalbumin, Journal of Biological Chemistry 277(13) (2002) 10922-10930.
[288] P. Roach, D. Farrar, C.C. Perry, Interpretation of protein adsorption: Surface-induced conformational changes, Journal of the American Chemical Society 127(22) (2005) 8168-8173.

Chapter 4: Phage display on carbamylated Human Serum Albumin

4.1 Introduction

Clearance of carbamylated albumin, as well as other proteins, has long been a problem, as it cannot be differentiated from normal albumin by conventional treatment such as hemodialysis, which is solely based on size difference. Accumulation of carbamylated HSA (cHSA) in uremic patients underwent hemodialysis seems to be inevitable [21]. Therefore more specific strategy has to be developed to enable selectively removal of carbamylated albumin.

In fact, presence of the anti-homocitrulline-containing protein antibodies has been found in autoantibody system for rheumatoid arthritis (RA) patients [55]. In addition, immunizing animals with peptides or proteins containing homocitrulline produces antibodies against this carbamylated proteins. For instance, polyclonal antibodies against carbamylated low density lipoprotein (cLDL) were produced by immunizing guinea pig [289] and rabbits [290] with cLDL. The anti-cLDL antibody produced from rabbit showed low cross-reactivity towards native LDL or other LDL isoforms. Likewise, in another study rabbits immunized with carbamylated HSA produced serum that has equal strong binding to homocitrulline-containing collagen telopeptides as serum generated from carbamylated type I collagen immunization [57]. From western blotting of anti-carbamylated protein antibodies for fetal calf serum with carbamylation, carbamylated albumin was found with the most intense band [291], this should suggest carbamylated albumin being the main antigen target. All these findings indicate that carbamylated protein antibody is in fact specific towards homocitrulline- containing species, but may not differentiate among

protein types.

Despite the fact that antibody against carbamylated albumin has been identified from anti-sera, production of these antibodies has to go through hybridoma technique, which involves complicated long period of preparation process including animal immunization and hybridoma cell culture, with only limited yield and poor repeatability [54]. In comparison, phage display technique allows for antibody or peptide generation with an easier procedure and a larger scale of production [39]. Despite the advantages in production, phage display allows for generation of target specific peptides, which should be more suitable for achieving our purpose of carbamylated protein removal. Once immobilized on surface, small peptides shall present more binding sites with higher density than antibodies. In addition, small peptides shall have higher nature stability under complex media environment and is more suitable for long term applications such as sensor or substrate for adsorption [43]. Although antibodies against carbamylated protein has been found in RA patient [55] and the monoclonal antibody has been prepared by way of hybridoma [56, 57], till now there has been no phage display derived peptide identified for carbamylated protein, not even any sequence of antibody for homocitrulline containing protein has been reported to our best knowledge. Realizing that peptide ligands may have great potential in selective protein removal [292], in this study we works on identifying such peptide ligands that are possible for isolation of carbamylated protein toxins without affecting the native ones.

4.2 Experiments

4.2.1 Materials

Albumin from human serum (HSA, lyophilized, fatty acid free) was purchased from Sigma-Aldrich. Sodium cyanate, 2-aminobenzoic acid (ABA), trichloroacetic acid (TCA), sodium tetraborate (ST), were also provided by Sigma-Aldrich. Amicon ultra-15

centrifugal filter unit was provided by Millipore Sigma. M13KE phage display kit (Ph.D-12) was provided by New England Biolabs. Homocitrulline/Citrulline Assay Kit was provided by Cell Biolabs for quantification of carbamylation. QIAprep Spin M13 Kit was provided by QIAGEN for template purification. Anti-M13 Antibody (HRP) (Mouse Monoclonal antibody) was provided by Sino Biological. ELISA Substrate Solution (1-Step™ Ultra TMB) was provided by ThermoFisher Scientific. Protein targets used were filtering sterilized before biopanning, and all solutions or supplied used in biopanning were autoclaved in advance. Sodium dodecyl sulphate-polyacrylamide gel electrophoresis (SDS-PAGE) precast gels (10% Mini-PROTEAN TGX Stain-Free Protein Gels) and protein standard ladder (Precision Plus Protein Dual Color Standards) were provided by Bio-Rad. All candidate peptides were synthesized by GL Biochem and the purity was verified by high-performance liquid chromatography (HPLC) with 98%, and the composition was confirmed by mass spectrometry.

4.2.2 *In vitro* carbamylation of HSA

In vitro carbamylation of HSA was done as reported before [28]. In brief, carbamylation was carried out by incubating HSA sample (0.6 mM) under 0.1 M phosphate buffer (PB, pH 7.4) with sodium cyanate at room temperature with stirring for 8 days. Initial concentration of sodium cyanate was varied for different degree of carbamylation. Unbound free cyanate was removed by three cycles of ultrafiltration with PB. ABA assay, as reported elsewhere [259] was used to prove absence of residual cyanate. In brief, 0.5 ml of solution that may contain residual cyanate was added into a solution of 6 N HCl with 2-aminobenzoic acid for 1 min in boiling water bath and then cooled to room temperature, and the absorbance at 310 nm was recorded for quantification of residual cyanate. Solution

protein concentration was determined using UV-Vis from absorbance at 280 nm and was then diluted to desired concentrations. Extent of carbamylation was quantified by the percentage of carbamylated lysine, marked as Hcit%, and was measured through homocitrulline assay following manufactory's protocol. In brief, samples were treated with Proteinase K with the presence of SDS at 37 ºC for 2 hrs, and was then incubated with urea-nitrogen reagent and diacetyl monoxime at 97°C for 30 minutes. Precipitates were removed by centrifuge at 18000 g for 10 mins, and the supernatant was transferred into a 96-well plate and analyzed at 550 nm with a plate reader. A standard curve of homocitrulline solution provided in the kit (0 to 600 μM) was made for determination of homocitrulline in sample. Hcit% was calculated by dividing the measured homocitrulline with the total lysine amount estimated (59 for one HSA molecule).

4.2.3 Protein characterization

The size and zeta-potential for both HSA and cHSA were measured through Malvern Nano-ZS DLS. For zeta-potential measurement, protein solution was concentrated to 8 mg/ml with 1 mM PB (pH 7.4). For size measurement, protein solution was diluted to 0.25 mg/ml with 0.1 M PB (pH 7.4). All measurements were taken at 25 ºC and each reported data represent average of three measurements. To verify the structure integrity of HSA after carbamylation, SDS-PAGE was performed on a Bio-Rad mini-protean electrophoresis system. The test was done following the standard protocol provided by Bio-Rad. In brief, both HSA and CHSA solution were denatured by mixing with SDS and heating at 60 ºC for 5 mins. After loading samples into wells of a precast gel, electrophoresis was performed at 200 V for ~ 30 mins. The gel was stained with 0.2 % Commassie Brilliant Blue, followed by destaining in acetic acid solution.

4.2.4 Biopanning against CHSA

4.2.4.1 Biopanning

Six wells of a 96-well ELISA plate were filled with CHSA target (100 μg/ml in 0.1 M carbonate buffer, pH 8.6) with 150 μl each well. Incubate the plate in a moisture environment at 4 ºC overnight, followed by discarding that target solution and refill fully with HSA blocking (5 mg/ml in 0.1 M carbonate buffer, pH 8.6) buffer for another 1 hr at 4 ºC. Prior to binding to target, the phage library was firstly screened on HSA for negative panning. The phage library was prepared at 10^{11} pfu/ml in TBST, and was added by pipetting 100 μl into wells pre-blocked with HSA only. After incubation for 1 hr at room temperature, the library solution was transferred to the plate with target, and was incubated for another 1 hr with gentle shaking. Unbound phages were removed by washing the wells with TBST-0.1% for 10 times, and the tween concentration was increased to 0.5 % after the first round. Surface bound phages were eluted with 100 μl glycine elution buffer (pH 2.2, containing 1 mg/ml HSA) for 15 mins and were neutralized with Tris-HCl buffer (pH 9.1). Elution was performed 3 times for each well and the collected eluates were denoted as E1, E2 and E3.

4.2.4.2 Phage amplification and purification

With a 250 ml Erlenmeyer flask, 20 ml of *E.coli* early log (OD_{600} 0.01-0.05) culture was mixed with 500 μl of each eluate and was incubated for 4.5 hr at 37 ºC with vigorous shaking. Bacteria were then separated by centrifuging at 12,000 g for 10 mins. Supernatant was collected and stored at 4 ºC overnight, with addition of 1/6 volume of PEG/NaCl to precipitate the phage. The precipitate was then centrifuged and further purified by re-dissolving in 1 ml TBS and precipitate again with 0.167 ml PEG/NaCl. The purified pellet was re-dissolved in 200 μl TBS and stored at 4 ºC.

4.2.4.3 Phage titration

Each amplified eluate was titrated with the blue plague titration method given in the supplier's manual. In brief, 200 µl of *E.coli* middle log (OD_{600} ~0.5) culture was mixed with 10 µl of eluate (10-fold serial dilution in TBS in the range of 10^8-10^{14}) and 790 µl melted top agar, and was poured onto a pre-warmed LB/IPTG/Xgal plate. All plates were incubated at 37 ºC overnight, and the blue plagues were counted as plaque-forming units (pfu).

4.2.4.4 Phage clone separation and template isolation for sequencing

For single clone phage collection, each separate blue plague for amplified eluate was picked and suspended into 100 µl TBS in a 96-well plate. The plate was heated at 60 ºC for 45 mins for sterilization. By mixing with 50 µl of 80% glycerol, each phage suspension was stored in -20 ºC. The single-stranded phage DNA was isolated with the QIAprep Spin M13 Kit following supplier's manual. In brief, each single clone phage suspension was amplified by adding 10 µl into 4 ml of *E.coli* early log (OD_{600} 0.01-0.05) culture and incubating for 4 hr at 37 ºC. After removing bacteria by centrifuge, 1/100 volume of buffer MP was added to each phage supernatant to incubate for 2 mins, and a total of 2.1 ml phage solution was loaded into QIAprep spin column and centrifuged to flow-through the column. To enable M13 phage lysis and template purification, 0.7 ml buffer PB was loaded into the column and flow-through by centrifuge, followed by 0.7 ml buffer PE loading and flow-through by centrifuge. Template was eluted by loading 100 µl EB. After incubating for 10 mins, eluate was collected by centrifuge. The template concentration (20-80 ng/ ul) and purity was verified by a NanoDrop UV-Vis spectrophotometer in its ssDNA measurement mode. For sequencing, 10 µl of each template was mixed with 1 µl -96 gIII sequencing primer, and the template sequence was obtained through standard Sanger DNA sequencing.

4.2.5 Phage binding specificity test: Enzyme-linked immunosorbent assay (ELISA)

To each well of a ELISA 96-well plate, 300 µl of protein of interest (1 mg/ml in 0.1 M carbonate buffer, pH 8.6) was added and was incubated in a moisture environment at 4 ºC overnight, followed by discarding protein solution and refill fully with TBST-0.5% blocking buffer for another 1 hr at 4 ºC. After washing the wells with TBST-0.5% to remove unbound protein, 20 µl of amplified single clone phage solution (10^{13} pfu/ml) was added with 180 µl TBST-0.5% buffer and was incubated for 2 hr. After washing the wells with TBST-0.5% to remove unbound phages, 200 µl of TBST-0.5% containing 1 µl HRP-AntiM13 (0.55 µg/ml) was added to each well and was incubated for 1 hr. After washing the wells with TBST-0.5% to send away unbound antibodies, 100 µl of HRP substrate was added to each well and was incubated for 10 mins. Reaction was quenched by adding 100 µl of 1 M H_2SO_4 and the absorbance at 450 nm was collected.

4.2.6 Peptide binding specificity test: Isothermal titration calorimetry (ITC)

ITC experiment was performed on a Nano ITC Low Volume isothermal titration calorimeters (TA instrument) with an active cell volume of 170 µL and injection syringe volume of 50 µL. All proteins and peptides were dissolved using the 0.1 M sodium phosphate buffer (pH 7.4). For titration of HSA/cHSA, protein concentration was 0.1 mM and peptide concentration was 2mM. For titration of Fgn/cFgn, protein concentration was 4 µM and peptide concentration was 0.21 mM. Titration was performed with 50 consecutive injections of 0.95 µL peptide solution with 200 s spacing between each injection. For titration of peptide into cHSA with antibody, cHSA was incubated with anti-Hcit for 2 hours at 25 ºC before titration, and both tirant and titrate solution were prepared

with 0.01 M PBS (pH 7.4) containing 50% glycerol and 0.02% NaN_3. The stirring rate and isotherm temperature were set at 150 rpm and 25 °C. The ITC data was processed by NanoAnalyze Data Analysis v3.10.0 for baseline subtraction and model fitting (independent model). Heat of peptide dilution was subtracted from signal by doing control titration tests. All data were repeated at least twice, and the data presented is a representative curve since only very small variations among repeats were observed. The fitted curves were analyzed through the statistical test program. The Gaussian distribution of results were obtained through repeated simulation with controlled random data perturbations for 1000 trials, and the 95% confidence interval were given and shown in the fitting graph.

4.2.7 Sodium dodecyl sulfate–polyacrylamide gel electrophoresis (SDS-PAGE)

SDS-PAGE was performed on a Bio-Rad mini-protean electrophoresis system. The test was done following the standard protocol provided by Bio-Rad. In brief, protein samples were denatured by mixing with SDS and heating at 60 ºC for 5 mins. After loading samples into wells of a precast gel, electrophoresis was performed at 200 V for ~ 30 mins. The gel was stained with 0.2 % Commassie Brilliant Blue, followed by destaining in acetic acid solution.

4.2.8 Molecular docking

Structure of cH2-p1 was created through I-TASSER Protein Structure and Function Prediction Services. [293-295] The potential binding sites for this predicted model were also provided in the result. A total of three possible binding sites were determined, with the top binding site (marked as cH2-p1-C1, and the surface is shown by the blue area in Figure 4-1b) showing significantly higher C-score [296] (0.33) compared to the other two, 0.14

and 0.13. To simulate homocitrulline residue present in protein, a model molecule Hcit-res (Figure 4-1c) was created. The docking grids set up in Python Molecule Viewer (PMV), version 1.5.6, were centered in the pocket of cH2-p1-C1. The box for docking was set to 8 Å × 16 Å × 14 Å to fully enclose the surface regions of all residues involved in cH2-p1-C1. AutoDock Vina was used for the docking experiment.[297]

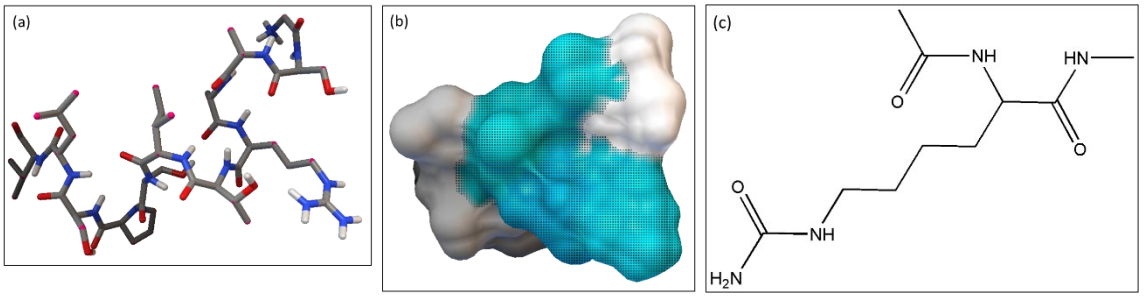

Figure 4-1 (a) Modeling conformation of cH2-p1 (b) Top ranked potential binding site, cH2-p1-C1, of cH2-p1 (c) Model molecule Hcit-res to mimic homocitrulline residue.

4.3 Result and discussion

4.3.1 *In vitro* carbamylation

In order to mimic the real target *in vivo*, the extent of carbamylation should be controlled to a value similar to that contained in uremic patients. However, the problem is that in uremic patients carbamylated albumin is always mixed with uncarbamylated ones and can hardly be distinguished for precise measurement. One study has determined that the proportion of HSA carbamylated at its most carbamylation susceptible site Lys-549 varied from 0.1% to 3% [28], implying that only a small fraction of HSA was carbamylated in whatever extent. Mapping of carbamylation sites through fragmentation and multiple reaction monitoring (MRM) studies identified up to 2 lysine sites (Lys-549 and Lys-160) much more susceptible to carbamylation than other sites. Hence we may roughly estimate the real carbamylation extent, or Hcit%, from 1.7% (1/59) to 3.4% (2/59).

In our study, the *in vitro* carbamylated HSA was prepared as a model carbamylation target. Homocitrulline level was used as a measure for degree of carbamylation. We have prepared cHSA with varied concentration of cyanate, which resulted in Hcit% of 0.54% (cHSA-1) and 2.7% (cHSA-2) (see Table 4-1). Purity of cHSA was verified through ABA assay, and the 0 absorbance at 310 nm proved the absence of residual cyanate. To verify the *in vitro* stability over carbamylation or time, SDS-PAGE study was performed. Both the bands for control HSA and cHSA-2 were stayed at the location in the range from 55 to 75 kDa, with no additional bands below or above (Figure 4-2), which is not surprising as cyanate only binds to a small fraction of lysine side chain to gain almost negligible molecular weight, nor will it cleave the peptide bond. It has been reported that the stoke's radius of BSA increased slightly after carbamylation [32]. Through DLS study we confirmed the protein diameter of native HSA increased from 9.4 nm to 12.6 nm for cHSA-1, and remained without further change for cHSA-2 (Figure 4-3). This might indicate that the protein size is only sensitive to change at a very slight degree of carbamylation.

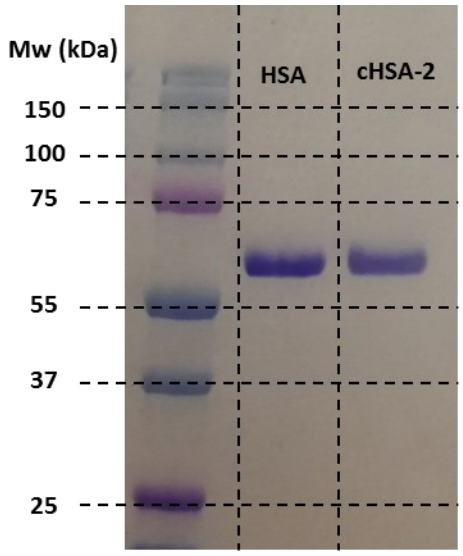

Figure 4-2 SDS-PAGE bands of native HSA and cHSA-2

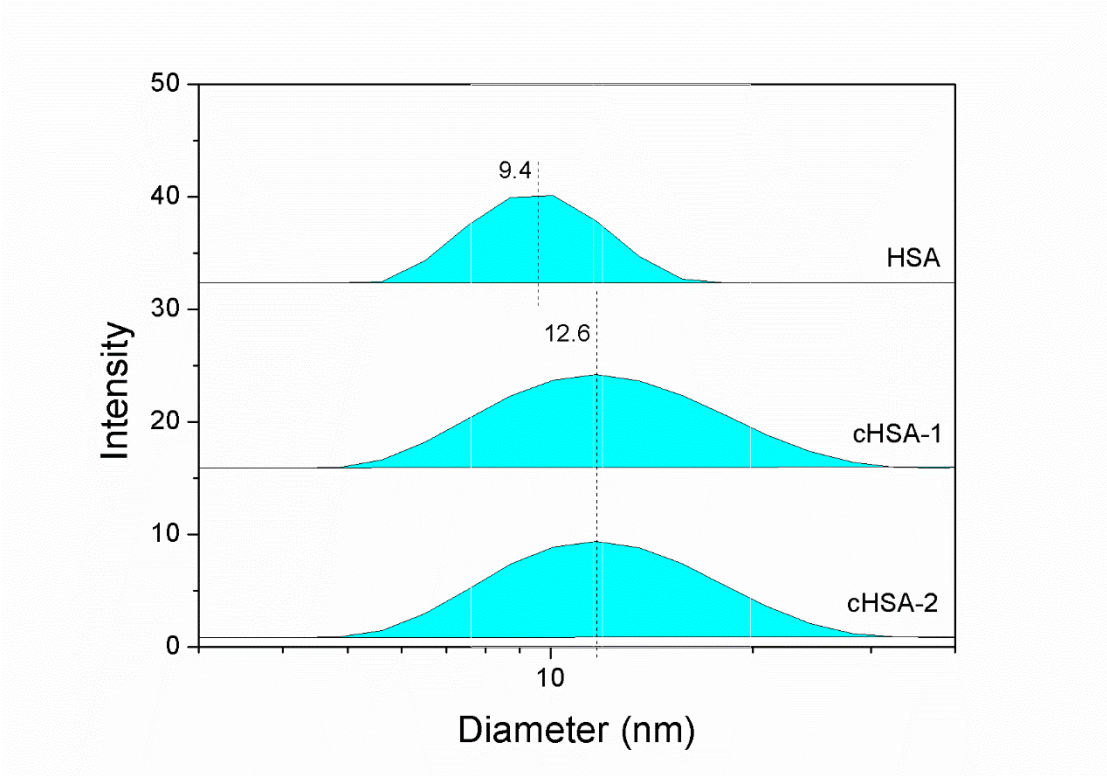

Figure 4-3 DLS size distribution of HSA, cHSA-1 and cHSA-2 (0.25 mg/ml in 0.1 M PB (pH 7.4), 25 ^{o}C, each curve represents average of three measurements)

Table 4-1 cHSA prepared through *In vitro* carbamylation

Sample	Hcit% (%)	zeta-potential (mV)
HSA	0	-7.46
cHSA-1	0.54	-7.84
cHSA-2	2.7	-10.8
cHSA-3	3.7	-11.7

4.3.2 Identification of candidate phage clones specific to cHSA

The Ph.D. -12 library was chosen for selecting carbamylation specific peptides towards cHSA. The 12mer random library gives a complexity of 10^9 variant clones and allows for more complicated folding structure than 7mer library. In our attempts to search for antibodies against homocitrulline containing species, we found no such antibody sequence recorded in IMGT databases [298, 299]. However, there were 31 sequences listed, with the acc. number from AJ430734 to AJ430772, for antibodies against citrulline containing peptide, submitted by Raats [300]. It is worthy of note that one commercial antibody, considered citrulline specific, has been found to be able to recognize both homocitrulline- and citrulline- containing albumins [57]. We noticed each of three Complementarity-determining regions (CDR) for these items generally consists of 7 to 15 amino acids, which makes 12mer peptides ideal choice for mimic these CDR. Since cHSA is derived from HSA, it is important to exclude the HSA binding phages during biopanning process. In fact, HSA binding motif with high affinity has been identified through phage display work before [301], with disulfide-constrained cyclic peptide phage-display libraries derived from M13mp18. Therefore in our work phage library was bound to HSA coated 96-well

plate surface in double repeats as negative biopanning to remove possible HSA binding phages, and hence cHSA specific phages were chosen from only weak HSA binding phage pool.

From biopanning on cHSA-1, we found only one sequence (APPHVSSTVSWL) present for all picked plagues after the first round. Although this sequence did not match any TUP record stored in SAROTUP database, we found this still could be one TUP with high propagation rate, as it is similar to one notorious propagation-related TUP APWHLSSQYSRT as reported in many biopanning result [302-304]. PHD7FASTER prediction revealed that it has a 0.96 probability to be with propagation advantage. While through the ELISA assay the obtained phage isolates (cH1-p1) failed to exhibit significantly higher absorbance on cHSA-1 compared to HSA to prove it as cHSA specific phages, we speculate cHSA-1 may lack the sufficient feature from HSA to be recognized by any phages and therefore unable to be bound by carbamylation specific phages. To increase the specificity cHSA-2 with higher Hcit% was used as target for phage display. After four rounds of biopanning, a number of sequences with high variability were resulted (Figure 4-4). Although it is expected that with repeated biopanning and amplification, clone variation should be reduced and more consensus sequence should appear, we did not find any such trend in our result, and even after four rounds we still found new sequences never appeared before. Sequence alignment did not yield any highly conservative motifs (Figure 4-4). Generally, the clones with high binding strength would be enriched after just one or two rounds, so further biopanning after four rounds in such case would not help, or it may just result in enrichment of phages with growing advantages. Nevertheless, there were several clones appeared more frequently than others. The top 6 clones were picked together with cH1-p1 and were listed in Table 4-2. Among all the clone sequences for cHSA-2 phage display, the amino acid population was ranked according to their occurrence frequency (Table 4-3). We found serine, alanine, proline, leucine and threonine are the most abundant

amino acids, and they are all constitutes in both cH1-p1 and cH2-p1. One thing in common is that these are considered small amino acids except for leucine [305]. Also negatively charged amino acids aspartate and glutamate are far less than positively charged amino acids lysine, histidine and arginine.

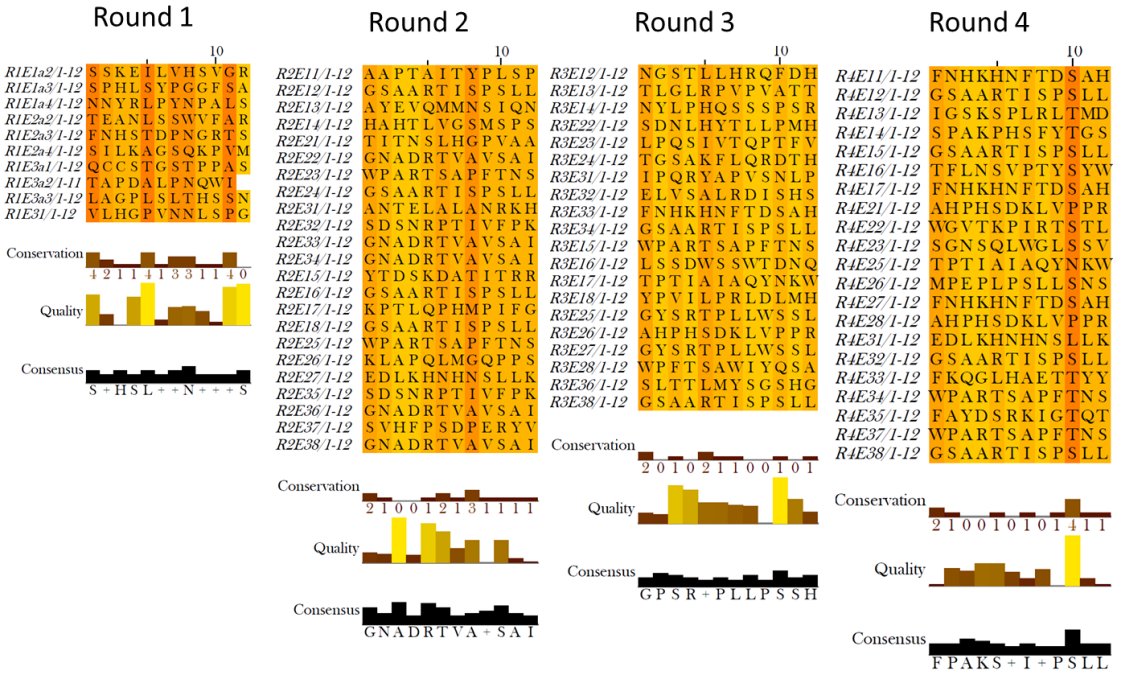

Figure 4-4 Sequence alignment results of four rounds of biopanning on cHSA-2

Table 4-2 Lists of candidate peptide sequences obtained through the phage display biopanning targeting cHSA

Sequence	frequency (%) [a]	pI [b]	Target	Label	Reference
GSAARTISPSLL	11.9	9.75	cHSA-2	cH2-p1	[306]
FNHKHNFTDSAH	6.0	7.02	cHSA-2	cH2-p2	This work
WPARTSAPFTNS	6.0	9.75	cHSA-2	cH2-p3	This work
AHPHSDKLVPPR	3.6	8.8	cHSA-2	cH2-p4	[306]
TPTIAIAQYNKW	2.4	8.26	cHSA-2	cH2-p5	This work
TLGLRPVPVATT	1.2	9.41	cHSA-2	cH2-p6	[306, 307]
APPHVSSTVSWL	100	6.79	cHSA-1	cH1-p1	This work

[a] The frequency was the percentage of the sequences appeared in sequencing data from all rounds of biopanning, with the sum of 36 and 61 sequences for biopanning against cHSA-1 and cHSA-2 respectively.

[b] The Isoelectric point (pI) value of peptide was given by ProtParam tool for protein analysis [308]

Table 4-3 Frequency of amino acids included in result of biopanning on cHSA-2

Amino acid	Frequency (%)
S	**14.8**
A	**9.7**
P	**9.5**
L	**9.5**
T	**8.8**
N	**5.6**
R	**5.1**
H	**5.0**
G	**4.7**
I	**4.2**
V	**4.1**
D	**3.4**
K	**3.2**
F	**3.2**
Y	**2.6**
Q	**2.4**
W	**2.0**
M	**1.2**
E	**1.1**
C	**0.2**
U	**0.0**

An ELISA assay was performed for all peptide candidates for cHSA-1, cHSA-2, and native HSA (control). In cHSA-1 ELISA of all phages were shown to have similar binding to cHSA-1, despite they have almost no sequence similarities (Figure 4-5). Among them cH2-p1, cH2-p3, cH2-p4, cH2-p5 and cH2-p6 had significantly lower binding to HSA. In cHSA-2 ELISA (Figure 4-6), all phages were shown to be cHSA-2 specific, with the absorbance difference between HSA and cHSA more significantly than in cHSA-1 ELISA. Besides that, cH2-p1 was also found to be with higher binding affinity to cFgn, when comparing to native Fgn as control (Figure 4-6).

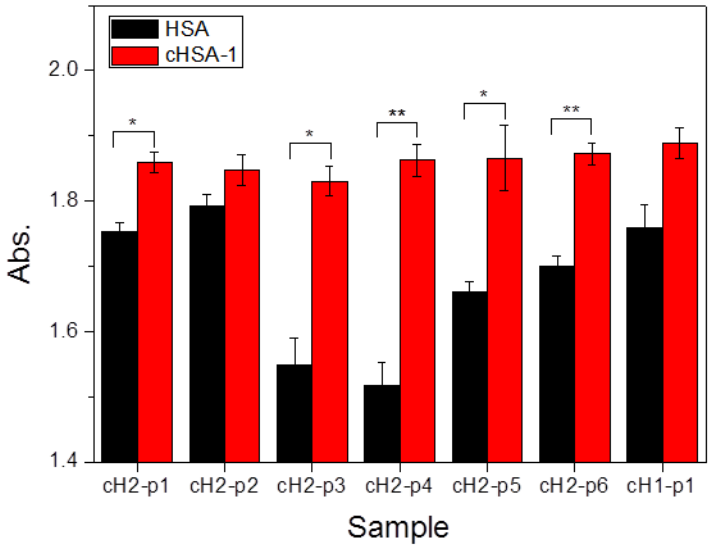

Figure 4-5 Affinity of candidate phages obtained through the phage display biopanning targeting cHSA to native HSA and carbamylated HSA (cHSA-1) (Data represent mean ±1 SD, n=3; *, $p < 0.01$; **, $p<0.001$)

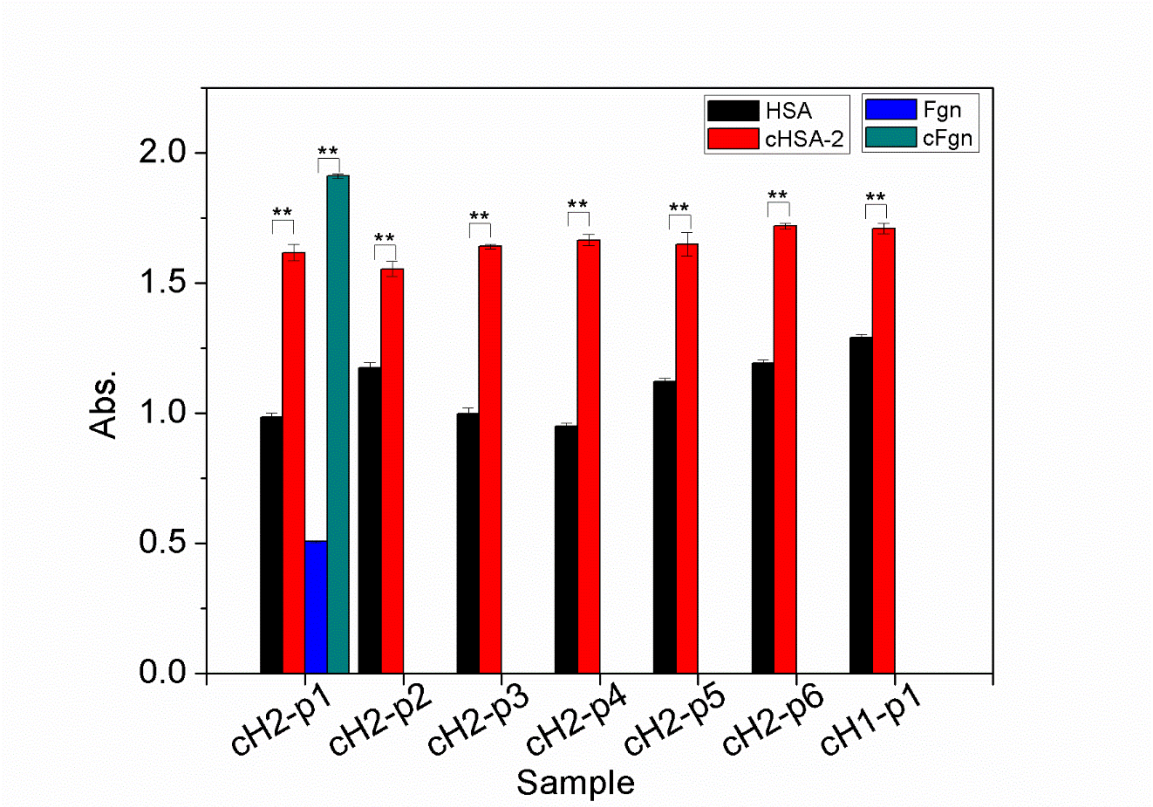

Figure 4-6 Affinity of candidate phages obtained through the phage display biopanning targeting cHSA to native HSA, carbamylated HSA (cHSA-2), Fgn and carbamylated Fgn (cFgn) (Data represent mean ±1 SD, n=3; *, $p < 0.01$; **, $p<0.001$)

4.3.3 Identification of peptide specific to cHSA through ITC

Since from ELISA result it was revealed that cH2-p1, cH2-p3, cH2-p4, cH2-p5 and cH2-p6 were shown to be cHSA specific towards both cHSA-1 and cHSA-2, they could be potential peptide ligands for cHSA. For optimal binding test convenience and to minimize non-specific interaction with other plasma proteins for future application, we only picked water soluble peptides cH2-p1, cH2-p4 and cH2-p6 for synthesis and exclude cH2-p3 and cH2-p5 due to their poor expected aqueous solubility.

For the ITC binding studies of cH2-p1, cH2-p4, cH2-p6 to cHSA/HSA, we found in general

that the K_d values ranged of from 10^{-5} M to 10^{-3} M for all data (Figure 4-7, Figure 4-8, Figure 4-9). Aaron et al. in his work used disulfide-constrained cyclic peptide phage display libraries to select binding peptide against HSA, and determined that the highest binding peptide with K_d values from 10^{-6} to 10^{-5} M in PBS (pH 6.2), and the K_d increased dramatically at higher pH of 7.4 and 9.4 [301]. In our work we did not find any peptide binding to HSA/cHSA with K_d less than 10^{-5} M, this is possibly because we performed negative panning with HSA in phage display which removes those high binding clones towards HSA. The downward ITC titration peaks suggest that the binding process is exothermic. The such obtained curve of ITC fell in the case with the dimensionless parameter $c=[M]_0/K_d$ to be ~1, under which circumstance only K_d can be determined, while the stoichiometry n and the binding enthalpy ΔH can only be roughly estimated [309, 310]. For cH2-p1, the titration peak for titration to HSA is so weak as small amounts of enthalpy was generated from interaction between cH2-p1 and HSA, with the K_d value of 1.0×10^{-3} M, while the binding to cHSA is more significant with K_d value of 1.0×10^{-4} M. For cH2-p4 and cH2-p6, the titration curve to both HSA and cHSA are significant, with the K_d value from 10^{-5} to 10^{-4} M, and the cH2-p4 has even a lower K_d for binding to HSA than binding to cHSA. As the main effect of carbamylation is the positive charge elimination, for HSA with a slightly negative charge, carbamylated samples shall have a more negative surface charge [311], and this was verified through our zeta-potential result for different Hcit% samples shown in Figure 4-11a. We also measured the pI value of cHSA through zeta-potential as 4.13, which was shifted from 4.83 for native HSA, shown in Figure 4-11b. Therefore nonspecific electrostatic interaction may have an impact on the peptide binding to cHSA. The pI of p1, p4 and p6 were calculated to be 9.75, 8.8 and 8.26 separately through ProtParam tool [308] as they would be positively charged at pH 7.4. However, despite the fact that cH2-p1 has a higher pI than cH2-p4, cH2-p1 does not have a lower K_d when binding to both HSA and cHSA. This indicates that the interaction between cH2-p1 and HSA/cHSA is not just electrostatic, and specific interactions should be responsible for

binding. Also it would be a great merit for peptides with low interactions with proteins other than the real target, as the nonspecific protein binding may block the binding sites and affects its activity. Therefore cH2-p1 is the best identified candidate peptide for our purpose so far. ITC results showed that the binding affinity of peptide to HSA/cHSA was not always consistent to their corresponding phages. Although cH2-p1 showed consistent higher binding to cHSA than HSA in both ITC and ELISA, that binding specificity for cH2-p4 or cH2-p6 was not inherited by their peptide. It should be noted that in phage displayed peptides the C- terminals are not present as they are fused to the phage and therefore should miss one negatively charged carboxylate compared to the synthesized peptides, which may show different binding properties with changed the electrostatic properties. Moreover, HSA/cHSA coated on surface may underwent some extent of structural refolding and then expose only certain parts to phages for binding, so the process of binding to HSA/cHSA may not be exactly in the same way between surface and solution cases.

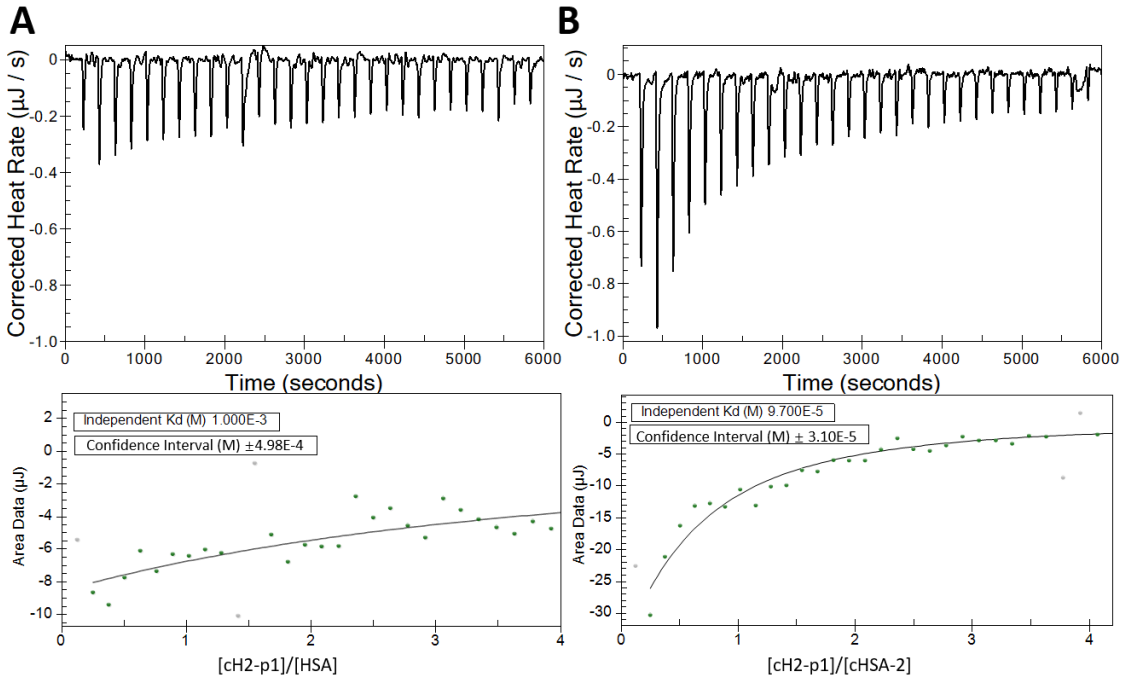

Figure 4-7 ITC raw titration data and fitting of integrated heat plots of peptide cH2-p1 titration into (A)

native HSA and (B) cHSA-1

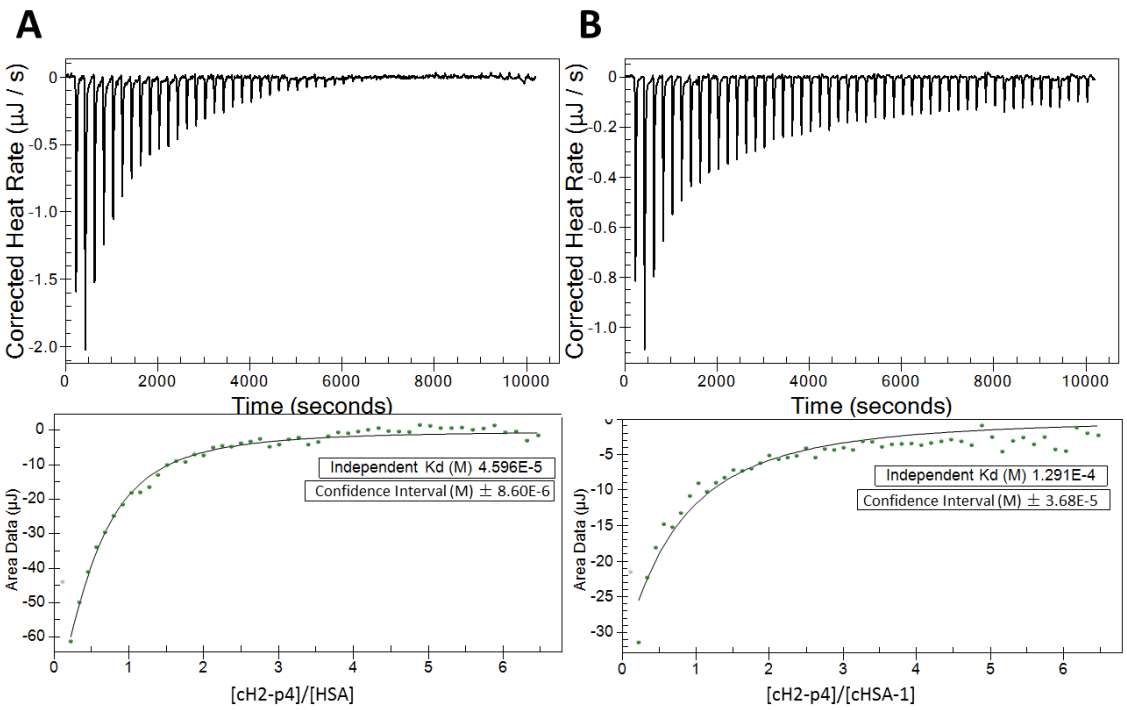

Figure 4-8 ITC raw titration data and fitting of integrated heat plots of peptide cH2-p4 titration into (A) native HSA and (B) cHSA-1

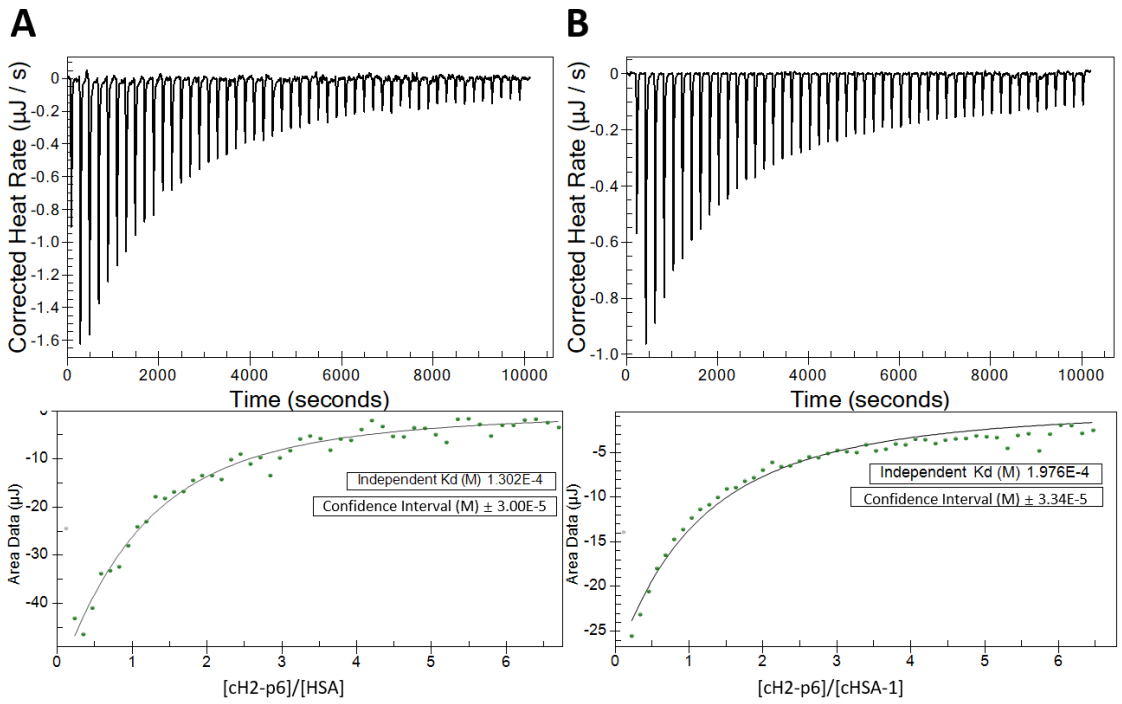

Figure 4-9 ITC raw titration data and fitting of integrated heat plots of peptide cH2-p6 titration into (A) native HSA and (B) cHSA-1

4.3.4 cH2-p1 binding to cHSA with different Hcit%

Since the interaction between cH2-p1 and cHSA was shown to be specific, it is interesting to know if this specificity would vary if the extent of carbamylation changed. Here in this study cHSA-1, cHSA-2 and cHSA-3 with different Hcit% were compared for binding to cH2-p1. The resulting K_d were similar, with 1.2×10^{-4} M for binding to cHSA-1 and 1.0×10^{-4} M for binding to cHSA-2, and 9.9×10^{-5} M for binding to cHSA-3 (Figure 4-10). Although it has been noted that from Figure 4-11 that zeta-potential of cHSA was shifted from -7.84 mV for cHSA-1 to -10.76 mV for cHSA-2, that difference in surface charge did not affect the binding affinity. The similar K_d should just be due to the fact that the ligand binding is only specific to homocitrulline with homocitrulline as the target.

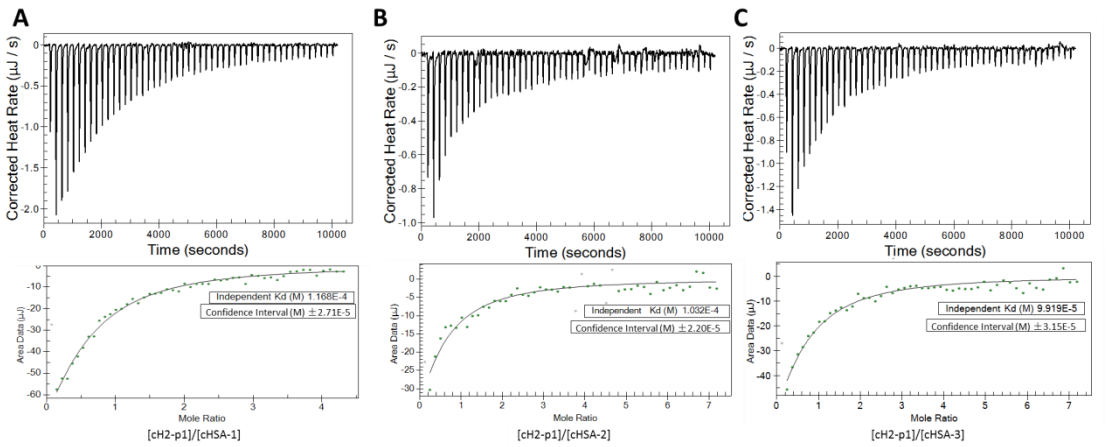

Figure 4-10 ITC raw titration data and fitting of integrated heat plots of peptide cH2-p1 titration into (A) cHSA-1, (B) cHSA-2 and (C) cHSA-3

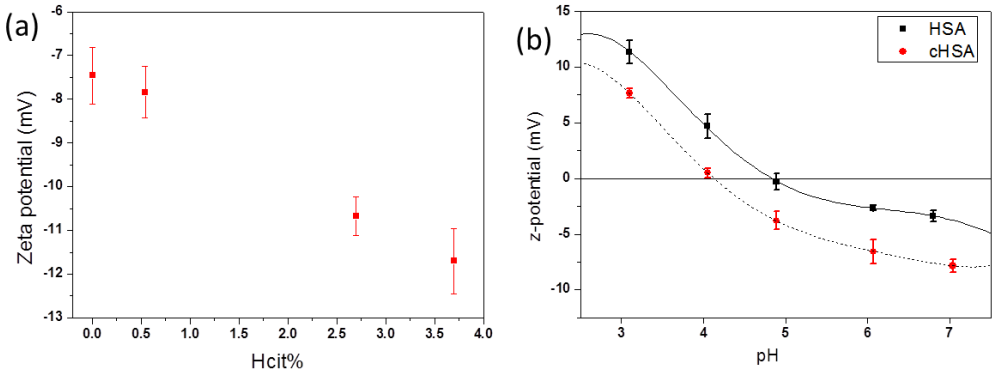

Figure 4-11(a) Zeta-potential and (b) Isoelectric point of native HSA and carbamylated HSA

4.3.5 cH2-p1 binding to other carbamylated protein species

One previous research collected sera from rabbits immunized with carbamylated HSA, and revealed that such sera contains antibodies recognized homocitrulline-containing collagen telopeptides [57]. To verify if cH2-p1 is homocitrulline specific regardless of protein types, cH2-p1 binding to another important plasma protein fibrinogen (Fgn) with and without

carbamylation were tested. For cH2-p1 binding to Fgn, we found no exothermic or endothermic peaks generated during the whole titration, which makes it even not possible to generate a fitting curve (Figure 4-12a). While for cH2-p1 binding to cFgn the titration was exhibited to be a endothermic with strong upward titration peaks, with a K_d value fitted to be 8.4×10^{-5} M (Figure 4-12b). The result of cH2-p1 titration to Fgn showed cH2-p1 does not bind to this protein without carbamylation. Unlike cHSA, binding of cH2-p1 to cFgn was found to be endothermic, which suggests that the binding is entropy driven. The Hcit% for cFgn was measured to be 11.9 %, yet still with similar K_d for binding to cH2-p1 compared to cHSA. The endothermic binding may involve complex conformational change that may require further study to determine. We speculate that this is possibly because peptide binding to carbamylated fibrinogen destabilize its structure and cause unfolding or disentanglement of its three subchains for the entropy gains.

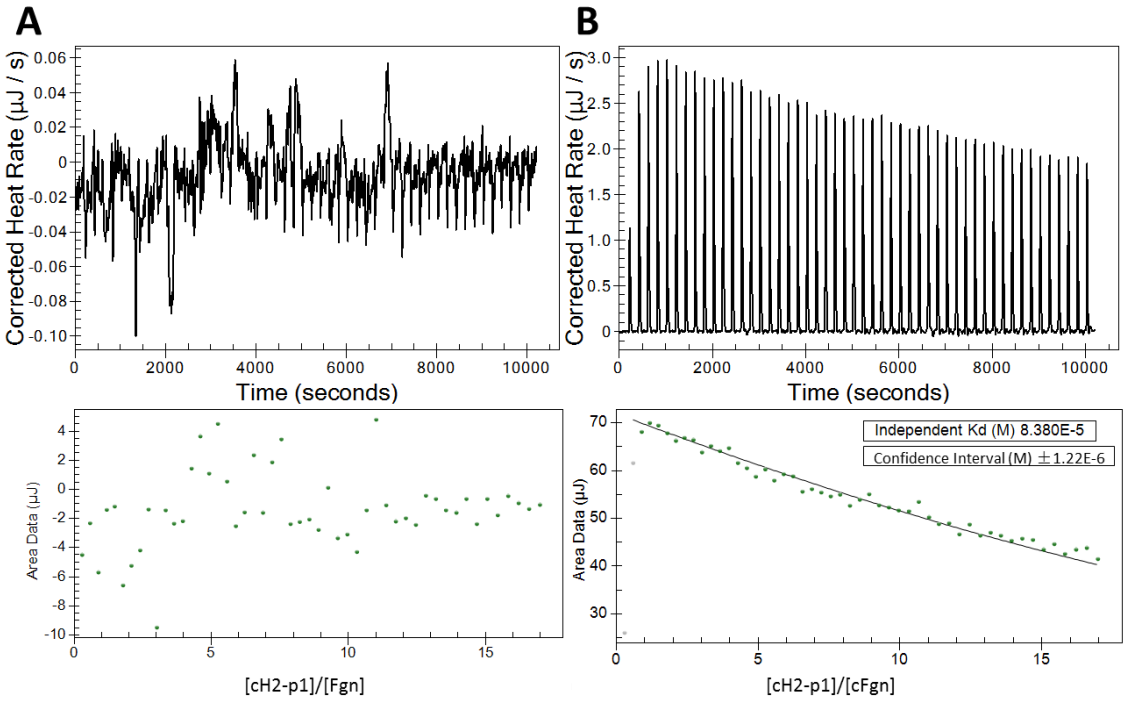

Figure 4-12 ITC raw titration data and fitting of integrated heat plots of peptide cH2-p1 titration into (A) native Fgn and (B) cFgn

4.3.6 Binding mechanism study through titration of cH2-p1 to cHSA with anti-Hcit

To study if the binding sites on cHSA for cH2-p1 are the same for antibody targets homocitrulline, cHSA was incubated with anti-Hcit prior to cH2-p1 titration test. The control test was done by titration of cH2-p1 into the solution containing only anti-Hcit, and the result proved that cH2-p1 has a very low binding affinity towards anti-Hcit, with the K_d fitted to be 1×10^{-3} M, therefore the interaction between cH2-p1 and antibody is not to be considered in later tests. To fit the titration data for cH2-p1 to cHSA with and without the presence of anti-Hcit, a fixed K_d of 9.7×10^{-5} M as we determined before for cH2-p1 titrated into cHSA was used, and good fitting results were obtained for both cases (Figure 4-13). To accommodate the low concentration of obtained antibody, the concentration of both cHSA and cH2-p1 have been lowered by 10 times, thus resulting in a lower c value and more linear and flatter fitting curve. Nevertheless, a difference was found on binding enthalpy, that the binding enthalpy is less for cH2-p1 to cHSA when anti-Hcit is present. However, due to the low c binding nature, the binding enthalpy cannot be precisely quantified. If we assume that the cH2-p1 targets the same binding sites with anti-Hcit, it is reasonable to regard the difference as the result of decreased n value due to the occupancy of binding sites by anti-Hcit.

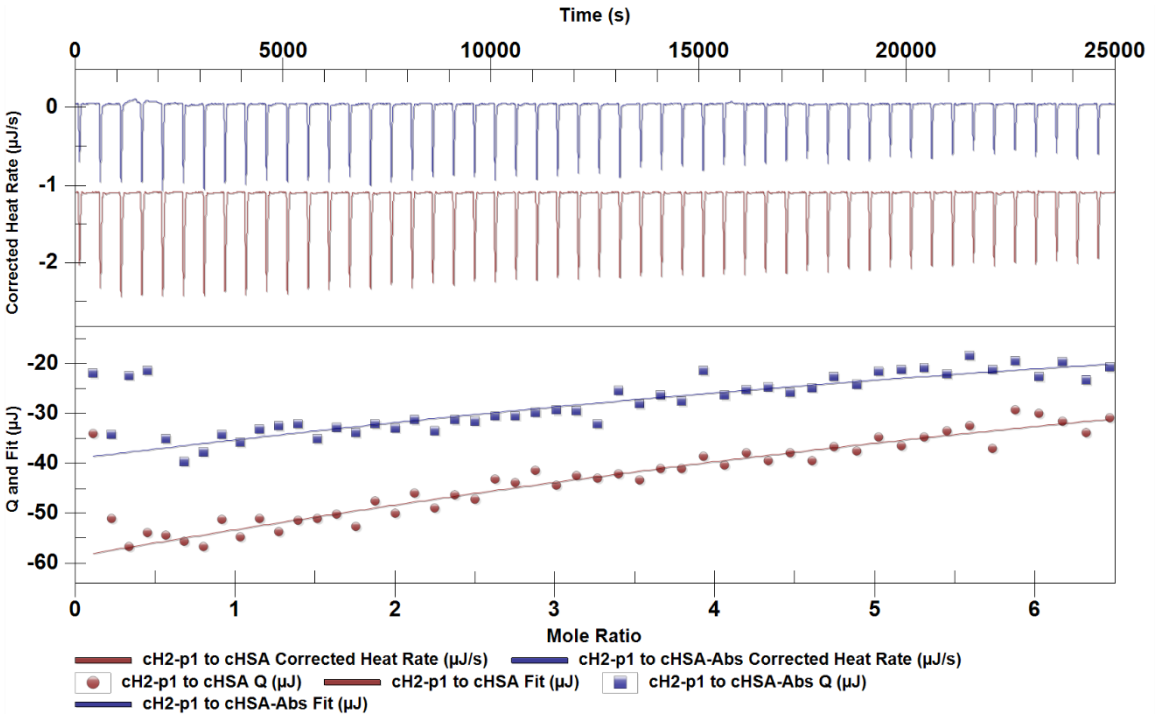

Figure 4-13 ITC raw titration data and fitting of integrated heat plots of peptide cH2-p1 titration into cHSA with (cHSA-Abs) and without (cHSA) been incubated with anti-Hcit

4.3.7 Binding mechanism study through molecular docking

Since cH2-p1 binds to both cHSA and cFgn with high affinity, we assume that cH2-p1 have the binding site for homocitrulline residues. To explore the possible binding mode of homocitrulline, molecular docking was studied. The model ligand Hcit-res instead of its amino acid form was created to simulate the carbamylated lysine residue as a simplification. The peptide chain of Hcit-res was simplified with two peptide bonds terminated with methyl groups. Longer peptide chains are not preferable as they may require a larger box for docking and reduce the site specificity. With the purpose to search for the best pose of the side chain and avoid trapping of peptide chains into binding pockets, all non-side chain bonds of Hcit-res were set to be non-rotatable and only the side chain bonds were allowed to be rotatable.[312] The top ranked binding site cH2-p1-C1 is composed of four residues,

Ala3, Arg5, Thr6 and Ile7. Figure 4-14 shows the top 2 scored poses, with the binding affinity of -3.1 kcal/mol for both conformations. Since the surface of pocket is mainly low electrostatic potential area, docking of carbamoyl group containing ligand should be expected. The same affinity score for both poses suggests that they are equally favorable. Pose a has the primary amine buried inside the pocket, and pose b has the secondary amine buried inside the pocket. Since the positively charged Arg5 is involved in the binding pocket, docking of lysine residues should not be considered as favorable as homocitrulline residues. Although it is possible that homocitrulline residues may dock into other binding sites, by doing docking experiments on all other two potential binding pockets provided by I-TASSER, we found none of the top scored poses are reasonable with homocitrulline side chain docked into the pocket.

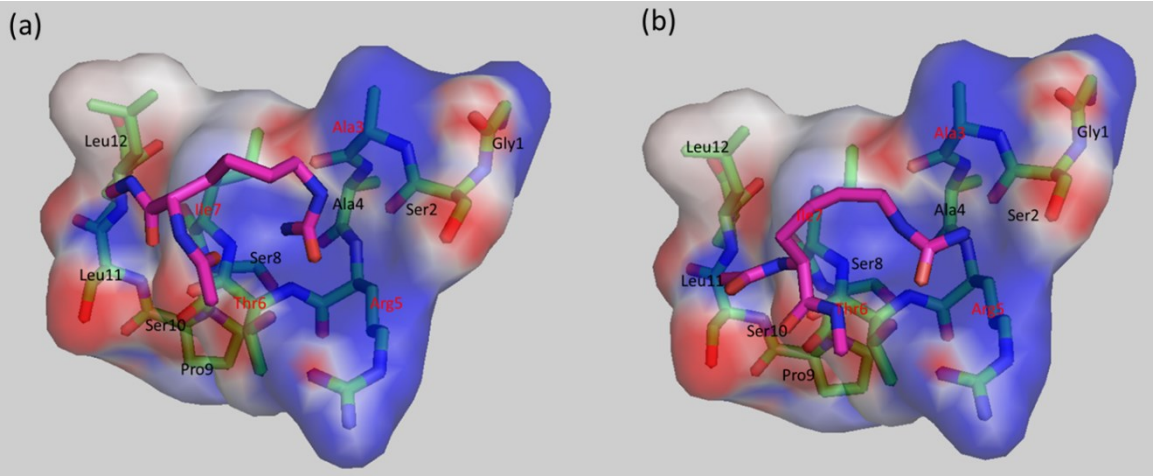

Figure 4-14 Two ways, (a) pose a and (b) pose b, the designed model Hcit-res (Pink carbon chain) docked into the candidate pocket of cH2-p1 (Green carbon chain) by AutoDock Vina. The surface of cH2-p1 is shown with electrostatic potential map.

Based on all results obtained above, the avidity of cH2-p1 to carbamylated proteins was significantly higher than to the native protein. However, it is still relatively low compared to antibody binding of even native HSA. This could arise from the fact that according to the molecular docking result, only four residues in cH2-p1 are involved in binding of

homocitrulline to form a binding pocket. This limited interaction between peptide amino acids and the small fraction of homocitrulline residues trapped inside may present the maximum limit of the binding affinity – short of further engineering of the amino acids involved in binding homocitrulline.

4.4 Conclusion

Several peptide sequences were identified using a Ph.D.-12 phage display library against carbamylated HSA. ELISA results revealed that the phage clone obtained through biopanning on cHSA-1 might be a TUP and does not have a significantly high binding specificity, while several phage clones obtained from cHSA-2 biopanning showed high binding specificity to both cHSA-1 and cHSA-2. ITC results were used to identify GSAARTISPSLL (cH2-p1) to have a dissociation constant (K_d) of 9.7×10^{-5} M when exothermic binding to cHSA, and was almost one order of magnitude lower than its K_d to native HSA. The binding affinity for cH2-p1 towards cHSA was not found to be influenced by the extent of carbamylation. Moreover, cH2-p1 was found to bind cFgn over the native protein. This process was endothermic, but yielded a similar K_d (8.4×10^{-5} M) as that for cHSA binding. The binding of cH2-p1 to cHSA was weakened when anti-Hcit is present in cHSA solution, suggesting that anti-Hcit occupied the same sites where cH2-p1 binds to cHSA. Through molecular docking study, we identified two poses homocitrulline residues may have when docking into cH2-p1 pocket. The potential of cH2-p1 to bind carbamylated proteins over native ones is the baseline for looking at removal of these proteins from CKD patients for further treatment.

4.5 Reference

[21] T. Niwa, Removal of Protein-Bound Uraemic Toxins by Haemodialysis, Blood purification 35 (2013) 20-25.
[28] A.H. Berg, C. Drechsler, J. Wenger, R. Buccafusca, T. Hod, S. Kalim, W. Ramma, S.M. Parikh, H. Steen, D.J. Friedman, J. Danziger, C. Wanner, R. Thadhani, S.A. Karumanchi, Carbamylation of Serum Albumin as a Risk Factor for Mortality in Patients with Kidney Failure, Science translational medicine 5(175) (2013).
[32] K.M. Fazili, M.M. Mir, M.A. Qasim, Changes in Protein Stability Upon Chemical Modification of Lysine Residues of Bovine Serum-Albumin by Different Reagents, Biochem Mol Biol Int 31(5) (1993) 807-816.
[39] J. Pande, M.M. Szewczyk, A.K. Grover, Phage display: Concept, innovations, applications and future, Biotechnol Adv 28(6) (2010) 849-858.
[43] Y.Y. Tan, T. Tian, W.L. Liu, Z. Zhu, C.Y.J. Yang, Advance in phage display technology for bioanalysis, Biotechnology journal 11(6) (2016) 732-745.
[54] F.W. Falkenberg, Monoclonal antibody production: problems and solutions, Res Immunol 149(6) (1998) 542-547.
[55] J. Shi, R. Knevel, P. Suwannalai, M.P. van der Linden, G.M.C. Janssen, P.A. van Veelen, N.E.W. Levarht, A.H.M. van der Helm-van Mil, A. Cerami, T.W.J. Huizinga, R.E.M. Toes, L.A. Trouw, Autoantibodies recognizing carbamylated proteins are present in sera of patients with rheumatoid arthritis and predict joint damage, Proceedings of the National Academy of Sciences of the United States of America 108(42) (2011) 17372-17377.
[56] J.S. Dekkers, M.K. Verheul, J.N. Stoop, B.S. Liu, A. Ioan-Facsinay, P.A. van Veelen, A.H. de Ru, G.M.C. Janssen, M. Hegen, S. Rapecki, T.W.J. Huizinga, L.A. Trouw, R.E.M. Toes, Breach of autoreactive B cell tolerance by post-translationally modified proteins, Annals of the rheumatic diseases 76(8) (2017) 1449-1457.
[57] S. Turunen, M.K. Koivula, L. Risteli, J. Risteli, Anticitrulline Antibodies Can Be Caused by Homocitrulline-Containing Proteins in Rabbits, Arthritis Rheum 62(11) (2010) 3345-3352.
[259] M. Guilloton, F. Karst, A Spectrophotometric Determination of Cyanate Using Reaction with 2-Aminobenzoic Acid, Analytical biochemistry 149(2) (1985) 291-295.
[289] L.M. Kraus, S. Miyamura, B.R. Pecha, A.P. Kraus, Carbamoylation of Hemoglobin in Uremic Patients Determined by Antibody Specific for Homocitrulline (Carbamoylated Epsilon-N-Lysine), Mol Immunol 28(4-5) (1991) 459-463.
[290] E.O. Apostolov, S.V. Shah, E. Ok, A.G. Basnakian, Quantification of carbamylated LDL in human sera by a new sandwich ELISA, Clinical chemistry 51(4) (2005) 719-728.
[291] S. Nakabo, M. Hashimoto, S. Ito, M. Furu, H. Ito, T. Fujii, H. Yoshifuji, Y. Imura, R. Nakashima, K. Murakami, N. Kuramoto, M. Tanaka, J. Satoh, A. Ishigami, S. Morita, T. Mimori, K. Ohmura, Carbamylated albumin is one of the target antigens of anti-carbamylated protein antibodies, Rheumatology 56(7) (2017) 1217-1226.
[292] Y.M. Fang, D.Q. Lin, S.J. Yao, Review on biomimetic affinity chromatography with short peptide

ligands and its application to protein purification, Journal of Chromatography A 1571 (2018) 1-15.
[293] Y. Zhang, I-TASSER server for protein 3D structure prediction, BMC bioinformatics 9 (2008).
[294] A. Roy, A. Kucukural, Y. Zhang, I-TASSER: a unified platform for automated protein structure and function prediction, Nature protocols 5(4) (2010) 725-738.
[295] J.Y. Yang, A. Roy, Y. Zhang, Protein-ligand binding site recognition using complementary binding-specific substructure comparison and sequence profile alignment, Bioinformatics 29(20) (2013) 2588-2595.
[296] J. Yang, A. Roy, Y. Zhang, BioLiP: a semi-manually curated database for biologically relevant ligand-protein interactions, Nucleic acids research 41(Database issue) (2013) D1096-103.
[297] O. Trott, A.J. Olson, Software News and Update AutoDock Vina: Improving the Speed and Accuracy of Docking with a New Scoring Function, Efficient Optimization, and Multithreading, J Comput Chem 31(2) (2010) 455-461.
[298] M.P. Lefranc, V. Giudicelli, P. Duroux, J. Jabado-Michaloud, G. Folch, S. Aouinti, E. Carillon, H. Duvergey, A. Houles, T. Paysan-Lafosse, S. Hadi-Saljoqi, S. Sasorith, G. Lefranc, S. Kossida, IMGT (R), the international ImMunoGeneTics information system (R) 25 years on, Nucleic acids research 43(D1) (2015) D413-D422.
[299] V. Giudicelli, P. Duroux, C. Ginestoux, G. Folch, J. Jabado-Michaloud, D. Chaume, M.P. Lefranc, IMGT/LIGM-DB, the IMGT comprehensive database of immunoglobulin and T cell receptor nucleotide sequences, Nucleic acids research 34(Database issue) (2006) D781-4.
[300] R. J.M.H., Recombinant human autoantibodies specific for citrullinecontaining peptides from RA patient derived phage display libraries (Unpublished).
[301] A.K. Sato, D.J. Sexton, L.A. Morganelli, E.H. Cohen, Q.L. Wu, G.P. Conley, Z. Streltsova, S.W. Lee, M. Devlin, D.B. DeOliveira, J. Enright, R.B. Kent, C.R. Wescott, T.C. Ransohoff, A.C. Ley, R.C. Ladner, Development of mammalian serum albumin affinity purification media by peptide phage display, Biotechnol Progr 18(2) (2002) 182-192.
[302] D. Gaser, B. Strukelj, T. Bratkovic, S. Kreft, J. Pungercar, M. Lunder, Cross-affinity of Peptide Ligands Selected from Phage Display Library Against Pancreatic Phospholipase A2 and Ammodytoxin C, Acta chimica Slovenica 56(3) (2009) 712-717.
[303] W.X. Zhao, H. Yuan, X. Xu, L. Ma, Isolation and Initial Application of a Novel Peptide That Specifically Recognizes the Neural Stem Cells Derived from Rhesus Monkey Embryonic Stem Cells, Journal of biomolecular screening 15(6) (2010) 687-694.
[304] S.J. Segvich, H.C. Smith, D.H. Kohn, The adsorption of preferential binding peptides to apatite-based materials, Biomaterials 30(7) (2009) 1287-1298.
[305] C. Pommie, S. Levadoux, R. Sabatier, G. Lefranc, M.P. Lefranc, IMGT standardized criteria for statistical analysis of immunoglobulin V-REGION amino acid properties, J Mol Recognit 17(1) (2004) 17-32.
[306] G. Fan, C.M. Dundas, C. Zhang, N.A. Lynd, B.K. Keitz, Sequence-Dependent Peptide Surface Functionalization of Metal-Organic Frameworks, ACS Applied Materials & Interfaces 10(22) (2018) 18601-18609.
[307] N. Schonberger, R. Braun, S. Matys, F.L. Lederer, F. Lehmann, K. Flemming, K. Pollmann, Chromatopanning for the identification of gallium binding peptides, Journal of Chromatography A 1600 (2019) 158-166.

[308] H.C. Gasteiger E., Gattiker A., Duvaud S., Wilkins M.R., Appel R.D., Bairoch A.;, Protein Identification and Analysis Tools on the ExPASy Server; (In) John M. Walker (ed): The Proteomics Protocols Handbook, Humana Press (2005). (2005) 571-607.
[309] W.B. Turnbull, A.H. Daranas, On the value of c: Can low affinity systems be studied by isothermal titration calorimetry?, Journal of the American Chemical Society 125(48) (2003) 14859-14866.
[310] L.D. Hansen, G.W. Fellingham, D.J. Russell, Simultaneous determination of equilibrium constants and enthalpy changes by titration calorimetry: Methods, instruments, and uncertainties, Analytical biochemistry 409(2) (2011) 220-229.
[311] S. Jaisson, C. Pietrement, P. Gillery, Carbamylation-Derived Products: Bioactive Compounds and Potential Biomarkers in Chronic Renal Failure and Atherosclerosis, Clinical chemistry 57(11) (2011) 1499-1505.
[312] E. Aghaee, J.B. Ghasemi, F. Manouchehri, S. Balalaie, Combined docking, molecular dynamics simulations and spectroscopic studies for the rational design of a dipeptide ligand for affinity chromatography separation of human serum albumin, Journal of molecular modeling 20(10) (2014).

Chapter 5: Protein adsorption based on peptide immobilized non-fouling surface

5.1 Introduction

With the aim to selective removal of carbamylated albumin from blood by peptide ligand, we have identified the cHSA binding peptide in our previous studies through phage display. For real application it is necessary to immobilize this peptide onto a surface which will then function as adsorbent material. To our knowledge we have never seen any adsorbent used in blood purification system coupled with protein binding peptide ligand. However, peptide ligands targeting certain proteins have been widely involved in preparing affinity chromatographic column for protein separation or purification [312-315]. For example, small peptide ligands WW for HSA, determined through molecular docking and molecular dynamics (MD) simulation, was proved able to stabilize the ligand-HSA complex after

immobilized onto ECH-lysine sepharose 4 gel with a space arm [312]. In another study α-Lactalbumin binding peptide WHWRKR was attached to a resin for isolation of α-lactalbumin from whey proteins, and a highly purified α-lactalbumin (100%) with a yield of 35.2% was achieved [315]. For application of peptide ligands in blood purification, one critical requirement is to minimize nonspecific protein adsorption on the blood adsorbent interface. A low level of fibrinogen adsorption may lead to blood coagulation, and adsorption of non-target protein on substrate may influence the affinity of peptide ligand. For optimization of specificity of surface peptide, the so called "non-fouling" polymer brushes could be used to avoid non-specific protein adsorption on substrate. For example, poly(hydroxyethyl methacrylate) (p(HEMA)) film coated surface has been shown to be nonfouling [71] with ultralow protein adsorption amount in single protein solution and diluted or undiluted serum and plasma. With the optimal thickness of polymer brushes, the protein adsorption for undiluted human blood serum and plasma is only ~3.0 and 3.5 ng/cm^2, which may prove its potential as blood contacting materials. Moreover, p(HEMA) brush could be used as a platform for functionalization with bioactive molecules [316-319]. Anodisc porous alumina membranes have been modified with p(HEMA) brushes derivatized with nitrilotriacetate-Ni^{2+} (NTA-Ni^{2+}) complexes, and was shown with purification ability to polyhistidine-tagged ubiquitin (HisU) in less than 30 min with a binding capacity of 120 mg of HisU/cm^3 [71]. In another study, p(HEMA) brushes grown on surface was modified with cell adhesion promoting RGD containing peptide ligands. It was found human umbilical vascular endothelial cells (HUVECs) are able to adhere and spread rapidly on such surface [319]. It was found in another study β-glucosidase (GLU) and β-galactosidase (GAL) are specifically adsorbed to p(HEMA) brushes, and it is proposed molecular recognition between the hydroxyl groups of PHEMA and the active sites of glycosidases occured during adsorption [314].

Since the p(HEMA) surface is with ultralow protein adsorption, it might be challenging to

quantify the specific adsorbed protein amount as it is lower than the detecting limit in many assays such as BCA [320] or ellipsometry [285]. Therefore one way is to use a more sensitive method such as radiolabeling method, which allows for detecting of protein in a more precise level [321, 322].

To improve hemocompatibility for materials used in hemodialysis, there are examples using poly(ethylene glycol) methacrylate (PEGMA) to improve hemocompatibility of PVDF membrane [323], or forming pHEMA brushes on PVDF membrane through atom transfer radical polymerization (ATRP) to improve its anti-protein adsorption property [324].

Based on our knowledge and previous studies, pHEMA brushes bound with antibody mimic peptides might be a promising way to develop specific adsorbent surface for removal of carbamylated proteins.

5.2 Experiments

5.2.1 Materials

HEMA (≥99%, contains ≤50 ppm inhibitor), copper(I) bromide, ascorbic acid, N,N,N',N'',N''-Pentamethyldiethylenetriamine (PMDETA), sodium azide (NaN_3), triphenylphosphine (PPh3), N-Hydroxysuccinimide (NHS), N-(3-Dimethylaminopropyl)-N'-ethylcarbodiimide hydrochloride (EDAC), succinic anhydride (SA), 4-(Dimethylamino) pyridine (DMAP), triethylamine (TEA), sodium citrate and sodium cyanate were purchased from Sigma-Aldrich (Canada). Albumin from human serum (HSA, lyophilized, fatty acid free) and fibrinogen from bovine plasma (Fgn, ≥75% clottable) were purchased from Sigma-Aldrich (Canada). ω-Mercaptoundecyl bromoisobutyrate (MBIB) was purchased from Regent Science Industry Limited. Silicon

wafers (100 mm, DSP) were purchased from University Wafer, Inc, and were sputtered with an adhesion layer of Cr (20 nm) followed by a layer of Au (20 nm) before use. Peptide used in this study was synthesized by GL Biochem and the purity was verified by high-performance liquid chromatography (HPLC) with 98%, and the composition was confirmed by mass spectrometry. Homocitrulline/Citrulline Assay Kit was provided by Cell Biolabs. Iodine-125 radionuclide in 0.1 M NaOH (1 mCi) was provided by Perkin Elmer. Pierce Pre-Coated Iodination Tubes and Micro BCA Protein Assay Kit were purchased from Thermo Fisher Scientific. Econo-Pac 10DG Desalting column was purchased from Bio-Rad. All other reagents were used as received without further purification. All dilutions and buffers were prepared with syringe filtered (0.22 μm) milli-Q deionized water

5.2.2 Preparation of p(HEMA) nonfouling surface

5.2.2.1 Synthesis of initiator (BiBUT) used for surface-initiated Atom Transfer Radical Polymerization (SI-ATRP)

For synthesis of surface initiator, the thiol group of 11-bromoundecanol was first protected by dissolving 1 g of 11-bromoundecanol and 0.9 g of potassium thioacetate in 5 ml dimethylformamide (DMF) and reacting with stirring overnight at room temperature. Then to the solution ethyl acetate was added and was filtered to remove precipitate, and the filtrate with product was extracted after washing with brine several times. The obtained solution was dried with N_2SO_4 and was then spin-dried, and was further dried under high vacuum (85% yield). For esterification, the yield product was mixed with 0.47 ml 2-bromoisobutyryl bromide, 1.04 ml triethylamine, 47 mg DMAP in 50 ml dichloromethane (DCM) with stirring for 24 hr at room temperature. The product from mixture solution was extracted after washing with brine several times. The obtained solution was dried with

N_2SO_4 and was then spin-dried, and was further dried under high vacuum. For thiol deprotection, the yield product was firstly dissolved in 30 ml of DCM/Methanol (1:1) and degassed with nitrogen for 30 mins, then 0.2 eq. molar of tetrabutylammonium cyanide was added and the reaction was kept in room temperature overnight. The mixture solution was spin-dried, followed by addition of 50 ml H_2O and was extracted by 50 ml ethyl acetate. The obtained solution was dried with N_2SO_4 and was then spin-dried, and was further purified by passing through a silica gel column (18% yield).

5.2.2.2 Gold sputtering on silicon wafer

The gold substrate was prepared by sputtering of an adhesion Ti/W 10%/90% layer (20 nm) and a gold layer (20 nm) onto both sides of the previously piranha cleaned Si wafer. The coated wafer was then sliced into pieces of 0.4 cm * 0.4 cm and rinsed with ethanol prior to use.

5.2.2.3 Immobilization of BiBUT on gold surface

The initiator was immobilized on gold surface by incubating the substrates in 1 mM ethanol solution of BiBUT overnight at room temperature. The substrate was then rinsed with ethanol and dried with nitrogen flow and kept in argon atmosphere before use.

5.2.2.4 Surface-initiated polymerization of HEMA on gold substrate through SI-ATRP

46 mg CuBr and 70 mg ascorbic acid were added into one flask, which was then purged with argon. Into this flask 60 ml of H_2O/Methanol 1:1 solvent was added. In another flask 34 ml of H_2O/Methanol 1:1 solvent and 2 ml of HEMA were added. After 30 mins of

purging both flasks, 140 ul of PMEDTA was added into the CuBr flask. After another 15 mins of purging, 6 ml of solution was transferred from the flask with CuBr into the other flask with HEMA, and after fully mixing 15 ml solution was injected into the substrate container to start polymerization. After polymerization substrates were taken out into H2O/Methanol 1:1 for quenching and was sonicated twice for one minute each time, followed by rinsing with isopropanol and drying with nitrogen flow.

5.2.3 Immobilization of peptide on p(HEMA) film

Two routes of peptide immobilization were used in this study, as illustrated in Figure 5-1.

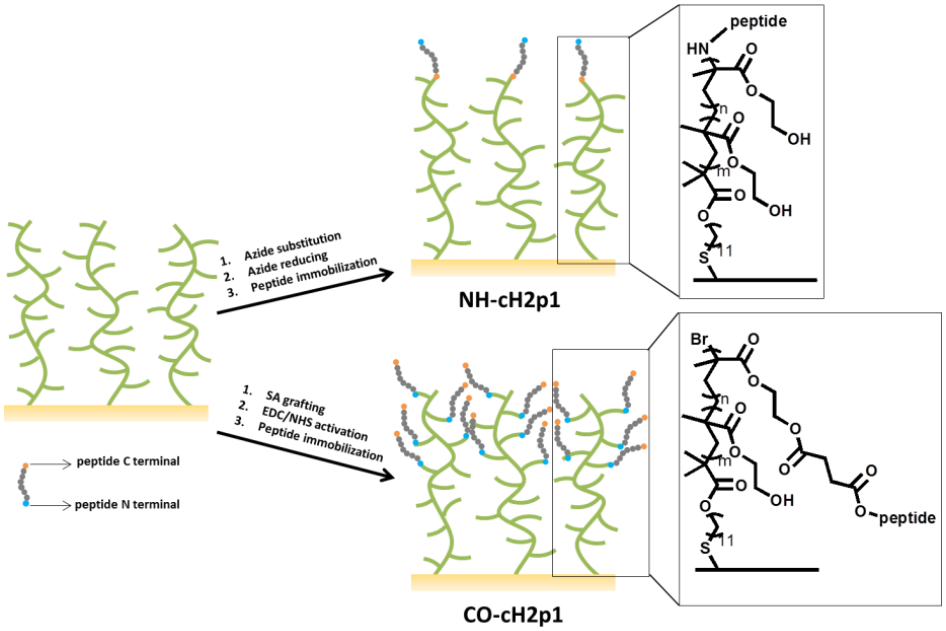

Figure 5-1 Schematic diagram showing the route of immobilization of p(HEMA) and peptide on gold surface

5.2.3.1 Peptide attached to p(HEMA) chain end groups (NH-cH2p1)

For azide substitution, p(HEMA) brush coated substrates were immersed into 10 ml H_2O with 65 mg NaN_3 with stirring and were kept for 24 hrs at room temperature. After

completion of azidation the substrates were rinsed with H_2O and ethanol and were dried with nitrogen flow. For azide reducing into primary amine, the substrates were immersed into 10 ml ethanol with 0.1 g PPh3 and 0.1 ml H_2O for 24 hrs at room temperature. After that the substrates were rinsed with ethanol and dried with nitrogen flow. For peptide immobilization on substrates, 2.5 mg of peptide was dissolved into 0.5 ml of sodium citrate buffer (0.01 M, pH 4.7). 10 mg of NHS and 100 mg of EDAC were dissolved into another 0.5 ml of sodium citrate buffer. Upon mixing of these two solutions, the mixture was added to fully immerse substrates. The reaction was kept for 24 hrs at 4 ºC. After reaction, substrates were rinsed with sodium citrate buffer and milli-Q water, followed by drying with nitrogen flow. The obtained substrate samples were denoted as NH-cH2p1.

5.2.3.2 Peptide attached to with p(HEMA) side chain groups (CO-cH2p1)

For grafting of succinic anhydride (SA), p(HEMA) brush coated substrates were immersed into 8 mL of anhydrous dioxane containing 0.1 g of SA, 0.12 g of DMAP, and 0.3 mL of TEA. The reaction was allowed to proceed for 24 hrs at room temperature. The substrates were then washed with copious amounts of methanol and water and were dried with nitrogen flow. For peptide immobilization on substrates, the substrate was preactivated for 1 hr at room temperature in 2 ml of phosphate buffered saline (PBS, pH 7.4) containing 2 mg of NHS and 20 mg of EDAC. The substrates were then transferred to 2 ml PBS solution containing 2.4 mg peptide. The reaction was allowed to proceed for 24 hrs at 4 ºC. After the reaction, substrates were rinsed with PBS and milli-Q water, followed by drying with nitrogen flow. The obtained substrate samples were denoted as CO-cH2p1.

5.2.4 Surface characterization

5.2.4.1 Characterization of polymer film thickness and grafting density

The thickness of the formed p(HEMA) layer on substrate was measured using ellipsometry (M-2000V J.A. Woollam Ellipsometer) and was fitted by PMMA model provided in the database. The optical constant (ks, ns) and gold layer thickness was obtained for bare gold sputtered wafers prior to pHEMA layer formation and was used in fitting of substrate model. For measurement, scanning wavelength was ranged from 300~1000 nm and three incidental angles (65º, 70º, 75º) were applied. The grafting density of p(HEMA) layer was measured through Quartz Crystal Microbalance (QCM200m, Stanford Research Systems). The oscillation frequency of QCM chips before and after polymerization was measured, and the frequency difference was converted to mass through Sauerbrey equation for grafting density.

5.2.4.2 Characterization of surface chemistry: X-ray photoelectron spectroscopy (XPS)

X-ray photoelectron spectroscopy (Kratos AXIS 165) was used to characterize substrates. Both survey scan and elemental core-level scan was obtained. Peaks from elemental core-level scan were background subtracted and integrated for quantification of each element.

5.2.4.3 Water contact angle characterization

An FTA-200 video system was used for contact angle measurement. Static contact angle was obtained through sessile drop method, with a drop size of 2 μl. For determination of contact angle, images of droplets were continuously captured for 5 s at an interval of 0.1 s, and the optimal model and results were automatically determined by the software.

5.2.5 Nonspecific protein adsorption test: Surface plasmon resonance imaging (SPRi)

A SPRi (SPRimager®II ARRAY, GWC TEchnologies) system was used to test nonspecific protein adsorption on p(HEMA) coated substrates. p(HEMA) was grafted from the SPRi sensors using methods described above. Prior to SPRi measurements, the angle of incident was adjusted to reach the minimum pixel intensity, and regions of interest (ROIs) on arrayed gold spots was picked for signal monitoring. Sensors were pre-immersed in PBS (0.01 M pH 7.4) for 30 mins, followed by protein solution running with 1 mg/ml HSA in PBS with the flow rate of 60 µl/mins. After adsorption equilibrium was reached, protein solution was replaced by PBS buffer and was kept running until desorption equilibrium had been reached. S-polarized images of the same ROIs were taken for data correction. For reflectivity to mass calculation, 15.8 ng/cm2 per 1% ΔR was applied, according to a calibration test study [325].

5.2.6 Radiolabeled protein adsorption

5.2.6.1 Protein radiolabeling through I^{125} iodination tube

Proteins were radiolabeled through direct iodination protocols provided by the manufacturer. In brief, 50 µg protein sample was mixed with 100 µCi of $Na^{125}I$ in 100 µl of PBS and was then added into iodination tube. The reaction was kept for 10 mins for HSA/cHSA and 5 mins for Fgn/cFgn. Upon completion, 1 ml of PBS with NaI (1 mM) was added into the tube, and then all mixtures were transferred to 10DG desalting column.

The desalting was done following manufacturer's procedure. In brief, the column was first eluted with 30 ml of PBS for equilibration, followed by addition of radiolabeled protein solutions and allow the sample to run completely into the gel. 10 ml of PBS was added to

elute the sample, and each eluted fraction contains 1 ml of solution. The radioactivity for each fraction was counted by measuring CPM of 10 µl aliquot in a gamma counter (2470 Wizard^2, PerkinElmer Inc). The fraction with the peak CPM value was transferred to a micro dialysis cassette for 1-day dialysis in PBS with 5 mol% NaI at 4 ºC. The residual amount of free $Na^{125}I$ after column separation and dialysis was estimated by a standard trichloroacetic acid (TCA) assay. In brief, 5 µl of radiolabeled sample was mixed with 20 µl of BSA (50 mg/ml in PBS), followed by addition of 100 µl of 20 % TCA. After incubation at 4 ºC for 20 mins, the precipitates were centrifuged down at 5000 g for 10 mins. The percentage of free $^{125}I^-$ in sample was calculated by the following equation:

$$I^{125}\% = \frac{CPM_{supernatant}}{CPM_{solution}} \times 100\%$$

Where $I^{125}\%$ represents the presence of free $^{125}I^-$ as percentage to the total ^{125}I, $CPM_{supernatant}$ represents the CPM of supernatant after centrifuge for free $^{125}I^-$, and $CPM_{solution}$ represents the CPM of radiolabeled sample for total ^{125}I.

5.2.6.2 Protein adsorption test

The obtained radiolabeled protein was mixed with unlabeled protein with the hot/cold ratio of 1:10 in PBS (pH 7.4) containing 5 mol% NaI. For binary competitive adsorption test, either radiolabeled carbamylated protein or radiolabeled native protein was added into their cold mixture for quantification of adsorption of each component. Carbamylated and native proteins were mixed at different molar ratio and the total protein concentration was fixed at 0.05 mg/ml in PBS-NaI (pH 7.4, 5 mol% NaI). For plasma protein adsorption, 10% plasma was prepared by 10 folds dilution of human plasma in PBS-NaI (pH 7.4, 5 mol% NaI). For cHSA adsorption under plasma, cHSA was added into the plasma with the final concentration of 0.04-0.24 mg/ml, which corresponds to 1%-6% of plasma HSA. For cFgn adsorption under plasma, cFgn was added into the plasma with the final concentration of 0.016-0.065 mg/ml, which corresponds to 5%-20% of plasma Fgn. Prior to protein

adsorption, all substrates were pre-immersed in PBS for 30 mins. Then all substrates were put on a flat surface under humid environment, with filter papers to absorb residual buffer droplets from surface. Protein solution was then introduced and fully immerses each substrate surface. Adsorption was allowed to proceed for 120 mins at room temperature. Then each substrate was flushed with copious amount of PBS and dried with a filter paper. The radioactivity was counted using a gamma counter by placing the substrates into the detector's counting tubes, with triplicate measurements for each sample. The count for each sample was averaged and surface concentration (S.C.) is to be calculated by the equation:

$$\text{S. C.}\,(\text{ng}/cm^2) = \frac{counts(c.p.m.)}{Sp.Ac.\,(cpm/ng) \times SA(cm^2)}$$

Where the counts are the radioactivity of the substrate; Sp.Ac. is the specific activity per ng of protein, determined through the solution radioactivity measurement; and SA is the surface area of substrate exposed to protein solution (0.16 cm^2 in this study).

5.2.6.3 Radiolabeled protein characterization

SDS-PAGE was performed on a Bio-Rad mini-protean electrophoresis system for characterization of radiolabeled protein and verify the structural integrity after radiolabeling. In brief, 10 µl of protein sample was mixed with 10 µl of 0.1 % SDS and was heated at 60 ºC for 5 mins. After loading samples into wells of a precast gel, electrophoresis was performed at 200 V for ~ 30 mins. Upon completion, gels were sliced into pieces with different molecular ranges (55-100 kDa, 25-55 kDa) marked by bands of standard molecular ladder and were then sent for CPM counts. BCA assay was performed to determine the protein yield after radiolabeling, following protocols provided by the manufacturer. In brief, 0.15 ml of radiolabeled sample after dialysis or reference solution was mixed with 0.15 ml of working reagent (WR) in a microplate well. After incubating the plate at 37 ºC for 2 hrs, absorbance at 562 nm was read.

5.3 Result and discussion

In order to immobilize peptides of interests on surface with minimized unwanted non-specific protein adsorption ability, p(HEMA) brushes were grown on gold surface through SI-ATRP, followed by grafting of peptide on top of polymer film.

5.3.1 Synthesis of SI-ATRP initiator BiBUT

The initiator (BiBUT) was synthesized following Figure 5-2, which was composed of three steps: (1) Substitution of bromide with protected thiol (2) Esterification of hydroxyl group with 2-bromoisobutyryl bromide (3) Deprotection to give thiol group. The chemical structure of BiBUT was characterized through ^{1}H-NMR with the spectrum shown in Figure 5-3. Characteristic peaks of BiBUT were displayed at 2.44 ppm ($HSCH_2$-, peak a), 1.2-1.6 ppm (-CH_2-, peak b), 4.10 ppm (-CH_2OC=O-, peak c), and 1.87 ppm (-CH_3, peak d).

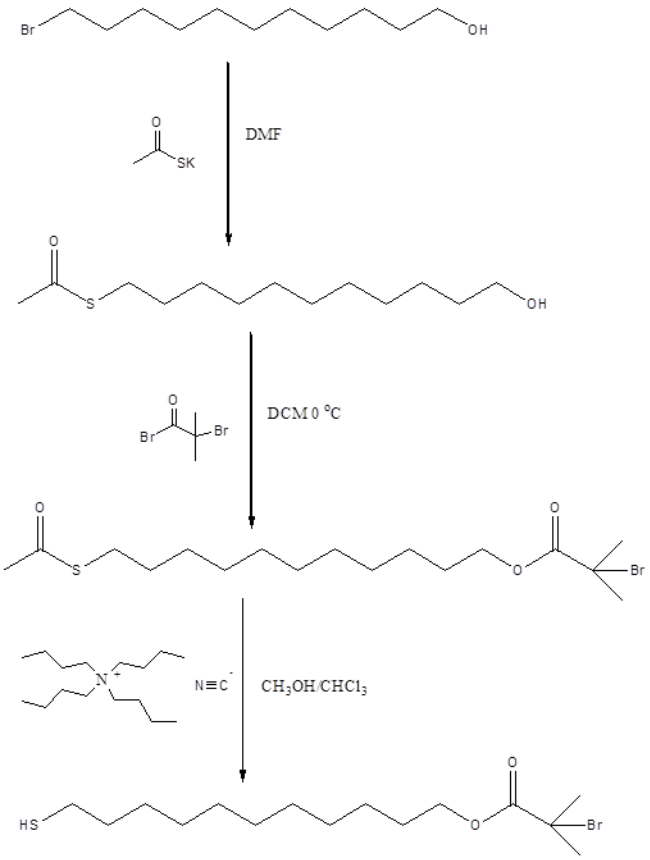

Figure 5-2 Schematic diagram illustrating the synthesis of SI-ATRP initiator BiBUT

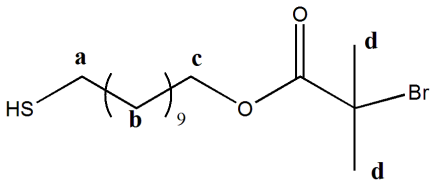

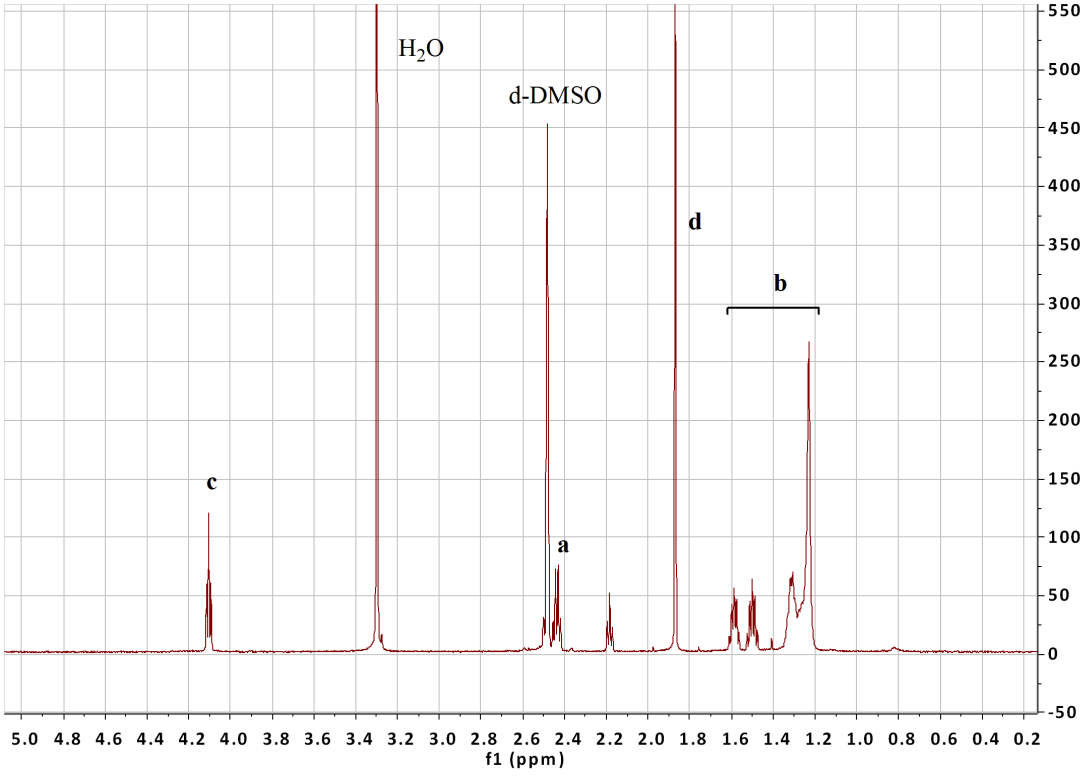

2-bromoisobutyryl undecanethiol (BiBUT)

Figure 5-3 ^{1}H-NMR spectrum of SI-ATRP initiator 2-bromoisobutyryl undecanethiol (BIBUT)

5.3.2 SI-ATRP of HEMA on gold surface

The success of p(HEMA) polymerization on gold surface can be confirmed through XPS spectra shown in Figure 5-4a. Au-pHEMA represents gold substrates after immobilization of BiBUT and SI-ATRP of HEMA. Compared with bare Au with only signals for Au, all Au signals disappeared for spectrum of Au-pHEMA, with only C and O present. C/O ratio for Au-pHEMA was determined as 2.2 shown in Table 5-1, which is in proximity with theoretical 2.0 value for C/O. The absence of Au signal after polymerization should suggest the full coverage of p(HEMA) coating on Au surface with no defect.

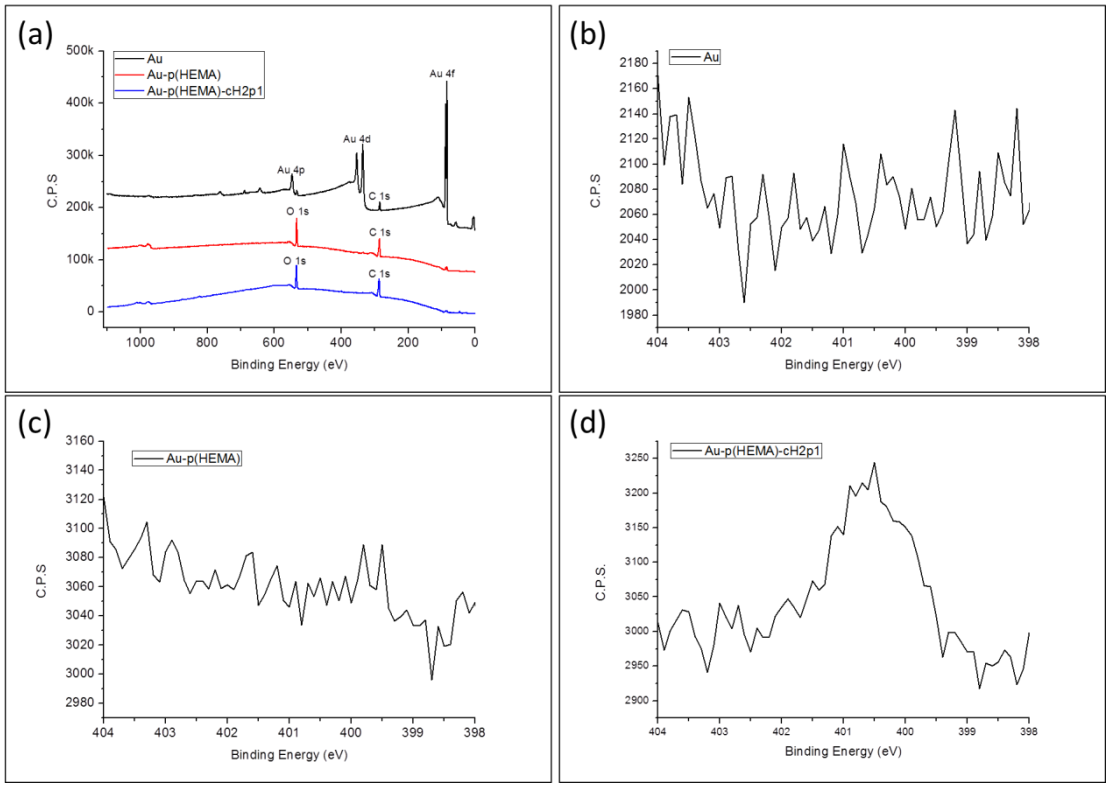

Figure 5-4 X-ray photoelectron spectroscopy (XPS) characterization for immobilization of polymer and peptide based on gold. (a) Survey scan of bare Au, Au-pHEMA, NH-cH2p1, (b) N 1s core-level scan of bare Au (c) N 1s core-level scan of Au-pHEMA (d) N 1s core-level scan of NH-cH2p1

Table 5-1 XPS elemental composition and water contact angle for Au, Au-Br, Au-pHEMA, NH-cH2p1 and CO-cH2p1

Sample	Elemental composition (%)						C/O ratio	Contact angle (°)
	O 1s	C 1s	Au 4f	S 2p	Br 3d	N 1s		
Bare Au	7.8	29.6	62.5	0	0	0	3.8	74.9±4.6
Au-Br	8.0	31.4	55.8	1.4	3.2	0	3.9	75.0±0.8
Au-pHEMA-5min	30.8	67.2	1.8	0	0	0	2.2	55.0±3.7
Au-pHEMA-15min	31.0	67.6	1.27	0	0	0	2.2	57.3±1.9
Au-pHEMA-30min	27.9	72.0	0.04	0	0	0	2.6	56.4±2.2
Au-pHEMA-60min	28.3	71.2	0.3	0	0	0	2.5	57.1±1.9
NH-cH2p1	28.3	69.8	0	0	0	1.9	2.5	55.6±0.5
CO-cH2p1	26.4	68.5	0.9	0	0	4.2	2.6	62.8±0.8

Polymerization time has been used to control the thickness of polymer film. As shown in Figure 5-5, the film thickness increased rapidly from 0 to ~46 nm in the first 30 mins of polymerization, and was then increased slowly to ~52 nm after 1 hr of polymerization. The nonlinear thickness growth with time may due to the termination of reactions as the polymerization proceeds, or steric hinderance between monomers and radicals as the polymer chains grow larger [71]. Even though, a fairly good control over thickness in the range of 10 to 50 nm can be achieved by adjusting the polymerization time from 5 to 60 mins. It has been reported before that the optimal anti-fouling thickness of p(HEMA) brushes prepared by SI-ATRP was found to be ~20-45 nm [326]. We therefore adjusted the polymerization to 12 mins for subsequent use, and the film thickness of 24 ± 2 nm was constantly achieved.

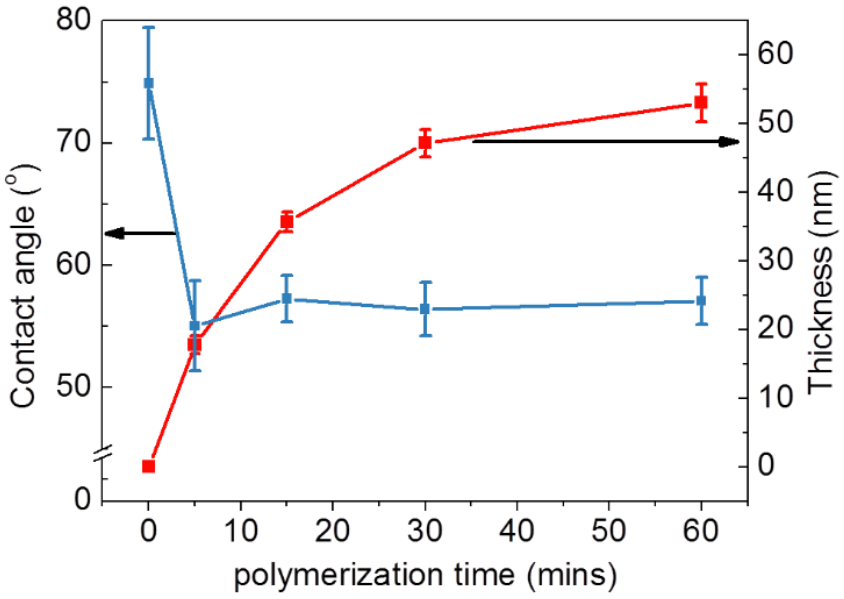

Figure 5-5 Dependence of film thickness of p(HEMA) as a function of polymerization time

Water contact angle was used for analysis of surface hydrophilicity of p(HEMA) film. As shown in Figure 5-5, static contact angle of bare Au surface was measured to be 75°. After polymerization of HEMA, the surface hydrophilicity was greatly improved by lowing contact angle from 75° for bare Au to ~55 ° for Au-p(HEMA) with different polymerization time. The time of polymerization seems to have little effect in determining the static contact angle.

The grafting density of p(HEMA) was measured by QCM. For p(HEMA) layer with thickness of 23.8±1.1 nm on a QCM chip, surface density of p(HEMA) was measured to be 3248±345 ng/cm^2. Since the molecular weight of p(HEMA) cannot be measured directly, the chain density was estimated by comparison with similar studies. By assuming that the p(HEMA) film is uniform spatially, the density of monomer entities in top 10 nm was

calculated to be 10.5 nmol/cm^2, or 63.2/nm^2. For closely packed p(HEMA) reported before, the chain density was found to be 0.7/nm^2, which can be converted to a HEMA density of 43/nm^2 for 10 nm of p(HEMA) brushes [327]. According to this, we may estimate the chain density of our p(HEMA) film to be similar to 0.7/nm^2, and should be present as brush region [328].

5.3.3 Non-specific protein adsorption on p(HEMA) film based on gold surface

p(HEMA) film was tested for its ability to resist non-specific protein adsorption in single solution of HSA. It can be noted that in Figure 5-6, the net HSA adsorption on bare gold surface after PB rinsing is 79 ng/cm^2. With p(HEMA) film, the net adsorption is as low as 0 and the difference between the end and beginning reflectivity is almost undetectable. The slight difference in reflectivity could be converted to a net adsorption of 0.4ng/cm^2, and this may just be caused by shift in background.

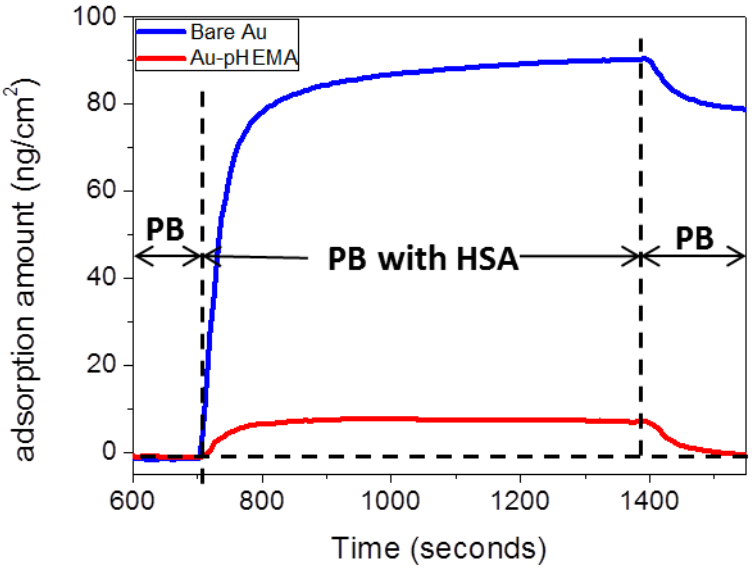

Figure 5-6 Adsorption process of HSA (1 mg/ml) on SPRi sensors of Au coating with and without p(HEMA) film.

5.3.4 Immobilization of candidate peptides on p(HEMA) film

The peptide cH2p1 with the sequence GSAARTISPSLL has been reported in our previous study as a ligand that binds to carbamylated proteins. Therefore, cH2p1 may serve as a potential binding element for carbamylated proteins when immobilized on surface. To demonstrate the feasibility of this application, immobilization of cH2p1 onto pHEMA brushes was studied with two strategies, through covalent bond with C-terminal (NH-cH2p1) and N-terminal (CO-cH2p1) of cH2p1. For NH-cH2p1, cH2p1 was attached to the pHEMA chain ends after substitution of terminal bromide with azide groups, followed by reduction of azide groups to primary amine (Figure 5-1). For CO-cH2p1, cH2p1 was attached to the pHEMA side chains after coupling of SA to hydroxyl groups (Figure 5-1). Presence of cH2p1 on both NH-cH2p1 and CO-cH2p1 was confirmed through the

appearance of N 1s signal in XPS spectra, which is absent in pHEMA film (Figure 5-7). Although azide substitution for NH-cH2p1 also introduce nitrogen on surface, XPS fails to detect any N 1s signal on pHEMA film after azide substitution or azide reduction, possibly due to the low nitrogen density. The N 1s peak at 400.3 eV for both NH-cH2p1 and CO-cH2p1 was typical for amide nitrogen (-NH-C=O-) in peptide backbone [329]. CO-cH2p1 was found with a C/N ratio of 16.5, lower than C/N of 37.6 for NH-cH2p1 (Table 5-1), which suggests a higher surface density of cH2p1 in CO-cH2p1. The higher cH2p1 density for CO-cH2p1 should be simply due to higher availability of sites for peptide attachment in side chains than in chain ends of pHEMA.

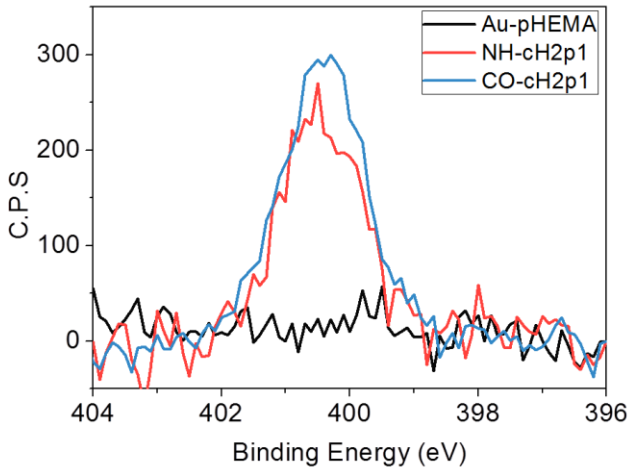

Figure 5-7 XPS N 1s core-level scan for Au-pHEMA, NH-cH2p1 and CO-cH2p1

From Table 5-1, we found the water contact angle is shown to be 55.6° for NH-cH2p1, and is almost the same as 57.3° for Au-pHEMA without peptides, and CO-cH2p1 has only a slightly higher contact angle of 62.8°. The difference between CO-cH2p1 and Au-pHEMA should be due to replacement of surface composition from p(HEMA) to cH2p1, which slightly alters the surface wettability. For NH-cH2p1, it is possible the peptide density not high enough to cause changes on surface wettability.

5.3.5 Radiolabeled protein adsorption

Both cHSA and cFgn samples for adsorption test were prepared following protocols we used previously, with the homocitrulline level measured to be 3.1% and 15.7% for cHSA and cFgn, respectively. The Hcit% of 3.1% for cHSA falls in range of 1.7%-3.4% estimated from fragmentation and multiple reaction monitoring (MRM) data of carbamylated albumin from uremic patients reported before [28]. However, till now we have not yet found any study providing the Hcit% data for cFgn in uremic patients. In any case, it was found only a small fraction of protein been carbamylated to any extent *in vivo*. Both the low Hcit% level with high similarity to native protein and their low plasma concentrations pose great challenges to the target of carbamylated protein removal in real applications.

To label proteins with radioactive iodine isotopes, it is important to be cautious on the oxidative iodination reaction, which may cause protein degradation. Therefore we first did a SDS-PAGE of radiolabeled proteins with different iodination time (Figure 5-8), and then determined the optimized reaction time of 10 mins for HSA/cHSA and 5 mins for Fgn/cFgn, to achieve a sufficiently high radioactivity counts while minimizing degradation. Radio counts of residual free iodide in radiolabeled protein samples was below 2% of total counts, as determined through TCA assay. The yield of labeled HSA, cHSA, Fgn, and cFgn was determined as 45.3%, 44.9%, 52.6% and 58.6%, with a specific activity of 15.3, 18.4, 27.8, and 63.0 cpm/ng, respectively for their single protein solution at a cold concentration of 0.05 mg/ml.

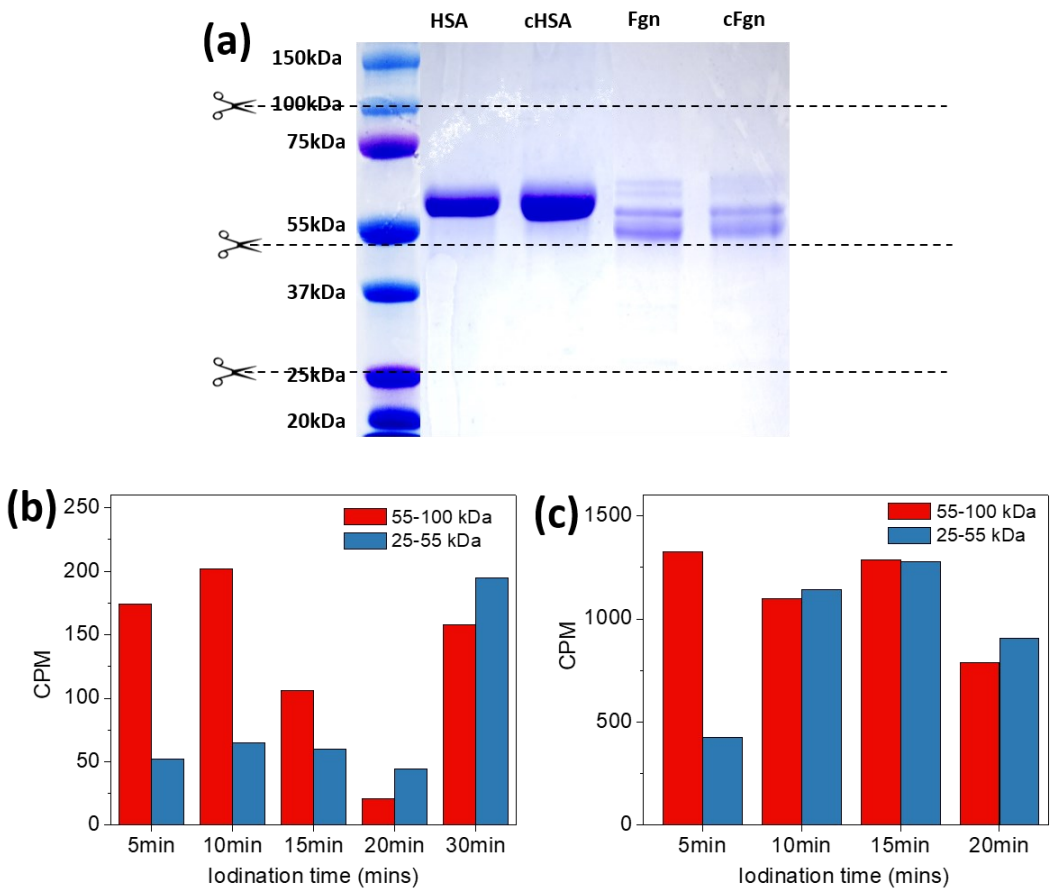

Figure 5-8 (a) SDS-PAGE bands of HSA/cHSA and Fgn/cFgn, (b) CPM counts for eluted fractions from 10DG column obtained by direct radiolabeling method for HSA and cHSA, (c) CPM counts for eluted fractions from 10DG column obtained by direct radiolabeling method for Fgn and cFgn.

It has been reported before iodide has a strong tendency to bind with gold [330]. The residual $^{125}I^-$, even at a low level, may interfere with our protein adsorption performed on gold based surface. We do have noticed that adsorption of I-HSA (0.4 mg/ml in PBS, hot/cold=4:1) on Au-p(HEMA) resulted in a CPM of 143, which suggests an unreasonable high surface adsorption amount 590 ng/cm^2 and should be mainly due to adsorption of $^{125}I^-$. We then include NaI into the solution of I-HSA for adsorption on Au-p(HEMA), and the CPM was dropped to below the detection limit. For protein adsorption on Au-p(HEMA), we have determined through SPRi the net adsorption amount be lower than 0.5 ng/cm^2,

which would be converted to CPM values less than 1 in this case.

5.3.5.1 HSA/cHSA competitive binding on NH-cH2p1 and CO-cH2p1

Competitive binding test between HSA and cHSA was done with varied [HSA]/[cHSA] ratio from 0:1 to 3:1 at a total concentration of 0.05 mg/ml. As shown in Figure 5-9, cHSA were adsorbed more or at a similar amount to HSA on both surfaces from 1:3 to 3:1, which suggests both NH-cH2p1 and CO-cH2p1 surface have specific binding affinity to cHSA. For either HSA or cHSA adsorption, CO-cH2p1 showed a higher adsorption amount than NH-cH2p1. By comparing adsorption amount between HSA and cHSA, however, we find NH-cH2p1 was with better selectivity of cHSA ($p<0.1$ for 1:3 and 1:1) than CO-cH2p1 ($p<0.1$ for 1:3). Although Au-pHEMA showed ultralow adsorption of HSA, the surface after peptide immobilization was no longer to be nonfouling against protein adsorption, as 5 to 20 ng/cm2 of HSA were adsorbed and 10 to 35 ng/cm2 of cHSA were adsorbed. We have found in our previous studies that cH2p1 in solution binds to both HSA and cHSA with Kd of $\sim 1\times10^{-3}$ M and $\sim 1\times10^{-4}$ M, which enables their binding to surface and explains the difference in their adsorption amount. For NH-cH2p1 with a higher cHSA selectivity over HSA than CO-cH2p1, it is possible that in NH-cH2p1 the N terminal of cH2p1 was exposed for binding, while in CO-cH2p1 it is the C terminal exposed, so the N terminal exposed surface is a better mimic of phage tails, that the N terminal of phage random peptide segment is to be in contact with target during biopanning. On the other hand, peptide anchored to pHEMA chains, especially in CO-cH2p1 where peptide anchored to polymer side chains, may break the hydration layer and increase the amount of protein nonspecific adsorption and weaken the desired surface selectivity.

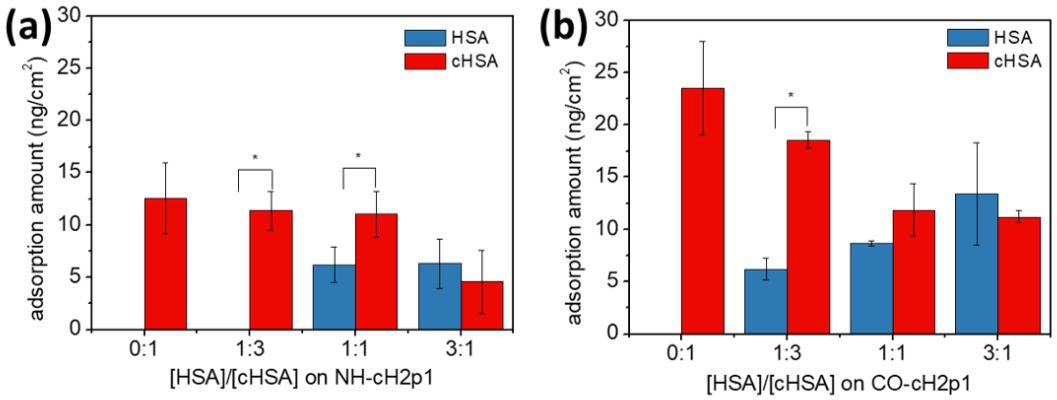

Figure 5-9 Competitive binding of HSA/cHSA at different ratios, Data represent mean ±1 SD, n=3; *, $p<0.1$

5.3.5.2 Fgn/cFgn competitive binding on NH-cH2p1 and CO-cH2p1

Both NH-cH2p1 and CO-cH2p1 adsorb a significant amount of cFgn compared to Fgn at different ratios (Figure 5-10). For NH-cH2p1, the adsorption amount of cFgn was significantly higher than Fgn at 1:3 ($p<0.1$). While for CO-cH2p1, the adsorption amount of Fgn and cFgn was similar at all tested ratios. This result is similar to that obtained in HSA/cHSA binding that NH-cH2p1 shows higher selectivity than CO-cH2p1 towards carbamylated protein, and is consistent with our previous findings that cH2p1 in solution binds with cFgn at a Kd of 8×10^{-5} M, but did not interact with Fgn. Another fact to be noted is that on some model surfaces, such as bare gold, -OH terminated and –CH3 terminated self-assembled monolayer (SAM) surface we have tested before, cFgn always adsorbs less than its native form. Therefore, carbamylation reduces the protein nonspecific adsorption, and removal of cHSA or cFgn has to go through carbamylation specific interactions instead of nonspecific ones.

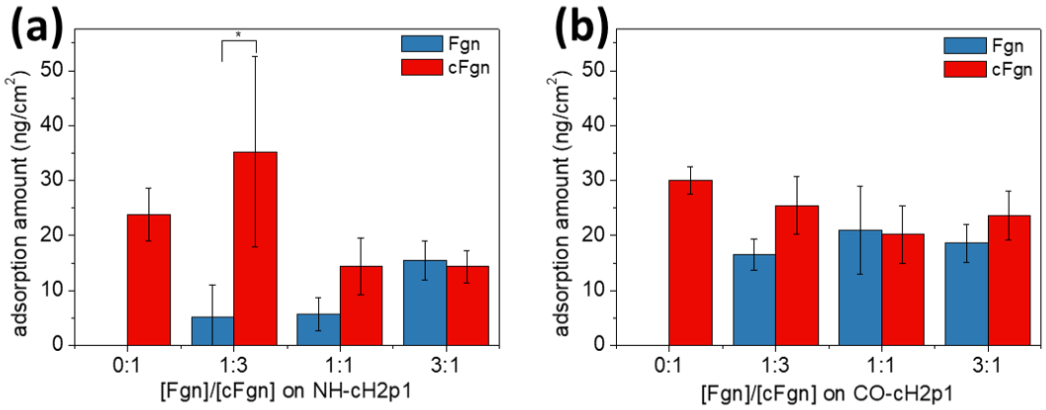

Figure 5-10 Competitive binding of HSA/cHSA at different ratios, Data represent mean ±1 SD, n=3; *, $p<0.1$

5.3.5.3 cHSA and cFgn adsorption in diluted plasma on NH-cH2p1 and CO-cH2p1

For cHSA or cFgn adsorption in plasma, we spiked 2%-6% of cHSA or 5%-20% of cFgn as compared to estimated HSA or Fgn concentrations. Although the plasma sample for our study may contain cHSA or cFgn and affect the total concentration of carbamylated proteins, this influence should be limited, because for healthy people carbamylated HSA takes only 0.4% of total HSA [28], and carbamylated Fgn even less [240]. Due to the low concentration of radiolabeled protein solution (~25 ug/ml) and the need to maintain the hot/cold ratio for a high detection resolution, plasma samples have to be diluted and we find 10 folds dilution is the minimum to meet all concentration needs.

For plasma cHSA adsorption, the adsorption amount increases with the cHSA concentration, and both surfaces have the similar adsorption (Figure 5-11a). For NH-cH2p1 the adsorption amount was ranged from 1.5 ng/cm^2 to 12.2 ng/cm^2, and for CO-cH2p1 the adsorption amount was ranged from 3.4 ng/cm^2 to 15.0 ng/cm^2. Although much more HSA

was present than cHSA in tested plasma samples, compared to competitive binding test, and with more complexed medium environment, the adsorption amount of cHSA at 4% and 6% varied from 10 ng/cm^2 to 15.0 ng/cm^2 for either surface and is close to the adsorption amount of ~11 ng/cm^2 obtain in HSA/cHSA of 1:1 in binary competitive binding test (Figure 5-9). This suggests that for both NH-cH2p1 and CO-cH2p1, a high HSA/cHSA ratio, even up to 25 to 1 for 4% sample, did not resulted in a big compromise in the binding capacity to cHSA, nor did the cHSA binding affected by the complex environment of plasma.

For plasma cFgn adsorption, the trend of adsorption amount increase is consistent to that of plasma cHSA adsorption, and NH-cH2p1 adsorbs a higher amount of cFgn than CO-cH2p1 (Figure 5-11b). For NH-cH2p1, the adsorption amount of cFgn at 15% and 20% is 13.7 ng/cm^2 and 15.7 ng/cm^2 and is very close to 14.3 ng/cm^2 obtained in Fgn/cFgn of 1:1 in binary competitive binding test (Figure 5-10a). However for CO-cH2p1, the adsorption amount of cFgn was ranged from 0.5 ng/cm^2 to 7.4 ng/cm^2 (Figure 5-11b), far below the adsorption amount of 20.2 ng/cm^2 obtained in Fgn/cFgn of 1:1 in binary competitive binding test (Figure 5-10b). This result suggests that only for NH-cH2p1 the binding capacity to cFgn was maintained in plasma, as shown by adsorption amount for cFgn concentration higher than 15%, but the cFgn binding capacity for CO-cH2p1 was significantly weakened.

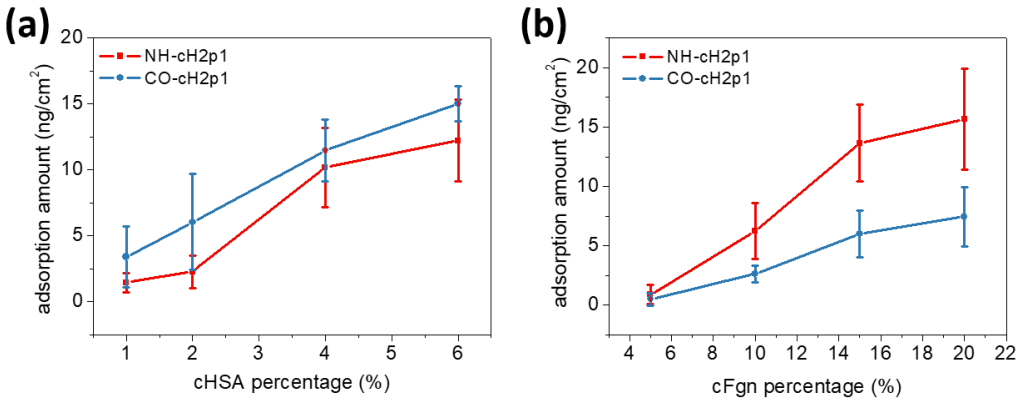

Figure 5-11 Adsorption of (a) cHSA and (b) cFgn in diluted plasma on NH-cH2p1 and CO-cH2p1, Data represent mean ±1 SD, n=3.

Based on all binary and plasma protein binding test, we may therefore conclude that NH-cH2p1 is a superior surface than CO-cH2p1 with higher carbamylated protein selectivity and better maintained adsorption capacity in diluted plasma. To better understand the selective adsorption performance of NH-cH2p1 in diluted plasma, we further did a protein adsorption test to measure adsorption of HSA, cHSA, Fgn and cFgn when they are all present in diluted plasma with radiolabeling, and the result is shown in Figure 5-12. It was be found that HSA was the most adsorbed protein, which was 17.7 ng/cm^2 at 10 mins and then was increased to 113.5 ng/cm^2 to reach a saturation after 1hr. However, we found the adsorption of Fgn is undetectable throughout the entire adsorption process. According to the specific activity of radiolabeled Fgn, this should mean an adsorption amount below a low limit of 2.6 ng/cm^2 for 1 cpm. Moreover, the adsorption of cHSA remained almost unchanged at ~6 ng/cm^2 throughout the adsorption time, and the adsorption of cFgn was gradually increased from 0.3 ng/cm^2 at 10 mins to 13.6 ng/cm^2 at 120 mins.

Despite the high adsorption amount of HSA, still a high adsorption amount was achieved for cHSA or cFgn. Although at the initial 10 mins far more amount of cHSA (6.1 ng/cm^2) was adsorbed than cFgn (0.3 ng/cm^2), we saw a near linear growth of cFgn over time. The increase of cFgn adsorption did not come with a decrease of adsorbed cHSA. As is like what causes Vroman effect, cFgn was continuously adsorbed by replacement of earlier adsorbed HSA instead of cHSA, since HSA has a higher concentration but much less affinity to this cH2p1 immobilized surface. Interestingly what unlike Vroman effect is that this replacement occurs only for cFgn, but not for Fgn at all.

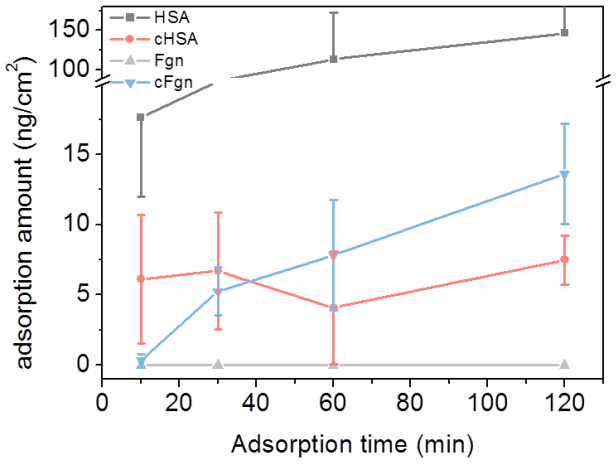

Figure 5-12 Adsorption of HSA, cHSA, Fgn and cFgn in diluted plasma on NH-cH2p1. Data represent mean ±1 SD, n=3. (The adsorption profile for HSA was not fully shown for better graph view)

The high amount of HSA adsorption should be due to the structural change of pHEMA brushes when functionalized with biomolecules, which breaks its hydration layer that prevents proteins from adsorption [113]. Although in NH-cH2p1 only chain end groups were functionalized with peptide, it is not very likely all these chain ends were fully exposed on surface, and hence peptide immobilized onto partially buried chain ends may generate gaps on hydration layer and cause nonspecific protein adsorption. It has been reported before that pHEMA brushes with streptavidin immobilization showed a nonspecific protein adsorption amount of ~110 ng/cm^2 under 10% fetal bovine serum (FBS), similar to the adsorption amount of HSA in our case [108]. Likewise, antibody functionalized pHEMA brushes showed ~60 ng/cm^2 of plasma protein adsorption [113]. Unlike cases of plasma protein adsorption driven merely by nonspecific interactions [331], we found in this study a huge difference in adsorption behavior between HSA and Fgn. This difference should be related to their affinity difference to cH2p1. With moderate binding affinity to cH2p1 as shown before, HSA was adsorbed to NH-cH2p1 almost nonspecifically that can be replaced by a more affinitive substrate. Since Fgn has no

binding interaction with cH2p1, the surface immobilized cH2p1 does not even allow Fgn to approach the polymer layer. Although HSA was adsorbed to surface with a high amount, it did not completely block the active peptide sites for specific binding, as revealed by the continuous growth of cFgn adsorption. It should be noted that adsorption of HSA is usually not a concern, and in fact albumin coatings have been shown in many studies to reach improved blood compatibility, with a passivate effect [332-334]. For better outcomes in hemocompatibility, it is important to minimize Fgn adsorption to avoid platelet adhesion and activation [256, 335], and a low Fgn adsorption has been determined as the most important criteria determining the hemocompatibility [336]. Therefore, the ultralow adsorption of Fgn (<2.6 ng/cm^2) achieved for NH-cH2p1 surface may provide an additional hemocompatibility benefit.

5.4 Conclusion

In this study, a novel adsorbent strategy for removal of carbamylated protein is proposed by combining carbamylation specific peptide with nonfouling polymer brushes. A well-controlled pHEMA brush thickness of 20-45 nm was achieved through surface-initiated atom-transfer radical polymerization and the obtained polymer film was proved with ultralow adsorption of HSA. Peptide cH2p1 was immobilized onto the pHEMA brushes by attachment of its N terminal or C terminal. cH2p1 functionalized surface were shown with selective binding towards cHSA and cFgn, and NH-cH2p1 were found with better selectivity and better maintained binding activity in diluted plasma than CO-cH2p1. More importantly for NH-cH2p1, although the nonspecific adsorption of HSA is high in diluted plasma, the adsorption of Fgn is quite low, which may suggest good hemocompatibility of such surface.

5.5 References

[28] A.H. Berg, C. Drechsler, J. Wenger, R. Buccafusca, T. Hod, S. Kalim, W. Ramma, S.M. Parikh, H. Steen, D.J. Friedman, J. Danziger, C. Wanner, R. Thadhani, S.A. Karumanchi, Carbamylation of Serum Albumin as a Risk Factor for Mortality in Patients with Kidney Failure, Science translational medicine 5(175) (2013).
[71] C. Zhao, L.Y. Li, Q.M. Wang, Q.M. Yu, J. Zheng, Effect of Film Thickness on the Antifouling Performance of Poly(hydroxy-functional methacrylates) Grafted Surfaces, Langmuir 27(8) (2011) 4906-4913.
[108] J. Trmcic-Cvitas, E. Hasan, M. Ramstedt, X. Li, M.A. Cooper, C. Abell, W.T.S. Huck, J.E. Gautrot, Biofunctionalized Protein Resistant Oligo(ethylene glycol)-Derived Polymer Brushes as Selective Immobilization and Sensing Platforms, Biomacromolecules 10(10) (2009) 2885-2894.
[113] H. Vaisocherova, V. Sevcu, P. Adam, B. Spackova, K. Hegnerova, A.D. Pereira, C. Rodriguez-Emmenegger, T. Riedel, M. Houska, E. Brynda, J. Homola, Functionalized ultra-low fouling carboxy- and hydroxy-functional surface platforms: functionalization capacity, biorecognition capability and resistance to fouling from undiluted biological media, Biosensors & bioelectronics 51 (2014) 150-157.
[240] V. Binder, B. Bergum, S. Jaisson, P. Gillery, C. Scavenius, E. Spriet, A.K. Nyhaug, H.M. Roberts, I.L.C. Chapple, A. Hellvard, N. Delaleu, P. Mydel, Impact of fibrinogen carbamylation on fibrin clot formation and stability, Thromb Haemostasis 117(5) (2017) 899-910.
[256] S.N. Rodrigues, I.C. Goncalves, M.C.L. Martins, M.A. Barbosa, B.D. Ratner, Fibrinogen adsorption, platelet adhesion and activation on mixed hydroxyl-/methyl-terminated self-assembled monolayers, Biomaterials 27(31) (2006) 5357-5367.
[285] D.K. Goyal, A. Subramanian, In-situ protein adsorption study on biofunctionalized surfaces using spectroscopic ellipsometry, Thin Solid Films 518(8) (2010) 2186-2193.
[312] E. Aghaee, J.B. Ghasemi, F. Manouchehri, S. Balalaie, Combined docking, molecular dynamics simulations and spectroscopic studies for the rational design of a dipeptide ligand for affinity chromatography separation of human serum albumin, Journal of molecular modeling 20(10) (2014).
[313] R.Z. Wang, D.Q. Lin, W.N. Chu, Q.L. Zhang, S.J. Yao, New tetrapeptide ligands designed for antibody purification with biomimetic chromatography: Molecular simulation and experimental validation, Biochem Eng J 114 (2016) 194-204.
[314] D.B. Kaufman, M.E. Hentsch, G.A. Baumbach, J.A. Buettner, C.A. Dadd, P.Y. Huang, D.J. Hammond, R.G. Carbonell, Affinity purification of fibrinogen using a ligand from a peptide library, Biotechnology and bioengineering 77(3) (2002) 278-289.
[315] P.V. Gurgel, R.G. Carbonell, H.E. Swaisgood, Fractionation of whey proteins with a hexapeptide ligand affinity resin, Bioseparation 9(6) (2000) 385-392.
[316] P. Jain, L. Sun, J.H. Dai, G.L. Baker, M.L. Bruening, High-capacity purification of his-tagged proteins by affinity membranes containing functionalized polymer brushes, Biomacromolecules 8(10) (2007) 3102-3107.
[317] F. Xu, J.H. Geiger, G.L. Baker, M.L. Bruening, Polymer Brush-Modified Magnetic Nanoparticles for His-Tagged Protein Purification, Langmuir 27(6) (2011) 3106-3112.

[318] S. Tugulu, P. Silacci, N. Stergiopulos, H.A. Klok, RGD - Functionalized polymer brushes as substrates for the integrin specific adhesion of human umbilical vein endothelial cells, Biomaterials 28(16) (2007) 2536-2546.
[319] Y. Fang, W. Xu, X.L. Meng, X.Y. Ye, J. Wu, Z.K. Xu, Poly(2-hydroxyethyl methacrylate) Brush Surface for Specific and Oriented Adsorption of Glycosidases, Langmuir 28(37) (2012) 13318-13324.
[320] F. Causa, E. Battista, R. Della Moglie, D. Guarnieri, M. Iannone, P.A. Netti, Surface Investigation on Biomimetic Materials to Control Cell Adhesion: The Case of RGD Conjugation on PCL, Langmuir 26(12) (2010) 9875-9884.
[321] F.Y. Liu, M.Y. Zhou, F. Zhang, I-125 labelling of human serum albumin and fibrinogen and a study of protein adsorption properties on the surface of titanium oxide film, Appl Radiat Isotopes 49(1-2) (1998) 67-72.
[322] E. Jansson, P. Tengvall, Adsorption of albumin and IgG to porous and smooth titanium, Colloid Surf. B-Biointerfaces 35(1) (2004) 45-51.
[323] Y. Chang, Y.J. Shih, C.Y. Ko, J.F. Jhong, Y.L. Liu, T.C. Wei, Hemocompatibility of Poly(vinylidene fluoride) Membrane Grafted with Network-Like and Brush-Like Antifouling Layer Controlled via Plasma-Induced Surface PEGylation, Langmuir 27(9) (2011) 5445-5455.
[324] Y. Sui, X.L. Gao, Z.N. Wang, C.J. Gao, Antifouling and antibacterial improvement of surface-functionalized poly(vinylidene fluoride) membrane prepared via dihydroxyphenylalanine-initiated atom transfer radical graft polymerizations, J Membrane Sci 394 (2012) 107-119.
[325] B.P. Nelson, T.E. Grimsrud, M.R. Liles, R.M. Goodman, R.M. Corn, Surface plasmon resonance imaging measurements of DNA and RNA hybridization adsorption onto DNA microarrays, Analytical chemistry 73(1) (2001) 1-7.
[326] C. Zhao, L. Li, Q. Wang, Q. Yu, J. Zheng, Effect of film thickness on the antifouling performance of poly (hydroxy-functional methacrylates) grafted surfaces, Langmuir 27(8) (2011) 4906-4913 %@ 0743-7463.
[327] C. Yoshikawa, A. Goto, N. Ishizuka, K. Nakanishi, A. Kishida, Y. Tsujii, T. Fukuda, Size-Exclusion Effect and Protein Repellency of Concentrated Polymer Brushes Prepared by Surface-Initiated Living Radical Polymerization, Macromolecular Symposia 248(1) (2007) 189-198.
[328] C. Yoshikawa, A. Goto, N. Ishizuka, K. Nakanishi, A. Kishida, Y. Tsujii, T. Fukuda, Size-exclusion effect and protein repellency of concentrated polymer brushes prepared by surface-initiated living radical polymerization, Macromolecular Symposia 248 (2007) 189-198.
[329] H. Lu, M.A. Hood, S. Mauri, J.E. Baio, M. Bonn, R. Munoz-Espi, T. Weidner, Biomimetic vaterite formation at surfaces structurally templated by oligo(glutamic acid) peptides, Chemical Communications 51(88) (2015) 15902-15905.
[330] Y.J. Du, R.M. Cornelius, J.L. Brash, Measurement of protein adsorption to gold surface by radioiodination methods: suppression of free iodide sorption, Colloid Surf. B-Biointerfaces 17(1) (2000) 59-67.
[331] Y.X. Ding, V. Hlady, Competitive Adsorption of Three Human Plasma Proteins onto Sulfhydryl-to-sulfonate Gradient Surfaces, Croat Chem Acta 84(2) (2011) 193-202.
[332] G. Jin, Q.H. Yao, S.Z. Zhang, L. Zhang, Surface modifying of microporous PTFE capillary for bilirubin removing from human plasma and its blood compatibility, Mat Sci Eng C-Bio S 28(8) (2008)

1480-1488.
[333] R.C. Eberhart, M.S. Munro, J.R. Frautschi, M. Lubin, F.J. Clubb, C.W. Miller, V.I. Sevastianov, Influence of Endogenous Albumin Binding on Blood-Material Interactions, Ann Ny Acad Sci 516 (1987) 78-95.
[334] K. Kottke-Marchant, J.M. Anderson, Y. Umemura, R.E. Marchant, Effect of albumin coating on the in vitro blood compatibility of Dacron® arterial prostheses, Biomaterials 10(3) (1989) 147-155.
[335] J.M. Grunkemeier, W.B. Tsai, C.D. McFarland, T.A. Horbett, The effect of adsorbed fibrinogen, fibronectin, von Willebrand factor and vitronectin on the procoagulant state of adherent platelets, Biomaterials 21(22) (2000) 2243-2252.
[336] T.A. Horbett, Fibrinogen adsorption to biomaterials, Journal of Biomedical Materials Research Part A 106(10) (2018) 2777-2788.

Chapter 6: Conclusion and Future Work

6.1 Conclusion

For better understand of carbamylation, the effect of carbamylation on three protein models were studied in terms of the secondary structure, tertiary structure, charge and water bound states. While the molecular integrity and secondary structure were well preserved after carbamylation, it was found carbamylation increases the surface charge negativity of protein and will significantly change its folding structure. For HSA and LA, carbamylation increases the accessibility of fluorescence quencher, which should suggest a more exposed folding structure. For Fgn, carbamylation increased the fraction of accessible tryptophan, which may be due to occurrence of subchain disentanglement. Also, all studied carbamylated proteins were found to be with less interaction with surrounding water. A model of impact of carbamylation on globular protein structure such as HSA was proposed based on the above findings. To study the adsorption behaviors of carbamylated protein, two model SAM surfaces were prepared, with each terminated with $–CH_3$ and –OH separately. Protein adsorption study revealed that carbamylated proteins generally have a lower amount of adsorption, and the type of substrates influences the overall amount of adsorption. To our knowledge it was for the first time tertiary structure and hydration state change characterized for carbamylated proteins, and adsorption of carbamylated and native protein on model SAM surface been compared.

To determine the potential ligand for carbamylated protein, phage display was performed against carbamylated HSA. Two sets of biopanning were performed with different extent of carbamylation for HSA. A total of seven candidate phage clones were identified from phage display. ELISA result showed that some of these phage clones were with specificity towards carbamylated HSA compared to uncarbamylated HSA. ITC identified one

particular peptide GSAARTISPSLL (cH2-p1) with the dissociation constant (K_d) of 1.0 × 10^{-4} M when binding to cHSA, and was almost one magnitude lower than its K_d to native HSA. The binding affinity for cH2-p1 towards cHSA was found to be little influenced by the extent of carbamylation. Moreover, cH2-p1 was found to be cFgn binding, with a similar K_d (8.4×10^{-5} M) to the case of cHSA binding, while there seems to be no interaction between cH2-p1 and cFgn. This work demonstrates the presence of carbamylation specific peptide targets homocitrulline containing proteins, and the reported peptide makes it possible for further research aiming at therapeutic effects for carbamylation related diseases.

Furthermore, the candidate peptide cH2p1 was immobilized onto surface to investigate the possibility of using this ligand for selective binding and removal of cHSA. In the first step, we prepared a nonspecific protein adsorption resistant surface based on p(HEMA). A well-controlled pHEMA brush thickness of 20-45 nm was achieved through surface-initiated atom-transfer radical polymerization. The surface density of polymer brush and peptide were quantified, and the obtained polymer film was proved with ultralow adsorption of HSA. Then peptide cH2p1 was immobilized to the polymer film by attachment of its N terminal or C terminal. Both cH2p1 functionalized surfaces were shown with selective binding towards cHSA and cFgn, and NH-cH2p1 were found with better selectivity and better maintained binding activity in diluted plasma than CO-cH2p1. To reach N terminal attachment of peptide we developed a novel method including terminal substitution with azide, reduction of azide and NHS/EDC coupling. This method has the advantages of simple to perform, with mild conditions for reaction, highly repeatable, and without need of any toxic solvent, which makes it highly practical for functionalization of different substrates, polymer brushes or applications. In this work, we provided one strategy to remove carbamylated protein from plasma, through immobilizing carbamylation specific peptide onto nonfouling polymer brushes, and then exposing the peptide modified surface

to the media containing carbamylated proteins.

6.2 Future work

We have identified one carbamylation specific peptide through phage display, but it turns out that the binding affinity towards carbamylated protein is not as high as that for a typical antibody-antigen interaction. This could be largely due to to negative panning process that excluded many HSA specific clones. It is also possible due to the limitation of the direct panning process or the phage library we have used. It is possible that a higher affinitive peptide ligand exists, and it might be determined through biopanning on biotinylated HSA in solution phase and capture, followed by capture with a streptavidin coated surface, or through biopanning with another type of phage library.

For further studies for clinic applications in hemodialysis, challenges have to be met when blood was the media. Although we have found that the fibrinogen adsorption is low when contacted with diluted plasma for peptide immobilized pHEMA film, performing more standard hemocompatibility tests would be needed to prove its blood compatibility.

It should also be noted that peptide immobilized in the flat surface we studied here has a very low amount of protein adsorption due to limited surface area, or low peptide density. To enable adsorption of target in a higher level, the ligand has to be immobilized on substrates with much higher surface area ratio such as porous beads or nanofibers. To this end, an optimized substrate material for peptide immobilization would be another subject to be studied.

Bibliography

[1] R. Vanholder, R. De Smet, G. Glorieux, A. Argiles, U. Baurmeister, P. Brunet, W. Clark, G. Cohen, P.P. De Deyn, R. Deppisch, B. Descamps-Latscha, T. Henle, A. Jorres, H.D. Lemke, Z.A. Massy, J. Passlick-Deetjen, M. Rodriguez, B. Stegmayr, P. Stenvinkel, C. Tetta, C. Wanner, W. Zidek, E. Grp, Review on uremic toxins: Classification, concentration, and interindividual variability, Kidney international 63(5) (2003) 1934-1943.

[2] R. Vanholder, R. De Smet, G. Glorieux, A. Argiles, U. Baurmeister, P. Brunet, W. Clark, G. Cohen, P.P. De Deyn, R. Deppisch, B. Descamps-Latscha, T. Henle, A. Jorres, H.D. Lemke, Z.A. Massy, J. Passlick-Deetjen, M. Rodriguez, B. Stegmayr, P. Stenvinkel, C. Tetta, C. Wanner, W. Zidek, G. European Uremic Toxin Work, Review on uremic toxins: classification, concentration, and interindividual variability, Kidney Int 63(5) (2003) 1934-43.

[3] H.A. Mutsaers, E.G. Stribos, G. Glorieux, R. Vanholder, P. Olinga, Chronic kidney disease and fibrosis: the role of uremic retention solutes, Frontiers in medicine 2 (2015) 60.

[4] C. Drechsler, S. Kalim, J.B. Wenger, P. Suntharalingam, T. Hod, R.I. Thadhani, S.A. Karumanchi, C. Wanner, A.H. Berg, Protein carbamylation is associated with heart failure and mortality in diabetic patients with end-stage renal disease, Kidney international 87(6) (2015) 1201-1208.

[5] R. Vanholder, E. Schepers, A. Pletinck, E.V. Nagler, G. Glorieux, The Uremic Toxicity of Indoxyl Sulfate and p-Cresyl Sulfate: A Systematic Review, Journal of the American Society of Nephrology 25(9) (2014) 1897-1907.

[6] J.B. Stokes, Consequences of frequent hemodialysis: comparison to conventional hemodialysis and transplantation, Trans Am Clin Climatol Assoc 122 (2011) 124-36.

[7] S. Liabeuf, T.B. Drueke, Z.A. Massy, Protein-Bound Uremic Toxins: New Insight from Clinical Studies, Toxins 3(7) (2011) 911-919.

[8] L. Dou, E. Bertrand, C. Cerini, V. Faure, J. Sampol, R. Vanholder, Y. Berland, P. Brunet, The uremic solutes p-cresol and indoxyl sulfate inhibit endothelial proliferation and wound repair, Kidney international 65(2) (2004) 442-451.

[9] S.C. Leong, T.L. Sirich, Indoxyl sulfate—review of toxicity and therapeutic strategies, Toxins 8(12) (2016) 358.

[10] A.W. Martinez, N.S. Recht, T.H. Hostetter, T.W. Meyer, Removal of p-cresol sulfate by hemodialysis, Journal of the American Society of Nephrology 16(11) (2005) 3430-3436.

[11] H. de Loor, B. Bammens, P. Evenepoel, V. De Preter, K. Verbeke, Gas chromatographic-mass spectrometric analysis for measurement of p-cresol and its conjugated metabolites in uremic and normal serum, Clinical chemistry 51(8) (2005) 1535-1538.

[12] T. Niwa, K. Maeda, T. Ohki, A. Saito, K. Kobayashi, A gas chromatographic-mass spectrometric analysis for phenols in uremic serum, Clinica chimica acta; international journal of clinical chemistry 110(1) (1981) 51-57.

[13] N. Ogata, N. Matsushima, T. Shibata, Pharmacokinetics of wood creosote: glucuronic acid and sulfate conjugation of phenolic compounds, Pharmacology 51(3) (1995) 195-204.
[14] L. Koppe, N.J. Pillon, R.E. Vella, M.L. Croze, C.C. Pelletier, S. Chambert, Z. Massy, G. Glorieux, R. Vanholder, Y. Dugenet, H.A. Soula, D. Fouque, C.O. Soulage, p-Cresyl Sulfate Promotes Insulin Resistance Associated with CKD, Journal of the American Society of Nephrology 24(1) (2013) 88-99.
[15] H. Watanabe, Y. Miyamoto, D. Honda, H. Tanaka, Q. Wu, M. Endo, T. Noguchi, D. Kadowaki, Y. Ishima, S. Kotani, M. Nakajima, K. Kataoka, S. Kim-Mitsuyama, M. Tanaka, M. Fukagawa, M. Otagiri, T. Maruyama, p-Cresyl sulfate causes renal tubular cell damage by inducing oxidative stress by activation of NADPH oxidase, Kidney international 83(4) (2013) 582-592.
[16] T. Niwa, Uremic Toxicity of Indoxyl Sulfate, Nagoya journal of medical science 72(1-2) (2010) 1-11.
[17] L. Viaene, P. Annaert, H. de Loor, R. Poesen, P. Evenepoel, B. Meijers, Albumin is the main plasma binding protein for indoxyl sulfate and p-cresyl sulfate, Biopharmaceutics & drug disposition 34(3) (2013) 165-75.
[18] E. Devine, D.H. Krieter, M. Ruth, J. Jankovski, H.D. Lemke, Binding Affinity and Capacity for the Uremic Toxin Indoxyl Sulfate, Toxins 6(2) (2014) 416-429.
[19] A. Dhondt, R. Vanholder, W. Van Biesen, N. Lameire, The removal of uremic toxins, Kidney international 58 (2000) S47-S59.
[20] A. Enomoto, M. Takeda, A. Tojo, T. Sekine, S.H. Cha, S. Khamdang, F. Takayama, I. Aoyama, S. Nakamura, H. Endou, T. Niwa, Role of organic anion transporters in the tubular transport of indoxyl sulfate and the induction of its nephrotoxicity, Journal of the American Society of Nephrology 13(7) (2002).
[21] T. Niwa, Removal of Protein-Bound Uraemic Toxins by Haemodialysis, Blood purification 35 (2013) 20-25.
[22] C.M. Balion, T.F. Draisey, R.J. Thibert, Carbamylated hemoglobin and carbamylated plasma protein in hemodialyzed patients, Kidney international 53(2) (1998) 488-495.
[23] W. Qin, J.B. Smith, D.L. Smith, Rates of Carbamylation of Specific Lysyl Residues in Bovine Alpha-Crystallins, Journal of Biological Chemistry 267(36) (1992) 26128-26133.
[24] S.S. Sun, J.Y. Zhou, W.M. Yang, H. Zhang, Inhibition of protein carbamylation in urea solution using ammonium-containing buffers, Analytical biochemistry 446 (2014) 76-81.
[25] P.M. Angel, R. Orlando, Quantitative carbamylation as a stable isotopic labeling method for comparative proteomics, Rapid Commun Mass Sp 21(10) (2007) 1623-1634.
[26] J.J.T. Gerding, A. Koppers, P. Hagel, H. Bloemendal, Cyanate Formation in Solutions of Urea .I. Effect of Urea on Eye Lens Protein Alpha-Crystallin, Biochimica et biophysica acta 243(3) (1971) 374-+.
[27] W. Qin, J.B. Smith, D.L. Smith, Rates of carbamylation of specific lysyl residues in bovine alpha-crystallins, The Journal of biological chemistry 267(36) (1992) 26128-33.
[28] A.H. Berg, C. Drechsler, J. Wenger, R. Buccafusca, T. Hod, S. Kalim, W. Ramma, S.M. Parikh, H. Steen, D.J. Friedman, J. Danziger, C. Wanner, R. Thadhani, S.A. Karumanchi, Carbamylation of Serum Albumin as a Risk Factor for Mortality in Patients with Kidney Failure, Science translational medicine 5(175) (2013).
[29] G.R. Stark, [53] Modification of proteins with cyanate, Methods in enzymology 25 (1972) 579-84.
[30] L. Gorissea, C. Pietrement, V. Vuiblet, C.E.H. Schmelzer, M. Kohler, L. Duca, L. Debelle, P. Fornes, S. Jaisson, P. Gillery, Protein carbamylation is a hallmark of aging, Proceedings of the National Academy

of Sciences of the United States of America 113(5) (2016) 1191-1196.
[31] S. Jaisson, S. Lorimier, S. Ricard-Blum, G.D. Sockalingum, C. Delevallee-Forte, G. Kegelaer, M. Manfait, R. Garnotel, P. Gillery, Impact of carbamylation on type I collagen conformational structure and its ability to activate human polymorphonuclear neutrophils, Chem Biol 13(2) (2006) 149-159.
[32] K.M. Fazili, M.M. Mir, M.A. Qasim, Changes in Protein Stability Upon Chemical Modification of Lysine Residues of Bovine Serum-Albumin by Different Reagents, Biochem Mol Biol Int 31(5) (1993) 807-816.
[33] H.T. Beswick, J.J. Harding, High-Molecular-Weight Crystallin Aggregate Formation Resulting from Nonenzymatic Carbamylation of Lens Crystallins - Relevance to Cataract Formation, Experimental eye research 45(4) (1987) 569-578.
[34] M.-L.P. Gross, G. Piecha, A. Bierhaus, W. Hanke, T. Henle, P. Schirmacher, E. Ritz, Glycated and carbamylated albumin is more" nephrotoxic" than unmodified albumin in the amphibian kidney, American Journal of Physiology-Heart and Circulatory Physiology (2011).
[35] J. Shi, P.A. van Veelen, M. Mahler, G.M.C. Janssen, J.W. Drijfhout, T.W.J. Huizinga, R.E.M. Toes, L.A. Trouw, Carbamylation and antibodies against carbamylated proteins in autoimmunity and other pathologies, Autoimmunity reviews 13(3) (2014) 225-230.
[36] F.H. Verbrugge, W.H.W. Tang, S.L. Hazen, Protein carbamylation and cardiovascular disease, Kidney international 88(3) (2015) 474-478.
[37] B.G. Stegmayr, New insight in impaired binding capacity for albumin in uraemic patients, Acta Physiol 215(1) (2015) 5-8.
[38] B.P. Gray, K.C. Brown, Combinatorial Peptide Libraries: Mining for Cell-Binding Peptides, Chemical reviews 114(2) (2014) 1020-1081.
[39] J. Pande, M.M. Szewczyk, A.K. Grover, Phage display: Concept, innovations, applications and future, Biotechnol Adv 28(6) (2010) 849-858.
[40] G.P. Smith, V.A. Petrenko, Phage display, Chemical reviews 97(2) (1997) 391-410.
[41] J.K. Scott, G.P. Smith, Searching for Peptide Ligands with an Epitope Library, Science 249(4967) (1990) 386-390.
[42] J. Mccafferty, A.D. Griffiths, G. Winter, D.J. Chiswell, Phage Antibodies - Filamentous Phage Displaying Antibody Variable Domains, Nature 348(6301) (1990) 552-554.
[43] Y.Y. Tan, T. Tian, W.L. Liu, Z. Zhu, C.Y.J. Yang, Advance in phage display technology for bioanalysis, Biotechnology journal 11(6) (2016) 732-745.
[44] C.F. Barbas, A.S. Kang, R.A. Lerner, S.J. Benkovic, Assembly of Combinatorial Antibody Libraries on Phage Surfaces - the Gene-Iii Site, Proceedings of the National Academy of Sciences of the United States of America 88(18) (1991) 7978-7982.
[45] H.B. Lowman, S.H. Bass, N. Simpson, J.A. Wells, Selecting High-Affinity Binding-Proteins by Monovalent Phage Display, Biochemistry 30(45) (1991) 10832-10838.
[46] N.C. Wrighton, F.X. Farrell, R. Chang, A.K. Kashyap, F.P. Barbone, L.S. Mulcahy, D.L. Johnson, R.W. Barrett, L.K. Jolliffe, W.J. Dower, Small peptides as potent mimetics of the protein hormone erythropoietin, Science 273(5274) (1996) 458-463.
[47] W. Arap, R. Pasqualini, E. Ruoslahti, Cancer treatment by targeted drug delivery to tumor vasculature in a mouse model, Science 279(5349) (1998) 377-380.

[48] J. Andris-Widhopf, P. Steinberger, C.F. Barbas Iii, Bacteriophage Display of Combinatorial Antibody Libraries, eLS (2001).
[49] M.S. Dennis, M. Zhang, Y.G. Meng, M. Kadkhodayan, D. Kirchhofer, D. Combs, L.A. Damico, Albumin binding as a general strategy for improving the pharmacokinetics of proteins, Journal of Biological Chemistry 277(38) (2002) 35035-35043.
[50] L.B. Giebel, R. Cass, D.L. Milligan, D. Young, R. Arze, C.J.B. Johnson, Screening of cyclic peptide phage libraries identifies ligands that bind streptavidin with high affinities, 34(47) (1995) 15430-15435.
[51] M. Krook, K. Mosbach, O.J.J.o.i.m. Ramström, Novel peptides binding to the Fc-portion of immunoglobulins obtained from a combinatorial phage display peptide library, 221(1-2) (1998) 151-157.
[52] C. Heilmann, M. Herrmann, B.E. Kehrel, G.J.T.J.o.i.d. Peters, Platelet-binding domains in 2 fibrinogen-binding proteins of Staphylococcus aureus identified by phage display, 186(1) (2002) 32-39.
[53] A.F. Kolodziej, S.A. Nair, P. Graham, T.J. McMurry, R.C. Ladner, C. Wescott, D.J. Sexton, P.J.B.c. Caravan, Fibrin specific peptides derived by phage display: characterization of peptides and conjugates for imaging, 23(3) (2012) 548-556.
[54] F.W. Falkenberg, Monoclonal antibody production: problems and solutions, Res Immunol 149(6) (1998) 542-547.
[55] J. Shi, R. Knevel, P. Suwannalai, M.P. van der Linden, G.M.C. Janssen, P.A. van Veelen, N.E.W. Levarht, A.H.M. van der Helm-van Mil, A. Cerami, T.W.J. Huizinga, R.E.M. Toes, L.A. Trouw, Autoantibodies recognizing carbamylated proteins are present in sera of patients with rheumatoid arthritis and predict joint damage, Proceedings of the National Academy of Sciences of the United States of America 108(42) (2011) 17372-17377.
[56] J.S. Dekkers, M.K. Verheul, J.N. Stoop, B.S. Liu, A. Ioan-Facsinay, P.A. van Veelen, A.H. de Ru, G.M.C. Janssen, M. Hegen, S. Rapecki, T.W.J. Huizinga, L.A. Trouw, R.E.M. Toes, Breach of autoreactive B cell tolerance by post-translationally modified proteins, Annals of the rheumatic diseases 76(8) (2017) 1449-1457.
[57] S. Turunen, M.K. Koivula, L. Risteli, J. Risteli, Anticitrulline Antibodies Can Be Caused by Homocitrulline-Containing Proteins in Rabbits, Arthritis Rheum 62(11) (2010) 3345-3352.
[58] C.N. Pace, Conformational stability of globular proteins, Trends in biochemical sciences 15(1) (1990) 14-7.
[59] V. Hlady, J. Buijs, Protein adsorption on solid surfaces, Curr Opin Biotech 7(1) (1996) 72-77.
[60] M.E. Callow, J.A. Callow, Marine biofouling: a sticky problem, Biologist 49(1) (2002) 1-5.
[61] R.J.C. McLean, M. Whiteley, D.J. Stickler, W.C. Fuqua, Evidence of autoinducer activity in naturally occurring biofilms, FEMS microbiology letters 154(2) (1997) 259-263.
[62] G. Crotts, T.G. Park, Protein delivery from poly(lactic-co-glycolic acid) biodegradable microspheres: release kinetics and stability issues, Journal of microencapsulation 15(6) (1998) 699-713.
[63] W.B. Tsai, J.M. Grunkemeier, T.A. Horbett, Human plasma fibrinogen adsorption and platelet adhesion to polystyrene, J Biomed Mater Res 44(2) (1999) 130-139.
[64] S. Herrwerth, W. Eck, S. Reinhardt, M. Grunze, Factors that determine the protein resistance of oligoether self-assembled monolayers - Internal hydrophilicity, terminal hydrophilicity, and lateral packing density, Journal of the American Chemical Society 125(31) (2003) 9359-9366.
[65] J.M. Harris, Introduction to biomedical and biotechnical applications of polyethylene glycol., Abstr

Pap Am Chem S 213 (1997) 21-Poly.
[66] M.C. Shen, L. Martinson, M.S. Wagner, D.G. Castner, B.D. Ratner, T.A. Horbett, PEO-like plasma polymerized tetraglyme surface interactions with leukocytes and proteins: in vitro and in vivo studies, Journal of Biomaterials Science-Polymer Edition 13(4) (2002) 367-390.
[67] Y.Y. Luk, M. Kato, M. Mrksich, Self-assembled monolayers of alkanethiolates presenting mannitol groups are inert to protein adsorption and cell attachment, Langmuir 16(24) (2000) 9604-9608.
[68] M.C. Shen, M.S. Wagner, D.G. Castner, B.D. Ratner, T.A. Horbett, Multivariate surface analysis of plasma-deposited tetraglyme for reduction of protein adsorption and monocyte adhesion, Langmuir 19(5) (2003) 1692-1699.
[69] S. Martwiset, A.E. Koh, W. Chen, Nonfouling characteristics of dextran-containing surfaces, Langmuir 22(19) (2006) 8192-8196.
[70] M. Wyszogrodzka, R. Haag, Synthesis and Characterization of Glycerol Dendrons, Self-Assembled Monolayers on Gold: A Detailed Study of Their Protein Resistance, Biomacromolecules 10(5) (2009) 1043-1054.
[71] C. Zhao, L.Y. Li, Q.M. Wang, Q.M. Yu, J. Zheng, Effect of Film Thickness on the Antifouling Performance of Poly(hydroxy-functional methacrylates) Grafted Surfaces, Langmuir 27(8) (2011) 4906-4913.
[72] Z. Zhang, S.F. Chen, Y. Chang, S.Y. Jiang, Surface grafted sulfobetaine polymers via atom transfer radical polymerization as superlow fouling coatings, Journal of Physical Chemistry B 110(22) (2006) 10799-10804.
[73] G. Cheng, Z. Zhang, S.F. Chen, J.D. Bryers, S.Y. Jiang, Inhibition of bacterial adhesion and biofilm formation on zwitterionic surfaces, Biomaterials 28(29) (2007) 4192-4199.
[74] W. Yang, H. Xue, W. Li, J.L. Zhang, S.Y. Jiang, Pursuing "Zero" Protein Adsorption of Poly(carboxybetaine) from Undiluted Blood Serum and Plasma, Langmuir 25(19) (2009) 11911-11916.
[75] R. Barbey, L. Lavanant, D. Paripovic, N. Schuwer, C. Sugnaux, S. Tugulu, H.A. Klok, Polymer Brushes via Surface-Initiated Controlled Radical Polymerization: Synthesis, Characterization, Properties, and Applications, Chemical reviews 109(11) (2009) 5437-5527.
[76] K. Matyjaszewski, Atom Transfer Radical Polymerization (ATRP): Current Status and Future Perspectives, Macromolecules 45(10) (2012) 4015-4039.
[77] D.J. Siegwart, J.K. Oh, K. Matyjaszewski, ATRP in the design of functional materials for biomedical applications, Progress in Polymer Science 37(1) (2012) 18-37.
[78] G. Moad, E. Rizzardo, S.H. Thang, Radical addition-fragmentation chemistry in polymer synthesis, Polymer 49(5) (2008) 1079-1131.
[79] R.B. Grubbs, Nitroxide-Mediated Radical Polymerization: Limitations and Versatility, Polym Rev 51(2) (2011) 104-137.
[80] W. Feng, R.X. Chen, J.L. Brash, S.P. Zhu, Surface-initiated atom transfer radical polymerization of oligo(ethylene glycol) methacrylate: Effect of solvent on graft density, Macromolecular rapid communications 26(17) (2005) 1383-1388.
[81] A.A. Brown, N.S. Khan, L. Steinbock, W.T.S. Huck, Synthesis of oligo(ethylene glycol) methacrylate polymer brushes, Eur Polym J 41(8) (2005) 1757-1765.
[82] D.M. Jones, A.A. Brown, W.T.S. Huck, Surface-initiated polymerizations in aqueous media: Effect of

initiator density, Langmuir 18(4) (2002) 1265-1269.
[83] C.D. Bain, E.B. Troughton, Y.T. Tao, J. Evall, G.M. Whitesides, R.G. Nuzzo, Formation of Monolayer Films by the Spontaneous Assembly of Organic Thiols from Solution onto Gold, Journal of the American Chemical Society 111(1) (1989) 321-335.
[84] C. Perruchot, M.A. Khan, A. Kamitsi, S.P. Armes, T. von Werne, T.E. Patten, Synthesis of well-defined, polymer-grafted silica particles by aqueous ATRP, Langmuir 17(15) (2001) 4479-4481.
[85] K. Ohno, T. Morinaga, K. Koh, Y. Tsujii, T. Fukuda, Synthesis of monodisperse silica particles coated with well-defined, high-density polymer brushes by surface-initiated atom transfer radical polymerization, Macromolecules 38(6) (2005) 2137-2142.
[86] C.L. Huang, T. Tassone, K. Woodberry, D. Sunday, D.L. Green, Impact of ATRP Initiator Spacer Length on Grafting Poly(methyl methacrylate) from Silica Nanoparticles, Langmuir 25(23) (2009) 13351-13360.
[87] H.W. Ma, D.J. Li, X. Sheng, B. Zhao, A. Chilkoti, Protein-resistant polymer coatings on silicon oxide by surface-initiated atom transfer radical polymerization, Langmuir 22(8) (2006) 3751-3756.
[88] B. Lego, M. Francois, W.G. Skene, S. Giasson, Polymer Brush Covalently Attached to OH-Functionalized Mica Surface via Surface-Initiated ATRP: Control of Grafting Density and Polymer Chain Length, Langmuir 25(9) (2009) 5313-5321.
[89] B. Lego, W.G. Skene, S. Giasson, Unprecedented covalently attached ATRP initiator onto OH-functionalized mica surfaces, Langmuir 24(2) (2008) 379-382.
[90] M. Steenackers, A.M. Gigler, N. Zhang, F. Deubel, M. Seifert, L.H. Hess, C.H.Y.X. Lim, K.P. Loh, J.A. Garrido, R. Jordan, M. Stutzmann, I.D. Sharp, Polymer Brushes on Graphene, Journal of the American Chemical Society 133(27) (2011) 10490-10498.
[91] A. Badri, M.R. Whittaker, P.B. Zetterlund, Modification of graphene/graphene oxide with polymer brushes using controlled/living radical polymerization, J Polym Sci Pol Chem 50(15) (2012) 2981-2992.
[92] J. Majoinen, A. Walther, J.R. McKee, E. Kontturi, V. Aseyev, J.M. Malho, J. Ruokolainen, O. Ikkala, Polyelectrolyte Brushes Grafted from Cellulose Nanocrystals Using Cu-Mediated Surface-Initiated Controlled Radical Polymerization, Biomacromolecules 12(8) (2011) 2997-3006.
[93] T. Ameringer, F. Ercole, K.M. Tsang, B.R. Coad, X.L. Hou, A. Rodda, D.R. Nisbet, H. Thissen, R.A. Evans, L. Meagher, J.S. Forsythe, Surface grafting of electrospun fibers using ATRP and RAFT for the control of biointerfacial interactions, Biointerphases 8 (2013).
[94] A.M. Telford, C. Neto, L. Meagher, Robust grafting of PEG-methacrylate brushes from polymeric coatings, Polymer 54(21) (2013) 5490-5498.
[95] A. Hucknall, A.J. Simnick, R.T. Hill, A. Chilkoti, A. Garcia, M.S. Johannes, R.L. Clark, S. Zauscher, B.D. Ratner, Versatile synthesis and micropatterning of nonfouling polymer brushes on the wafer scale, Biointerphases 4(2) (2009) Fa50-Fa57.
[96] F.J. Xu, Z.H. Wang, W.T. Yang, Surface functionalization of polycaprolactone films via surface-initiated atom transfer radical polymerization for covalently coupling cell-adhesive biomolecules, Biomaterials 31(12) (2010) 3139-3147.
[97] A.M. Jonas, Z.J. Hu, K. Glinel, W.T.S. Huck, Effect of Nanoconfinement on the Collapse Transition of Responsive Polymer Brushes, Nano Letters 8(11) (2008) 3819-3824.
[98] T. Wu, K. Efimenko, J. Genzer, Combinatorial study of the mushroom-to-brush crossover in surface

anchored polyacrylamide, Journal of the American Chemical Society 124(32) (2002) 9394-9395.
[99] M. Furuya, M. Haramura, A. Tanaka, Reduction of nonspecific binding proteins to self-assembled monolayer on gold surface, Bioorganic & medicinal chemistry 14(2) (2006) 537-543.
[100] M. Furuya, Y. Tsushima, S. Tani, T. Kamimura, Development of affinity chromatography using a bioactive peptide as a ligand, Bioorganic & medicinal chemistry 14(15) (2006) 5093-5098.
[101] H. Chen, Y. Chen, H. Sheardown, M.A. Brook, Immobilization of heparin on a silicone surface through a heterobifunctional PEG spacer, Biomaterials 26(35) (2005) 7418-7424.
[102] H.W. Liu, C.H. Chen, C.L. Tsai, I.H. Lin, G.H. Hsiue, Heterobifunctional poly(ethylene glycol)-tethered bone morphogenetic protein-2-stimulated bone marrow mesenchymal stromal cell differentiation and osteogenesis, Tissue Eng 13(5) (2007) 1113-1124.
[103] J.E. Raynor, J.R. Capadona, D.M. Collard, T.A. Petrie, A.J. Garcia, Polymer brushes and self-assembled monolayers: Versatile platforms to control cell adhesion to biomaterials (Review), Biointerphases 4(2) (2009) Fa3-Fa16.
[104] M.A. Mintzer, E.E. Simanek, Nonviral Vectors for Gene Delivery, Chemical reviews 109(2) (2009) 259-302.
[105] D. Oupicky, Design and development strategies of polymer materials for drug and gene delivery applications, Adv Drug Deliver Rev 60(9) (2008) 957-957.
[106] D.W. Pack, A.S. Hoffman, S. Pun, P.S. Stayton, Design and development of polymers for gene delivery, Nat Rev Drug Discov 4(7) (2005) 581-593.
[107] W.J. Yang, K.G. Neoh, E.T. Kang, S.S.C. Lee, S.L.M. Teo, D. Rittschof, Functional polymer brushes via surface-initiated atom transfer radical graft polymerization for combating marine biofouling, Biofouling 28(9) (2012) 895-912.
[108] J. Trmcic-Cvitas, E. Hasan, M. Ramstedt, X. Li, M.A. Cooper, C. Abell, W.T.S. Huck, J.E. Gautrot, Biofunctionalized Protein Resistant Oligo(ethylene glycol)-Derived Polymer Brushes as Selective Immobilization and Sensing Platforms, Biomacromolecules 10(10) (2009) 2885-2894.
[109] J. Trmcic-Cvitas, E. Hasan, M. Ramstedt, X. Li, M.A. Cooper, C. Abell, W.T. Huck, J.E.J.B. Gautrot, Biofunctionalized protein resistant oligo (ethylene glycol)-derived polymer brushes as selective immobilization and sensing platforms, 10(10) (2009) 2885-2894.
[110] B.S. Lee, J.K. Lee, W.-J. Kim, Y.H. Jung, S.J. Sim, J. Lee, I.S.J.B. Choi, Surface-initiated, atom transfer radical polymerization of oligo (ethylene glycol) methyl ether methacrylate and subsequent click chemistry for bioconjugation, 8(2) (2007) 744-749.
[111] N.D. Brault, A.D. White, A.D. Taylor, Q. Yu, S.J.A.c. Jiang, Directly functionalizable surface platform for protein arrays in undiluted human blood plasma, 85(3) (2013) 1447-1453.
[112] H. Vaisocherová, V. Ševců, P. Adam, B. Špačková, K. Hegnerová, A. de los Santos Pereira, C. Rodriguez-Emmenegger, T. Riedel, M. Houska, E.J.B. Brynda, Bioelectronics, Functionalized ultra-low fouling carboxy-and hydroxy-functional surface platforms: functionalization capacity, biorecognition capability and resistance to fouling from undiluted biological media, 51 (2014) 150-157.
[113] H. Vaisocherova, V. Sevcu, P. Adam, B. Spackova, K. Hegnerova, A.D. Pereira, C. Rodriguez-Emmenegger, T. Riedel, M. Houska, E. Brynda, J. Homola, Functionalized ultra-low fouling carboxy- and hydroxy-functional surface platforms: functionalization capacity, biorecognition capability and resistance to fouling from undiluted biological media, Biosensors & bioelectronics 51 (2014) 150-157.

[114] N.D. Brault, H.S. Sundaram, C.-J. Huang, Y. Li, Q. Yu, S.J.B. Jiang, Two-layer architecture using atom transfer radical polymerization for enhanced sensing and detection in complex media, 13(12) (2012) 4049-4056.
[115] M.H. Rahman, S.S. Haqqie, M.D. McGoldrick, Acute hemolysis with acute renal failure in a patient with valproic acid poisoning treated with charcoal hemoperfusion, Hemodialysis international. International Symposium on Home Hemodialysis 10(3) (2006) 256-9.
[116] J. Winchester, A. Boldur, C. Oleru, C. Kitiyakara, Use of dialysis and hemoperfusion in treatment of poisoning, Handbook of dialysis. Boston: Boston Little Brown (1994).
[117] D.S. Terman, G. Buffaloe, G. Cook, M. Sullivan, C. Mattioli, R. Tillquist, J.C. Ayus, Extracorporeal Immunoadsorption - Initial Experience in Human Systemic Lupus-Erythematosus, Lancet 2(8147) (1979) 824-826.
[118] A. Ault, New direction for treatment of rheumatoid arthritis offered in USA, Lancet 353(9158) (1999) 1071-1071.
[119] J. Caldwell, R.M. Gendreau, D. Furst, A pilot study using a staph protein A column (Prosorba (R)) to treat refractory rheumatoid arthritis, Journal of Rheumatology 26(8) (1999) 1657-1662.
[120] R.M. Hakim, E. Milford, J. Himmelfarb, R. Wingard, J.M. Lazarus, R.M. Watt, Extracorporeal Removal of Anti-Hla Antibodies in Transplant Candidates, American Journal of Kidney Diseases 16(5) (1990) 423-431.
[121] S. Yamamoto, J.J. Kazama, T. Wakamatsu, Y. Takahashi, Y. Kaneko, S. Goto, I. Narita, Removal of uremic toxins by renal replacement therapies: a review of current progress and future perspectives, Renal Replacement Therapy 2(1) (2016) 43.
[122] R.A. Van Wagenen, M. Steggall, D.J. Lentz, J.D. Andrade, Activated carbons for medical applications. In vitro microparticle characterization and solute adsorption, Biomaterials, medical devices, and artificial organs 3(3) (1975) 319-64.
[123] V. Wernert, O. Schaf, V. Faure, P. Brunet, L. Dou, Y. Berland, P. Boulet, B. Kuchta, R. Denoyel, Adsorption of the uremic toxin p-cresol onto hemodialysis membranes and microporous adsorbent zeolite silicalite, Journal of biotechnology 123(2) (2006) 164-173.
[124] G. Dunea, Replacement of Renal-Function by Dialysis - a Textbook of Dialysis, 2nd Edition - Drukker,W, Parsons,Fm, Maher,Jf, Jama-J Am Med Assoc 252(13) (1984) 1768-1768.
[125] J. Mulder, Basic principles of membrane technology, Springer Science & Business Media2012.
[126] V. Gura, C. Ronco, A. Davenport, The Wearable Artificial Kidney, Why and How: From Holy Grail to Reality, Seminars in dialysis 22(1) (2009) 13-17.
[127] C. Ronco, A. Davenport, V. Gura, Toward the wearable artificial kidney, Hemodialysis International 12 (2008) S40-S47.
[128] C. Ronco, A. Davenport, V. Gura, A wearable artificial kidney: dream or reality?, Nat Clin Pract Nephr 4(11) (2008) 604-605.
[129] H.D. Polaschegg, Wearable Dialysis: What is Missing?, Hemodialysis: New Methods and Future Technology 171 (2011) 226-230.
[130] M. Pascual, N. TolkoffRubin, J.A. Schifferli, Is adsorption an important characteristic of dialysis membranes?, Kidney international 49(2) (1996) 309-313.
[131] A.K. Cheung, Biocompatibility of Hemodialysis Membranes, Journal of the American Society of

Nephrology 1(2) (1990) 150-161.
[132] H. Vonbaeyer, F. Kochinke, R. Schwerdtfeger, Cascade Plasmapheresis with Online Membrane Regeneration - Laboratory and Clinical-Studies, J Membrane Sci 22(2-3) (1985) 297-315.
[133] G.V. Chapman, P.W.E. Hone, W. Bolton, A. Blogg, C. Stokoe, T. Cahill, J.F. Mahony, P.C. Farrell, Evaluation of Hemodiafiltration and Sorbent Membrane Dialysis .1. Invivo and Invitro Dialyzer Performance, Dialysis Transplant 11(9) (1982) 758-&.
[134] G.V. Chapman, P.W.E. Hone, M.J. Shirlow, W. Bolton, A. Blogg, C. Stokoe, T. Cahill, J.F. Mahony, P.C. Farrell, Evaluation of Hemodiafiltration and Sorbent Membrane Dialysis .2. Clinical, Nutritional, and Middle Molecule Assessment, Dialysis Transplant 11(10) (1982) 871-&.
[135] K. Maeda, A. Saito, S. Kawaguchi, R. Sezaki, T. Niwa, M. Naotsuka, K. Kobayashi, H. Asada, Y. Yamamoto, K. Ohta, Problems with Activated-Charcoal and Alumina as Sorbents for Medical Use, Artificial organs 3(4) (1979) 336-340.
[136] D.H. Randerson, H.J. Gurland, B. Schmidt, P.C. Farrell, P.W.E. Hone, C. Stokoe, A. Zuber, A. Blogg, A. Fatehmoghadam, I. Marschner, W. Kopcke, Sorbent Membrane Dialysis in Uremia, Contributions to nephrology 29 (1982) 53-64.
[137] M.S.L. Tijink, M. Wester, J.F. Sun, A. Saris, L.A.M. Bolhuis-Versteeg, S. Saiful, J.A. Joles, Z. Borneman, M. Wessling, D.F. Stamatialis, A novel approach for blood purification: Mixed-matrix membranes combining diffusion and adsorption in one step, Acta Biomaterialia 8(6) (2012) 2279-2287.
[138] E.C. Dillon, J.H. Wilton, J.C. Barlow, W.A. Watson, Large Surface-Area Activated-Charcoal and the Inhibition of Aspirin Absorption, Ann Emerg Med 18(5) (1989) 547-552.
[139] T.M.S. Chang, Removal of Endogenous and Exogenous Toxins by a Microencapsulated Absorbent, Can J Physiol Pharm 47(12) (1969) 1043-&.
[140] H. Marsh, F. Rodríguez-Reinoso, CHAPTER 1 - Introduction to the Scope of the Text, in: H. Marsh, F. Rodríguez-Reinoso (Eds.), Activated Carbon, Elsevier Science Ltd, Oxford, 2006, pp. 1-12.
[141] S. Stefoni, L. Coli, G. Feliciangeli, L. Baldrati, V. Bonomini, Regular Hemoperfusion in Regular Dialysis Treatment - a Long-Term Study, International Journal of Artificial Organs 3(6) (1980) 348-353.
[142] J. Chen, W. Han, J. Chen, W. Zong, W. Wang, Y. Wang, G. Cheng, C. Li, L. Ou, Y. Yu, High performance of a unique mesoporous polystyrene-based adsorbent for blood purification, Regenerative biomaterials 4(1) (2016) 31-37.
[143] R.C. Bansal, J.-B. Donnet, F. Stoeckli, Active carbon, Marcel Dekker1988.
[144] M.C. Annesini, V. Piemonte, L. Turchetti, Removal of albumin-bound toxins from albumin-containing solutions: Tryptophan fixed-bed adsorption on activated carbon, Chem Eng Res Des 88(8A) (2010) 1018-1023.
[145] Crystallization, Air–Water Operations, Drying, Adsorption, Membrane Separations, and Other Mass Transfer Processes, Fluid Mechanics, Heat Transfer, and Mass Transfer.
[146] J. Pires, M.L. Pinto, A. Carvalho, M.B. de Carvalho, Assessment of hydrophobic-hydrophilic properties of microporous materials from water adsorption isotherms, Adsorption 9(4) (2003) 303-309.
[147] V. Wernert, O. Schaf, H. Ghobarkar, R. Denoyel, Adsorption properties of zeolites for artificial kidney applications, Micropor Mesopor Mat 83(1-3) (2005) 101-113.
[148] R.R. Willis, D.S. Bem, D.L. Ellig, Process and composition for removing toxins from bodily fluids, Google Patents, 2003.

[149] B.G. Trewyn, J.A. Nieweg, Y. Zhao, V.S.Y. Lin, Biocompatible mesoporous silica nanoparticles with different morphologies for animal cell membrane, penetration, Chem Eng J 137(1) (2008) 23-29.
[150] W.K. Cheah, Y.L. Sim, F.Y. Yeoh, Amine-functionalized mesoporous silica for urea adsorption, Mater Chem Phys 175 (2016) 151-157.
[151] D. Fine, A. Grattoni, R. Goodall, S.S. Bansal, C. Chiappini, S. Hosali, A.L. van de Ven, S. Srinivasan, X.W. Liu, B. Godin, L. Brousseau, I.K. Yazdi, J. Fernandez-Moure, E. Tasciotti, H.J. Wu, Y. Hu, S. Klemm, M. Ferrari, Silicon Micro- and Nanofabrication for Medicine, Adv Healthc Mater 2(5) (2013) 632-666.
[152] Q. Wei, H.Q. Chen, Z.R. Nie, Y.L. Hao, Y.L. Wang, Q.Y. Li, J.X. Zou, Preparation and characterization of vinyl-functionalized mesoporous SBA-15 silica by a direct synthesis method, Mater Lett 61(7) (2007) 1469-1473.
[153] G.S. Wu, P.H. Li, H.Q. Feng, X.M. Zhang, P.K. Chu, Engineering and functionalization of biomaterials via surface modification, Journal of Materials Chemistry B 3(10) (2015) 2024-2042.
[154] K.Y. Ho, G. McKay, K.L. Yeung, Selective adsorbents from ordered mesoporous silica, Langmuir 19(7) (2003) 3019-3024.
[155] M.D. Branković, A.R. Zarubica, T.D. Anđelković, D.H. Anđelković, Mesoporous silica (MCM-41): Synthesis/modification, characterization and removal of selected organic micro-pollutants from water, Advanced Technologies 6(1) (2017) 50-57.
[156] H. Sugaya, Y. Sakai, Polymethylmethacrylate: from polymer to dialyzer, Polymethylmethacrylate, Karger Publishers1999, pp. 1-8.
[157] P. Fabbrini, S. Sirtori, E. Casiraghi, F. Pieruzzi, S. Genovesi, D. Corti, R. Brivio, G. Gregorini, G. Como, M.L. Carati, M.R. Vigano, A. Stella, Polymethylmethacrylate Membrane and Serum Free Light Chain Removal: Enhancing Adsorption Properties, Blood purification 35 (2013) 52-58.
[158] S. Furuyoshi, M. Nakatani, J. Taman, H. Kutsuki, S. Takata, N. Tani, New Adsorption Column (Lixelle) to Eliminate (β2-Microglobulin for Direct Hemoperfusion, Therapeutic Apheresis 2(1) (1998) 13-17.
[159] T. Abe, K. Uchita, H. Orita, M. Kamimura, M. Oda, H. Hasegawa, H. Kobata, M. Fukunishi, M. Shimazaki, T. Abe, T. Akizawa, S. Ahmad, Effect of beta(2)-microglobulin adsorption column on dialysis-related amyloidosis, Kidney international 64(4) (2003) 1522-1528.
[160] N. Homma, F. Gejyo, S. Hasegawa, T. Teramura, I. Ei, H. Maruyama, M. Arakawa, Effects of a new adsorbent column for removing beta-2-microglobulin from circulating blood of dialysis patients, Dialysis-Related Amyloidosis 112 (1995) 164-171.
[161] F. Gejyo, T. Teramura, I. Ei, M. Arakawa, R. Nakazawa, N. Azuma, M. Suzuki, S. Furuyoshi, T. Nankou, S. Takata, A. Yasuda, Long-term clinical evaluation of an adsorbent column (BM-O1) of direct hemoperfusion type for beta(2)-microglobulin on the treatment of dialysis-related amyloidosis, Artificial organs 19(12) (1995) 1222-1226.
[162] V. Davankov, L. Pavlova, M. Tsyurupa, J. Brady, M. Balsamo, E. Yousha, Polymeric adsorbent for removing toxic proteins from blood of patients with kidney failure, Journal of Chromatography B 739(1) (2000) 73-80.
[163] E. Menegatti, C. Ronco, J.F. Winchester, A. Dragonetti, D. Di Simone, A. Davit, G. Mengozzi, G. Marietti, G. Loduca, M. Mansouri, G.P. Sancipriano, L.M. Sena, D. Roccatello, Absence of NF-kappa B activation by a new polystyrene-type adsorbent designed for hemoperfusion, Blood purification 23(1)

(2005) 91-98.
[164] M. Santin, M.A. Wassall, G. Peluso, S.P. Denyer, Adsorption of alpha-1-microglobulin from biological fluids onto polymer surfaces, Biomaterials 18(11) (1997) 823-827.
[165] M.D. Morena, D.Q. Guo, V.S. Balakrishnan, J.A. Brady, J.F. Winchester, B.L. Jaber, Effect of a novel adsorbent on cytokine responsiveness to uremic plasma, Kidney international 63(3) (2003) 1150-1154.
[166] R.A. Odell, P. Slowiaczek, J.E. Moran, K. Schindhelm, Beta2-Microglobulin Kinetics in End-Stage Renal-Failure, Kidney international 39(5) (1991) 909-919.
[167] K.E. Hagstam, L.E. Larsson, H. Thysell, Experimental Studies on Charcoal Haemoperfusion in Phenobarbital Intoxication and Uraemia Including Histopathologic Findings, Acta Med Scand 180(5) (1966) 593-+.
[168] M. Ghannoum, J. Bouchard, T.D. Nolin, G. Ouellet, D.M. Roberts, Hemoperfusion for the Treatment of Poisoning: Technology, Determinants of Poison Clearance, and Application in Clinical Practice, Seminars in dialysis 27(4) (2014) 350-361.
[169] C.A. Howell, S.R. Sandeman, Y. Zheng, S.V. Mikhalovsky, V.G. Nikolaev, L.A. Sakhno, E.A. Snezhkova, New dextran coated activated carbons for medical use, Carbon 97 (2016) 134-146.
[170] N.N. Cai, Q.S. Li, J.M. Zhang, T. Xu, W.Q. Zhao, J. Yang, L. Zhang, Antifouling zwitterionic hydrogel coating improves hemocompatibility of activated carbon hemoadsorbent, Journal of colloid and interface science 503 (2017) 168-177.
[171] J.D. Andrade, K. Kunitomo, Vanwagen.R, B. Kastigir, D. Gough, W.J. Kolff, Coated Adsorbents for Direct Blood Perfusion - Hema/Activated Carbon, T Am Soc Art Int Org 17(Apr) (1971) 222-&.
[172] N. Cai, Q. Li, J. Zhang, T. Xu, W. Zhao, J. Yang, L. Zhang, Antifouling zwitterionic hydrogel coating improves hemocompatibility of activated carbon hemoadsorbent, Journal of colloid and interface science 503 (2017) 168-177.
[173] C.J. Lee, S.T. Hsu, Preparation of Spherical Encapsulation of Activated Carbons and Their Adsorption Capacity of Typical Uremic Toxins, J Biomed Mater Res 24(2) (1990) 243-258.
[174] C.J. Liu, X.Y. Liang, X.J. Liu, Q. Wang, L. Zhan, R. Zhang, W.M. Qiao, L.C. Ling, Surface modification of pitch-based spherical activated carbon by CVD of NH(3) to improve its adsorption to uric acid, Applied Surface Science 254(21) (2008) 6701-6705.
[175] T. Mitome, Y. Uchida, Y. Egashira, K. Hayashi, A. Nishiura, N. Nishiyama, Adsorption of indole on KOH-activated mesoporous carbon, Colloid Surf. A-Physicochem. Eng. Asp. 424 (2013) 89-95.
[176] R. Sipehia, R.A.B. Bannard, T.M.S. Chang, Poly(Vinylidene Fluoride)-Coated or Poly(Vinylidene Chloride Vinyl Chloride)-Coated Activated-Charcoal for the Adsorption of Large Lipophilic Molecules with Exclusion of Small Hydrophilic Molecules, J Membrane Sci 47(3) (1989) 293-299.
[177] D.J. Malik, G.L. Warwick, M. Venturi, M. Streat, K. Hellgardt, N. Hoenich, J.A. Dale, Preparation of novel mesoporous carbons for the adsorption of an inflammatory cytokine (IL-1 beta), Biomaterials 25(15) (2004) 2933-2940.
[178] X.P. Deng, T. Wang, F. Zhao, L.J. Li, C.S. Zhao, Poly(ether sulfone)/activated carbon hybrid beads for creatinine adsorption, J Appl Polym Sci 103(2) (2007) 1085-1092.
[179] C. Jackson, Design and In-vitro Characterisation of Novel Sorbent Device for Extracorporeal Blood Filtration and Other Applications, McGill University, 2012.
[180] Y.J. Jia, X.Y. Li, J.C. Jiang, K. Sun, Adsorption of creatinine on polyaniline-poly(styrene sulfonate)

hydrogels based activated carbon particles, Iran Polym J 24(9) (2015) 775-781.
[181] R.K. Singh, S. Kumar, S. Kumar, A. Kumar, Development of parthenium based activated carbon and its utilization for adsorptive removal of p-cresol from aqueous solution, J Hazard Mater 155(3) (2008) 523-535.
[182] I. Bakas, K. Elatmani, S. Qourzal, N. Barka, A. Assabbane, I. Aît-Ichou, A comparative adsorption for the removal of p-cresol from aqueous solution onto granular activated charcoal and granular activated alumina, J. Mater. Environ. Sci 5(3) (2014) 675-682.
[183] V.K. Upadhyayula, S. Deng, M.C. Mitchell, G.B. Smith, Application of carbon nanotube technology for removal of contaminants in drinking water: a review, Science of the total environment 408(1) (2009) 1-13.
[184] K.H. Chan, E.T. Wong, M.I. Khan, A. Idris, N.M. Yusof, Fabrication of polyvinylidene difluoride nano-hybrid dialysis membranes using functionalized multiwall carbon nanotube for polyethylene glycol (hydrophilic additive) retention, Journal of Industrial and Engineering Chemistry 20(5) (2014) 3744-3753.
[185] R. Sipehia, R. Bannard, T. Chang, Poly (vinylidene fluoride)-or poly (vinylidene chloride/vinyl chloride)-coated activated charcoal for the adsorption of large lipophilic molecules with exclusion of small hydrophilic molecules, Journal of membrane science 47(3) (1989) 293-299.
[186] D. Malik, G. Warwick, M. Venturi, M. Streat, K. Hellgardt, N. Hoenich, J. Dale, Preparation of novel mesoporous carbons for the adsorption of an inflammatory cytokine (IL-1β), Biomaterials 25(15) (2004) 2933-2940.
[187] X. Deng, T. Wang, F. Zhao, L. Li, C. Zhao, Poly (ether sulfone)/activated carbon hybrid beads for creatinine adsorption, Journal of applied polymer science 103(2) (2007) 1085-1092.
[188] S.R. Ash, Dialysis material and method for removing uremic substances, Google Patents, 1986.
[189] V. Wernert, O. Schäf, H. Ghobarkar, R. Denoyel, Adsorption properties of zeolites for artificial kidney applications, Microporous and Mesoporous Materials 83(1-3) (2005) 101-113.
[190] K. Namekawa, M.T. Schreiber, T. Aoyagi, M. Ebara, Fabrication of zeolite–polymer composite nanofibers for removal of uremic toxins from kidney failure patients, Biomaterials Science 2(5) (2014) 674-679.
[191] L. Lu, C. Samarasekera, J.T. Yeow, Creatinine adsorption capacity of electrospun polyacrylonitrile (PAN)-zeolite nanofiber membranes for potential artificial kidney applications, Journal of Applied Polymer Science 132(34) (2015).
[192] L. Lu, J.T. Yeow, An adsorption study of indoxyl sulfate by zeolites and polyethersulfone–zeolite composite membranes, Materials & Design 120 (2017) 328-335.
[193] G. Lesaffer, R. De Smet, N. Lameire, A. Dhondt, P. Duym, R. Vanholder, Intradialytic removal of protein-bound uraemic toxins: role of solute characteristics and of dialyser membrane, Nephrol Dial Transpl 15(1) (2000) 50-57.
[194] V. Wernert, O. Schäf, V. Faure, P. Brunet, L. Dou, Y. Berland, P. Boulet, B. Kuchta, R. Denoyel, Adsorption of the uremic toxin p-cresol onto hemodialysis membranes and microporous adsorbent zeolite silicalite, Journal of biotechnology 123(2) (2006) 164-173.
[195] V. Davankov, L. Pavlova, M. Tsyurupa, J. Brady, M. Balsamo, E. Yousha, Polymeric adsorbent for removing toxic proteins from blood of patients with kidney failure, Journal of Chromatography B: Biomedical Sciences and Applications 739(1) (2000) 73-80.

[196] M.D. Morena, D. Guo, V.S. Balakrishnan, J.A. Brady, J.F. Winchester, B.L. Jaber, Effect of a novel adsorbent on cytokine responsiveness to uremic plasma, Kidney international 63(3) (2003) 1150-1154.
[197] J. Li, L. Han, S. Liu, S. He, Y. Cao, J. Xie, L. Jia, Removal of indoxyl sulfate by water-soluble poly-cyclodextrins in dialysis, Colloids and Surfaces B: Biointerfaces 164 (2018) 406-413.
[198] S. Kang, J.E. Yang, J. Kim, M. Ahn, H.J. Koo, M. Kim, Y.S. Lee, S.R. Paik, Removal of intact β2-microglobulin at neutral ph by using seed-conjugated polymer beads prepared with β2-microglobulin-derived peptide (58–67), Biotechnology progress 27(2) (2011) 521-529.
[199] H.-A. Tsai, M.-J. Syu, Synthesis of creatinine-imprinted poly (β-cyclodextrin) for the specific binding of creatinine, Biomaterials 26(15) (2005) 2759-2766.
[200] H.-A. Tsai, M.-J. Syu, Preparation of imprinted poly (tetraethoxysilanol) sol–gel for the specific uptake of creatinine, Chemical engineering journal 168(3) (2011) 1369-1376.
[201] M. Tijink, J. Kooman, M. Wester, J. Sun, S. Saiful, J. Joles, Z. Borneman, M. Wessling, D. Stamatialis, Mixed matrix membranes: a new asset for blood purification therapies, Blood purification 37(1) (2014) 1-3.
[202] M.S. Tijink, M. Wester, G. Glorieux, K.G. Gerritsen, J. Sun, P.C. Swart, Z. Borneman, M. Wessling, R. Vanholder, J.A. Joles, Mixed matrix hollow fiber membranes for removal of protein-bound toxins from human plasma, Biomaterials 34(32) (2013) 7819-7828.
[203] C. Nie, L. Ma, Y. Xia, C. He, J. Deng, L. Wang, C. Cheng, S. Sun, C. Zhao, Novel heparin-mimicking polymer brush grafted carbon nanotube/PES composite membranes for safe and efficient blood purification, Journal of Membrane Science 475 (2015) 455-468.
[204] D. Berge-Lefranc, H. Pizzala, R. Denoyel, V. Hornebecq, J.L. Berge-Lefranc, R. Guieu, P. Brunet, H. Ghobarkar, O. Schaf, Mechanism of creatinine adsorption from physiological solutions onto mordenite, Micropor Mesopor Mat 119(1-3) (2009) 186-192.
[205] K. Namekawa, M.T. Schreiber, T. Aoyagi, M. Ebara, Fabrication of zeolite-polymer composite nanofibers for removal of uremic toxins from kidney failure patients, Biomater Sci-Uk 2(5) (2014) 674-679.
[206] R. Takai, R. Kurimoto, Y. Nakagawa, Y. Kotsuchibashi, K. Namekawa, M. Ebara, Towards a Rational Design of Zeolite-Polymer Composite Nanofibers for Efficient Adsorption of Creatinine, J Nanomater (2016).
[207] L.M. Lu, C. Samarasekera, J.T.W. Yeow, Creatinine adsorption capacity of electrospun polyacrylonitrile (PAN)-zeolite nanofiber membranes for potential artificial kidney applications, J Appl Polym Sci 132(34) (2015).
[208] L.M. Lu, J.T.W. Yeow, An adsorption study of indoxyl sulfate by zeolites and polyethersulfone-zeolite composite membranes, Mater Design 120 (2017) 328-335.
[209] J.Y. Li, L.L. Han, S.X. Liu, S. He, Y.M. Cao, J. Xie, L.Y. Jia, Removal of indoxyl sulfate by water-soluble poly-cyclodextrins in dialysis, Colloid Surf. B-Biointerfaces 164 (2018) 406-413.
[210] S. Kang, J.E. Yang, J. Kim, M. Ahn, H.J. Koo, M. Kim, Y.S. Lee, S.R. Paik, Removal of Intact beta 2-Microglobulin at Neutral pH by Using Seed-Conjugated Polymer Beads Prepared with beta 2-Microglobulin-Derived Peptide (58-67), Biotechnol Progr 27(2) (2011) 521-529.
[211] J.H. Huang, Treatment of phenol and p-cresol in aqueous solution by adsorption using a carbonylated hypercrosslinked polymeric adsorbent, J Hazard Mater 168(2-3) (2009) 1028-1034.

[212] B.J. Gao, Y. Yang, J. Wang, Y. Zhang, Preparation and adsorption characteristic of polymeric microsphere with strong adsorbability for creatinine, J Biochem Mol Toxic 22(3) (2008) 166-174.
[213] G. Selvolini, G. Marrazza, MIP-based sensors: Promising new tools for cancer biomarker determination, Sensors 17(4) (2017) 718.
[214] H.A. Tsai, M.J. Syu, Synthesis of creatinine-imprinted poly(beta-cyclodextrin) for the specific binding of creatinine, Biomaterials 26(15) (2005) 2759-2766.
[215] C. Baggiani, L. Anfossi, C. Giovannoli, Molecular imprinted polymers as synthetic receptors for the analysis of myco-and phyco-toxins, Analyst 133(6) (2008) 719-730.
[216] K. Haupt, Peer Reviewed: Molecularly Imprinted Polymers: The Next Generation, Analytical chemistry 75(17) (2003) 376 A-383 A.
[217] H.A. Tsai, M.J. Syu, Preparation of imprinted poly(tetraethoxysilanol) sol-gel for the specific uptake of creatinine, Chem Eng J 168(3) (2011) 1369-1376.
[218] P.S. Malchesky, W. Varnes, W. Piatkiewicz, Y. Nose, Membranes Containing Sorbents for Blood Detoxification, T Am Soc Art Int Org 23 (1977) 659-666.
[219] E. Denti, J.M. Walker, D. Brancaccio, V. Tessore, Evaluation of Novel Sorbent Systems for Joint Hemodialysis and Hemoperfusion, Med Instrum 11(4) (1977) 212-216.
[220] P.S. Malchesky, W. Piatkiewicz, W.G. Varnes, L. Ondercin, Y. Nose, Sorbent Membranes - Device Designs, Evaluations and Potential Applications, Artificial organs 2(4) (1978) 367-371.
[221] E. Klein, F.F. Holland, K. Eberle, F.C. Morton, I. Cabasso, Sorbent-Filled Hollow Fibers for Hemopurification, T Am Soc Art Int Org 24 (1978) 127-130.
[222] H.J. Gurland, L.A. Castro, W. Samtleben, J.C. Fernandez, Combination of Hemodialysis and Hemoperfusion in a Single Unit for Treatment of Uremia, Clinical nephrology 11(3) (1979) 167-172.
[223] S. Saiful, Mixed matrix membrane adsorbers for protein and blood purification, (2007).
[224] M.S.L. Tijink, M. Wester, G. Glorieux, K.G.F. Gerritsen, J.F. Sun, P.C. Swart, Z. Borneman, M. Wessling, R. Vanholder, J.A. Joles, D. Stamatialis, Mixed matrix hollow fiber membranes for removal of protein-bound toxins from human plasma, Biomaterials 34(32) (2013) 7819-7828.
[225] D. Pavlenko, E. van Geffen, M.J. van Steenbergen, G. Glorieux, R. Vanholder, K.G.F. Gerritsen, D. Stamatialis, New low-flux mixed matrix membranes that offer superior removal of protein-bound toxins from human plasma, Scientific reports 6 (2016).
[226] C.X. Nie, L. Ma, Y. Xia, C. He, J. Deng, L.R. Wang, C. Cheng, S.D. Sun, C.S. Zhao, Novel heparin-mimicking polymer brush grafted carbon nanotube/PES composite membranes for safe and efficient blood purification, J Membrane Sci 475 (2015) 455-468.
[227] S. Ito, M. Yoshida, Protein-Bound Uremic Toxins: New Culprits of Cardiovascular Events in Chronic Kidney Disease Patients, Toxins 6(2) (2014) 665-678.
[228] D.H. Krieter, A. Hackl, A. Rodriguez, L. Chenine, H.L. Moragues, H.D. Lemke, C. Wanner, B. Canaud, Protein-bound uraemic toxin removal in haemodialysis and post-dilution haemodiafiltration, Nephrol Dial Transpl 25(1) (2010) 212-218.
[229] Y. Yoshida, T. Sakai, M. Ise, Effects of Oral Adsorbent in the Rat Model of Chronic-Renal-Failure, Nephron 62(3) (1992) 305-314.
[230] P. Owada, M. Nakao, J. Koike, K. Ujiie, K. Tomita, T. Shiigai, Effects of oral adsorbent AST-120 on the progression of chronic renal failure: A randomized controlled study, Kidney international (1997) S188-

S190.
[231] T. Miyazaki, I. Aoyama, M. Ise, H. Seo, T. Niwa, An oral sorbent reduces overload of indoxyl sulphate and gene expression of TGF-beta 1 in uraemic rat kidneys, Nephrol Dial Transpl 15(11) (2000) 1773-1781.
[232] K. Shimoishi, M. Anraku, K. Kitamura, Y. Tasaki, K. Taguchi, M. Hashimoto, E. Fukunaga, T. Maruyama, M. Otagiri, An oral adsorbent, AST-120 protects against the progression of oxidative stress by reducing the accumulation of indoxyl sulfate in the systemic circulation in renal failure, Pharmaceut Res 24(7) (2007) 1283-1289.
[233] Y. Iwasaki, H. Yamato, T. Nii-Kono, A. Fujieda, M. Uchida, A. Hosokawa, M. Motojima, M. Fukagawa, Administration of oral charcoal adsorbent (AST-120) suppresses low-turnover bone progression in uraemic rats, Nephrol Dial Transpl 21(10) (2006) 2768-2774.
[234] M. Asai, S. Kumakura, M. Kikuchi, Review of the efficacy of AST-120 (KREMEZIN((R))) on renal function in chronic kidney disease patients, Renal failure 41(1) (2019) 47-56.
[235] G. Schulman, R. Vanholder, T. Niwa, AST-120 for the management of progression of chronic kidney disease, International journal of nephrology and renovascular disease 7 (2014) 49-56.
[236] D. Falkenhagen, W. Strobl, G. Vogt, A. Schrefl, I. Linsberger, F.J. Gerner, M. Schoenhofen, Fractionated plasma separation and adsorption system: A novel system for blood purification to remove albumin bound substances, Artificial organs 23(1) (1999) 81-86.
[237] W. Laleman, A. Wilmer, P. Evenepoel, C. Verslype, J. Fevery, F. Nevens, Review article: non-biological liver support in liver failure, Aliment Pharm Therap 23(3) (2006) 351-363.
[238] B.K. Meijers, V. Weber, B. Bammens, W. Dehaen, K. Verbeke, D. Falkenhagen, P. Evenepoel, Removal of the uremic retention solute p-Cresol using fractionated plasma separation and adsorption, Artificial organs 32(3) (2008) 214-219.
[239] F. Brettschneider, M. Tolle, M. von der Giet, J. Passlick-Deetjen, S. Steppan, M. Peter, V. Jankowski, A. Krause, S. Kuhne, W. Zidek, J. Jankowski, Removal of protein-bound, hydrophobic uremic toxins by a combined fractionated plasma separation and adsorption technique, Artificial organs 37(4) (2013) 409-16.
[240] V. Binder, B. Bergum, S. Jaisson, P. Gillery, C. Scavenius, E. Spriet, A.K. Nyhaug, H.M. Roberts, I.L.C. Chapple, A. Hellvard, N. Delaleu, P. Mydel, Impact of fibrinogen carbamylation on fibrin clot formation and stability, Thromb Haemostasis 117(5) (2017) 899-910.
[241] V.V. Sarnatskaya, A.I. Ivanov, V.G. Nikolaev, E. Rotellar, K. von Appen, M. Haspar, V.N. Maslenny, H. Klinkmann, Structure and binding properties of serum albumin in uremic patients at different periods of hemodialysis, Artificial organs 22(2) (1998) 107-115.
[242] V.V. Sarnatskaya, W.E. Lindup, P. Walther, V.N. Maslenny, L.A. Yushko, A.S. Sidorenko, A.V. Nikolaev, V.G. Nikolaev, Albumin, bilirubin, and activated carbon: New edges of an old triangle, Artificial Cells Blood Substitutes and Immobilization Biotechnology 30(2) (2002) 113-126.
[243] V.G. Nikolaev, V.V. Sarnatskaya, A.N. Sidorenko, K.I. Bardakhivskaya, E.A. Snezhkova, L.A. Yushko, V.N. Maslenny, L.A. Sakhno, S.V. Mikhalovsky, O.P. Kozynchenko, A.V. Nikolaev, Deliganding Carbonic Adsorbents for Simultaneous Removal of Protein-Bound Toxins, Bacterial Toxins and Inflammatory Cytokines, Nato Sci Peace Sec A (2011) 289-+.
[244] V.V. Sarnatskaya, L.A. Yushko, L.A. Sakhno, V.G. Nikolaev, A.V. Nikolaev, D.V. Grinenko, S.V. Mikhalovsky, New approaches to the removal of protein-bound toxins from blood plasma of uremic

patients, Artif Cell Blood Sub 35(3) (2007) 287-308.
[245] M.W. Mosesson, Fibrinogen and fibrin structure and functions, Journal of Thrombosis and Haemostasis 3(8) (2005) 1894-1904.
[246] D. Brian, P. Chowdary, Coagulation in Kidney Disease, in: M. Harber (Ed.), Practical Nephrology, Springer London, London, 2014, pp. 603-612.
[247] E.A. Permyakov, L.J. Berliner, alpha-Lactalbumin: structure and function, FEBS letters 473(3) (2000) 269-274.
[248] S.Y. Jung, S.M. Lim, F. Albertorio, G. Kim, M.C. Gurau, R.D. Yang, M.A. Holden, P.S. Cremer, The Vroman effect: A molecular level description of fibrinogen displacement, Journal of the American Chemical Society 125(42) (2003) 12782-12786.
[249] T. Peters, Serum-Albumin, Adv.Protein Chem. 37 (1985) 161-245.
[250] L.M. Siegel, K.J. Monty, Determination of Molecular Weights and Frictional Ratios of Proteins in Impure Systems by Use of Gel Filtration and Density Gradient Centrifugation . Application to Crude Preparations of Sulfite and Hydroxylamine Reductases, Biochimica et biophysica acta 112(2) (1966) 346-&.
[251] H.O. Ho, C.C. Hsiao, T.D. Sokoloski, C.Y. Chen, M.T. Sheu, Fibrin-Based Drug-Delivery Systems .3. The Evaluation of the Release of Macromolecules from Microbeads, Journal of Controlled Release 34(1) (1995) 65-70.
[252] C. Bramaud, P. Aimar, G. Daufin, Whey protein fractionation: Isoelectric precipitation of alpha-lactalbumin under gentle heat treatment, Biotechnology and bioengineering 56(4) (1997) 391-397.
[253] K. Gast, D. Zirwer, M. Muller-Frohne, G. Damaschun, Trifluoroethanol-induced conformational transitions of proteins: Insights gained from the differences between alpha-lactalbumin and ribonuclease A, Protein Science 8(3) (1999) 625-634.
[254] K.L. Prime, G.M. Whitesides, Adsorption of Proteins onto Surfaces Containing End-Attached Oligo(Ethylene Oxide) - a Model System Using Self-Assembled Monolayers, Journal of the American Chemical Society 115(23) (1993) 10714-10721.
[255] M.C.L. Martins, B.D. Ratner, M.A. Barbosa, Protein adsorption on mixtures of hydroxyl- and methylterminated alkanethiols self-assembled monolavers, Journal of Biomedical Materials Research Part A 67A(1) (2003) 158-171.
[256] S.N. Rodrigues, I.C. Goncalves, M.C.L. Martins, M.A. Barbosa, B.D. Ratner, Fibrinogen adsorption, platelet adhesion and activation on mixed hydroxyl-/methyl-terminated self-assembled monolayers, Biomaterials 27(31) (2006) 5357-5367.
[257] V.A. Tegoulia, S.L. Cooper, Leukocyte adhesion on model surfaces under flow: Effects of surface chemistry, protein adsorption, and shear rate, J Biomed Mater Res 50(3) (2000) 291-301.
[258] J.C. Lin, W.H. Chuang, Synthesis, surface characterization, and platelet reactivity evaluation for the self-assembled monolayer of alkanethiol with sulfonic acid functionality, J Biomed Mater Res 51(3) (2000) 413-423.
[259] M. Guilloton, F. Karst, A Spectrophotometric Determination of Cyanate Using Reaction with 2-Aminobenzoic Acid, Analytical biochemistry 149(2) (1985) 291-295.
[260] S.L. Snyder, P.Z. Sobocinski, An improved 2, 4, 6-trinitrobenzenesulfonic acid method for the determination of amines, Analytical biochemistry 64(1) (1975) 284-288.

[261] M. Binazadeh, H. Zeng, L.D. Unsworth, Effect of peptide secondary structure on adsorption and adsorbed film properties on end-grafted polyethylene oxide layers, Acta Biomaterialia 10(1) (2014) 56-66.
[262] S. Abraham, A. So, L.D. Unsworth, Poly(carboxybetaine methacrylamide)-Modified Nanoparticles: A Model System for Studying the Effect of Chain Chemistry on Film Properties, Adsorbed Protein Conformation, and Clot Formation Kinetics, Biomacromolecules 12(10) (2011) 3567-3580.
[263] S. Meiboom, D. Gill, Modified Spin-Echo Method for Measuring Nuclear Relaxation Times, Rev Sci Instrum 29(8) (1958) 688-691.
[264] B.P. Hills, S.F. Takacs, P.S. Belton, The Effects of Proteins on the Proton Nmr Transverse Relaxation-Times of Water .1. Native Bovine Serum-Albumin, Mol Phys 67(4) (1989) 903-918.
[265] T.T. Ehler, N. Malmberg, L.J. Noe, Characterization of self-assembled alkanethiol monolayers on silver and gold using surface plasmon spectroscopy, The Journal of Physical Chemistry B 101(8) (1997) 1268-1272.
[266] M.C. Sun, J. Deng, Z.C. Tang, J.D. Wu, D. Li, H. Chen, C.Y. Gao, A correlation study of protein adsorption and cell behaviors on substrates with different densities of PEG chains, Colloid Surf. B-Biointerfaces 122 (2014) 134-142.
[267] L.C. Kurz, D. LaZard, C. Frieden, Protein structural changes accompanying formation of enzymic transition states: tryptophan environment in ground-state and transition-state analog complexes of adenosine deaminase, Biochemistry 24(6) (1985) 1342-1346.
[268] J. Oakes, Protein hydration. Nuclear magnetic resonance relaxation studies of the state of water in native bovine serum albumin solutions, Journal of the Chemical Society, Faraday Transactions 1: Physical Chemistry in Condensed Phases 72 (1976) 216-227.
[269] J. Clifford, J. Oakes, G. Tiddy, Nuclear magnetic resonance studies of water in disperse systems, Special Discussions of the Faraday Society 1 (1970) 175-186.
[270] P.A. Cuypers, J.W. Corsel, M.P. Janssen, J.M.M. Kop, W.T. Hermens, H.C. Hemker, The Adsorption of Prothrombin to Phosphatidylserine Multilayers Quantitated by Ellipsometry, Journal of Biological Chemistry 258(4) (1983) 2426-2431.
[271] S.J. McClellan, E.I. Franses, Adsorption of bovine serum albumin at solid/aqueous interfaces, Colloid Surf. A-Physicochem. Eng. Asp. 260(1-3) (2005) 265-275.
[272] M. Dargahi, S. Omanovic, A comparative PM-IRRAS and ellipsometry study of the adsorptive behaviour of bovine serum albumin on a gold surface, Colloid Surf. B-Biointerfaces 116 (2014) 383-388.
[273] P.A. Cuypers, J.W. Corsel, M.P. Janssen, J. Kop, W.T. Hermens, H.C. Hemker, The adsorption of prothrombin to phosphatidylserine multilayers quantitated by ellipsometry, Journal of Biological Chemistry 258(4) (1983) 2426-2431.
[274] J.-F. Hsieh, S.-T. Chen, Comparative studies on the analysis of glycoproteins and lipopolysaccharides by the gel-based microchip and SDS-PAGE, Biomicrofluidics 1(1) (2007) 014102.
[275] P. Weathersby, T. Horbett, A. Hoffman, Solution stability of bovine fibrinogen, Thromb Res 10(2) (1977) 245-252.
[276] A.A. Rashin, B. Honig, On the environment of ionizable groups in globular proteins, Journal of molecular biology 173(4) (1984) 515-521.
[277] C. Koro, A. Hellvard, N. Delaleu, V. Binder, C. Scavenius, B. Bergum, I. Główczyk, H.M. Roberts, I.L. Chapple, M.M. Grant, Carbamylated LL-37 as a modulator of the immune response, Innate immunity

22(3) (2016) 218-229.
[278] A. Le Dean, F. Mariette, M. Marin, (1)H nuclear magnetic resonance relaxometry study of water state in milk protein mixtures, Journal of agricultural and food chemistry 52(17) (2004) 5449-5455.
[279] G.H. Goetz, M. Shalaeva, Leveraging chromatography based physicochemical properties for efficient drug design, Admet Dmpk 6(2) (2018) 85-104.
[280] I. Zaccari, B.G. Catchpole, S.X. Laurenson, A.G. Davies, C. Walti, Improving the Dielectric Properties of Ethylene-Glycol Alkanethiol Self-Assembled Monolayers, Langmuir 30(5) (2014) 1321-1326.
[281] G. Greczynski, L.J.P.i.M.S. Hultman, X-ray photoelectron spectroscopy: Towards reliable binding energy referencing, 107 (2020) 100591.
[282] Y. Kamon, Y. Kitayama, A.N. Itakura, K. Fukazawa, K. Ishihara, T. Takeuchi, Synthesis of grafted phosphorylcholine polymer layers as specific recognition ligands for C-reactive protein focused on grafting density and thickness to achieve highly sensitive detection, Physical Chemistry Chemical Physics 17(15) (2015) 9951-9958.
[283] Y. Arima, H. Iwata, Effects of surface functional groups on protein adsorption and subsequent cell adhesion using self-assembled monolayers, Journal of Materials Chemistry 17(38) (2007) 4079-4087.
[284] L.Y. Li, S.F. Chen, S.Y. Jiang, Protein adsorption on alkanethiolate self-assembled monolayers: Nanoscale surface structural and chemical effects, Langmuir 19(7) (2003) 2974-2982.
[285] D.K. Goyal, A. Subramanian, In-situ protein adsorption study on biofunctionalized surfaces using spectroscopic ellipsometry, Thin Solid Films 518(8) (2010) 2186-2193.
[286] J. Benesch, A. Askendal, P. Tengvall, Quantification of adsorbed human serum albumin at solid interfaces: a comparison between radioimmunoassay (RIA) and simple null ellipsometry, Colloid Surf. B-Biointerfaces 18(2) (2000) 71-81.
[287] M.F.M. Engel, C.P.M. van Mierlo, A.J.W.G. Visser, Kinetic and structural characterization of adsorption-induced unfolding of bovine alpha-lactalbumin, Journal of Biological Chemistry 277(13) (2002) 10922-10930.
[288] P. Roach, D. Farrar, C.C. Perry, Interpretation of protein adsorption: Surface-induced conformational changes, Journal of the American Chemical Society 127(22) (2005) 8168-8173.
[289] L.M. Kraus, S. Miyamura, B.R. Pecha, A.P. Kraus, Carbamoylation of Hemoglobin in Uremic Patients Determined by Antibody Specific for Homocitrulline (Carbamoylated Epsilon-N-Lysine), Mol Immunol 28(4-5) (1991) 459-463.
[290] E.O. Apostolov, S.V. Shah, E. Ok, A.G. Basnakian, Quantification of carbamylated LDL in human sera by a new sandwich ELISA, Clinical chemistry 51(4) (2005) 719-728.
[291] S. Nakabo, M. Hashimoto, S. Ito, M. Furu, H. Ito, T. Fujii, H. Yoshifuji, Y. Imura, R. Nakashima, K. Murakami, N. Kuramoto, M. Tanaka, J. Satoh, A. Ishigami, S. Morita, T. Mimori, K. Ohmura, Carbamylated albumin is one of the target antigens of anti-carbamylated protein antibodies, Rheumatology 56(7) (2017) 1217-1226.
[292] Y.M. Fang, D.Q. Lin, S.J. Yao, Review on biomimetic affinity chromatography with short peptide ligands and its application to protein purification, Journal of Chromatography A 1571 (2018) 1-15.
[293] Y. Zhang, I-TASSER server for protein 3D structure prediction, BMC bioinformatics 9 (2008).
[294] A. Roy, A. Kucukural, Y. Zhang, I-TASSER: a unified platform for automated protein structure and function prediction, Nature protocols 5(4) (2010) 725-738.

[295] J.Y. Yang, A. Roy, Y. Zhang, Protein-ligand binding site recognition using complementary binding-specific substructure comparison and sequence profile alignment, Bioinformatics 29(20) (2013) 2588-2595.
[296] J. Yang, A. Roy, Y. Zhang, BioLiP: a semi-manually curated database for biologically relevant ligand-protein interactions, Nucleic acids research 41(Database issue) (2013) D1096-103.
[297] O. Trott, A.J. Olson, Software News and Update AutoDock Vina: Improving the Speed and Accuracy of Docking with a New Scoring Function, Efficient Optimization, and Multithreading, J Comput Chem 31(2) (2010) 455-461.
[298] M.P. Lefranc, V. Giudicelli, P. Duroux, J. Jabado-Michaloud, G. Folch, S. Aouinti, E. Carillon, H. Duvergey, A. Houles, T. Paysan-Lafosse, S. Hadi-Saljoqi, S. Sasorith, G. Lefranc, S. Kossida, IMGT (R), the international ImMunoGeneTics information system (R) 25 years on, Nucleic acids research 43(D1) (2015) D413-D422.
[299] V. Giudicelli, P. Duroux, C. Ginestoux, G. Folch, J. Jabado-Michaloud, D. Chaume, M.P. Lefranc, IMGT/LIGM-DB, the IMGT comprehensive database of immunoglobulin and T cell receptor nucleotide sequences, Nucleic acids research 34(Database issue) (2006) D781-4.
[300] R. J.M.H., Recombinant human autoantibodies specific for citrullinecontaining peptides from RA patient derived phage display libraries (Unpublished).
[301] A.K. Sato, D.J. Sexton, L.A. Morganelli, E.H. Cohen, Q.L. Wu, G.P. Conley, Z. Streltsova, S.W. Lee, M. Devlin, D.B. DeOliveira, J. Enright, R.B. Kent, C.R. Wescott, T.C. Ransohoff, A.C. Ley, R.C. Ladner, Development of mammalian serum albumin affinity purification media by peptide phage display, Biotechnol Progr 18(2) (2002) 182-192.
[302] D. Gaser, B. Strukelj, T. Bratkovic, S. Kreft, J. Pungercar, M. Lunder, Cross-affinity of Peptide Ligands Selected from Phage Display Library Against Pancreatic Phospholipase A2 and Ammodytoxin C, Acta chimica Slovenica 56(3) (2009) 712-717.
[303] W.X. Zhao, H. Yuan, X. Xu, L. Ma, Isolation and Initial Application of a Novel Peptide That Specifically Recognizes the Neural Stem Cells Derived from Rhesus Monkey Embryonic Stem Cells, Journal of biomolecular screening 15(6) (2010) 687-694.
[304] S.J. Segvich, H.C. Smith, D.H. Kohn, The adsorption of preferential binding peptides to apatite-based materials, Biomaterials 30(7) (2009) 1287-1298.
[305] C. Pommie, S. Levadoux, R. Sabatier, G. Lefranc, M.P. Lefranc, IMGT standardized criteria for statistical analysis of immunoglobulin V-REGION amino acid properties, J Mol Recognit 17(1) (2004) 17-32.
[306] G. Fan, C.M. Dundas, C. Zhang, N.A. Lynd, B.K. Keitz, Sequence-Dependent Peptide Surface Functionalization of Metal-Organic Frameworks, ACS Applied Materials & Interfaces 10(22) (2018) 18601-18609.
[307] N. Schonberger, R. Braun, S. Matys, F.L. Lederer, F. Lehmann, K. Flemming, K. Pollmann, Chromatopanning for the identification of gallium binding peptides, Journal of Chromatography A 1600 (2019) 158-166.
[308] H.C. Gasteiger E., Gattiker A., Duvaud S., Wilkins M.R., Appel R.D., Bairoch A.;, Protein Identification and Analysis Tools on the ExPASy Server; (In) John M. Walker (ed): The Proteomics Protocols Handbook, Humana Press (2005). (2005) 571-607.
[309] W.B. Turnbull, A.H. Daranas, On the value of c: Can low affinity systems be studied by isothermal

titration calorimetry?, Journal of the American Chemical Society 125(48) (2003) 14859-14866.
[310] L.D. Hansen, G.W. Fellingham, D.J. Russell, Simultaneous determination of equilibrium constants and enthalpy changes by titration calorimetry: Methods, instruments, and uncertainties, Analytical biochemistry 409(2) (2011) 220-229.
[311] S. Jaisson, C. Pietrement, P. Gillery, Carbamylation-Derived Products: Bioactive Compounds and Potential Biomarkers in Chronic Renal Failure and Atherosclerosis, Clinical chemistry 57(11) (2011) 1499-1505.
[312] E. Aghaee, J.B. Ghasemi, F. Manouchehri, S. Balalaie, Combined docking, molecular dynamics simulations and spectroscopic studies for the rational design of a dipeptide ligand for affinity chromatography separation of human serum albumin, Journal of molecular modeling 20(10) (2014).
[313] R.Z. Wang, D.Q. Lin, W.N. Chu, Q.L. Zhang, S.J. Yao, New tetrapeptide ligands designed for antibody purification with biomimetic chromatography: Molecular simulation and experimental validation, Biochem Eng J 114 (2016) 194-204.
[314] D.B. Kaufman, M.E. Hentsch, G.A. Baumbach, J.A. Buettner, C.A. Dadd, P.Y. Huang, D.J. Hammond, R.G. Carbonell, Affinity purification of fibrinogen using a ligand from a peptide library, Biotechnology and bioengineering 77(3) (2002) 278-289.
[315] P.V. Gurgel, R.G. Carbonell, H.E. Swaisgood, Fractionation of whey proteins with a hexapeptide ligand affinity resin, Bioseparation 9(6) (2000) 385-392.
[316] P. Jain, L. Sun, J.H. Dai, G.L. Baker, M.L. Bruening, High-capacity purification of his-tagged proteins by affinity membranes containing functionalized polymer brushes, Biomacromolecules 8(10) (2007) 3102-3107.
[317] F. Xu, J.H. Geiger, G.L. Baker, M.L. Bruening, Polymer Brush-Modified Magnetic Nanoparticles for His-Tagged Protein Purification, Langmuir 27(6) (2011) 3106-3112.
[318] S. Tugulu, P. Silacci, N. Stergiopulos, H.A. Klok, RGD - Functionalized polymer brushes as substrates for the integrin specific adhesion of human umbilical vein endothelial cells, Biomaterials 28(16) (2007) 2536-2546.
[319] Y. Fang, W. Xu, X.L. Meng, X.Y. Ye, J. Wu, Z.K. Xu, Poly(2-hydroxyethyl methacrylate) Brush Surface for Specific and Oriented Adsorption of Glycosidases, Langmuir 28(37) (2012) 13318-13324.
[320] F. Causa, E. Battista, R. Della Moglie, D. Guarnieri, M. Iannone, P.A. Netti, Surface Investigation on Biomimetic Materials to Control Cell Adhesion: The Case of RGD Conjugation on PCL, Langmuir 26(12) (2010) 9875-9884.
[321] F.Y. Liu, M.Y. Zhou, F. Zhang, I-125 labelling of human serum albumin and fibrinogen and a study of protein adsorption properties on the surface of titanium oxide film, Appl Radiat Isotopes 49(1-2) (1998) 67-72.
[322] E. Jansson, P. Tengvall, Adsorption of albumin and IgG to porous and smooth titanium, Colloid Surf. B-Biointerfaces 35(1) (2004) 45-51.
[323] Y. Chang, Y.J. Shih, C.Y. Ko, J.F. Jhong, Y.L. Liu, T.C. Wei, Hemocompatibility of Poly(vinylidene fluoride) Membrane Grafted with Network-Like and Brush-Like Antifouling Layer Controlled via Plasma-Induced Surface PEGylation, Langmuir 27(9) (2011) 5445-5455.
[324] Y. Sui, X.L. Gao, Z.N. Wang, C.J. Gao, Antifouling and antibacterial improvement of surface-functionalized poly(vinylidene fluoride) membrane prepared via dihydroxyphenylalanine-initiated atom

transfer radical graft polymerizations, J Membrane Sci 394 (2012) 107-119.
[325] B.P. Nelson, T.E. Grimsrud, M.R. Liles, R.M. Goodman, R.M. Corn, Surface plasmon resonance imaging measurements of DNA and RNA hybridization adsorption onto DNA microarrays, Analytical chemistry 73(1) (2001) 1-7.
[326] C. Zhao, L. Li, Q. Wang, Q. Yu, J. Zheng, Effect of film thickness on the antifouling performance of poly (hydroxy-functional methacrylates) grafted surfaces, Langmuir 27(8) (2011) 4906-4913 %@ 0743-7463.
[327] C. Yoshikawa, A. Goto, N. Ishizuka, K. Nakanishi, A. Kishida, Y. Tsujii, T. Fukuda, Size-Exclusion Effect and Protein Repellency of Concentrated Polymer Brushes Prepared by Surface-Initiated Living Radical Polymerization, Macromolecular Symposia 248(1) (2007) 189-198.
[328] C. Yoshikawa, A. Goto, N. Ishizuka, K. Nakanishi, A. Kishida, Y. Tsujii, T. Fukuda, Size-exclusion effect and protein repellency of concentrated polymer brushes prepared by surface-initiated living radical polymerization, Macromolecular Symposia 248 (2007) 189-198.
[329] H. Lu, M.A. Hood, S. Mauri, J.E. Baio, M. Bonn, R. Munoz-Espi, T. Weidner, Biomimetic vaterite formation at surfaces structurally templated by oligo(glutamic acid) peptides, Chemical Communications 51(88) (2015) 15902-15905.
[330] Y.J. Du, R.M. Cornelius, J.L. Brash, Measurement of protein adsorption to gold surface by radioiodination methods: suppression of free iodide sorption, Colloid Surf. B-Biointerfaces 17(1) (2000) 59-67.
[331] Y.X. Ding, V. Hlady, Competitive Adsorption of Three Human Plasma Proteins onto Sulfhydryl-to-sulfonate Gradient Surfaces, Croat Chem Acta 84(2) (2011) 193-202.
[332] G. Jin, Q.H. Yao, S.Z. Zhang, L. Zhang, Surface modifying of microporous PTFE capillary for bilirubin removing from human plasma and its blood compatibility, Mat Sci Eng C-Bio S 28(8) (2008) 1480-1488.
[333] R.C. Eberhart, M.S. Munro, J.R. Frautschi, M. Lubin, F.J. Clubb, C.W. Miller, V.I. Sevastianov, Influence of Endogenous Albumin Binding on Blood-Material Interactions, Ann Ny Acad Sci 516 (1987) 78-95.
[334] K. Kottke-Marchant, J.M. Anderson, Y. Umemura, R.E. Marchant, Effect of albumin coating on the in vitro blood compatibility of Dacron® arterial prostheses, Biomaterials 10(3) (1989) 147-155.
[335] J.M. Grunkemeier, W.B. Tsai, C.D. McFarland, T.A. Horbett, The effect of adsorbed fibrinogen, fibronectin, von Willebrand factor and vitronectin on the procoagulant state of adherent platelets, Biomaterials 21(22) (2000) 2243-2252.
[336] T.A. Horbett, Fibrinogen adsorption to biomaterials, Journal of Biomedical Materials Research Part A 106(10) (2018) 2777-2788.